



UNIVERSIDAD DE CHILE
FACULTAD DE CIENCIAS FÍSICAS Y MATEMÁTICAS
DEPARTAMENTO DE FÍSICA

TESIS PARA OPTAR AL GRADO DE
MAGÍSTER EN CIENCIAS, MENCIÓN FÍSICA

BASTIÁN PRADENAS MÁRQUEZ

PROFESOR GUÍA:
GONZALO PALMA QUILODRÁN

MIEMBROS DE LA COMISIÓN:

SANTIAGO DE CHILE
JULIO 2018

RESUMEN DE LA MEMORIA PARA OPTAR
AL TÍTULO DE MAGÍSTER EN CIENCIAS, MENCIÓN FÍSICA
POR: BASTIÁN PRADENAS MÁRQUEZ
FECHA: JULIO 2018
PROF. GUÍA: GONZALO PALMA QUILODRÁN

The journey is the destination, man.
Gerald Johanssen

Agradecimientos

Me gustaría expresar mi gratitud por los siguientes humanos, animales e instituciones:

A toda mi familia en general por animarme a dar lo mejor y estar pendiente en cada uno de mis pasos. En particular, a mis padres que sin su cariño, afecto y apoyo incondicional durante todo este tiempo esto no sería posible; también a mi tío Salva por estar siempre presente y atento; a mis abuelitas por su amor, afecto, cazuelas y sopas de misterio.

Al caballito y a todos mis perros que por su lealtad y agasajo siempre me sacan una sonrisa.

A mis amigos del DFI y de Universidad de Chile, en especial al Rafa, Chelo, a los Pipes, Susana, Ualter, Esteban, Bryan, Bruno, Isi, Pablito, Vitoco, Xorin, Tomás, Carlitos y al Mancilla. Que entre buenas conversaciones, anécdotas, historias, risas y pichangas me mantuvieron cuerdo durante todos estos años generando momentos que atesoraré con nostalgia.

A toda la comunidad del DFI, que gracias a su dedicación, pasión y compromiso con la docencia de alguna u otra forma hicieron encantarme aún más por la Física, particularmente a Rodrigo Soto, Marcel Clerc, Claudio Falcón y Gonzalo Palma, en especial a estos dos últimos. A Falcón por transmitir su entusiasmo y energía; al Gonzalo por brindarme de su tiempo, disposición y confianza; y que sin su apoyo este trabajo no sería posible.

A los integrantes de la colaboración CLASS por su pasión, esfuerzo y compromiso; en especial a Toby por brindarme la oportunidad y de un espacio; finalmente también a Zhilei, John, Manwei y Sumit por su hospitalidad, humor, energía y amistad.

A Conicyt por el soporte económico brindado durante estos dos años de magíster.

Contents

1	Introduction	1
1.1	Standard Λ CDM Cosmology	2
1.1.1	Einstein equations	3
1.1.2	Concordance model	5
1.1.3	Thermal History	6
2	Inflation	12
2.1	Causal structure	12
2.1.1	Flatness problem	14
2.1.2	Horizon Problem	14
2.2	Background	15
2.2.1	Single field slow-roll inflation	17
2.2.2	Slow And Ultra Slow Roll Inflation	19
2.3	Quantum initial conditions	19
2.3.1	Free Scalar spectator Field In dS_4	20
2.3.2	Canonical quantization	21
2.3.3	Choice of the vacuum	22
2.4	Two point correlation function	23
2.4.1	Light field limit	24
2.4.2	Heavy field limit	24
2.5	Curvature power spectrum	25
2.5.1	Comoving gauge	25
2.5.2	Tensor Perturbations	27
2.5.3	Observations	29
2.6	Non-gaussianity	31
2.6.1	Non-gaussian CMB statistic	31
2.6.2	Fields non-gaussianity	32
2.6.3	Local non-Gaussianity	33
2.7	In-In formalism	35
3	Cosmic Microwave Background	40
3.1	CMB anisotropies	40
3.2	Radiative transfer: from recombination to today.	45
3.3	Large scales: The Sachs-Wolfe effect	47
3.3.1	Acoustic peaks	48
3.4	The damping tail	50

3.5	Cosmology from the CMB power spectrum	52
3.6	CMB Polarization	53
3.6.1	Polarized Boltzmann equation	53
3.7	CMB systematics	63
4	Features	66
4.1	Correlation of power spectra	68
4.1.1	Preliminaries	68
4.1.2	Rapidly time varying backgrounds	69
4.1.3	In-in formalism	70
4.1.4	Features from varying Hubble parameters	72
4.1.5	Including the effects of a varying sound speed	73
4.2	A quantitative discussion	74
4.2.1	Resonant features	74
4.2.2	Predictions for the low ℓ tensor power spectrum	75
4.3	Conclusions	76
4.4	Figures	77
5	Consistency relations	80
5.1	Review of the consistency relation derivation	81
5.2	A generalized consistency relation	84
5.2.1	Case with $\varepsilon \rightarrow 0$	85
5.2.2	Non-Gaussianity in ultra slow-roll inflation	86
5.2.3	Case with $\varepsilon \neq 0$	87
5.3	Discussion	89
5.4	Conclusions	90
6	Conformal Fermi Coordinates and vanishing f_{NL}	92
6.1	Fermi Normal Coordinates	93
6.1.1	Geometric construction	94
6.1.2	Coordinates transformation	95
6.2	Congruence of timelike geodesics	98
6.3	Transverse metric	98
6.3.1	Kinematics	98
6.4	Geodesic deviation	99
6.4.1	Raychaudhuri's equation	100
6.5	Fermi Normal Coordinates (FNC) in FRW	102
6.5.1	Unperturbed FLRW Universe	104
6.5.2	Perturbed FLRW Universe	106
6.6	Conformal Fermi Coordinates (CFC)	108
6.6.1	Construction of the CFC	109
6.6.2	Mapping to CFC	110
6.7	Power Spectrum Of Short Modes in CFC	122
6.8	Bispectrum Squeezed Limit	123
6.8.1	Observed f_{NL} in single field Attractor models	123
6.8.2	Observed f_{NL} in single field Non-attractor models	124
6.9	Discussion and conclusions	125

7	Window Functions and Deconvolution Method for The Cosmology Large Angular Scale Surveyor(CLASS)	128
7.1	Beams and window functions	128
7.2	Moon temperature model	132
7.2.1	Beam fitting and deconvolution	133
7.2.2	Uncertainty propagation	136
7.3	Conclusions	138
7.4	Chapter Appendix	140

List of Tables

1.1	Parameter 68% confidence levels for the base Λ CDM cosmology computed from the <i>Planck</i> CMB power spectra, in combination with the CMB lensing likelihood.	6
1.2	Termal history of the universe.	7
6.1	In this table we collect the relevant CFC conformal metric Christoffel coefficients from [1]. We separate them into contributions from $\eta_{\mu\nu} + h_{\mu\nu}$ and those from the scale factor a^2/a_F^2 . The terms of the left(right) are useful for (non-)attractor models.	120
6.2	Results: this is a summary of the derived perturbative quantities for the CFC construction evaluated at the central geodesic. All the geometrical objects of interest are displayed here; in particular, notice the tetrad vectors for both types of scenarios in which is the unobservable long modes have been absorbed either in the spatial components or the temporal components. In the last two lines the coordinates $(\bar{\tau}, \bar{\mathbf{x}}_c)$ was omitted for brevity.	121
7.1	Notation	129
7.2	Window function parameters	136

List of Figures

1.1	Supernova recession: Evidence for dark energy, found in 1998 by the Supernova Cosmology Project and Calan-Tololo Supernovae Survey.	5
1.2	Homogeneity and contrast of the CMB: Pictorially if we take a CMB picture and then we tune its contrast we would notice the anisotropies structure, corresponding to a different temperature at a different point on the sky.	8
1.3	Universe evolution. Credit: http://www.damtp.cam.ac.uk/user/db275/concepts/Lecture7.pdf	9
1.4	Cosmology Large Angular Scale Surveyor Aka. CLASS telescope located in cerro Toco, San Pedro de Atacama, Chile.	10
2.1	Space time foliation. Credit:[14].	26
2.2	Primordial curvature power spectrum from Planck collaboration 2015. The nearly scale-invariant of this spectrum, tell us about a quasi de Sitter expansion of the early universe and its duration, more importantly, it is obtained by naturally deconvolving the angular power temperature power spectrum or the C_l^{TT} 's, which makes of this image a remarkably beautiful and at the same time thrilling plot in concordance with basic inflationary predictions. Nevertheless, it is worth mentioning that the information(amplitude and the scalar tilt) of this spectrum is not sufficient to break the physical parameter degeneracy between its $H_{\text{inflation}}$ and ε , furthermore, the scenario is even worst, making the energy inflationary scale one of the worst constrained parameters in physics. This is why we need an ultimate and independent primordial source to break this degeneracy, such as B -modes from primordial gravitational waves [32].	30
2.3	Schematic probability distribution for the primordial curvature perturbation. Positive f_{NL} correspond to the red curve in the figure. Negative f_{NL} correspond to an axial reflection at $\zeta = 0$ of the red curve. The constrained f_{NL} is should be represented much smaller in this plot. Credit:[14].	34
3.1	Measurements of the CMB intensity vs. frequency together with a fit to the data. Superposed are the expected black body curves for $T = 2\text{K}$ and $T = 40\text{K}$. They are the most precise measurements of the CMB spectrum at the millimeter wavelengths near its peak were made by the Far Infrared Absolute Spectrophotometer(FIRAS) instrument aboard the Cosmic Background Explorer (COBE) satellite. Credit: https://lambda.gsfc.nasa.gov/product/cobe/	41
3.2	Angular anisotropies. https://www.cosmos.esa.int/web/planck/planck-collaboration . 42	

3.3 Modes evolution: Overdensities are generated during the inflation as quantum fluctuations. As the horizon shrinks the wavelength of the curvature modes becomes larger than the horizon(aka. they exit the horizon) and consequently they freeze and become classical. After the hot big bang era or recombination, these modes re-enter the horizon and they start to grow according to the underlying subhorizon physics, finally at decoupling or recombination, they leave defined statistical fingerprints which are transported and projected through incoming photons from the CMB toward us. Credit: http://www.damtp.cam.ac.uk/user/db275/Cosmology/Lectures.pdf	44
3.4 TT -angular power spectrum by Planck collaboration 2015. The dashed vertical line at $l = 30$ correspond to the change of map between commander($l = 2 - 29$) and SMICA($l = 30 - 2500$). Data shows an astonishing matching with the CMB model for higher l , however, al low l is cosmic variance(theoretical error) dominated. The unique easy solution to fix these statistical mismatch is to switch from this universe to another, take data and combine them. Credit: https://www.cosmos.esa.int/web/planck/planck-collaboration	53
3.5 E-modes and B-modes patterns: The E-modes or curl free patterns are symmetric under reflection, whereas the B-modes or divergenless pattern are antisymmetric under reflection. Credit: https://writescience.wordpress.com/2014/04/11/	59
3.6 The transformation of quadrupole anisotropies into linear polarization. In different regions the plane wave modulation of the quadrupole can change its sign but not its polarization sense. (a) The orientation of the quadrupole moment with respect to the scatterig direction \hat{n} determines the sense and magnitude of the polarization. It is aligned with the cold(red, long) lobe in the $e_\theta \otimes e_\phi$ tangent plane. (b) In spherical coordinates where $n \cdot k = \cos \theta$, the polarization points north-south Q with magnitude varying as $\sin 2\theta$ for scalar fluctuations. Credit: http://background.uchicago.edu/~whu/polar/webversion/polar.html	61
3.7 EE and TE angular power spectrum. Remarkably the red curves are not a fit, they are the model using the parameters inferred from the TT -angular power spectrum. Therefore these plot show the consistency of the theoretical framework [32].	62
3.8 LFI at 30GHz Commander map: The top figure shows the magnetic fields and the intensity of polarized radiation synchrotron radiation measured from LFI at 30GHz. The bottom figure shows the magnetic fields and the intensity of polarized radiation synchrotron radiation measured from HFI at 353GHz. These two figures are important to understand the status of the current observation of B modes from CMB. They correspond to the main spurious sources on the galactic plane that must be characterized and eliminated. Credit: https://www.cosmos.esa.int/web/planck/planck-collaboration	65
4.1 The first two slow-roll parameters $\Delta\eta$ and $\Delta\varepsilon$ (left panels) using eq. (4.39) and $\frac{\Delta P_S}{P_S^0}(k)$, $\frac{\Delta P_T}{P_T^0}(k)$ (right panels) related by eq. (4.34), in the case of the resonant feature (4.41). We have used $A = 0.028$, $\Omega = 30$, $\phi/2\pi = 0.634$, $k_* = 0.05[\text{Mpc}]^{-1}$ and $\varepsilon_0 = 0.0068$.	77

4.2	The first two slow-roll parameters $\Delta\eta$ and $\Delta\varepsilon$ (left panels) using eq. (4.40) and $\frac{\Delta P_S}{P_S^0}(k)$, $\frac{\Delta P_T}{P_T^0}(k)$ (right panels) related by eq. (4.38), in the case of the resonant feature (4.41). We have used $A = 0.028$, $\Omega = 30$, $\phi/2\pi = 0.634$, $k_* = 0.05[\text{Mpc}]^{-1}$ and $\varepsilon_0 = 0.0068$	78
4.3	The first two slow-roll parameters $\Delta\eta$ and $\Delta\varepsilon$ (left panels) using eq. (4.39) and $\frac{\Delta P_S}{P_S^0}(k)$, $\frac{\Delta P_T}{P_T^0}(k)$ (right panels) related by eq. (4.34), in the case of the Gaussian feature (4.42). We have used $A = -0.15$, $\lambda = 15$, $k^* = 0.002[\text{Mpc}]^{-1}$ and $\varepsilon_0 = 0.0068$	78
4.4	Plot of the first two slow-roll parameters $\Delta\eta$ and $\Delta\varepsilon$ (left panels) using eq. (4.40) and $\frac{\Delta P_S}{P_S^0}(k)$, $\frac{\Delta P_T}{P_T^0}(k)$ (right panels) related by eq. (4.38), in the case of the Gaussian feature (4.42). We have used $A = -0.15$, $\lambda = 15$, $k^* = 0.002[\text{Mpc}]^{-1}$ and $\varepsilon_0 = 0.0068$	79
6.1	Geometrical construction of Fermi coordinates	93
6.2	Geodesic congruence	99
6.3	Geometrical construction of Fermi coordinates	103
7.1	Average beam profile. The shaded region denotes a $1-\sigma$ of uncertainty envelope around the beam average along the season.	133
7.2	Beam profile: the red line represents the symmetrized convolved signal between the moon and the beam($T * B$) with its respective fit using Eq.(7.38)(green line), whereas the blue dashed line represent the deconvolved beam.	135
7.3	Temperature-temperature window function: The upper panel show the l dependence of the window function acting as low pass filter. The bottom panel shows its fractional uncertainty.	136
7.4	Fractional uncertainty comparison: The blue and the light blue contours represent the fractional uncertainty of beam and the convolved beam, respectively. The red line correspond to the fractional deviation between the convolved beam and the deconvolved beam, this effect is significant for higher l . The negative tendency can be interpreted as a lack of power for higher l since the convolution soften the small beam features that adds extra amplitude.	137
7.5	Temperature-temperature beam covariance matrix in harmonic representation.	138
7.6	Temperature-Temperature window function: The upper panel show the l dependence of the window function acting as low pass filter. The bottom panel shows its fractional uncertainty.	140
7.7	Temperature-Polarization window function. $P = E, B$. The upper panel show the l dependence of the window function acting as low pass filter. The bottom panel shows its fractional uncertainty.	140
7.8	Polarization-Polarization window function. $P = E, B$. The upper panel show the l dependence of the window function acting as low pass filter. The bottom panel shows its fractional uncertainty.	141
7.9	Temperature-Temperature beam covariance matrix in harmonic representation.	141
7.10	Polarization-Polarization beam covariance matrix in harmonic representation.	142
7.11	Polarization-Temperature beam covariance matrix in harmonic representation.	142

Chapter 1

Introduction

The last one hundred of years have been an epoch of great physics achievements. Particularly, the Cosmology started with the Einstein's discovery of General Relativity, then Hubble observed other galaxies and derive an empiric relation between distance and velocity that could be explained by the expansion of the universe by introducing the cosmological constant Λ . The discovery of the Cosmic Microwave Background signal in 1964 by Arno Penzias and Robert Wilson which was the first observational indication of a cosmological phase of the universe proposed in 1948 by George Gamow and Ralph A. Alpher known as big bang nucleosynthesis; The discovery of the actual inflationary paradigm to explain the homogeneity and the flatness of our universe in 1982 by Alan Guth, Andrei Linde, Andreas Albrecht and Paul Steinhardt; The particular surprise that density fluctuation during inflation serves as seeds to the structures of late time universe; The measurements of an almost perfect Blackbody CMB spectrum from COBE, hereafter, we say that cosmology started to be considered a precision science; The discovery of the accelerating universe by The early idea of the expansion of the universe was that this expansion would be decelerating due to gravitational attraction. The significant discovery appeared in 1998 when the Supernova Cosmology Project and the High-Z Supernova Search Team used type Ia supernovae to measure the rate of deceleration. They found out, surprisingly, that our universe was accelerating and therefore diluting its content quicker; The significant improvement in temperature anisotropies by WMAP and Planck satellites they improved with high precision the primordial power spectra, and finally the detection of gravitational waves from the black holes and neutron stars coalescence by LIGO in 2016.

Most of these findings helped to set the foundations of the standard model of cosmology known as the Λ CDM model, or concordance model. This way of looking our universe encompasses different concepts for its description: First, we have the Λ component which tells us about the expanding universe at late times, and second, we have the CDM which stands for cold dark matter. Under this model, our universe is made of $\sim 70\%$ of dark energy, encoded in the cosmological constant Λ , and around a 26% of cold dark matter which is used to explain the formation of galaxies. Its real composition and why it does not interact with ordinary matter is still a remaining mystery. The last part is the 4% containing all the baryonic matter of our universe, these are the particles contained in planets, stars and gas clouds. It is worth mentioning that Λ CDM describe a complex system as our universe in just

six parameters, therefore our universe is complex as simple at the same time, these parameters depend on others coming from Quantum theory, General Relativity, Nuclear Physics, Electrodynamics and Kinetic theory. Nevertheless, there are still some unknown ingredients for example dark matter, dark energy whose microscopic origin is not understood, after all, cosmology has become a mainstream topic within particle physics, largely because cosmology provides several of the main pieces of observational evidence for the incompleteness of the Standard Model of particle physics.

1.1 Standard Λ CDM Cosmology

Cosmology became a science once Einstein's discovery of General Relativity (GR) related the observed distribution of stress-energy to the measurable geometry of spacetime. This implies the geometry of the universe as a whole can be tied to the overall distribution of matter at the largest scales. It used to be an article of faith that this geometry should be assumed to be homogeneous and isotropic, the so-called cosmological principle, but these days it is pretty much an experimental fact that the stress-energy of the universe is homogeneous and isotropic on the largest scales visible.

On such large scales, the geometry of space-time should, therefore, be homogeneous and isotropic, and the Friedmann-Robertson-Walker(FRW) metric describes the most general of such a geometry in 3+1 dimensions. The line-element for this metric can be written as

$$ds^2 = g_{\mu\nu}dx^\mu dx^\nu = -dt^2 + a^2(t) \left[\frac{dr^2}{1 - kr^2} + r^2(d\theta^2 + \sin^2\theta d\phi^2) \right] \quad (1.1)$$

where $a(t)$ is the scale factor describing the relative size of a spacelike hypersurface Σ_t at different times. The FRW geometry is characterized by the curvature of such spatial slices, where the parameter k is 0 for flat Euclidean space; 1 for positive curvature space and -1 for negative ones.

To study this class of spacetime it is useful to analyze the propagation of signals emitted by a source at a given time t_1 , and observed by us today at a time t_0 . Because of the expansion of space, this signals become stretched while they travel through the universe. We define the redshift of light between the time of departure t_1 and arrival t_0 as

$$1 + z = \frac{a(t_0)}{a(t_1)} \quad (1.2)$$

Then if $a(t)$ is increasing with time, the frequency is shifted towards the infrared(redshift today), by a factor $a(t_1)/a(t_0)$, and z is different from 0. Additionally, the expansion rate is characterized by the Hubble parameter $H = \dot{a}/a$, which is positive for an expanding universe and negative for contracting universes. It is convenient and usual to define $a(t_0) = 1$ and recognize $H(t_0) = H_0$ as the Hubble rate today or the Hubble constant. The comoving distance to an object at redshift z ,

$$\chi(z) = \int_0^z \frac{dz'}{H(z')} \quad (1.3)$$

allow us to define two important cosmological distance measures:

- **Angular diameter distance.** Is defined as the ratio of an objects physical transverse size to its angular size at emission time. This is given by

$$d_A(z) = \frac{1}{1+z} \chi(z) \quad (1.4)$$

- **Luminosity distance.** Measure the corrected distance, due to redshifting of the luminous distance emitted by an object as observed on Earth. It is given by

$$d_L(z) = (1+z)\chi(z) \quad (1.5)$$

The importance of these measures is that they give us the possibility to consider measurements of distances at large redshifts, say $z > 0, 1$ when the effects of cosmological expansion are considerable. Measurements at large redshift, tell us whether the universe is expanding or contracting and how fast.

1.1.1 Einstein equations

To describe the dynamics of the FRW spacetime defined previously, we should solve the Einstein's equations. As a first approximation, we assume that the interaction between different matter components is negligible. Therefore the universe can be modeled as filled with a perfect fluid of pressure p and density ρ . This type of matter is consistent with the symmetries of the spacetime considered previously, and is described by the following energy-momentum tensor:

$$T_{\nu}^{\mu} = \begin{pmatrix} \rho(t) & & & \\ & -p(t) & & \\ & & -p(t) & \\ & & & -p(t) \end{pmatrix} \quad (1.6)$$

Einstein equations $G_{\mu\nu} = 8\pi T_{\mu\nu}$ become

$$H^2 + \frac{k^2}{a^2} = \frac{1}{3M_{\text{pl}}^2}\rho, \quad \dot{H} + H^2 = -\frac{1}{6M_{\text{pl}}^2}(\rho + 3p). \quad (1.7)$$

On the other hand, conservation of energy-momentum tensor $T^{0\nu}_{;\nu}$, gives:

$$\dot{\rho} + 3H(\rho + p) = 0 \quad (1.8)$$

Solving this set of equations will allow us to study the evolution of the factor a as a function of the matter content that fills the universe. To proceed we will consider low-density fluids, such that they will satisfy a barotropic state equation. So the pressure as a function of the density is $p = w\rho$. Therefore Eq.(1.8) can be rewritten as

$$\frac{d \ln \rho}{d \ln a} = -3(1+w), \quad (1.9)$$

thus implying that $a \sim \rho^{-3(1+w)}$, which gives us the scale factor as a function of time:

$$a(t) = \begin{cases} t^{\frac{2}{3(1+w)}} & \text{for } w = -1 \\ e^{Ht} & \text{for } w = -1 \end{cases} \quad (1.10)$$

Therefore we notice that depending on the matter content that we consider, we get a different evolution of the scale factor $a(t)$ and thus the Hubble parameter $H(t)$. As the universe is filled with a mixture of different matter components, then it is useful to classify them by their contribution to the pressure. Let us examine four important cases:

- **Matter.** We will use the term matter, to refer to any form of matter for which the pressure is much smaller than energy density $|p| \ll \rho$. This is the case for a gas of non-relativistic particles, where the energy density is dominated by the mass term. This includes cold dark matter and baryons(nuclei and electrons). Setting $w = 0$, we get:

$$\rho \propto a^{-3} \quad (1.11)$$

This dilution of the energy density simply reflects the expansion of a volume $V \propto a^3$.

- **Radiation.** Radiation denotes anything for which the pressure is about a third of energy density, $p = \rho/3$. This is the case for a gas of relativistic particles, for which the energy is dominated by the kinetic energy. This includes photons, neutrinos, and gravitons.

$$\rho \propto a^{-4} \quad (1.12)$$

The dilution now includes an extra factor a^{-1} due to the redshifting of the photon energy $E \propto a^{-1}$.

- **Vacuum energy.** Or better know as *Dark Energy*. The Einstein's equations allow another source $T_{\mu\nu} \propto g_{\mu\nu}$, producing a negative pressure component characterized by an equation of state $p = -\rho$. This is unlike anything we have encountered in the lab but is hypothesized as the cause of the actual expansion of the universe. We find that the energy density is constant

$$\rho \propto a^0 \quad (1.13)$$

Since in this case, the energy density does not dilute, energy has to be created as the universe expands.

- **Curvature.** We can also include the effect of the curvature of spacetime as a type of fluid characterized by an energy density:

$$\rho \propto a^{-2}. \quad (1.14)$$

It will be useful to rewrite the different components of the stress-energy tensor in terms of the critical density for a flat Universe $\rho_c = 3M_{\text{pl}}^2 H^2$, which evaluated today becomes,

$$\rho_{c,0} = \frac{3H_0^2}{8\pi G} \quad (1.15)$$

The dimensionless densities evaluated today are:

$$\Omega_{i,0} = \frac{\rho_{i,0}}{\rho_{c,0}} \quad (1.16)$$

Then Friedmann eq. (1.7) becomes

$$H^2 = H_0^2 [\Omega_{r,0}a^{-4} + \Omega_{m,0}a^{-3} + \Omega_{k,0}a^{-2} + \Omega_\Lambda] \quad (1.17)$$

Where we have defined

$$\Omega_{k,0}(a) = -\frac{k}{a^2 H_0^2} \quad (1.18)$$

as a measure of the relative curvature contribution. In the literature is usual to drop the today index '0'. Moreover, observations suggest that $\Omega_k = 0$ so we will drop it hereafter.

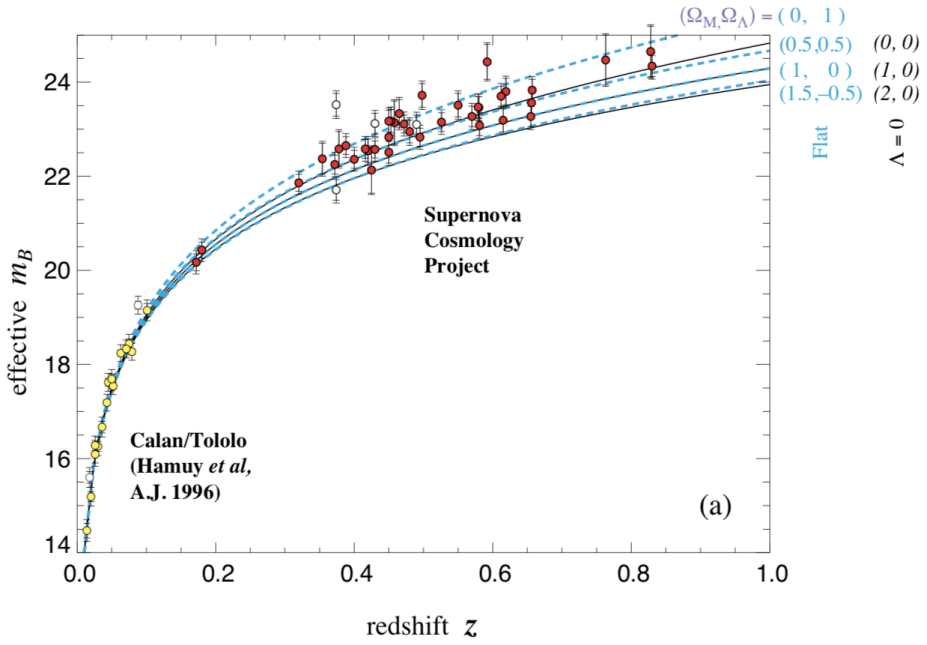


Figure 1.1: Supernova recession: Evidence for dark energy, found in 1998 by the Supernova Cosmology Project and Calan-Tololo Supernovae Survey.

1.1.2 Concordance model

The concordance or Λ CDM model is based on well-tested physical principles, including general relativity that describes the dynamics of an expanding universe, the quantum mechanical laws that govern the creation of species during early times, and the Boltzmann equation which allows us to track the evolution of each of these species. However, most of the parameter in the concordance model contains information about physics we still have no detailed understanding. The relative fractions of baryons, dark matter and dark energy in the universe are all governed by fundamental processes that still lie outside the current Standard Model of particle physics, and may extend up to the TeV, GUT or even Planck scales. The set of variables required by the concordance cosmology is not fixed but is dictated by the quality of the available data and our ignorance of fundamental physical parameters and interactions.

Table 1.1 details the six parameter used in the Λ CDM model and their current values according to Planck combined with supernovae data and LSS observations. From 1.1 can be deduced that the current model favors a flat universe dominated by a 68.25% of dark energy, 26.8% of dark matter and a 4.9% of ordinary or baryonic matter. This parametrization also includes data about the initial condition necessary to produce the CMB power spectrum. Assuming that the initial state of the universe was filled with small adiabatic curvature perturbations parametrized by a power spectrum of the form:

$$\mathcal{P}_R(k) \propto A_s k^{n_s - 1} \quad (1.19)$$

Table 1.1 indicates that Eq.1.19 forms a near scale invariant power spectrum.

Parameter	Planck $TT+lowP+lensing$
$\Omega_b h^2$	0.02226 ± 0.00023
$\Omega_c h^2$	0.1186 ± 0.0020
$100\theta_{MC}$	1.04103 ± 0.00046
τ	0.066 ± 0.016
n_s	0.9677 ± 0.0060
H_0	67.8 ± 0.9
Ω_m	0.308 ± 0.012
$\Omega_m h^2$	0.1415 ± 0.0019
$\Omega_m h^3$	0.09591 ± 0.00045
σ_8	0.815 ± 0.009
$\sigma_8 \Omega_m^{0.5}$	0.4521 ± 0.0088
Age/Gyr	13.799 ± 0.038
r_{drag}	147.60 ± 0.43
k_{eq}	0.01027 ± 0.00014

Table 1.1: Parameter 68% confidence levels for the base Λ CDM cosmology computed from the *Planck* CMB power spectra, in combination with the CMB lensing likelihood.

1.1.3 Thermal History

The concordance models describes how the universe is now dominated by dark energy, and it is composed of a determined number of species. Since dark energy remains constant in time, at early time, matter and radiation should have dominated. We examine now, briefly, the evolution of different types of matter, that produces the universe we see nowadays.

At the beginning, our universe was hot and dense, and spacetime was expanding. This means that early epochs are characterized by high energies, at which certainly broken symmetries in the laws of physics were restored, and by the fact that the expansion rate $H(t)$ plays an important role as a timescale. The interaction between particles freeze out or decouple when the interaction rate drops below the expansion rate. Table 1.2 summarizes the various phase transitions related to symmetry breaking events. We will give a quick summary of the most important events in the evolution of the Universe. This description will start at 100 GeV where we still have a detailed picture of the physics present.

Above 100 GeV the electroweak symmetry is restored and the Z and W_{\pm} bosons are massless. Interactions are strong enough to keep quarks and leptons in thermal equilibrium. Below 100 GeV the symmetry between the electromagnetic and the weak forces is broken, Z and W_{\pm} bosons acquire mass, and the cross-section of weak interactions decreases as the temperature of the universe drops. As a result, at 1 MeV, neutrinos decouple from the rest of the matter. Shortly after, at 1 second, the temperature drops below the electron rest mass and electrons and positrons annihilate efficiently. Only an initial matter-antimatter asymmetry of one part in a billion survives. The resulting photon-baryon fluid is in equilibrium. Around 2.2 MeV the strong interaction becomes important and protons and neutrons combine into the light elements (H, He, Li) during Big Bang nucleosynthesis (~ 200 s). The successful prediction of the light elements (H, He and Li) abundances is one of the most striking consequences of

the Big Bang theory. The matter and radiation densities are equal at around 1 eV (10^{11} s). Charged matter particles and photons are strongly coupled in the plasma and fluctuations in the density propagate as cosmic sound waves. Around 0.1 eV (380,000 yrs) protons and electrons combine into neutral hydrogen atoms. This epoch, at which the first atoms start to form (H) is referred to as recombination, despite the fact that electrons had never before combined into atoms. At a temperature greater than about 3000K the Universe consisted of

Event	time t	redshift z	temperature T
Electroweak phase transition	10^{-10} s	10^{15}	100 GeV
QCD phase transition	10^{-9} s	10^{12}	150 MeV
Neutrino decoupling	1 s	$6 \cdot 10^9$	1 MeV
$e^- - e^+$ annihilation	6 s	$2 \cdot 10^9$	500 KeV
Big bang nucleosynthesis	180 s	$4 \cdot 10^8$	0.75 eV
Matter-radiation equality	60 kyr	3200	0.75 eV
CMB decoupling	380 kyr	1100	0.23eV
Reionization	100 Myr	11	2.6meV
Dark energy-matter equality	9Gyr s	0.4	0.33meV
Present	13.7 Gyr	0	0.24meV

Table 1.2: Termal history of the universe.

an ionized plasma of mostly protons, electrons and photons, with a few helium nuclei and a tiny trace of lithium. The important characteristic of this plasma is that it was opaque, or more precisely, the mean free path of a photon was smaller than the Hubble length. As the universe cooled and expanded, the plasma recombines into neutral atoms, first the helium, then a little later the hydrogen.

After recombination, and once the gas is in a neutral state, the mean free path for a photon becomes much larger than the Hubble length. The universe is then full of a background of freely propagating photons with a black body distribution of frequencies. At the time of recombination. the background radiation has a temperature of $T = 3000\text{K}$, and as the universe expands photons redshifted, so that the temperature of photons drops with the increase of the scale factor $T \propto a^{-1}$. We can detect these photons today. Looking at the sky, this background of photons come to us evenly from all directions, with an observed average temperature of $T_0 = 2.73\text{K}$. This is the cosmic microwave background. Since by looking at higher and higher redshift objects, we are looking further and further back in time, we can view the observation of CMB photons as imaging a uniform surface of the last scattering at redshift 1100.

To the extent that recombination happens at the same time and in the same way everywhere, the CMB will be of precisely uniform temperature. While the observed CMB is highly isotropic, it is not perfectly isotropic. The first anisotropy discovered was the dipole which was first measured in the 1970's by several groups. It was until more than a decade after, that the first observation for the anisotropy was made $l > 2$, by COBE satellite:

The natural basis to describe these anisotropies are the spherical harmonics $Y_{lm}(\theta, \phi)$. The motion of earth with respect to the CMB comoving frame induces a Doppler shift in temperature, this intrinsic dipole effect can be average out, additionally, any locally uniform

perturbation will contribute to the effective background, making indistinguishable to notice it. Technically, we typically say that $l = 0, 1$ (monopole and dipole) contribution are gauge dependent in a part in $\sim 10^5$, so it does not make any sense have an extremely precise measurement for them. Nevertheless, the multipoles $l \geq 2$ are genuinely gauge invariant and well defined:

$$\frac{\Delta T}{T_0} = \sum_{l=0}^{\infty} \sum_{m=-l}^{m=l} a_{lm} Y_{lm}(\theta, \phi). \quad (1.20)$$

If we assume statistical isotropy, then there is no preferred direction in the universe, and we expect that the statistical properties of $\Delta T/T_0$ to be independent of the index m . In consequence, we can define the power spectrum estimator

$$C_l = \frac{1}{(2l+1)} \sum_m |a_{lm}|^2 \quad (1.21)$$

which is better known as the rotationally invariant temperature angular power spectrum. Which technically is the variance of the probability distribution for a_{lm} 's. This quantity simplifies the information contained in a CMB map pixel and thus is used to analyze the CMB power spectrum.

$$\frac{\Delta T}{T} \approx 10^{-5}, \quad (1.22)$$

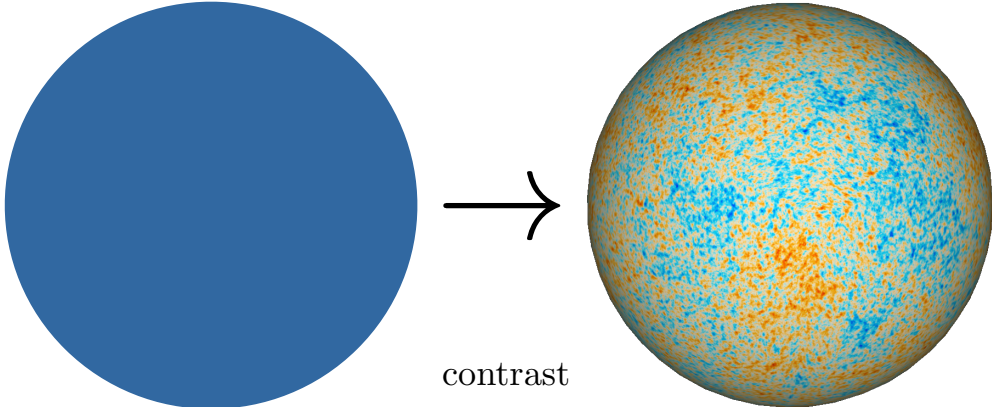


Figure 1.2: Homogeneity and contrast of the CMB: Pictorially if we take a CMB picture and then we tune its contrast we would notice the anisotropies structure, corresponding to a different temperature at a different point on the sky.

The anisotropies represent the tiny primordial density fluctuations in the cosmological matter present at the time of recombination. These small density perturbations, grow via gravitational instability to form the large-scale structures observed in the late universe. A competition between the background pressure and gravity determines the details of the growth of structure. During radiation domination the growth of the overdensities is slow $\delta\rho \propto \ln a$. Clustering becomes more efficiently after matter dominates the background density, $\delta\rho \propto a$. Small scales become non-linear when $\delta\rho \sim 1$, and form gravitationally bound objects that decouple from the overall expansion that leads to a picture of hierarchical structure formation with small-scale structures (like stars and galaxies) forming and then merging

in larger structures (clusters and superclusters of galaxies). Around redshift $z \approx 25$, high energy photons from the first stars begin to ionize the hydrogen in the intergalactic medium. This process of reionization is completed at $z \approx 6$. Meanwhile, the most massive stars run out of nuclear fuel and explode as supernovae. In these explosions the heavy elements (C, O, etc.) necessary for the formation of life. At $z \approx 1$ negative pressure dark energy start to dominate the universe expansion and the growth of structure ceases $\delta\rho \approx \text{constant}$.

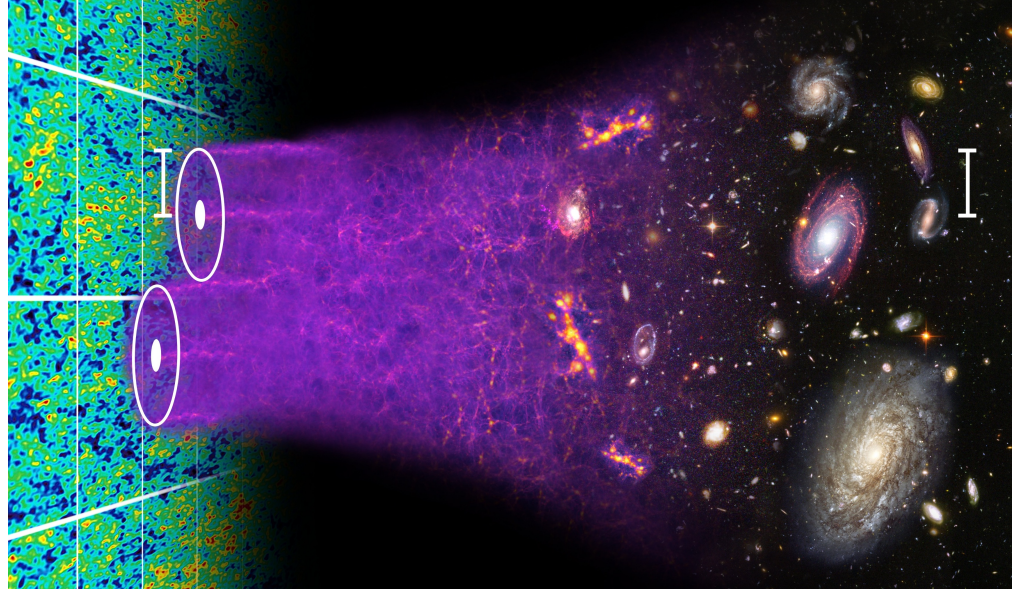


Figure 1.3: Universe evolution. Credit:<http://www.damtp.cam.ac.uk/user/db275/concepts/Lecture7.pdf>.

Nowadays, there are many groups such as CLASS, Simons Observatory, BICEP, Polar Bear among others, expanding the frontier by trying to detect the elusive B-modes and constraint the reionization depth, which is a challenging task due to the experimental effort. Mainly, the B-modes are entirely a quantum gravity phenomena, so fundamentally is important; additionally, it may give us the energy scale of inflation. We are not able to reach a signal fainter than $r \sim 0.001$, if inflation is a quantum phenomena we know that they must be there since it must excite light degree of freedom, but we do not know how energetic inflation was, these pure signal independently from the inflationary model will tell us something about its energy. For which a central claim is that quantum fluctuations explain the properties of primordial fluctuations presently found written large across the sky. If true, this claim would imply not only that quantum-gravity effects are observable; but that their imprint has already been observed cosmologically. Such claims sharpen the need to clarify what parameters control the size of quantum effects in gravity, and along the way more generally to identify the domain of validity of semi-classical methods in cosmology.

As we know so far, Inflation gave us the seeds for primordial structure formation; produces adiabatic modes that are conserved frozen until the hot big-bang epoch; it produces modes coherent phases that tell us that some event happened everywhere at the same time; and is characterized by a nearly scale-invariant power spectrum that tell us about a nearly de Sitter expansion. However, Inflation from the fundamental perspective is not well understood.

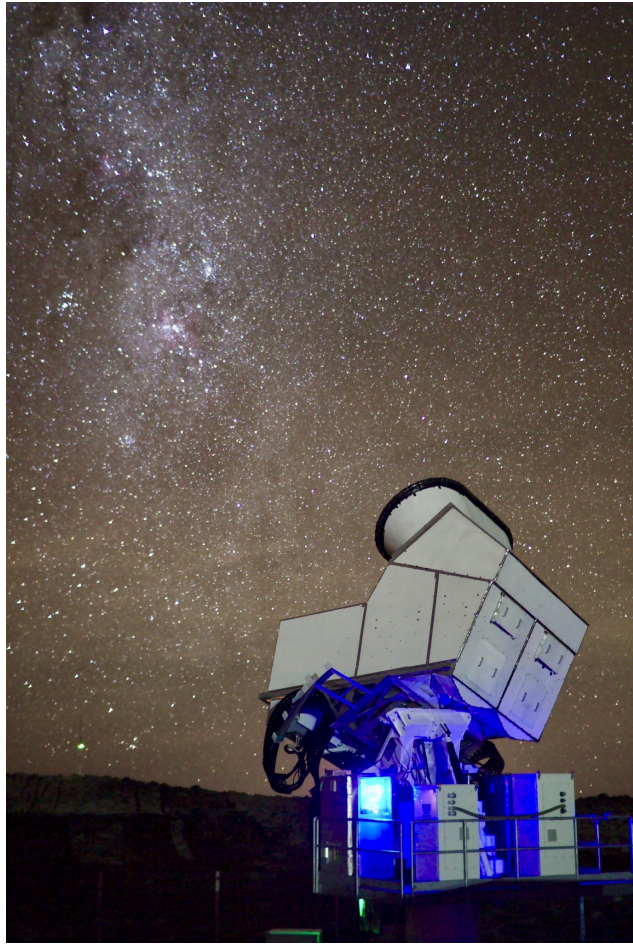


Figure 1.4: Cosmology Large Angular Scale Surveyor Aka. CLASS telescope located in cerro Toco, San Pedro de Atacama, Chile.

Nobody knows what happened precisely there, but we know that something happened at the same time everywhere. Theories embedded in string theories and supergravities as UV completions but the testability maintains us skeptic from it. The most significant advances in the understanding of inflation have been in the frame of Effective Field Theory(EFT), its success is based on the fact that it allows separating the physics valid at different energy scales. Therefore one can isolate the essential degrees of freedom valid up to a specific range of energy, while the remaining is encoded in operators of the low energy theory. This EFT allows unifying most of the single field models of inflation in just a few parameters.

The theory of cosmological perturbations assumes an external observer with unlimited access to all places and at all times with complete knowledge of the entire ensemble of modes of different fields and their properties; under this treatment, this type of observers are outside the experiment or "outside the box"(our universe). Nevertheless, that is not our case. Instead, we are observers confined in a 4-dimensional spacetime influenced and subordinated by its dynamics. Under this perspective, we are observers inside of the experiment, which at the same time is merely one realization of other similar alternatives, with limited access to the entire ensemble of fields modes.

Due to this fact, we can not have full access to the entire universe restricting our knowledge

and information available to just a causally connected small region of space from which we sample the local statistical distribution. The way in which we formally deal with the influence of spacetime dynamics on us is by using the Conformal Fermi Coordinates(CFC). First introduced [2], in the context of an observer trajectory near strong gravitational fields(Fermi coordinates), but ultimately incorporated and revived in a cosmological context [1] [3] adapted to a conformal scenario to study the primordial curvature power spectrum and bispectrum of our universe. Its construction follows from the *flatness theorem* and at the same time is a consequence of the *equivalence principle* on our Hubble local patch. These coordinates allow us to connect the global theory of fluctuations with observations whose precision scales as k_S^2/k_L^2 , where k_S is the observed fluctuation on a determined scale and k_L correspond to long modes that are scales longer than the scales of interest. The main prediction of this coordinates is the vanishing of the local measured squeezed limit of the bispectrum[3].

Additionally, current CMB observations show the existence anomalies such as the dipolar, quadrupole and octupole asymmetry, and a bumpy features at $l \sim 23$. During this work, we will focus on latter. First, we will use the time-dependent background of the de Sitter universe, commonly encoded in the slow roll parameters, to create a self-interaction term for the curvature perturbations[4]. In the chapter 4 of this thesis, we analyze the effect of such background quantities in the power spectrum of the tensor modes and establish a possible relation between both power spectra.

The outline of this thesis is the following: In chapter 1, We sketch the salient features of the standard cosmological model Λ CDM. In chapter 2, We introduce the standard paradigm of *Inflation*, we review its main features , non gaussianities to pave our the road in the subsequent sections. In chapter 3, We introduce the main features of CMB by dissecting it in different pieces. to understand qualitatively the main features. For temperature and polarization signal. In chapter 4, We analyze the implications of the time-dependent background quantities that parametrize inflation for the scale invariance of the tensor power spectrum. In chapter 5, We derive new relations for the the local Non-gaussianity for Slow and Ultraslow roll scenarios. In chapter 6, First introduce the notion of the Fermi coordinates, and then analyze their implications for the observed power spectrum and bispectrum. In chapter 7, We characterize the beams and the window functions for the 40GHz band of the Cosmology Large Angular Scale Surveyor(CLASS).

Finally, we will follow the natural units convention $c = \hbar = 1$. The reduced Planck mass: $M_{\text{pl}}^2 = 32G_N$. The Einstein summation over repeated indices. The Greek indices ranges from 0 to 3 and latin indices from 1 to 3. The boldface variable denotes spatial coordinates. e.g. \mathbf{x} .

Chapter 2

Inflation

The cosmic Inflation or simply Inflation is an early phase of exponentially expanding the universe, it explains the flatness, the near homogeneity and isotropy, and provides the origin of the large-scale structure of the cosmos as quantum fluctuations of a microscopic region that were amplified to cosmic scale as the universe expanded around 60 e-folds [5] [6].

Nowadays, Inflation is a piece of the current six cosmological parameter model, the Λ CDM model, providing two essential parameters that characterize the near scale-invariant primordial scalar power spectrum of the overdensities that seeded our universe: its amplitude A_s and slope, n_s [7]. The latter is a parameter that tells us about a quasi de Sitter expansion.

The predictive power of inflation relies on the adiabaticity of quantum fluctuations during this period: If they are adiabatic then are conserved or frozen when they exit the Hubble horizon until then re-enter after reheating [8]. The mesmerizing fact of the CMB fluctuations is that they are both adiabatic and coherent. These facts imply that observations can be connected with the fluctuations generated during inflation; additionally, they tell us that some event happened at the same time everywhere[9], respectively.

First, we will discuss about some cosmic problems solves that inflation solves, characterize the background and then we consider the quantum theory of fluctuations produced during inflation and its statistic.

This chapter is partially based on [10]

2.1 Causal structure

We now move to study the causal structure of flat FRW spacetimes. To do so we begin by changing from proper time t to conformal time τ using the following relation

$$d\tau = \frac{dt}{a(t)}. \quad (2.1)$$

We see that the FRW metric then factorizes into a Minkowski metric $\eta_{\mu\nu}$ multiplied by the scale factor $a(\tau)$

$$ds^2 = a^2(\tau) \eta_{\mu\nu} dx^\mu dx^\nu \quad (2.2)$$

therefore the radial propagation of particles is characterized by the following line element

$$ds^2 = a^2(\tau) [-d\tau^2 + dr^2] \quad (2.3)$$

In particular null geodesics followed by photons are represented by just straight lines at $\pm 45^\circ$ angles in the $\tau - r$ plane.

$$r(\tau) = \pm\tau + c \quad (2.4)$$

the maximal distance of a photon can travel between an initial time t_i and later time $t > t_i$ is given by:

$$\Delta r = \tau - \tau_i = \int_{t_i}^t \frac{dt'}{a(t')} \quad (2.5)$$

Thus the maximal distance traveled is equal to the amount of conformal time elapsed during the interval $t - t_i$. The initial time is often taken to be the origin of the universe $t_i = 0$, defined by the initial singularity $a_i = a(t_i) = 0$. We obtain

$$\Delta r_{\max}(t) = \int_0^t \frac{dt'}{a(t')} = \tau(t) - \tau(0), \quad (2.6)$$

which is the comoving particle horizon. If we rewrite the conformal time as

$$\tau = \int \frac{dt}{a(t)} = \int \frac{d \ln a}{a H} \quad (2.7)$$

from the above equation, we deduce that the elapsed conformal time depends on the evolution of the comoving Hubble radius $(aH)^{-1}$. For example, for a universe dominated by a barotropic state equation $w = p/\rho$, we find that this evolves as

$$(aH)^{-1} \approx a^{\frac{1}{2}(1+3w)} \quad (2.8)$$

Note the dependence of the exponent on the combination $1 + 3w$. All the familiar sources satisfy the strong energy condition (SEC), $1 + 3w > 0$, so it was reasonable, prior to the knowledge of the acceleration of the universe, to assume that the comoving Hubble radius increases as the universe expands. Performing the integral Eq.(2.7) gives

$$\tau \approx \frac{2}{(1+3w)} a^{\frac{1}{2}(1+3w)} \quad (2.9)$$

For conventional matter sources the initial singularity is at $\tau_i = 0$.

$$\tau_i \approx a_i^{\frac{1}{2}(1+3w)}, \quad \text{for } w > -1/3 \quad (2.10)$$

and the comoving horizon is finite

$$\Delta r_{\max}(t) \approx a^{\frac{1}{2}(1+3w)}, \quad \text{for } w > -1/3 \quad (2.11)$$

2.1.1 Flatness problem

Let us recall that the evolution of curvature in FRW spacetime, is described by the following density parameter:

$$\Omega_k(a) = -\frac{k}{a^2 H^2} \quad (2.12)$$

Then if we assume, for simplicity, that the expansion is dominated by some form of matter with an equation of state equal to w , we have $a \sim t^{\frac{2}{3(1+w)}}$ and we have the following expressions are satisfied:

$$\dot{\Omega}_k = \Omega_k H(1 + 3w) \rightarrow \frac{d\Omega_k}{dN} = \Omega_k(1 + 3w). \quad (2.13)$$

If we further assume that $w > 1/3$, then the solution $\Omega_k = 0$ is an unstable point. Thus if $\Omega_k > 0$ at some point, Ω_k will keep growing. And viceversa, if $\Omega_k < 0$ at some point, it will keep decreasing. Of course at most $|\Omega_k| = 1$ in which case w becomes $1/3$ if $k < 0$, or otherwise the universe collapses if $k > 0$.

The surprising fact is that Ω_k is now observed to be smaller than about 10^{-2} . Taking into account the content of matter of the universe, this means that at earlier times it was even closer to zero. For example, at BBN epoch, it has to be $|\Omega_k| < 10^{-18}$, at the Planck scale $|\Omega_k| < 10^{-63}$. In others words, since curvature depends on redshift as a^{-2} , it tends to dominate in the future with respect to other forms of matter. So, if today curvature is not already dominating, it means that it was almost negligible in the past. The value of Ω_k at those early times represents a remarkably small number.

A possible solution could be that $k = 0$ in the initial state of the universe. While this possibility could be true, it is unknown why the universe should choose such a precise state initially. A second possibility would be that in some epoch the universe would have been dominated by some matter content with $w < 1/3$.

2.1.2 Horizon Problem

Let us digress briefly to make a simple calculation. Given that the universe seems very homogeneous at large distances, it is valid to ask ourselves, if we can trace back this to the beginning of the universe. To do this let us compute the angle subtended by the comoving horizon at recombination. This is defined as the ratio of the comoving particle horizon at recombination and the comoving angular diameter distance from us (an observer at redshift $z = 0$) to recombination ($z \approx 1100$).

$$\theta_{\text{hor}} = \frac{d_{\text{hor}}}{d_A} \quad (2.14)$$

A fundamental quantity is the comoving distance between redshifts z_1 and z_2

$$\tau_2 - \tau_1 = \int_{z_1}^{z_2} \frac{dz}{H(z)} = \mathcal{I}(z_1, z_2). \quad (2.15)$$

The comoving particle horizon at recombination is

$$d_{\text{hor}} = \tau_{\text{rec}} - \tau_i \approx \mathcal{I}(z_{\text{rec}}, \infty) \quad (2.16)$$

the angular scale of the horizon at recombination therefore is

$$\theta_{\text{hor}} = \frac{d_{\text{hor}}}{d_A} = \frac{\mathcal{I}(z_{\text{rec}}, \infty)}{\mathcal{I}(0, z_{\text{rec}})} \quad (2.17)$$

Using $H(z)$ from Eq.(1.17)

$$H(z) = H_0 \sqrt{\Omega_m(1+z)^3 + \Omega_\gamma(1+z)^4 + \Omega_\Lambda} \quad (2.18)$$

it can be deduced that

$$\theta_{\text{hor}} = 1.16^\circ \quad (2.19)$$

Therefore in a matter or radiation dominated universe no physical influence could have smoothed out the initial inhomogeneities that are separated by more than $\theta > \theta_c = 2\theta_{\text{hor}} = 2.3^\circ$ to the same temperature, in contradiction with the nearly perfect isotropy of the microwave background at large angular scales observed ever since the background radiation was discovered. This striking fact tells us that even at the time of the last scattering, the largest scales were still outside the horizon. This is called the *Horizon Problem*.

2.2 Background

As we have seen Equation (2.7) implies that the comoving horizon is the logarithmic integral of the comoving Hubble radius $(aH)^{-1}$. The Hubble radius, as we mentioned previously, is the distance over which particles can travel in the course of one expansion time, i.e., it is roughly the time in which the scale factor doubles. So the Hubble radius is another way of measuring whether particles are causally connected with each other: If they are separated by distances larger than the Hubble radius then they cannot currently communicate.

There is a subtle distinction between the comoving horizon τ and the comoving Hubble radius $(aH)^{-1}$. If particles are separated by distances greater than τ , they never could have communicated with one another; if they are separated by distances greater than $(aH)^{-1}$ they cannot talk to each other now. It is, therefore, possible that τ could have been much larger than $(aH)^{-1}$ now so that particles cannot communicate today but were in causal contact early on. This might happen if the comoving Hubble radius early on was much larger than it is now so that the comoving horizon got most of its contribution from early times. This could happen but is not possible during matter or radiation dominated epochs, because in those cases, the comoving Hubble radius increases with time, so typically we expect the largest contribution to τ to come from most ancient times.

All this suggests a solution to the horizon problem. If there exists a brief time, where the universe was not dominated by radiation or matter, and moreover the Hubble radius decreased. Then the comoving horizon τ would get most of its contributions not from recent times but rather from primordial epochs. Particles separated by many Hubble radius today

would have been in causal contact before the epoch of rapid expansion and this could be explained the smoothness of the CMB observed today. This epoch of dramatically decreasing Hubble radius is called Inflation. As noted earlier, a decreasing Hubble radius requires a violation of the SEC, $1 + 3w < 0$. Therefore we notice that the Big Bang singularity is now pushed to negative conformal time,

$$\tau_i \propto \frac{2}{1+3w} a_i^{\frac{1}{2}(1+3w)} = -\infty, \text{ for } w < -\frac{1}{3} \quad (2.20)$$

This implies that there was much more conformal time between the singularity and decoupling than we had thought. The past light cone of widely separated points in the CMB now had time to intersect before the time $\tau = 0$ which is not the initial singularity, but instead becomes, what it is called, the time of reheating. There is time both before and after $\tau = 0$. A decreasing comoving horizon means that large scales entering the present universe were inside the horizon before inflation ending. Therefore, causal physics before inflation ending had time to establish spatial homogeneity. With a period of inflation, the uniformity of the CMB is not a mystery anymore. To continue with the discussion, let us notice that a shrinking Hubble radius $(aH)^{-1}$ corresponds to

$$\frac{d}{dt}(aH)^{-1} = \frac{d}{dt}\dot{a}^{-1} = -\frac{\ddot{a}}{\dot{a}^2} \quad (2.21)$$

Thus,

$$\frac{d^2a}{dt^2} > 0; \quad (2.22)$$

which in turns implies that a shrinking comoving horizon produces an accelerated expansion. Also, inflation implies some constraint on the evolution of the Einstein equations. If we write,

$$\frac{d}{dt}(aH)^{-1} = -\frac{\dot{a}H + a\dot{H}}{(aH)^2} = -\frac{1}{a}(1 - \varepsilon), \text{ where } \varepsilon = -\frac{\dot{H}}{H^2} > 0 \quad (2.23)$$

The shrinking Hubble sphere therefore also correspond to

$$\varepsilon = -\frac{\dot{H}}{H^2} = -\frac{d \ln H}{dN} < 1 \quad (2.24)$$

Here we have defined $dN = d \ln a = H dt$, which measures the number of e-folds N of inflationary expansion. Eq.(2.24) implies that the fractional change of the Hubble parameter per *e*-fold is small. Moreover, to solve the horizon problem, we want inflation to last for a sufficiently long time. To achieve this requires (2.24) to remain small for a sufficiently large number of Hubble times. This condition is measured by a second parameter,

$$\eta = \frac{\dot{\varepsilon}}{H\varepsilon} = \frac{d \ln \varepsilon}{dN} \quad (2.25)$$

Then, for $|\eta| \ll 1$ the fractional change of ε per Hubble time is small and inflation persists. we should also ask ourselves what form of stress-energy source permits accelerated expansion. Assuming a perfect fluid with p and density ρ , the Friedmann equations become:

$$\dot{H} + H^2 = -\frac{1}{6M_{\text{pl}}}(\rho + 3p) = -\frac{H^2}{2}(1 + 3\rho). \quad (2.26)$$

Then

$$\varepsilon = -\frac{\dot{H}}{H^2} = \frac{3}{2} \left(1 + \frac{p}{\rho} \right) < 1 \rightarrow w = \frac{p}{\rho} < -\frac{1}{3} \quad (2.27)$$

The question we would like to answer now is how we can implement inflation on a field theoretical context. To do this we have a large number of options. This is a big problem in inflation; up to date, it has been impossible to find a unique model that match all the predictions of inflation, but instead an enormous variety of models have appeared since inflation was first presented in the eighties. But to introduce inflation, we give a brief description of the simplest models.

2.2.1 Single field slow-roll inflation

The simplest discussion we can give to push forward our intuition is to consider inflation as embedded in a field theoretical context. We start by considering a scalar field ϕ , called inflaton with potential $V(\phi)$ whose dynamics is given by the Lagrangian (we now set $M_{\text{pl}}^2 = 1$)

$$\mathcal{L}(\phi) = -\frac{1}{2}g^{\mu\nu}\partial_\mu\phi\partial_\nu\phi - V(\phi) \quad (2.28)$$

The idea of inflation is to fill a small region of the initial universe with a homogeneously distributed scalar field sitting on top of its potential $V(\phi)$. The equations of motion described by the action of (2.28), using a FRW background, are

$$\ddot{\phi} + 3H\dot{\phi} + V'(\phi) = 0 \quad (2.29)$$

and

$$H^2 = \frac{1}{3} \left(\frac{1}{2}\dot{\phi}^2 + V(\phi) \right) \quad (2.30)$$

Using these equations we derive the continuity equation, which is found to be given by

$$\dot{H} = -\frac{1}{2}\dot{\phi}^2 \quad (2.31)$$

In addition, the stress-energy tensor is given by

$$T_{\mu\nu} = -\frac{2}{\sqrt{-g}}\frac{\delta S_\phi}{\delta g^{\mu\nu}} = \partial_\mu\partial_\nu\phi - g_{\mu\nu} \left(\frac{1}{2}\partial_\rho\partial^\rho\phi + V(\phi) \right). \quad (2.32)$$

This result leads to the following expressions for the energy-density and pressure

$$\rho_\phi = \frac{1}{2}\dot{\phi}^2 + V(\phi), \quad p_\phi = \frac{1}{2}\dot{\phi}^2 - V(\phi) \quad (2.33)$$

Therefore the equation of state is

$$w_\phi = \frac{p_\phi}{\rho_\phi} = \frac{\frac{1}{2}\dot{\phi}^2 - V(\phi)}{\frac{1}{2}\dot{\phi}^2 + V(\phi)} \quad (2.34)$$

So the condition for inflation is equivalent to have an Eq. of state with $w_\phi \approx -1 < \frac{1}{3}$. Thus the potential energy V , should dominate over the kinetic energy $\dot{\phi}^2$. This may be expressed using the *slow-roll* parameter ε . Then

$$\varepsilon = -\frac{\dot{H}}{H^2} = \frac{1}{2} \frac{\dot{\phi}^2}{H^2} \ll 1. \quad (2.35)$$

Also, notice that Eq.(2.29) is the same as the one of a particle rolling down a potential. This particle is subject to friction through the term $H\dot{\phi}$. Like for particle trajectory, this means that the solution where $\dot{\phi} \approx V_\phi/3H$ is a slow-roll attractor solution if the friction is large enough. This can be written in terms of the slow roll parameter η as

$$\eta = -\frac{\ddot{\phi}}{H\dot{\phi}} \ll 1. \quad (2.36)$$

Then we have found that the two slow-roll parameters have to be much smaller than 1. The first parameter ε meaning that we are on a background solution where the Hubble parameter means that we are on an attractor solution, and also that this phase of accelerated expansion ($w \approx -1, a \propto e^{Ht}$) will last for a long time. For this condition to persists the acceleration of scalar field has to be small to achieve this, it is useful to define dimensionless acceleration per Hubble time. We now use the above conditions, $\varepsilon \sim |\eta| \ll 1$ to simplify the equations of motion. This is the so-called "slow-roll approximation". First, we notice that the parameters can be written in terms of the potential as,

$$\varepsilon \approx \frac{M_{pl}^2}{2} \left(\frac{V'}{V} \right)^2 \quad (2.37)$$

$$\eta \approx M_{pl}^2 \left(\frac{V''}{V} \right)^2 - \frac{M_{pl}^2}{2} \left(\frac{V'}{V} \right)^2 \quad (2.38)$$

These conditions lead to the following simplification of the inflation equations, which now reduce to:

$$\dot{\phi} = \frac{V'}{3H}, \quad H^2 = \frac{V}{3M_{pl}^2}, \quad a \propto e^{Ht}, \quad (2.39)$$

Let us notice that inflation will end when w ceases to be ≈ -1 , which in terms of slow roll parameters is,

$$\varepsilon \sim \eta \sim 1 \quad (2.40)$$

In terms of the potential, this means that the field that starts on top of his potential will slowly roll down while the Hubble parameter H will decrease, providing less friction. Hence, it will be a point when the potential will become too steep to guarantee that the kinetic energy is negligible with respect to the potential energy. We will call the point in field space where this occurs ϕ_{end} . At that point (immediately after inflation occurs), a period dominated by a form of energy $w > 1/3$ is expected to begin. This period is called reheating.

The amount of inflation required to solve the cosmological problems is most easily measured using the number of e-foldings. These are defined as the logarithm of the ratio of the scale factor at the end and at the beginning of inflation. We then have

$$N(\phi) = \ln \left(\frac{a_{end}}{a_i} \right) = \int_{a_i}^{a_f} d \ln a = \int_{t_i}^{t_f} H dt = \int_{\phi}^{\phi_{end}} \frac{H}{\dot{\phi}} \approx \int_{\phi_{end}}^{\phi} \frac{V}{V'} d\phi \quad (2.41)$$

where we have used that $a \propto e^{Ht}$ and the slow roll approximations. The largest scales observed in the CMB are produced some 40 to 60 e-folds before the end of inflation, thus

$$N_{\text{CMB}} \sim \int_{\phi_{\text{end}}}^{\phi} d\phi \frac{V}{V'} \sim 40 - 60 \quad (2.42)$$

2.2.2 Slow And Ultra Slow Roll Inflation

Another interesting regime of inflation can be the ultra slow roll phase which is characterized by the flatness of its potential and can correspond to the previous phase of the slow-roll regime, more precisely a starting USR period followed by SR phase with a smooth phase transition. Such scenarios can arise in UV completions theories from higher-dimensional supergravities[11]. In this case, the expected form for the scalar potential during the inflationary regime could be

$$V(\phi) = V_0 - V_1 e^{-\phi/\phi_0} + \dots \quad (2.43)$$

for some scales V_0 , V_1 and ϕ_0 . The USR phase takes place when $\phi \gg \phi_0$, so the first potential term, V_0 , dominates, and so is chosen as needed for inflationary cosmology, with $H^2 = V_0/(3M_{\text{pl}}^2)$. In this regime, the scalar field dynamics reduces to:

$$\ddot{\phi} + 3H\dot{\phi} = 0 \quad (2.44)$$

Additionally, with this choice the relevant potential derivatives are $V' = (V_1/\phi_0)e^{-\phi/\phi_0}$ and $V'' = -(V_1/\phi_0^2)e^{\phi/\phi_0}$ leading to slow-roll parameters of the form:

$$\varepsilon = \frac{1}{2} \left(\frac{M_{\text{pl}} V_1}{\phi_0 V_0} \right)^2 e^{-2\phi/\phi_0}, \quad \eta = - \left(\frac{M_{\text{pl}}^2 V_1}{\phi_0^2 V_0} \right) e^{-\phi/\phi_0}, \quad (2.45)$$

thus,

$$\varepsilon = \frac{1}{2} \left(\frac{\phi_0}{M_{\text{pl}}} \right)^2 \eta^2 \quad (2.46)$$

which can easily be large so long as $\phi \gg \phi_0$ and ϕ_{end}/ϕ_0 is order unity. Notice that ε and η are generically small whenever $\phi \gg \phi_0$, even if $V_1 \sim V_0$, so there is no need to require ϕ_0 be larger than M_{pl} to ensure a slow roll. Typical examples of underlying UV theories give $\phi_0 \sim M_{\text{pl}}$, in which case $\varepsilon \propto \eta^2$. It turns out that this prediction provides better agreement with experiment that $\varepsilon \simeq \eta$ does, and the generic expectation $\varepsilon \propto \eta^2$ has potentially interesting observational consequences for measurements of primordial gravitational waves because it relates the as yet unmeasured tensor-to-scalar ratio $r < 0.07$, to the observed spectral tilt, $n_s = 0.96$, giving the prediction $r \simeq (n_s - 1)^2 \simeq 0.002$.

2.3 Quantum initial conditions

As we have seen the Inflaton field ϕ governs the primordial universe dynamics through a dominant scalar contribution to the stress-energy tensor $T_{\mu\nu}$, in particular, its energy density

ρ and pressure p . From the Friedmann equations this energy density controls how the universe evolves, particularly the inflationary mechanism and its duration, more importantly, implicitly determines a universal clock: more energy density means a smaller universe, hotter and younger, on the other hand, less energy density means a bigger universe cooler and older. Thus, it defines indirectly a universal clock whose flow its t ; but something remarkable happens when we consider quantum mechanics and general relativity at the same footing. In order to satisfy the Heisenberg's uncertainty principle from quantum mechanics, a precise time from precise clock is impossible to have, therefore this quantum mechanical clock, necessarily must locally fluctuate $\delta t(t, x) \sim \delta\phi/\dot{\phi} \sim H/\dot{\phi}$, this mechanism produces an intrinsic variation in the energy density field $\delta\rho$ in the primordial universe, that are amplified due to the universe expansion, providing the seeds for the formation of structures that we see today, such as the Cosmic Microwave Background (CMB), Large Scale Structures(LSS) and smaller objects therein.

2.3.1 Free Scalar spectator Field In dS_4

Let start with a free spectator scalar field in de Sitter space with mass m that carries an insignificant amount of energy and therefore the background does not react in presence of this field. The action for this theory is given by:

$$S = \frac{1}{2} \int d^4x \sqrt{-g} [-g^{\mu\nu} \partial_\mu \phi \partial_\nu \phi - m^2 \phi^2] \quad (2.47)$$

or in conformal time $a(\tau) = -1/H\tau$:

$$S = \frac{1}{2} \int d\tau d^3x a^2 [\phi'^2 - (\partial_i \phi)^2 - m^2 a^2 \phi^2] \quad (2.48)$$

It is useful define an auxiliary field: $v = a\phi$, so the action becomes,

$$S = \frac{1}{2} \int d\tau d^3x \left(v'^2 - \partial_i v^2 + \left(\frac{a''}{a} - m^2 a^2 \right) v^2 \right) \quad (2.49)$$

The Fourier representation for this theory is

$$S = \frac{1}{2} \int d\tau \frac{d^3k}{(2\pi)^3} [v_{\mathbf{k}}'^2 - \omega_k^2(\tau) v_{\mathbf{k}}^2] \quad (2.50)$$

One can see that this action is nothing but just a continuous sum of a set of decoupled harmonic oscillators with time-varying effective mass and angular frequencies defined by whose dispersion relation is:

$$\omega^2(\tau) = k^2 + m_{\text{eff}}^2(\tau) = k^2 + \left(\frac{m^2}{H^2} - 2 \right) \tau^{-2} \quad (2.51)$$

where the field Fourier mode,

$$v_{\mathbf{k}}(\tau) = \int d^3x v(\tau, \mathbf{x}) e^{i\mathbf{k}\mathbf{x}} \quad (2.52)$$

Varying the action it produces in the so-called *Mukhanov-Sasaki equation*:

$$v''_{\mathbf{k}} + \left(k^2 + \frac{m^2/H^2 - 2}{\tau^2} \right) v_{\mathbf{k}} = 0 \quad (2.53)$$

in de Sitter space this mode equation becomes

$$\tau^2 v''_k + \left(k^2 \tau^2 - \nu^2 + \frac{1}{4} \right) v_k = 0, \text{ with } \nu^2 = \frac{9}{4} - \frac{m^2}{H^2} \quad (2.54)$$

whose general solution:

$$v_k(\tau) = \sqrt{-k\tau} \left[c_k^{(1)} \mathcal{H}_{\nu}^{(1)}(-k\tau) + c_k^{(2)} \mathcal{H}_{\nu}^{(2)}(-k\tau) \right] \quad (2.55)$$

where $\mathcal{H}_{\nu}^{(1)}, \mathcal{H}_{\nu}^{(2)}$ are the Hankel function of the first and second kind. Notice that its time evolution does not depend on their wave vector, just its modulo k , that is to say they do not have a preferred direction to evolve; additionally, in the massless limit $\nu = 3/2$ and the Hankel functions are of the form of 'half-integer', and one recover the well know results for these mode equation:

$$v_k(\tau) = c_k^{(1)} \left(1 - \frac{i}{k\tau} \right) e^{-ik\tau} + c_k^{(2)} \left(1 + \frac{i}{k\tau} \right) e^{+ik\tau} \quad (2.56)$$

where $c_k^{(1)}, c_k^{(2)}$ were redefined to absorb some irrelevant remnant constants.

2.3.2 Canonical quantization

From the action we learn that the conjugate momentum for the auxiliary field $\pi = \partial \mathcal{L} / \partial \dot{v} = \dot{v}$. We promote those field to quantum operators $\hat{v}(\tau, x), \hat{\pi}(\tau, x)$. The operators satisfy que equal time commutator relation:

$$[\hat{v}(\tau, \mathbf{x}), \hat{\pi}(\tau, \mathbf{x}')] = i\delta^3(\mathbf{x} - \mathbf{x}') \quad (2.57)$$

where $\hbar = 1$. The delta function is required by locality: points at a different location in space are independent and the corresponding operator commutes. Moreover, if this relation is Fourier transformed immediately one obtain its equivalent representation:

$$[\hat{v}_{\mathbf{k}}(\tau), \hat{\pi}_{\mathbf{k}}(\tau)] = -i(2\pi)^3 \delta^3(\mathbf{k} + \mathbf{k}'). \quad (2.58)$$

Which means that the field operator modes are independent between them, unless they are the same. It is convenient to expand the quantum auxiliary field $v_{\mathbf{k}}(\tau)$ in terms of creation and annihilation time independent operators

$$\hat{v}_{\mathbf{k}} = v_k(\tau) \hat{a}_{\mathbf{k}} + v_k^*(\tau) \hat{a}_{-\mathbf{k}}^\dagger \quad (2.59)$$

where the mode function $v_k(\tau)$ and its complex conjugate $v_k^*(\tau)$ satisfies the classical field equation (2.55), $a_{\mathbf{k}}$ is a creation operator and $\hat{a}_{-\mathbf{k}}^\dagger$ its hermitian complex conjugate, that satisfies bosonic algebra:

$$[\hat{a}_{\mathbf{k}}, \hat{a}_{\mathbf{k}'}^\dagger] = (2\pi)^3 \delta^3(\mathbf{k} - \mathbf{k}'), \quad [\hat{a}_{\mathbf{k}}, \hat{a}_{\mathbf{k}'}] = [\hat{a}_{\mathbf{k}}^\dagger, \hat{a}_{\mathbf{k}'}^\dagger] = 0. \quad (2.60)$$

Which is the well-known commutation relation for the raising and lowering operators of a harmonic oscillator. The quantum states in its Hilbert space are constructed by defining the vacuum state $|0\rangle$ via

$$\hat{a}_k|0\rangle = 0 \quad (2.61)$$

and the repeated application of \hat{a}_k^\dagger produces excited states for this system.

2.3.3 Choice of the vacuum

The Wronskian of the mode function is:

$$W[v_k, v_k^*] = v'_k v_k^* - v_k v'^*_k = 2i\text{Im}(v'_k v_k^*) \quad (2.62)$$

From the Eq.(2.53) it is easy to show the Wronskian is time-independent, and therefore we can be freely chosen. In particular $W[v_k, v_k^*] = -i$, because it simplifies the commutation relations for raising and lowering operator in momentum space. Given this conservation property, it is a convenient choice a time in which the Wronskian computation simplifies, such as in the *early time limit*, where the Hankel functions have a friendly asymptotic representation:

$$\lim_{\tau \rightarrow -\infty} \mathcal{H}_\nu^{(1,2)}(-k\tau) = \sqrt{\frac{2}{-\pi k\tau}} e^{\mp ik\tau} e^{\mp \frac{\pi}{2}(\nu + \frac{1}{2})} \quad (2.63)$$

Therefore the mode function (2.55) behaves like:

$$\lim_{\tau \rightarrow \infty} v_k(\tau) = \tilde{c}_k^{(1)} e^{-ik\tau} + \tilde{c}_k^{(2)} e^{ik\tau} \quad (2.64)$$

where $\tilde{c}_k^{(1)}$ and $\tilde{c}_k^{(2)}$ were defined to absorb the remaining constant for this expansion. In this limit suitable these constants satisfies a simply constraint relation:

$$|\tilde{c}_k^{(1)}|^2 - |\tilde{c}_k^{(2)}|^2 = \frac{1}{2k}. \quad (2.65)$$

As it can be seen, there is a free set of choices that underlie in a hyperbola branch for each Fourier mode k , therefore there is a remnant arbitrariness for the solution of MS equation. Moreover, this constraint relation is unable to fix completely the vacuum condition because it is always possible to apply a Bogolyubov transformation by taking another linear combination of the 2 modes solution and find another set of raising and lowering operator. Thus it is fundamental and necessary to find a physical argument to fix completely the vacuum ket $|0\rangle$. This ambiguity can be untangled by minimizing the vacuum energy, that is to say, minimizing the vacuum expectation value of the Hamiltonian operator:

$$\hat{H}(\tau) = \frac{1}{2} \int d^3x [\hat{\pi}^2 + \partial_i \hat{v}^2 + m^2(\tau) \hat{v}^2]. \quad (2.66)$$

Whose momentum representation is:

$$\hat{H}(\tau) = \frac{1}{2} \int \frac{d^3k}{(2\pi)^3} [\hat{a}_k^- \hat{a}_{-k}^- F_k(\tau) + \hat{a}_{-k}^+ \hat{a}_k^+ F_k^*(\tau) + (2\hat{a}_k^+ \hat{a}_k^- + (2\pi)^3 \delta^{(3)}(0)) E_k] \quad (2.67)$$

with:

$$E_k(\tau) = |v'_k(\tau)|^2 + \omega_k^2(\tau)|v_k(\tau)|^2, \quad \text{and} \quad F_k(\tau) = v'_k(\tau)^2 + \omega_k^2(\tau)v_k(\tau) \quad (2.68)$$

where $\omega_k^2(\tau) = k^2 + m_{\text{eff}}^2(\tau)$. Computing its vacuum expectation value

$$\langle 0 | \hat{H} | 0 \rangle = \int \frac{d^3 k}{(2\pi)^3} (1 + (2\pi)^3 \delta^{(3)}(0)) E_k \quad (2.69)$$

where the divergence term comes from an infinite volume of integration and E_k is the energy for each mode, that has to be minimized by tuning the mode constants $c_k^{(1)}, c_k^{(2)}$. In the same manner that before, the spectral energy density simplifies in the early time limit, giving an expectation value(omitting the vacuum energy):

$$\langle 0 | \hat{H} | 0 \rangle = \int \frac{d^3 k}{(2\pi)^3} k^2 (|c_k^{(1)}|^2 + |c_k^{(2)}|^2) \quad (2.70)$$

Combining this relation with (2.62), this energy density is minimized when $|c_k^{(1)}| = \frac{1}{\sqrt{2k}}$ and $c_k^{(2)} = 0$. Thus the mode function reduces to:

$$v_k(\tau) = \frac{\sqrt{\pi}}{2} \sqrt{-\tau} \mathcal{H}_\nu^{(1)}(-k\tau) \quad (2.71)$$

2.4 Two point correlation function

Given the stochastic nature of the quantum field, it is impossible to predict with precision the exact field configuration in a given space-time point. Due to this impossibility we are concerned in the field statistical properties, such as its variance and higher statistical moments. With this in mind let start computing the most basic, useful and powerful quantity for a quantum field in cosmology: the 2-pt correlation function for a quantum field \hat{v}

$$\langle 0 | \hat{v}(\tau, \mathbf{x}) \hat{v}(\tau, \mathbf{y}) | 0 \rangle = \int \frac{d^3 k}{(2\pi)^3} e^{-\mathbf{k}(\mathbf{x}-\mathbf{y})} |v_k(\tau)|^2 \quad (2.72)$$

one of the remarkable features of this expression is that the field correlation function is real, position independent and only depends on the distance between the two spatial coordinates. Exploiting the fact that the power spectrum is rotationally invariant in momentum space one gets a reduced expression for the same 2-pt correlation function:

$$\langle 0 | \hat{v}(\tau, \mathbf{x}) \hat{v}(\tau, \mathbf{y}) | 0 \rangle = \int d \ln k j_0(kr) \frac{k^3 P_v(\tau, k)}{2\pi^2} \quad (2.73)$$

where j_0 is the 0-spherical Bessel function and $P(\tau, k) = |v_k(\tau)|^2$. Thus if we are interested in the power spectrum for the field ϕ Eq.(2.48), we get

$$P_\phi(\tau, k) = \frac{1}{a^2} \frac{k^3}{2\pi^2} P_v(\tau, k) \quad (2.74)$$

or more explicitly:

$$\mathcal{P}_\phi(\tau, k) = \frac{k^3}{2\pi^2} (H\tau)^2 \frac{-\pi\tau}{4} |\mathcal{H}_\nu^{(1)}(-k\tau)|^2. \quad (2.75)$$

In cosmology, we are interested in superhorizon adiabatic modes, since these modes get frozen after horizon crossing, allow us to connect theory with observations. Thus formally in the superhorizon limit, since

$$\lim_{k\tau \rightarrow 0} \mathcal{H}_\nu^{(1)}(-k\tau) = \frac{-i}{\pi} \Gamma(\nu) \left(\frac{-k\tau}{2} \right)^{-\nu}, \quad (2.76)$$

the power spectrum becomes

$$\mathcal{P}_\phi(\tau, k) = \frac{\Gamma^2(\nu)}{\pi^3} \left(-\frac{k\tau}{2} \right)^{3-2\nu} H^2. \quad (2.77)$$

2.4.1 Light field limit

A phenomenologically interesting limit is when the scalar field mass approaches to zero, the called *light field limit*, $m^2 \ll H^2$, in which ν from the power spectrum (2.77) reduces to $\frac{3}{2} - \frac{1}{3} \frac{m^2}{H^2}$ and the power spectrum becomes:

$$\mathcal{P}_\phi(\tau, k) = \left(\frac{H}{2\pi} \right)^2 \left(-\frac{k\tau}{2} \right)^{\frac{2}{3} \frac{m^2}{H^2}} \left(1 - \frac{2}{3} c_1 \frac{m^2}{H^2} \right) \quad (2.78)$$

Therefore its spectral index:

$$\frac{d \ln \mathcal{P}_\phi}{d \ln k} = \frac{2}{3} \frac{m^2}{H^2} \quad (2.79)$$

where $c_1 = (2 - \gamma - 2 \ln 2)$ and γ is the Euler-Mascheroni number. When $m \rightarrow 0$ the spectral index approaches to zero, and we get a scale invariant power spectrum for a massless field in de Sitter space.

2.4.2 Heavy field limit

Another interesting limit is when $m \gg \frac{3}{2}H$, the degree of the Hankel function becomes imaginary so $\nu = i\mu$

$$\mu = \sqrt{\frac{m^2}{H^2} - 9/4} \rightarrow m/H \quad (2.80)$$

and the Fourier modes are:

$$|v_k(\tau)| = \frac{\sqrt{\pi}}{2} e^{-\pi\mu/2} \sqrt{-\tau} \mathcal{H}_\mu^{(1)}(-k\tau) \quad (2.81)$$

thus the power spectrum of a very massive field with Bunch-Davis initial condition is suppressed by an exponential law $\mathcal{P}_\phi(k) \propto e^{-\pi \frac{m}{H}}$.

2.5 Curvature power spectrum

Due to we have already developed all the machinery sufficient and necessary to describe light scalar field in de Sitter space, now we will consider single-field slow-roll models of inflation

$$S = \frac{1}{2} \int d^4x \sqrt{-g} [R - g^{\mu\nu} \partial_\mu \phi \partial_\nu \phi - V(\phi)], \quad (2.82)$$

where we have set the Planckian mass, $M_{\text{pl}} = 1$. We will study both scalar and tensor fluctuations. For the scalar modes, we have to be careful to identify the true physical degrees of freedom. A priori, we have 5 scalar modes: 4 metric perturbations δg_{00} , δg_{ii} , $\delta g_{0i} \sim \partial_i B$ and $\delta g_{ij} \sim \partial_i \partial_j H$ and 1 scalar field perturbation $\delta\phi$. Gauge invariances associated with the invariance of Eq.(2.82) under scalar coordinate transformations $x^\mu \rightarrow x^\mu + \varepsilon^\mu$ remove two modes. The Einstein's constraint equations remove two more modes, so that we are left with 1 physical scalar mode.

2.5.1 Comoving gauge

We will work with a fixed gauge throughout. For a various reasons, it will be convenient to work in comoving gauge, defined by the vanishing momentum density $\delta T^{0i} = 0$. For slow-roll inflation, this becomes

$$\delta\phi = 0 \quad (2.83)$$

In this gauge, perturbations are characterized purely by fluctuations in the metric,

$$\delta g_{ij} = a^2(1 - 2\zeta)\delta_{ij} + h_{ij}. \quad (2.84)$$

Here, h_{ij} is a transverse ($\nabla_i h^{ij} = 0$), traceless (h_i^i) tensor and ζ is a scalar. One can show that the comoving spatial slices $\phi = \text{const}$ have three-curvature $R^{(3)} = \frac{4}{a^2} \nabla^2 \zeta$. Hence, ζ is referred to as the comoving curvature perturbation. The perturbation ζ has the crucial property that (for adiabatic matter fluctuations) it is time-independent on superhorizon scales:

$$\lim_{k \ll aH} \dot{\zeta}_{\vec{k}} = 0 \quad (2.85)$$

Solving the Einstein equations for the non-dynamical metric perturbations δg_{00} and δg_{0i} in terms of ζ is a bit tedious. In the ADM metric parametrization where N, N^i are respectively the lapse and the shift vector that define the foliation and where h_{ij} is the induced three-metric on the spatial hypersurface. One advantage of parametrizing in this way is that neither \dot{N} nor N^i do not appear in the action, hence they correspond to non-propagating fields that act as Lagrange's multipliers(constraints) with a just algebraic equation of motion. Furthermore, all the gravitational dynamics is encoded in the 3-metric h_{ij} on slices of constant time. Thus in ADM, the spacetime metric is

$$ds^2 = -N^2 dt^2 + h_{ij}(dx^i + N^i dt)(dx^j + N^j dt). \quad (2.86)$$

Ignoring the tensorial perturbation, the 3-metric reads,

$$h_{ij} = a^2(t) e^{-2\zeta(t, \mathbf{x})} \delta_{ij} \quad (2.87)$$

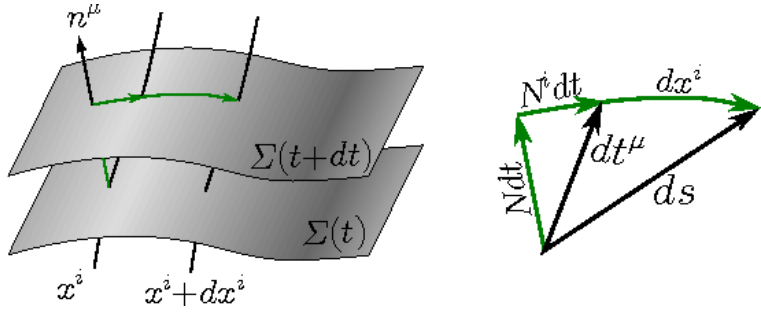


Figure 2.1: Space time foliation. Credit:[14].

where $\zeta(t, \mathbf{x})$ is the non-linear generalization [12] of the variable introduced by Bardeen, Steinhardt and Turner [13] in linear perturbation theory. This variable corresponds to a local rescaling of the scale factor that is equivalent to a local time reparametrization of the background evolution. The action (2.82) can be rewritten as:

$$S = \frac{1}{2} \int d^4x \sqrt{h} \left[NR^{(3)} - 2NV + N^{-1}(E_{ij}E^{ij} - E^2) + N^{-1}\dot{\phi}^2 \right] \quad (2.88)$$

Where $E = E_i^i$ and $K_{ij} = N^{-1}E_{ij}$ is the extrinsic curvature defined by:

$$K_{ij} = \frac{1}{2N}(\dot{h}_{ij} - \mathcal{D}_i N_j - \mathcal{D}_j N_i) \quad (2.89)$$

where \mathcal{D}_i is the covariant derivative on the 3-metric. The ADM action implies the following constraints equations for the Lagrange multipliers N and N^i or technically the Hamiltonian and the momentum constraint:

$$R^{(3)} - 2V - N^{-2}(E^{ij}E_{ij} - E^2) - N^{-2}\dot{\phi}^2 = 0, \quad \mathcal{D}_i [N^{-1}(E_j^i - \delta_j^i E)] = 0 \quad (2.90)$$

To solve these constraint equations, we split the shift vector N_i into an irrotational and incompressible part (scalar-vector decomposition):

$$N_i = \partial_i \psi + N_i^T \quad (2.91)$$

It is useful solve the constraint equation order by order in ζ so they admit a perturbative expansion and simplifying the non-trivial non-linearities in their algebraic equations:

$$N = 1 + \delta N^{(1)} + \delta N^{(2)} + \dots, \quad \psi = \psi^{(1)} + \psi^{(2)} + \dots, \quad N^{Ti} = N^{Ti(1)} + N^{Ti(2)} + \dots, \quad (2.92)$$

replacing in (2.88) one find that

$$\delta N^{(1)} = \frac{\dot{\zeta}}{H}, \quad \partial^2 N^{Ti(1)} = 0, \quad \psi^{(1)} = -\frac{\zeta}{H} + \frac{a^2}{H} \partial^{-2}(\varepsilon \dot{\zeta}) \quad (2.93)$$

Where ∂^{-2} is defined as $\partial^{-2}\partial^2 f = f$. Substituting the first-order constraint solution for N, N^i back into the action, and tediously integrating by parts one finds second order action for the curvature perturbation ζ :

$$S = \frac{1}{2} \int dx^4 a^3 \frac{\dot{\phi}^2}{H^2} \left[\dot{\zeta}^2 - \frac{1}{a^2} (\partial_i \zeta)^2 \right] \quad (2.94)$$

Defining the canonically normalized Mukhanov variable $v = z\zeta$, where $z^2 = a^2 \frac{\dot{\phi}^2}{H^2} = 2a^2\varepsilon$, and changing to conformal time, we get:

$$S = \frac{1}{2} \int d\tau d^3x [v'^2 - (\partial_i v)^2 - m_{\text{eff}}^2(\tau)v^2] \quad (2.95)$$

where $m_{\text{eff}}^2(\tau) = -\frac{z''}{z} = -\frac{H}{a\dot{\phi}} \frac{\partial^2}{\partial\tau^2}(\frac{a\dot{\phi}}{H})$. We see that this action is of the form Eq.(2.48), thus we can apply the entire machinery already derived. The effective mass can be obtained in terms of the background quantities with further manipulations one find:

$$\frac{z''}{z} = (aH)^2 \left[2 - \varepsilon + \frac{3}{2}\eta - \frac{1}{2}\varepsilon\eta + \frac{1}{4}\eta^2 + \eta k \right] \quad (2.96)$$

Additionally, the conformal time satisfies at first order in slow roll expansion:

$$aH = -\frac{1}{\tau}(1 + \varepsilon). \quad (2.97)$$

Therefore, the effective mass at the first order in slow roll expansion:

$$m_{\text{eff}}^2(\tau) = -\frac{1}{\tau^2} \left[2 + 3 \left(\varepsilon + \frac{1}{2}\eta \right) \right] \quad (2.98)$$

From the Eq.(2.54) we can identify the ν parameter to fix the mode equation $v_k(\tau)$, $m^2(\tau) = \frac{\nu^2 - 1/4}{\tau^2}$, where $\nu^2 = \frac{9}{4} + 3(\varepsilon + \frac{1}{2}\eta)$, thus the equivalent to the ratio m^2/H^2 in the equation (2.79) is $-3(\varepsilon + \frac{1}{2}\eta)$. If ε and η are sufficient small and nearly constant during inflation thus $\nu = \frac{3}{2} + \varepsilon + \frac{1}{2}\eta$. We can replace these values into (2.78) and (2.79) and divide by an additional 2ε factor that comes from Mukhanov variable $\zeta = z^{-1}v$ to get the power spectrum for ζ field:

$$\mathcal{P}_\zeta(\tau, k) = \frac{H^2}{8\pi^2 M_{\text{pl}}^2 \varepsilon} \left(-\frac{k\tau}{2} \right)^{-2\varepsilon-\eta} (1 - O(\varepsilon, \eta)) \quad (2.99)$$

where we have added M_{pl}^{-2} to reconstruct the units and. Additionally, observations suggest that this power spectrum can be accurately parametrized by

$$\mathcal{P}_\zeta(\tau, k) = A_s(k_*) \left(\frac{k}{k_*} \right)^{n_s-1} \quad (2.100)$$

where A_s is the amplitude of the power spectrum, k_* is some reference scale and n_s is the spectral index defined by:

$$n_s - 1 = \frac{d \ln \mathcal{P}_\zeta}{d \ln k} = -2\varepsilon - \eta \quad (2.101)$$

2.5.2 Tensor Perturbations

Primordial gravitational waves are tensor perturbations of the spacetime metric generated during inflation, they are gauge invariant objects and appear in the metric as:

$$ds^2 = a^2(\tau) [-d\tau^2 + (\delta_{ij} + h_{ij})dx^i dx^j] \quad (2.102)$$

where h_{ij} is a symmetric, traceless and transverse tensor, that is to say:

$$h_{ij} = h_{ji} \quad h_i^i = 0 \quad \partial_i h_j^i = 0, \quad (2.103)$$

respectively. These conditions imply that h_{ij} has only two degrees of freedom, which we shall denote as the helicity $p = \pm 2$. Moreover, we decompose h_{ij} in Fourier modes as:

$$h_{ij}(\tau, \mathbf{x}) = \sum_{p=\pm 2} \int \frac{d^3 k}{(2\pi)^3} h_{ij}^{(p)}(\tau, \mathbf{k}) e^{i\mathbf{k}\mathbf{x}} \quad (2.104)$$

For k along the \hat{z} -axis, we choose a set of basis tensors

$$m^{(\pm 2)}(\hat{z}) = \frac{1}{2} (\hat{x} \pm i\hat{y}) \otimes (\hat{x} \pm i\hat{y}) \quad (2.105)$$

satisfying the orthonormality and reality conditions:

$$m_{ij}^{(p)}(\hat{k})(m^{(q)ij}(\hat{k}))^* = \delta^{pq} \quad (2.106)$$

$$(m^{(p)ij}(\hat{k}))^* = m_{ij}^{(-p)}(\hat{k}) = m^{(p)ij}(-\hat{k}) \quad (2.107)$$

On such a basis, we have

$$h_{ij}^{(\pm 2)}(\tau, \mathbf{k}) = \frac{1}{\sqrt{2}} m_{ij}^{\pm 2}(\hat{k}) h^{(\pm 2)}(\tau, \mathbf{k}) \quad (2.108)$$

From the Einstein-Hilbert action the Ricci scalar contribution decouples at linear in perturbations and we find

$${}^{(2)}S = \frac{M_{\text{pl}}^2}{8} \int d\tau d^3 x a^2 \left(\dot{h}_{ij} \dot{h}^{ij} - \partial_i h_{jk} \partial^i h^{jk} \right) \quad (2.109)$$

after tedious algebra we get

$${}^{(2)}S = \frac{M_{\text{pl}}^2}{16} \sum_{p=\pm 2} \int d\tau d^3 k a^2 \left[(\dot{h}^{(p)})^2 + k^2 (h^{(p)})^2 \right]. \quad (2.110)$$

For quantizing this field is the same as the scalar field but replacing $\zeta \rightarrow (M_{\text{pl}}/\sqrt{8})h^{(p)}$ for each independently-evolving helicity state, one can derive the power spectrum by defining the two point correlator at an equal time:

$$\langle h^{(p)}(\mathbf{k}) h^{(q)}(\mathbf{k}')^* \rangle = \frac{2\pi^2}{k^3} \frac{\mathcal{P}_h(k)}{2} \delta^{pq} \delta(\mathbf{k} - \mathbf{k}') \quad (2.111)$$

at the horizon crossing, finally:

$$\mathcal{P}_h(k) = \frac{2H^2}{\pi^2 M_{\text{pl}}^2} \left(-\frac{k\tau}{2} \right)^{-2\varepsilon-\eta} (1 + \mathcal{O}(\varepsilon, \eta)) \quad (2.112)$$

whose tensor spectral index n_T is defined by

$$n_T = \frac{d \ln \mathcal{P}_h(k)}{d \ln k} = -2\varepsilon \quad (2.113)$$

as the same for the scalar power spectrum, Eq.(2.112) can be parametrized as

$$\mathcal{P}_h(k) = A_t(k_*) \left(\frac{k}{k_*} \right)^{n_T}. \quad (2.114)$$

Considering the expression Eq.(2.112) and Eq.(2.99), it is defined the slow-roll single field inflation consistency relation by defining *the scalar to tensor ratio* as:

$$r = \frac{A_t}{A_s} = 16\varepsilon = -8n_T. \quad (2.115)$$

This is the so called consistency relation for scalar and tensorial power spectrum. In addition to this, since $\mathcal{P}_\zeta(k)$ is fixed and $\mathcal{P}_h(k)$ is proportional to the Hubble scale H , the tensor to scalar ratio is a direct measure of the energy scale of inflation.

$$H^{1/4} \sim \left(\frac{r}{0.01} \right)^{1/4} 10^{16} \text{GeV} \quad (2.116)$$

2.5.3 Observations

According to observations, the power spectrum of the curvature perturbation is almost scale-invariant, with a value of order 10^{-9} . The scale dependence of the spectrum is characterized by the spectral index n_s . Scale invariance correspond to $n_s = 1$, and often the quantity $n_s - 1$ is called the spectral tilt. If n_s is constant then $\mathcal{P}_\zeta(k) \propto k^{n_s-1}$. If n_s depends on k one says that the spectral index is running. In that case, one usually assumes that that n_s can be approximated as a linear function on $\ln k$ so that the running is defined by $n'_s = dn_s/d\ln k$. Observations are compatible with the hypothesis that ζ is the primordial perturbation. Also from the Λ CDM model to current CMB observations anisotropies and galaxy distributions gives

$$\mathcal{P}_\zeta^{1/2} = (4.9 \pm 0.2) \cdot 10^{-5}, \quad n_s = 0.9655 \pm 0.0062 \quad (2.117)$$

The spectrum is defined at the pivot scale $k_0 = 0.002 \text{Mpc}^{-1}$. This observational value of the power spectrum is known as the COBE normalization. From the above equations, one see that the power spectrum depend weakly on the scale so one often refer this as a *nearly scale invariant* power spectrum, and this parameter tell us about a quasi-de Sitter early stage of our Universe. One can also define the running of the spectral index, as

$$\alpha_s = \frac{d \ln n_s}{d \ln k} = -2\eta\varepsilon - \frac{\dot{\eta}}{H\eta} \quad (2.118)$$

Thus is one order smaller than $n_s \sim 1$ in terms of slow roll parameters in the above simple model. The observational constraint for n_s is

$$\alpha_s = -0.0084 \pm 0.008, \quad (68\% \text{CL, Planck TT+lowP}) \quad (2.119)$$

Thus although inflation is nearly scale-invariant, an exact scale invariance with $n_s = 1$ is ruled out at over 5σ .

The production of a stochastic background of gravitational waves(GW) is a fundamental prediction of any cosmological inflationary model. Their observation would produce the

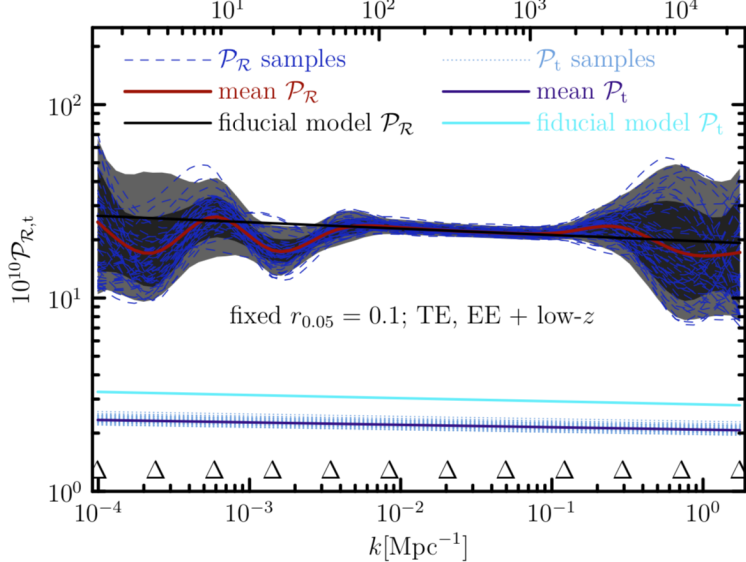


Figure 2.2: Primordial curvature power spectrum from Planck collaboration 2015. The nearly scale-invariant of this spectrum, tell us about a quasi de Sitter expansion of the early universe and its duration, more importantly, it is obtained by naturally deconvolving the angular power temperature power spectrum or the C_l^{TT} 's, which makes of this image a remarkably beautiful and at the same time thrilling plot in concordance with basic inflationary predictions. Nevertheless, it is worth mentioning that the information(amplitude and the scalar tilt) of this spectrum is not sufficient to break the physical parameter degeneracy between its $H_{\text{inflation}}$ and ϵ , furthermore, the scenario is even worst, making the energy inflationary scale one of the worst constrained parameters in physics. This is why we need an ultimate and independent primordial source to break this degeneracy, such as B -modes from primordial gravitational waves [32].

first experimental evidence of a quantum gravity phenomenon, thus represent an exciting, powerful window on the origin and evolution of the universe. The features of such a signal encode unique information about the physics of the Early Universe and the main observational signature of the inflationary GW background is a curl-like pattern (B -modes) in the polarization of the CMB.

In the same footing for the primordial curvature perturbation and in spite of all the efforts possible so far, primordial gravitational waves have not been detected on the CMB. The current best upper limit comes from the joint analysis of Planck, BICEP2, Keck Array ([15]) and other data, which correspond to a scalar-to-tensor ratio of

$$r < 0.07 \text{ (95% CL)}, \quad \text{with } k_* = 0.05 \text{ Mpc}^{-1} \quad (2.120)$$

assuming the consistency relation $r = -8n_T$, where n_T is the tensor spectral index. Excluding temperature data and assuming a scale-invariant GW power-spectrum, the bound becomes

$$r < 0.09 \text{ (95% CL)}, \quad \text{with } k_* = 0.05 \text{ Mpc}^{-1} \quad (2.121)$$

In light of all this, it is not at all surprising that primordial GW's are the object of a growing experimental effort, and that their detection will be a major goal for Cosmology

in the forthcoming decades. The state of the art corresponds to multiple projects at the different places around the world, mainly in the north of Chile and Antarctica, due to the privileged atmospheric conditions along the year. A number of, present or forthcoming, ground-based or balloon-borne experiments, such as ACTPol ([16]), Polarbear ([17]), CLASS ([18]), Piper ([19]) and Spider ([20]), are specifically aimed at B-mode detection. In addition, CMB satellites such as WMAP and Planck have, in recent years, provided bounds on r , such as the one reported above.

2.6 Non-gaussianity

The hopes and racing for detecting non-gaussianity keeps intact since the beginnings, and theoretically and experimentally we have the potential to constraint(measure) up to order 0.1 using multi-channel data from future CMB experiments and LSS. Particularly the CMB can provide us constraint on f_{NL} up to 1, from the modes larger than 10 Mpc projected on the last scattering 2-sphere ($(10^3)^2 \sim 10^6$ modes). Additionally, LSS will survey 3-dimensional fields, from scales larger than 10 Mpc and shorter than the horizon scale $\sim 10^4$ Mpc, capturing potentially $(10^4/10)^3 \sim 10^9$ independent modes, improving the sensitivity of non-gaussianity to 0.1. So this is the beginning of a vibrant epoch to keep pushing(as far as we can) our fundamental understanding up to the next level.

2.6.1 Non-gaussian CMB statistic

The measured temperature fluctuations in a CMB map from some experiment, with N_{pix} and ΔT_i the temperature fluctuation at the direction \hat{n} satisfy with good accuracy a Gaussian probability distribution(PDF)

$$P_g(\Delta T) = \frac{1}{(2\pi)^{N_{\text{pix}}} |\xi|^{1/2}} \exp \left(-\frac{1}{2} \sum_{ij} \Delta T_i \xi_{ij}^{-1} \Delta T_j \right) \quad (2.122)$$

where $\xi_{ij} = \langle \Delta T_i \Delta T_j \rangle$ is the covariance matrix or two point correlation function of the temperature anisotropy and $|\xi|$ is its determinant. It is usual practice to expand ΔT in spherical harmonics, $\Delta T(\hat{n}) = \sum_{lm} a_{lm} Y_{lm}(\hat{n})$. The Gaussian PDF for the a'_{lm} s becomes

$$P_g(a) = \frac{1}{N_{\text{harm}} |C|^{1/2}} \exp \left(-\frac{1}{2} \sum_{lm} \sum_{l'm'} a_{lm}^* [(C^{-1})_{lm, l'm'}] a_{l'm'} \right) \quad (2.123)$$

where $C_{lm, l'm'} = \langle a_{lm}^* a_{l'm'} \rangle$ and N_{harm} is the number multipoles that is summed over. For a Gaussian PDF for the CMB, its covariance matrix $[C_{lm, l'm'}]$, provides a full description of the data. All higher correlations either vanish, $\langle a_{lm} a_{l'm'} a_{l''m''} \rangle = 0$, or can be expressed in terms of $C_{lm, l'm'}$. Moreover, when the CMB is statistical homogeneous and isotropic

$$C_{lm, l'm'} = C_l \delta_{ll'} \delta_{mm'} \quad (2.124)$$

and Eq.(2.123) reduces to

$$P_g(a) = \prod_{lm} \frac{e^{-\frac{|a_{lm}|^2}{2C_l}}}{\sqrt{2\pi C_l}}. \quad (2.125)$$

To parameterize the CMB non-gaussianity, we know from observations that the CMB is very close to a Gaussian distribution. Therefore, it makes sense to Taylor expand the probability distribution(Gram-Charlier expansion) around a Gaussian distribution

$$P(a) = \left[1 - \frac{1}{6} \sum \langle a_{l_1 m_1} a_{l_2 m_2} a_{l_3 m_3} \rangle \frac{\partial}{\partial a_{l_1 m_1}} \frac{\partial}{\partial a_{l_2 m_2}} \frac{\partial}{\partial a_{l_3 m_3}} + \dots \right] \cdot P_g(a) \quad (2.126)$$

Evaluating the derivatives gives

$$\frac{P(a)}{P_g(a)} = 1 + \frac{1}{6} \sum \langle a_{l_1 m_1} a_{l_2 m_2} a_{l_3 m_3} \rangle ((C^{-1}a)_{l_1 m_1} (C^{-1}a)_{l_2 m_2} (C^{-1}a)_{l_3 m_3} - 3(C^{-1})_{l_1 m_1, l_2 m_2} (C^{-1}a)_{l_3 m_3}). \quad (2.127)$$

This formula tell us what we expected that the leading deviation from the Gaussian PDF is proportional to the angular bispectrum $\langle a_{l_1 m_1} a_{l_2 m_2} a_{l_3 m_3} \rangle$. The formula is also used to estimate the angular bispectrum from data by maximizing this PDF. In this chapter, we will concentrate on the primordial non-gaussianity of the curvature field ζ .

2.6.2 Fields non-gaussianity

As far as we have seen, within the inflationary cosmology, higher connected correlators of the primordial perturbations are generally expected to be small. The Fourier coefficients of a Gaussian perturbation have only the minimal correlation demanded by the reality condition. As a result, the stochastic properties of the perturbation are completely defined by its spectrum. In particular, the non-zero correlators of the Fourier coefficients are given by the spectrum that only depend on the magnitude of \mathbf{k} , corresponding to rotational invariance:

$$\langle \phi_{\mathbf{k}} \rangle = 0, \quad \langle \phi_{\mathbf{k}} \phi_{\mathbf{k}'} \rangle = (2\pi)^3 \delta^3(\mathbf{k} + \mathbf{k}') P_\phi(k), \quad \langle \phi_{\mathbf{k}_1} \phi_{\mathbf{k}_2} \phi_{\mathbf{k}_3} \rangle = 0 \quad (2.128)$$

moreover, trispectrum is related by the power spectrum as

$$\langle \phi_{\mathbf{k}_1} \phi_{\mathbf{k}_2} \phi_{\mathbf{k}_3} \phi_{\mathbf{k}_4} \rangle = (2\pi)^6 \delta^3(\mathbf{k}_1 + \mathbf{k}_2) \delta^3(\mathbf{k}_3 + \mathbf{k}_4) P_\phi(k_1) P_\phi(k_3) + \text{two permutations} \quad (2.129)$$

Nevertheless, the coefficients of a non-Gaussian perturbation have additional correlations, not specified by its spectrum; that means the additional correlation between modes. The following contribution is the three-point correlator that vanishes in the Gaussian case. Thus we define the bispectrum B given by

$$\langle \phi_{\mathbf{k}_1} \phi_{\mathbf{k}_2} \phi_{\mathbf{k}_3} \rangle = (2\pi)^3 \delta^3(\mathbf{k}_1 + \mathbf{k}_2 + \mathbf{k}_3) B(k_1, k_2, k_3). \quad (2.130)$$

Translational invariance demands that each correlator vanishes when the sum of the momenta \mathbf{k}_i vanishes and the fact that bispectrum depends only on the lengths of three sides of the

triangle formed by the momenta corresponds to invariance under rotations. It is convenient to define the reduced bispectrum B by going to position space

$$\langle \phi(\mathbf{x}_1 + \mathbf{x}_3)\phi(\mathbf{x}_2 + \mathbf{x}_3)\phi(\mathbf{x}_3) \rangle = \int \frac{d^3k_2}{(2\pi)^3} \frac{d^3k_1}{(2\pi)^3} B(k_1, k_2, k_3) e^{i(\mathbf{k}_1\mathbf{x}_1 + \mathbf{k}_2\mathbf{x}_2)} \quad (2.131)$$

Notice that \mathbf{x}_3 does not appear in the R.H.S. of the above equation because translational invariance, whereas \mathbf{x}_1 and \mathbf{x}_2 are needed to define a triangulated configuration. When $\mathbf{x}_1 = \mathbf{x}_2 = \mathbf{x}_3$, this configuration defines the skewness of the probability distribution defined by

$$S = \langle \phi^3 \rangle / \langle \phi^2 \rangle^{3/2} \quad (2.132)$$

2.6.3 Local non-Gaussianity

The simplest possibility for the form of the non-gaussianity at higher order

$$\zeta(\mathbf{x}) = \zeta_g(\mathbf{x}) + \zeta_{\text{N.G.}}(\mathbf{x}) = \zeta_g(\mathbf{x}) + \sum_{n>1} b_n [\zeta_g^n(\mathbf{x}) - \langle \zeta_g^n(\mathbf{x}) \rangle], \quad (2.133)$$

The second term in the summatory is to guarantee $\langle \zeta(\mathbf{x}) \rangle = 0$ at all orders. This ansatz was introduced in [21] in the context of Galaxy halo bias. For our purposes we can just keep the second order term and ignore the constant contribution, because it can always be absorbed via a gauge transformation by the unperturbed background, so

$$\zeta(\mathbf{x}) = \zeta_g(\mathbf{x}) + b\zeta_g^2(\mathbf{x}) + \dots = \zeta_g(\mathbf{x}) + \frac{3}{5}f_{\text{NL}}\zeta_g^2(\mathbf{x}) + \dots \quad (2.134)$$

thus is known as local non-gaussianity¹. Since $\zeta_g(\mathbf{x})$ is Gaussian to good accuracy, the first term must dominate. It is worth emphasizing that this is just an ansatz, instead of a generic expansion, as an example, the f_{NL} estimator could depend on position and terms like ζ_g^2 are not necessarily expanded at the same spatial point. As a result, the terms like $f_{\text{NL}}\zeta_g^2(\mathbf{x})$ has to be in general written as a convolution(as a non-local term). But hereafter we are going to consider just this term since the local ansatz has clear physical meaning: this ansatz assumes non-Gaussianities are generated independently at different spatial points. Translating this requirement into the context of inflation, typically implies the non-Gaussianity is generated on super-Hubble scales.

Qualitatively, for positive f_{NL} , the part of contribution from positive $\zeta_g(\mathbf{x})$ gets enhanced, and the part of contribution from negative ζ_g gets suppressed. This provides an intuitive way to visualize the sign of f_{NL} . In position space, this non-Gaussianity can be characterized by the probability distribution function of ζ . The probability distribution is plotted in Fig. 2.3. Note that the tail at large and positive ζ indicates where structures are formed in the universe. Thus positive f_{NL} means more galaxies are formed given a fixed power spectrum. For the CMB sky, positive f_{NL} means there are more very cold spots than very hot spots on the CMB, and more modestly hot spots than modestly cold spots. The position-space features of f_{NL} is intuitive to understand. However, the inflationary perturbation manifests

¹The numerical factor 3/5 in (2.134) comes its due to historical reason. f_{NL} originally was introduced in terms of the gravitational potential.

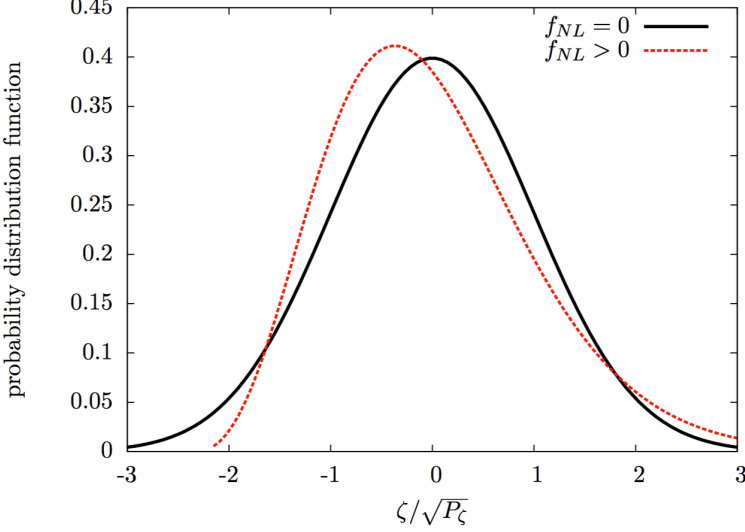


Figure 2.3: Schematic probability distribution for the primordial curvature perturbation. Positive f_{NL} correspond to the red curve in the figure. Negative f_{NL} correspond to an axial reflection at $\zeta = 0$ of the red curve. The constrained f_{NL} is should be represented much smaller in this plot. Credit:[14].

itself in momentum space. There are much more configurations of three-point function to look at, than just looking at position-space probability distributions point by point. Thus the momentum space correlation functions provide a much more powerful test of non-Gaussianity than the isolated position space test. In momentum space, the corresponding expression is:

$$\zeta_{\mathbf{k}} = \zeta_{\mathbf{k}}^g + \frac{3}{5} f_{\text{NL}} \int \frac{d^3 q}{(2\pi)^3} \zeta_{\mathbf{q}}^g \zeta_{\mathbf{q}-\mathbf{k}}^g. \quad (2.135)$$

Inserting this expression into the three point function

$$\langle \zeta_{\mathbf{k}_1} \zeta_{\mathbf{k}_2} \zeta_{\mathbf{k}_3} \rangle = (2\pi)^3 \delta^3(\mathbf{k}_1 + \mathbf{k}_2 + \mathbf{k}_3) B_{\zeta}(k_1, k_2, k_3) \quad (2.136)$$

with

$$B_{\zeta}(k_1, k_2, k_3) = \frac{18}{5} f_{\text{NL}} \frac{\mathcal{S}(k_1, k_2, k_3)}{(k_1 k_2 k_3)^2} \mathcal{P}^2(k_*) \quad (2.137)$$

where $\mathcal{P}_{\zeta}(k_*) = k_*^3 P_{\zeta}(k_*)$ is the quasi-scale invariant dimensionless power spectrum evaluated at the fiducial scale k_* with the shape function normalized to $\mathcal{S}(k, k, k) = 1$ and defined by

$$S_{\text{loc}}(k_1, k_2, k_3) = \frac{1}{3} \left(\frac{k_3^2}{k_1 k_2} + 2 \text{ permutations} \right) \quad (2.138)$$

The shapes of the bispectrum refers to the dependence \mathcal{S} on the momentum ratios k_2/k_1 and k_3/k_1 , while fixing the overall momentum scale $K = (k_1 + k_2 + k_3)/3$. Explicitly with this parametrization the bispectrum (??) becomes :

$$B_{\zeta}(k_1, k_2, k_3) = \frac{6}{5} f_{\text{NL}} \frac{\mathcal{P}^2(k_*)}{(k_1 k_2 k_3)^3} \left(\frac{k_1^2}{k_2 k_3} + \frac{k_2^2}{k_1 k_3} + \frac{k_3^2}{k_1 k_2} \right) \quad (2.139)$$

An interesting quantity appears when of the three momenta goes to zero, for example (assuming $k_3 \ll k_1 \approx k_2$) in whose case the shape function

$$\lim_{k_3 \rightarrow 0} S_{\text{loc}}(k_1, k_2, k_3) = \frac{2}{3} \frac{k_2}{k_1} \quad (2.140)$$

thus the bispectrum

$$\lim_{k_3 \rightarrow 0} B_\zeta(k_1, k_2, k_3) = \frac{12}{5} f_{\text{NL}} \mathcal{P}^2(k_*) \frac{1}{k_1^3 k_2 k_3^2} \cong \frac{12}{5} f_{\text{NL}} P_\zeta(k_1) P_\zeta(k_3) \quad (2.141)$$

this is known as the *squeezed limit* bispectrum and as a direct relevance since it provides a direct test for the local ansatz Eq.(2.134). The observational constraint for f_{NL} from Planck ([7]) is:

$$f_{\text{NL}} = 0.8 \pm 5.0, \text{ (68%CL, Planck TT + low P)} \quad (2.142)$$

2.7 In-In formalism

The in-in formalism is a systematic scheme to evaluate radiative corrections or higher order contributions to primordial cosmological perturbation, which is the basis (as well the ADM formalism) of modern calculations for higher-order contributions to the primordial spectrum. The importance of these tools for inflations relies upon its predictability and accuracy and its relative simplicity, therefore, it helps to capture all phenomena by finding the action of fields, how it behaves, what symmetries are hidden and respected by those fields and finally all possible couplings with others fundamental fields.

This subsection is organized as follow: firstly, we will introduce some formal aspects of the in-in formalism a la Weinberg [22] and secondly, we will compute the simplest radiative contribution from the lowest order interaction Hamiltonian H_I order 3. To have some intuition on the computation of the complete 3 point correlation function we will pick up the simplest term and compute its contribution through the in-in formalism in function to illustrate some aspect of this methodology. The remaining terms are analogous and straightforward, however, are a tedious task.

The in-in formalism scheme can be viewed as one of the initial conditions, in-in takes the initial states of some set of fields, $|in\rangle$, and calculates the expectation value of some set of operators \mathcal{O} with respect to these fields at a later time t , $|\Omega(t)\rangle$. Specifying the initial conditions typically amounts to choosing the Bunch-Davies vacuum: the dynamical degrees of freedom behave like harmonic oscillators at very small length scales(well inside the horizon), and each mode is assumed to be in its ground state. To evaluate an expectation value at some arbitrary time in the interaction picture one needs to evolve the 'in state' forward in time $|\Omega(t)\rangle$. Operationally, the simplest way of incorporating this initial condition is to include some evolution in imaginary time, $t \rightarrow t(1 + i\varepsilon)$ and compute the expectation value, $\langle O(t) \rangle$, of a product of operators $O(t)$ at time t , require that we evaluate

$$\langle O(t) \rangle = \langle \left(T e^{-i \int_{-\infty}^t H_I(t') dt'} \right)^\dagger O(t) \left(T e^{-i \int_{-\infty}^t H_I(t'') dt''} \right) \rangle \quad (2.143)$$

where the fields on the right-hand side are Heisenberg fields. The expectation value is taken with respect to the initial state, $|in\rangle$, which we assume to be the Bunch-Davies vacuum. The interaction Hamiltonian H_I is defined in the usual way so that the total Hamiltonian H is the combination of H_I and the free-field Hamiltonian, H_0 ,

$$H = H_0 + H_{int} \quad (2.144)$$

From the action one constructs the Hamiltonian by defining conjugate momenta, and separating out the quadratic from the higher order parts: H_0 consists of terms that are quadratic in the perturbative degrees of freedom (and thus free), while H_{int} consists of all third and higher order terms. The free Hamiltonian H_0 drives the evolution of the operators, while H_{int} evolves the states. This separation is natural since in a homogenous and isotropic background we can find the eigenstates of the free field Hamiltonian at past infinity. The interaction terms generally have derivative couplings even when the action contains only canonical kinetic terms. These derivative couplings are the end result of perturbatively expanding the action. If L_I is the portion of the action with terms third order and higher, the usual expression for the interaction Hamiltonian $H_{int} = -L_{int}$. In the more general case, there will be extra interaction terms.

$$\langle O \rangle = \sum_{n,m} \langle 0 | \left(T e^{-i \int_{-\infty}^t H_{int}(t') dt'} \right)^\dagger | n \rangle \langle n | O | m \rangle \langle m | \left(T e^{-i \int_{-\infty}^t H_{int}(t') dt'} \right) | 0 \rangle \quad (2.145)$$

The interpretation is clear, the 'in-in' correlation is the product of vacuum transition amplitudes ('in-out') and a matrix element $\langle n | O | m \rangle$, summed over all possible 'out' states. The 'in-in' formalism is simply standard QFT, rigged to compute correlation functions at a fixed time, given initial conditions instead of asymptotic boundary conditions. Initial conditions in QFT are usually specified by finding the eigenstates of the free Hamiltonian H_0 , and stipulating that the system begins in one (or some combination) of these eigenstates. If the system begins in the quantum mechanical vacuum, this amounts to putting our system in the vacuum state of H_0 at the initial time. Operationally, the vacuum is selected by redefining the range of t to include a small imaginary component, $t \rightarrow t + i\varepsilon|t|$. At the lowest order :

$$\langle O \rangle = \text{Re} \left\langle \left[-2iO^I(t) \int_{-\infty(1+i\varepsilon)}^t dt' H_{int}^I(t') \right] \right\rangle \quad (2.146)$$

This reduced form is due to the Hermiticity of the operator product. Let us consider a Lagrangian with generic fields ϕ_a ,

$$S = \int d^4x \mathcal{L}(\phi_a(\mathbf{x}, t), \dot{\phi}_a(\mathbf{x}, t)) \quad (2.147)$$

In a generic system, a range over all the fields in the theory, be it the metric, matter scalar fields, etc. We will keep the discussion general in this section, and specialize to a FRW cosmology in the next section. The canonical momenta for this system are defined as usual

$$\pi_a = \frac{\partial \mathcal{L}}{\partial \dot{\phi}_a} \quad (2.148)$$

and hence the Hamiltonian is then

$$H[\phi_a(t), \pi_a(t)] = \int d^3x \dot{\phi}_a \pi_a - L \quad (2.149)$$

In the quantum theory, the variables obey the equal time commutators relations

$$[\phi_a(\mathbf{x}, t), \pi_a(\mathbf{y}, t)] = i\delta_{ab}\delta(\mathbf{x} - \mathbf{y}) \quad (2.150)$$

and the other commutators vanish as usual. The Heisenberg equations of motion are then

$$\dot{\phi}_a(\mathbf{x}, t) = i[H[\phi(t), \pi(t)], \phi_a(\mathbf{x}, t)], \quad \dot{\pi}_a(\mathbf{x}, t) = i[H[\phi(t), \pi(t)], \pi_a(\mathbf{x}, t)] \quad (2.151)$$

so far, just the usual story. Now we want to consider the following system. We want to split the fields into a classical part ϕ and its quantum part $\delta\phi$:

$$\phi_a(\mathbf{x}, t) = \bar{\phi}_a(\mathbf{x}, t) + \delta\phi_a(\mathbf{x}, t), \quad \pi_a(\mathbf{x}, t) = \bar{\pi}_a(\mathbf{x}, t) + \delta\pi_a(\mathbf{x}, t) \quad (2.152)$$

where the classical part obey the classical equations of motion

$$\dot{\bar{\phi}}_a(\mathbf{x}, t) = \frac{\delta H[\bar{\phi}(t), \bar{\pi}(t)]}{\delta \bar{\pi}_a(\mathbf{x}, t)}, \quad \dot{\bar{\pi}}_a(\mathbf{x}, t) = \frac{\delta H[\bar{\phi}(t), \bar{\pi}(t)]}{\delta \bar{\phi}_a(\mathbf{x}, t)} \quad (2.153)$$

varying the Hamiltonian density

$$\dot{\bar{\phi}}_a(\mathbf{x}, t) = \int d^3y \frac{\delta H[\bar{\phi}(t), \bar{\pi}(t)]}{\delta \bar{\pi}_a(\mathbf{x}, t)} \delta(\mathbf{x} - \mathbf{y}) \quad (2.154)$$

And the 'background quantities' just commutes the Hamiltonian $[\bar{\phi}(\mathbf{x}, t), H] = [\bar{\pi}(\mathbf{x}, t), H] = 0$. Plugging this equation into (2.150), we see that the perturbations satisfies the commutator

$$[\delta\phi_a(\mathbf{x}, t), \delta\pi_b(\mathbf{y}, t)] = i\delta_{ab}\delta(\mathbf{x} - \mathbf{y}) \quad (2.155)$$

The way to think about this system is that it is a theory of quantized perturbations living on the classical time-dependent background. This should be familiar to you in the context of linear cosmological perturbation theory, but in this section, we will formalize it, and consider beyond linear order perturbation theory.

$$H[\phi(t), \pi(t)] = H[\bar{\phi}(t), \bar{\pi}(t)] + \frac{\delta H[\bar{\phi}(t), \bar{\pi}(t)]}{\delta \bar{\phi}(\mathbf{x}, t)} \delta\phi(\mathbf{x}, t) + \frac{\delta H[\bar{\phi}(t), \bar{\pi}(t)]}{\delta \bar{\pi}(\mathbf{x}, t)} \delta\pi(\mathbf{x}, t) + \tilde{H}[\delta\phi(t), \delta\pi(t); t] \quad (2.156)$$

the first piece describes the background quantities, the second order piece is proportional to the background equations of motion so vanishes and finally the quantum piece that starts at second order in perturbation. In other words, δH contains terms of quadratic and higher order in the quantized perturbations. The perturbation Hamiltonian $\tilde{H}[\delta\phi(t), \delta\pi(t); t]$ term is a functional of the perturbations, with an explicit time dependence on the background values $(\delta\phi(t), \delta\pi(t))$ which we denote by appending a 't' at the end.

To apply this toolkit to cosmology, particularly, we are interested in a Hamiltonian of an interacting theory of primordial curvature perturbation, since it encodes quantum radiative correction for higher order correlation function. This class of Hamiltonian can be split into 2 pieces: the free theory(quadratic) and the interacting(cubic and higher order):

$$H = H_0 + H_{int} \quad (2.157)$$

H_0 correspond to the quadratic y H_I to the interacting term². Concisely, the free theory is related with gaussian statistic and the power spectrum, whereas the second is related with the

²Hereafter: $\tilde{H} \rightarrow H$, $\delta\phi \rightarrow \zeta$

so-called non-gaussianities. Particularly, the quadratic Hamiltonian density for this theory is given by

$$\mathcal{H}_0 = 2\varepsilon \left[\frac{1}{2}\pi^2 - a\frac{1}{2}(\partial\zeta)^2 \right] \quad (2.158)$$

while the remaining higher order terms [23]:

$$\mathcal{H}_{int} = -a^3\varepsilon^2\zeta\pi^2 + 2a\varepsilon^2\zeta(\partial\zeta)^2 - 2a\varepsilon\pi(\partial\zeta)(\partial\chi) + \frac{a^3}{2}\varepsilon\dot{\eta}\zeta^2\pi + \frac{1}{2}\frac{\varepsilon}{a}(\partial\zeta)(\partial\chi)(\partial^2\chi) + \frac{\varepsilon}{4a}\partial^2\zeta(\partial\chi)^2 \quad (2.159)$$

where it has been defined $\partial^2\chi = a^2\varepsilon\dot{\zeta}$, $\varepsilon = -\dot{H}/H^2$ y $\eta = -\dot{\varepsilon}/H^2$. It is worth noting that the first three terms are $O(\varepsilon^2)$ while the rest three are $O(\varepsilon^3)$. For illustrative purposes let us consider only the first term in Eq.(2.159) and compute its contribution to 3-point correlation function of curvature modes by using the in-in formalism:

$$\langle \zeta_{\mathbf{k}_1} \zeta_{\mathbf{k}_2} \zeta_{\mathbf{k}_3} \rangle = \left\langle \left[\bar{T} \exp \left(i \int_{-\infty(1-i\varepsilon)}^{\tau} d\tilde{\tau} \mathcal{H}_{int}(\tilde{\tau}) \right) \right] \zeta_{\mathbf{k}_1}(\tau) \zeta_{\mathbf{k}_2}(\tau) \zeta_{\mathbf{k}_3}(\tau) \left[T \exp \left(-i \int_{-\infty(1+i\varepsilon)}^{\tau} d\tilde{\tau} \mathcal{H}_{int}(\tilde{\tau}) \right) \right] \right\rangle \quad (2.160)$$

where T is the ordering operator and \bar{T} is the anti-temporal ordering as already shown in the previous subsection. Picking up just first term in (2.159) its contribution becomes

$$\begin{aligned} \langle \zeta_{\mathbf{k}_1} \zeta_{\mathbf{k}_2} \zeta_{\mathbf{k}_3} \rangle &= \\ &- 2i\text{Re} \left(\left\langle \zeta_{\mathbf{k}_1} \zeta_{\mathbf{k}_2} \zeta_{\mathbf{k}_3} \int_{-\infty(1+i\varepsilon)}^{\tau} d\tilde{\tau} dx^3 a^2 \varepsilon^2 \zeta(x, \tilde{\tau}) \zeta'(x, \tilde{\tau}) \zeta'(x, \tilde{\tau}) \right\rangle \right) \end{aligned} \quad (2.161)$$

where the apostrophe on the function denotes derivation with respect τ

$$\begin{aligned} \langle \zeta_{\mathbf{k}_1} \zeta_{\mathbf{k}_2} \zeta_{\mathbf{k}_3} \rangle &= \\ &- 2i\text{Re} \left(\left\langle \zeta_{\mathbf{k}_1} \zeta_{\mathbf{k}_2} \zeta_{\mathbf{k}_3} \int \frac{dq_{123}^3}{(2\pi)^9} \int_{-\infty(1+i\varepsilon)}^{\tau} d\tilde{\tau} dx^3 a^2 \varepsilon^2 \zeta_{\mathbf{q}_1}(\tilde{\tau}) \zeta'_{\mathbf{q}_2}(\tilde{\tau}) \zeta'_{\mathbf{q}_3}(\tilde{\tau}) \right\rangle \cdot e^{-i(\mathbf{q}_1 + \mathbf{q}_2 + \mathbf{q}_3) \cdot \mathbf{x}} \right) \end{aligned} \quad (2.162)$$

contracting the internal and external legs

$$\begin{aligned} \langle \zeta_{\mathbf{k}_1} \zeta_{\mathbf{k}_2} \zeta_{\mathbf{k}_3} \rangle &= \\ &- 4i\text{Re} \left(u_{k_1}(0) u_{k_2}(0) u_{k_3}(0) \int \frac{dq_{123}^3}{(2\pi)^9} \int_{-\infty(1+i\varepsilon)}^{\tau} d\tilde{\tau} dx^3 a^2 \varepsilon^2 u_{q_1}^*(\tilde{\tau}) \frac{d}{d\tilde{\tau}} u_{q_2}^*(\tilde{\tau}) \frac{d}{d\tilde{\tau}} u_{q_3}^*(\tilde{\tau}) \right. \\ &\cdot (2\pi)^9 \delta^{(3)}(\mathbf{k}_1 - \mathbf{q}_1) \delta^{(3)}(\mathbf{k}_2 - \mathbf{q}_2) \delta^{(3)}(\mathbf{k}_3 - \mathbf{q}_3) \cdot e^{-i(\mathbf{q}_1 + \mathbf{q}_2 + \mathbf{q}_3) \cdot \mathbf{x}} + 1 \rightarrow 2 + 1 \rightarrow 3 \left. \right) \end{aligned} \quad (2.163)$$

using

$$\frac{du_k(\tau)}{d\tau} = \frac{H}{\sqrt{4\varepsilon k^3}} k^2 \tau e^{ik\tau}, \text{ and } \int dx^3 e^{-i(\mathbf{q}_1 + \mathbf{q}_2 + \mathbf{q}_3) \cdot \mathbf{x}} = (2\pi)^3 \delta^{(3)}(\mathbf{q}_1 + \mathbf{q}_2 + \mathbf{q}_3) \quad (2.164)$$

using $a = -1/H\tau$ for a de Sitter universe the three-point correlation function becomes

$$\begin{aligned} \langle \zeta_{\mathbf{k}_1} \zeta_{\mathbf{k}_2} \zeta_{\mathbf{k}_3} \rangle &\doteq \\ &\left[\frac{-4iH^6}{(4\varepsilon)^3} \frac{1}{(k_1 k_2 k_3)^3} \int_{-\infty(1-i\varepsilon)\tau} d\tilde{\tau} \frac{1}{(H\tilde{\tau})^2} \varepsilon^2 \times (k_2 k_3)^2 \tilde{\tau}^2 (1 + ik_1 \tilde{\tau}) e^{-i(k_1 + k_2 + k_3) \tilde{\tau}} \right] + \text{Sym} \end{aligned} \quad (2.165)$$

where \doteq denotes the equality and the factor $(2\pi)^3 \delta^{(3)}(\mathbf{k}_1 + \mathbf{k}_2 + \mathbf{k}_3)$ on the right hand side at the same time. Integrating the time out

$$\int_{-\infty(1+i\varepsilon)}^{\tau} d\tilde{\tau} (k_2 k_3)^2 (1 + ik_1 \tilde{\tau}) e^{-iK\tilde{\tau}} = (k_2 k_3)^2 \left(\frac{ik_1}{K^2} + \frac{i}{K} - \frac{k_1 \tilde{\tau}}{K} \right) e^{-i(K\tilde{\tau})} |_{-\infty(1+i\varepsilon)}^{\tau} \quad (2.166)$$

$$\langle \zeta_{\mathbf{k}_1} \zeta_{\mathbf{k}_2} \zeta_{\mathbf{k}_3} \rangle \doteq \frac{H^4}{16\varepsilon} \frac{1}{(k_1 k_2 k_3)^3} (k_2 k_3)^2 \left(\frac{1}{K} + \frac{k_1}{K^2} + 1 \rightarrow 2 + 1 \rightarrow 3 \right) \quad (2.167)$$

Obtaining the expression from the first contribution of (2.159) for the non-normalized shape function

$$B_1(k_1, k_2, k_3) = \frac{H^4}{16\varepsilon} \frac{1}{(k_1 k_2 k_3)^3} (k_2 k_3)^2 \left(\frac{1}{K} + \frac{k_1}{K^2} + 1 \rightarrow 2 + 1 \rightarrow 3 \right) \quad (2.168)$$

Considering the remaining terms order $O(\varepsilon^2)$ of (2.159) that contributes to the three point correlation function, it turns out.

$$B(k_1, k_2, k_3) = \frac{H^4}{M_{\text{pl}}^4} \frac{1}{(k_1 k_2 k_3)^3} \frac{1}{4\varepsilon^2} \left[\frac{\eta}{8} \sum k_i^3 + \frac{\varepsilon}{8} \left(- \sum k_i^3 + \sum_{i \neq j} k_i k_j^2 + \frac{8}{K} \sum_{i > j} k_i^2 k_j^2 \right) \right]. \quad (2.169)$$

We see if one of the modes is much longer than the others $k_2, k_3 \gg k_1$ hence $k_2 \sim k_3$, then Eq.(2.169) becomes:

$$\langle \zeta_{\mathbf{k}_1} \zeta_{\mathbf{k}_2} \zeta_{\mathbf{k}_3} \rangle = (2\pi)^3 \delta(\mathbf{k}_1 + \mathbf{k}_2 + \mathbf{k}_3) \frac{H^4}{M_{\text{pl}}^4} \frac{1}{4\varepsilon^2} \left[\frac{\eta + 2\varepsilon}{8} \sum k_i^3 \right] \quad (2.170)$$

identifying $n_s - 1 = -2\varepsilon - \eta$, the above expression reduces to

$$\langle \zeta_{\mathbf{k}_1} \zeta_{\mathbf{k}_2} \zeta_{\mathbf{k}_3} \rangle = (2\pi)^3 \delta^{(3)}(\mathbf{k}_1 + \mathbf{k}_2 + \mathbf{k}_3) (1 - n_s) P(k_1) P(k_2) \quad (2.171)$$

this is known as the **squeezed limit** since the triangle looks like a very squeezed triangle. Comparing to Eq.(2.141), we see that in this limit the slow-roll shape coincides with the local shape so:

$$f_{\text{NL}}^{\text{local}} = -\frac{5}{12}(n_s - 1). \quad (2.172)$$

Note that the two power spectra are of the short and long modes respectively and the slow roll parameters are evaluated at the time the short wavelength modes cross the horizon. In other words, there is a **consistency relation** between the index of the scalar power spectrum and the 3-pt correlation function in the squeezed limit. This is a fairly powerful relationship, the argument laid out above relies on the fact that the long wavelength mode ζ_1 remains frozen out outside the horizon and does not evolve, this is a feature of single scalar field models regardless of the exact details of the potential. Hence if this consistency relationship is not obeyed via observations, then we can rule out single scalar field models. In practice this is a particularly difficult observation to do: the squeezed limit requires $k_2, k_3 \gg k_1$, hence we need a very long wavelength mode. But we only have very few long wavelength modes in the sky due to cosmic variance, hence our ability to observe the squeezed limit of a 3-pt is basically constrained by cosmic variance.

Chapter 3

Cosmic Microwave Background

One of the most important features of the CMB is its Planck spectrum. It follows the blackbody curve to extremely high precision, over a factor of approximately 1000 in frequency Fig.3.1. This implies that the Universe was in thermal equilibrium when the radiation was released, which was at a temperature of approximately 3000K. Today it is near 3K. An even more important feature is that, to better than a part in 10^4 , this temperature is the same over the entire sky. This is surprising because it strongly implies that everything in the observable Universe was in thermal equilibrium at one time in its evolution. The most salient feature is that there are differences in the CMB temperature from place to place, at the level of 10^{-5} , and that these fluctuations have coherence beyond the horizon at the time of last scattering. In particular, for this chapter we are interested only in the photons density contrasts, since, it contain information of matter domination epoch, this time is called the decoupling, in which physically the photons are no longer interact with electrons via Thomson scattering, this contain relic information about how our universe began. Pictorially, the CMB can be viewed as a snapshot of our universe when it was just 380000 years old. Just a baby universe.

This chapter is partially based on [24], [25] and Lecture notes Physics 217bc, spring 2008, Caltech¹.

3.1 CMB anisotropies

Now we will see how the photons density evolves from early time to the present epoch. This anisotropy is observed today as the cosmic microwave background(CMB anisotropy). Photons in the early universe are in thermal equilibrium, with the blackbody distribution momenta. As the epoch of decoupling is approached, the distribution begins to fall out of equilibrium, developing anisotropy which is different for two polarization states. After decoupling at $z \sim 1000$, the redshifting of the photons through the inhomogeneous gravitational field generates more anisotropy, without affecting the polarization states. The reionization at $z \sim 10$ generates further anisotropy and more importantly polarization. The anisotropy

¹<http://www.tapir.caltech.edu/~chirata/ph217/index.html>

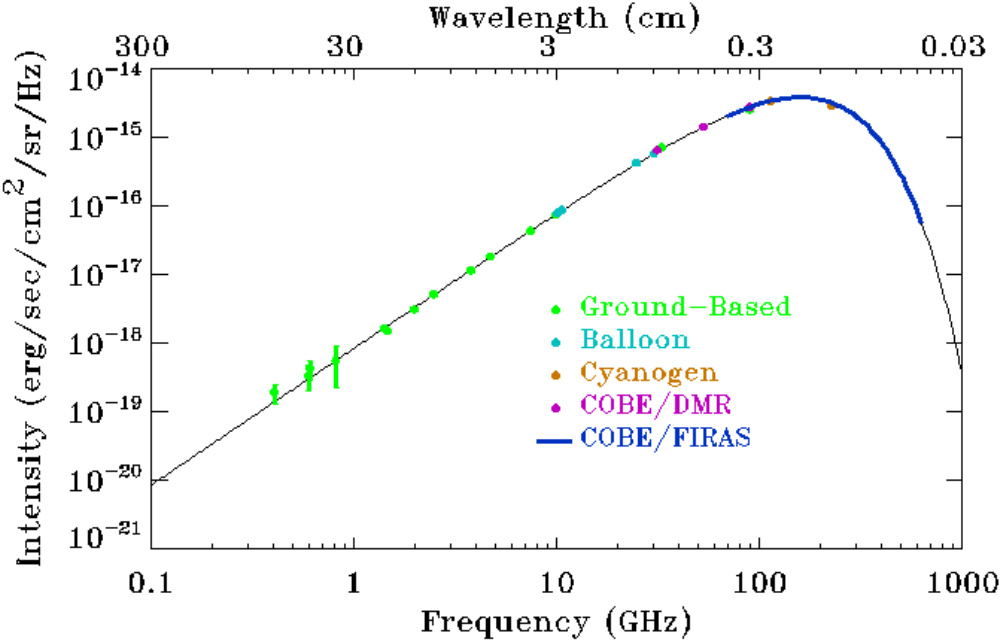


Figure 3.1: Measurements of the CMB intensity vs. frequency together with a fit to the data. Superposed are the expected black body curves for $T = 2\text{K}$ and $T = 40\text{K}$. They are the most precise measurements of the CMB spectrum at the millimeter wavelengths near its peak were made by the Far Infrared Absolute Spectrophotometer(FIRAS) instrument aboard the Cosmic Background Explorer (COBE) satellite. Credit: <https://lambda.gsfc.nasa.gov/product/cobe/>

is characterized by a perturbation in the intensity, which corresponds to a perturbation in the temperature of the blackbody distribution, and by two polarization parameters. In this chapter, we study the temperature and polarization fluctuations. The observed perturbation scales correspond to larger cosmological scales $k \sim 0.1 \text{ Mpc}^{-1}$. In this regime, first-order cosmological perturbation theory is almost always a good approximation, failing only on smaller scales and later times. We start our study with a perturbation called the *brightness function* Θ defined on the two-sphere for a given spacetime position.

$$\Theta(\eta, \mathbf{x}, \hat{n}) = \frac{\delta T(\eta, \mathbf{x}, \hat{n})}{T(\eta)} \quad (3.1)$$

where η^2 is the conformal time and $\hat{n} = \mathbf{p}/p$ is the direction of the incoming photons or equivalently in the direction where photons are seen $-\mathbf{e}$, and \mathbf{x} is the observer position. This field can be decomposed on the 2-sphere, such as

$$\Theta(\eta, \mathbf{x}, \hat{n}) = \sum_{l=0}^{\infty} \sum_{m=-l}^{m=l} (-1)^l \Theta_{lm}(\eta, \mathbf{x}) Y_{lm}(\hat{n}) = \sum_{l=0}^{\infty} \sum_{m=-l}^{m=l} \Theta_{lm}(\eta, \mathbf{x}) Y_{lm}(\mathbf{e}) \quad (3.2)$$

We see that the monopole $l = 0$ is related to photon energy density contrast by [26]:

$$\Theta_{00}(\eta, \mathbf{x}) = \frac{1}{4} \delta_{\gamma}(\eta, \mathbf{x}) \quad (3.3)$$

²often in matter domination epoch η is used instead of τ to denote the conformal time. While τ is reserved to the optical depth of reionization. This chapter will be the exception.

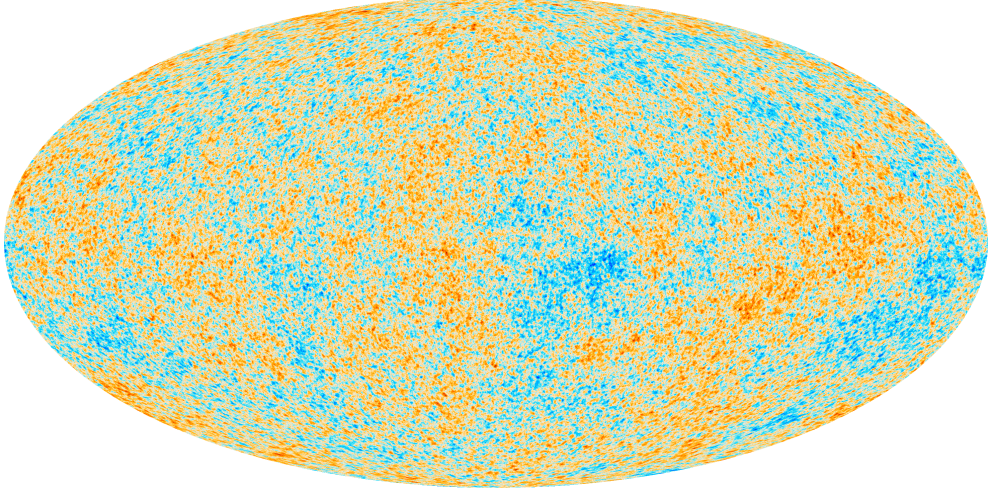


Figure 3.2: Angular anisotropies. <https://www.cosmos.esa.int/web/planck/planck-collaboration>.

that means that the dipole needs a slicing to be defined, but is independent of the threading since it is a scalar. Additionally, it means that we cannot determine the monopole, because there is no way of measuring the photon energy density at positions other than our own. The dipole $l = 1$ is the Doppler shift caused by the motion of the photon fluid relative to the observer,

$$\sum_m \Theta_{1m} Y_{1m}(\mathbf{e}) = -\mathbf{v}_\gamma \cdot \mathbf{e}. \quad (3.4)$$

We have evaluated the Doppler shift to first order in \mathbf{v}_γ (non-relativistic formula). At this point, we have to distinguish between an observer who moves with the gauge threading used to implement cosmological perturbation theory. It is easy to see that the dipole depends on the gauge threading, but not the slicing. For this observer, \mathbf{v}_γ is a cosmological perturbation and the evaluation of the Doppler shift to first order just corresponds to first order cosmological perturbation theory. The observed multipoles with $l \geq 2$, therefore, represent the intrinsic anisotropy of the CMB. They are denoted by Θ_{lm} :

$$a_{lm} = \Theta_{lm}(\eta = \eta_0, \mathbf{x} = 0) \quad (3.5)$$

where $\mathbf{x} = 0$ is our current position relative to the CMB rest frame and η_0 is the actual time. Therefore we need to understand the statistic of the local multipoles $a_{lm}(\eta, 0)$. To do this let first consider the Fourier decomposition of the field:

$$\Theta(\eta, \mathbf{x}, \hat{n}) = \int \frac{d^3 k}{(2\pi)^3} \Theta(\eta, \mathbf{k}, \hat{n}) e^{i\mathbf{k}\mathbf{x}} \quad (3.6)$$

At $\mathbf{x} = 0$, the last exponential is just equal to 1. Additionally, we can expand the angular Fourier components into spherical harmonics, such that:

$$\Theta(\eta, \mathbf{k}, \hat{n}) = \sum_{l=0}^{\infty} (-i)^l \sqrt{4\pi(2l+1)} \Theta_l(\eta, \mathbf{k}) Y_{l0}(\theta', \phi') \quad (3.7)$$

where θ', ϕ' are the angular variables with the 3-axis rotated in such a way that it points in the direction of the wavenumber \hat{k} , that is $\cos \theta = \hat{n} \cdot \hat{k}$. Since the spherical harmonics are

related to Legendre polynomials we have the following relation:

$$Y_{l0}(\theta', \phi') = \sqrt{\frac{2l+1}{4\pi}} P_l(\theta') \quad (3.8)$$

Therefore we have:

$$\Theta(\eta, \mathbf{k}, \hat{n}) = \sum_{l=0}^{\infty} (-i)^l (2l+1) \Theta_l(\eta, \mathbf{k}) P_l(\hat{n} \cdot \hat{k}) \quad (3.9)$$

whereas in real space

$$\Theta(\eta, 0, \hat{n}) = \int \frac{d^3 k}{(2\pi)^3} \sum_{l=0}^{\infty} (-i)^l (2l+1) \Theta_l(\eta, \mathbf{k}) P_l(\hat{n} \cdot \hat{k}). \quad (3.10)$$

In order to get a_{lm} we use the addition theorem:

$$P_l(\hat{n} \cdot \hat{k}) = \frac{4\pi}{(2l+1)} \sum_{m=-l}^{m=l} Y_{ml}^*(\hat{k}) Y_{ml}(\hat{n}) \quad (3.11)$$

so that Eq.(3.6) becomes

$$\Theta(\eta, 0, \hat{n}) = 4\pi \sum_{l,m} \int \frac{d^3 k}{(2\pi)^3} (-i)^l \Theta_l(\eta, \mathbf{k}) Y_{ml}^*(\hat{k}) Y_{ml}(\hat{n}) \quad (3.12)$$

we can read of the multipoles as

$$a_{lm}(\eta) = 4\pi (-i)^l \int \frac{d^3 k}{(2\pi)^3} \Theta_l(\eta, \mathbf{k}) Y_{lm}^*(\hat{k}) \quad (3.13)$$

The ensemble average of $\langle a_{lm} \rangle$ is equal zero, therefore they are equally positive or negative, this fact reflects the statistical isotropy of the primordial probability distribution, nevertheless the second moment of the multipoles are not, so we are interested in its variance. For doing that we compute the equal time correlation function:

$$\langle a_{lm}(\eta) a_{l'm'}^*(\eta) \rangle = 16\pi^2 \int \frac{d^3 k}{(2\pi)^3} \int \frac{d^3 k'}{(2\pi)^3} (-i)^{l'-l} \langle \Theta_l(\mathbf{k}, \eta) \Theta_{l'}(\mathbf{k}', \eta) \rangle Y_{l'm'}^*(\hat{k}') Y_{lm}(\hat{k}). \quad (3.14)$$

the field Θ can be written in terms of the primordial curvature perturbations generated by quantum fluctuation during inflation, whose relation is :

$$\langle \Theta_l(\mathbf{k}) \Theta_{l'}(\mathbf{k}') \rangle = \frac{\Theta_l(\mathbf{k})}{\zeta(\mathbf{k})} \frac{\Theta_{l'}^*(\mathbf{k}')}{\zeta^*(\mathbf{k}')} \langle \zeta(\mathbf{k}) \zeta^*(\mathbf{k}') \rangle = T_l(k) T_{l'}^*(k') \langle \zeta(\mathbf{k}) \zeta^*(\mathbf{k}') \rangle. \quad (3.15)$$

Notice that the ratios between Θ and ζ are direction independent. They are called transfer functions, $T_l(k)$, and encodes the adiabatic mode evolution, explicitly they depend on the physics between the horizon re-entry and its evolution afterward. Moreover, the correlation function on the R.H.S. satisfies:

$$\langle \zeta(\mathbf{k}) \zeta^*(\mathbf{k}') \rangle = (2\pi)^3 P_\zeta(k) \delta^3(\mathbf{k} - \mathbf{k}'), \quad (3.16)$$

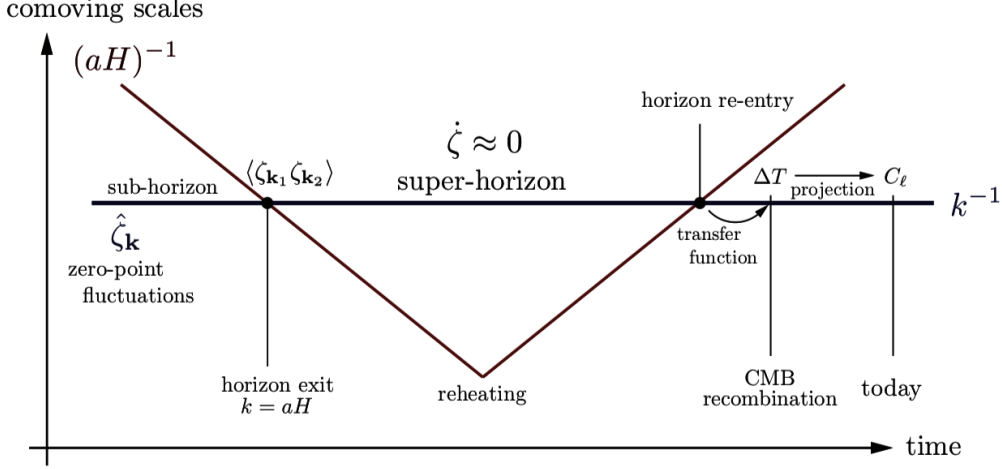


Figure 3.3: Modes evolution: Overdensities are generated during the inflation as quantum fluctuations. As the horizon shrinks the wavelength of the curvature modes becomes larger than the horizon(aka. they exit the horizon) and consequently they freeze and become classical. After the hot big bang era or recombination, these modes re-enter the horizon and they start to grow according to the underlying subhorizon physics, finally at decoupling or recombination, they leave defined statistical fingerprints which are transported and projected through incoming photons from the CMB toward us. Credit: <http://www.damtp.cam.ac.uk/user/db275/Cosmology/Lectures.pdf>.

where $P_\zeta(k)$ is the primordial curvature power spectrum. Therefore, the equal time correlation function (3.14) reduces to:

$$\langle a_{lm}(\eta) a_{l'm'}^*(\eta) \rangle = 16\pi^2 \int \frac{d^3k}{(2\pi)^3} (i)^{l'-l} T_l^2(k) P_\zeta(k) Y_{l'm'}^*(\hat{k}) Y_{lm}(\hat{k}). \quad (3.17)$$

Separating the k integral into a radial and an angular part to integrate the above expression,

$$\int \frac{d^3k}{(2\pi)^3} = \int \frac{k^3 d \ln k}{(2\pi^2)} \int \frac{d^2\hat{k}}{4\pi}. \quad (3.18)$$

Finally we get

$$\langle a_{lm} a_{l'm'}^* \rangle = 16\pi^2 (i)^{l'-l} \int \frac{d^2\hat{k}}{4\pi} Y_{lm}^*(\hat{k}) Y_{l'm'}(\hat{k}) \int \frac{k^3 d \ln k}{(2\pi^2)} T_l^2(k) P_\zeta(k) \quad (3.19)$$

$$\langle a_{lm} a_{l'm'}^* \rangle = \delta_{ll'} \delta_{mm'} 4\pi \int d \ln k T_l^2(k) \mathcal{P}_\zeta(k) \quad (3.20)$$

the above expression defines the angular power spectrum as:

$$\langle a_{lm} a_{l'm'}^* \rangle = \delta_{ll'} \delta_{mm'} C_l, \quad C_l = 4\pi \int d \ln k \mathcal{P}_\zeta(k) T_l^2(k), \quad (3.21)$$

where we have defined the dimensionless curvature power spectrum as $\mathcal{P}_\zeta(k) = k^3 P_\zeta(k)/(2\pi^2)$ and the power spectrum anisotropy as $C_l = \langle |a_{lm}|^2 \rangle$, is the variance of a gaussian distribution for a realization of the value a certain multipole a_{lm} . The above companion $\delta_{ll'} \delta_{mm'}$ (with the

condon-shorty phase convention) tell us that the different modes are statistical independent or simple do not have any correlation. While its variance, C_l , only depend on the angular number l reflect the fact of an ensemble rotationally invariant. The C_l 's are quantities that most of CMB observers aim to measure. The l number has associated an intrinsic angular scale $\theta \sim \pi/l$, thus a dominant physical scale $x \sim r_{\text{CMB}}\theta \sim \pi r_{\text{CMB}}$ with a wavenumber $k \sim l/r_{\text{CMB}}$.

Usually, the angular power spectrum is measured starting from $l = 2$. This is because the monopole is unobservable; we do not know the true mean value of the CMB temperature fluctuations, only its value in our location and technically it depends on the gauge time slicing and therefore gauge dependent. The dipole $l = 1$ depend on the observer velocity, so it has no absolute meaning. It does not make any sense to ask that is the CMB dipole in a frame relative to distant galaxies, but the latter frame is not known well. The multipole measured from $l \geq 2$ in the CMB rest frame are well defined and genuinely gauge invariant. The power spectrum defined here is dimensionless, but some of the CMB observers prefer to quote a_{lm} in mK i.e. they report the perturbations ΔT from the mean temperature T_γ rather than their fractional temperature $\Delta T/T_0$. In this case the power spectrum Eq.(3.21) must be multiplied by $T_{\gamma 0}^2$, where $T_{\gamma 0} = 2.73 \cdot 10^6 \mu\text{K}$.

Another important limitation is the fact that we just have one universe in which we have a limited access to sample its statistical distribution; a typical difference between C_l and actually measured multipole will be of order the rms deviation of $|a_{lm}|^2$ from C_l . The latter is given by

$$(\Delta C_l)^2 = \langle (|a_{lm}|^2 - C_l)^2 \rangle = \langle |a_{lm}|^4 - C_l^4 \rangle \quad (3.22)$$

This is the cosmic variance of C_l , similar to the cosmic variance of correlators of Fourier components. The real and imaginary parts of the multipoles will have independent Gaussian probability distributions, provided that the primordial distribution is Gaussian. If a single real or imaginary part is measured the cosmic variance is $2C_l^2$. If all $(2l + 1)$ independent components of a_{lm} are measured, the cosmic variance is reduced by a factor $(2l + 1)$. If the data are further binned by averaging over a range Δl around l , this reduces the cosmic variance by an additional factor Δl , giving

$$(\Delta C_l)^2 = \frac{2}{(2l + 1)\Delta l} C_l^2. \quad (3.23)$$

The cosmic variance is a serious limitation for low l but becomes negligible at higher l . It is worth remarking that direct observational constraints on non-gaussianity become very weak on large scales, corresponding to very low multipoles of CMB. Indeed, in this regime, they come only from CMB itself, and they depend on the assumed form of non-gaussianity. However, at least within an inflationary scenario, one does not expect an abrupt change from Gaussianity.

3.2 Radiative transfer: from recombination to today.

In this section, we consider what happens to photons after recombination. We clearly need to compute Θ_l and hence the CMB power spectrum. In absence of scattering, the photon

multipoles equations are:

$$\Theta_0 = -k\Theta_1 - \dot{\Phi}; \quad (3.24)$$

$$\dot{\Theta}_1 = \frac{k}{3}(\Theta_0 - 2\Theta_2) + \frac{1}{3}k\Psi; \quad (3.25)$$

$$\dot{\Theta}_l = \frac{k}{2l+1} [l\Theta_{l-1} - (l+1)\Theta_{l+1}]. \quad (3.26)$$

$$(3.27)$$

These equations simplify if we note that $\Psi = -\Phi$ once the photons and neutrinos do not contribute significantly to the energy density, and defining:

$$\bar{\Theta}_0 = \Theta_0 + \Psi = \Theta_0 - \Phi; \quad \bar{\Theta} = \Theta \quad (l \geq 1). \quad (3.28)$$

The system of equations reduces to:

$$\dot{\bar{\Theta}}_0 = -k\bar{\Theta}_1 - 2\dot{\Phi} \text{ and} \quad (3.29)$$

$$\dot{\bar{\Theta}}_l = \frac{k}{2l+1} [l\bar{\Theta}_{l-1} - (l+1)\bar{\Theta}_{l+1}]; \quad (l \geq 1) \quad (3.30)$$

Since the universe was optically thick(large $\dot{\tau}$) prior to recombination, we will have $\Theta_l(\eta_{\text{rec}}) = 0$ for $l \geq 2$. Thus the solutions to (3.29) are determined by the initial conditions $\bar{\Theta}_{0,1}(\eta_{\text{rec}})$ and the metric source $\dot{\Phi}(\eta)$. Since the equation is linear, these three contributions can be assessed separately.

- **Initial monopole perturbation.** Let us suppose first that at recombination $\bar{\Theta}_0 = 1$ and $\bar{\Theta}_l = 0(l \geq 1)$, and that $\dot{\Phi} = 0$. from the derivative relation for spherical Bessel functions,

$$(2l+1)j_l'(x) = l j_{l-1}(x) - (l+1)j_{l+1}(x), \quad (3.31)$$

we can see that the solutions are

$$\bar{\Theta}_l = j_l(k\Delta\eta), \quad \Delta\eta = \eta - \eta_{\text{rec}}. \quad (3.32)$$

This is not surprising: since in this approximation the photons are simple free-streaming, one would expect that at $k\Delta\eta < 1$ an observer should see only a monopole, but at late times an observer sees many ($\approx \Delta\eta/\lambda = k\Delta\eta/2\pi$) perturbation wavelength. In this case, the dominant multipole is:

$$l \sim k\Delta\eta. \quad (3.33)$$

Since $j_l(x)$ peaks at $x \sim l$ this is indeed what we get.

- **Initial dipole perturbation.** Now let us suppose that initially $\bar{\Theta}_1 = 1$, all other $\bar{\Theta}_l$ vanish. Also suppose $\dot{\Phi} = 0$ at all times. Since the equations of motion are η -independent, if $j_l(k\Delta\eta)$ is a solution, then the derivative with respect to η of this is also a solution.

$$\bar{\Theta} = 3j_l'(k\Delta\eta). \quad (3.34)$$

This is the solution that satisfies our initial conditions; recall that at small x , $j_l(x) \rightarrow x^l/(2l+1)!!$. At large l this is very similar to the monopole solution, expect that there is a factor 3, and the ' implies that the phase of oscillation is 90 out of phase from the monopole.

- **Time-varying potentials.** We take a Green's function approach. If initially $\bar{\Theta}_l = 0$, but $\dot{\Phi}$ is a delta function at some conformal time η_1 ,

$$\dot{\Phi} = \delta(\eta_1), \quad (3.35)$$

then immediately afterwards $\bar{\Theta}_0 = -2$, and the subsequent evolution is:

$$\bar{\Theta}_l = -2j_l(k(\eta - \eta_1)) \quad (3.36)$$

We can get the evolution for general $\dot{\Phi}$ by a superposition:

$$\bar{\Theta}_l = -2 \int_{\eta_{\text{rec}}}^{\eta} d\eta_1 \dot{\Phi}(\eta_1) j_l(k(\eta - \eta_1)) \quad (3.37)$$

- **Complete solution.** The complete solution to the problem is obtained by superposition:

$$\Theta_l = (\Theta_0(\eta_{\text{rec}}) - \Phi(\eta_{\text{rec}})) j_l(k\Delta\eta) + 3\Theta_1 j'_l(k\Delta\eta) - 2 \int_{\eta_{\text{rec}}}^{\eta} d\eta_1 \dot{\Phi}(\eta_1) j_l(k(\eta - \eta_1)) \quad (3.38)$$

for $l \geq 1$. These three terms are generally called the monopole, dipole, and the integrated Sachs-Wolfe(ISW) terms.

3.3 Large scales: The Sachs-Wolfe effect

We begin our study with the largest scales in the CMB, in which the Sachs-Wolfe(SW) effect takes place. The SW is a property of the CMB, in which photons from the CMB are gravitationally redshifted, causing the CMB spectrum to appear uneven. This effect is the predominant source of fluctuations in the CMB for angular scales above about ten degrees; those were outside the horizon at recombination, this condition requires $k\eta_{\text{rec}} < 1$ or:

$$l < \frac{r_{\text{CMB}}}{\eta_{\text{rec}}} \approx \frac{\eta_0}{\eta_{\text{rec}}} = 50 \quad (3.39)$$

In this case, at recombination, we may take as an initial condition the matter-dominated photons multipole moments:

$$\Theta_0 = \frac{3}{5}\Phi(0); \quad \Theta_1 = \frac{3}{5}i\Phi(0)(k\eta_0)^{1/2}; \quad \Phi = \frac{9}{10}\Phi(0) \quad (3.40)$$

The higher multipoles are zero at $\eta = \eta_{\text{rec}}$, since $k\eta_{\text{rec}} < 1$, the dipole term is negligible. We will also ignore the effects of the cosmological constant Λ , so that we are in matter domination, therefore $\Phi' = 0$, that is to say no integrated SW effect. Then:

$$\Theta_l(\eta_0) = -\frac{3}{10}\Phi(0)j_l(k(\eta_0 - \eta_{\text{rec}})) \approx -\frac{3}{10}\Phi(0)j_l(k\eta_0) = -\frac{1}{5}\zeta j_l(k\eta_0) \quad (3.41)$$

the CMB power spectrum is then:

$$C_l = \frac{4\pi}{25} \int d\ln k \mathcal{P}_{\zeta}(k) |j_l(k\eta_0)|^2. \quad (3.42)$$

Now let us suppose that $\mathcal{P}_\zeta(k)$ is a power law, as predicted by inflation with a smooth potential:

$$\mathcal{P}_\zeta(k) = \mathcal{P}_\zeta(\eta_0^{-1})(k\eta_0)^{n_s-1} \quad (3.43)$$

then

$$C_l = \frac{4\pi}{25} \mathcal{P}_\zeta(\eta_0^{-1}) \int_0^\infty d \ln k (k\eta_0)^{n_s-1} |j_l(k\eta_0)|^2 = \frac{4\pi}{25} \mathcal{P}_\zeta(\eta_0^{-1}) \int_0^\infty \frac{dx}{x} x^{n_s-1} |j_l(x)|^2 \quad (3.44)$$

The last integral can be evaluated to give:

$$C_l = \frac{2^{n_s-2}\pi^2}{25} \mathcal{P}_\zeta(\eta_0^{-1}) \frac{\Gamma(l+n_s/2-1/2)\Gamma(3-n_s)}{\Gamma(l+5/2-n_s/2)\Gamma^2(2-n_s/2)}. \quad (3.45)$$

An important case is when $n_s = 1$, for which we get:

$$\frac{l(l+1)}{2\pi} C_l = \frac{\mathcal{P}_\zeta(\eta_0^{-1})}{25} = \text{Constant}. \quad (3.46)$$

For this reason, CMB observers often make plots of angular power spectrum with $l(l+1)C_l/2\pi$ on the vertical axis. If $n_s \neq 1$, but $l \gg 1$, then we can apply Stirling's formula to the Γ 's and get:

$$C_l \approx \frac{2^{n_s-2}\pi^2\Gamma(3-n_s)}{25\Gamma^2(2-n_s/2)} \mathcal{P}_\zeta(\eta_0^{-1}) l^{n_s-3}, \quad (3.47)$$

so find the dependence:

$$\frac{l(l+1)}{2\pi} C_l \propto l^{n_s-1}. \quad (3.48)$$

For $n_s > 1$ this means the CMB power spectrum increases as one goes to smaller angular scales, while for $n_s < 1$ the opposite occurs. In principle, one can measure n_s this way. In practice the ISW effect is important at lowest range of l 's, where the Bessel function are slowly varying, and there is a limited range of l 's satisfying the condition $l < \eta_0/\eta_{\text{rec}}$. Therefore in order to measure n_s one resorts to a global fit to all the CMB data which includes scales that were inside the horizon at recombination. We will study next.

3.3.1 Acoustic peaks

Now let's consider the scale that was inside the horizon at the time of equality. Using (3.38), the anisotropy today is:

$$C_l = 4\pi \int d \ln k \mathcal{P}_\zeta(k) \left| \frac{\Theta_0(k)}{\zeta} j_l(k\Delta\eta) + 3 \frac{\Theta_0(k)}{\zeta} j'_l(k\Delta\eta) \right|^2 \quad (3.49)$$

where $\Delta\eta = \eta_0 - \eta_{\text{rec}}$. These terms correspond to the monopole photon perturbation, the dipole term o the last scattering surface. We can simplify the integrals if we go to late times, that is to say, $k\Delta\eta \gg 1$, and we use the asymptotic form of the spherical Bessel function for

$l \gg 1$. The function $j_l(x)$ goes to zero if $x < l + 1/2$, and for $x > l + 1/2$ we have:

$$j_l(x) \rightarrow \frac{1}{l + 1/2} \frac{\cos \beta}{\sqrt{\sin \beta}} \cos \left[\left(l + \frac{1}{2} \right) (\tan \beta - \beta) - \frac{\pi}{4} \right], \quad (3.50)$$

$$j'_l(x) \rightarrow \frac{-1}{l + 1/2} \cos \beta \sqrt{\sin \beta} \sin \left[\left(l + \frac{1}{2} \right) (\tan \beta - \beta) - \frac{\pi}{4} \right], \quad (3.51)$$

$$x = \left(l + \frac{1}{2} \right) \sec \beta, \quad (3.52)$$

where $x \leq \beta < \pi/2$. The above equations correspond the WKB solutions. Now we can exchange the integral form k to β , by using:

$$k = \frac{\sqrt{3}}{\eta_{\text{rec}}} \left(l + \frac{1}{2} \right) \sec \beta, \quad (3.53)$$

and $d \ln k = \tan \beta d\beta$. At large l , the arguments $(l + 1/2)(\tan \beta - \beta)$ are rapidly varying so we can replace the squares of Bessel functions with their cycle averages using $\cos^2, \sin^2 \rightarrow 1/2$ $\sin \cos \rightarrow 0$:

$$(j_l(x))^2 \rightarrow \frac{1}{2(l + 1/2)^2} \frac{\cos^2 \beta}{\sin \beta}, \quad (3.54)$$

$$(j'_l(x))^2 \rightarrow \frac{1}{2(l + 1/2)^2} \frac{\cos^2 \beta}{\sin \beta}, \quad (3.55)$$

$$(j_l(x))^2 (j'_l(x))^2 \rightarrow 0. \quad (3.56)$$

The last results mean that in the high l limit, the correlation between the monopole and the dipole terms vanish, which is what we should expect since the dipole is equally likely to point toward the observer as away so it ought to add incoherently to the monopole. In the C_l formula we have:

$$C_l = 2\pi \int d\beta \tan \beta \mathcal{P}_\zeta(k) \left| \frac{\bar{\Theta}_0}{\zeta} \right|^2 \frac{1}{(l + 1/2)^2} \frac{\cos^2 \beta}{\sin \beta} \tan \beta \quad (3.57)$$

$$+ 18\pi \int d\beta \tan \beta \mathcal{P}_\zeta(k) \left| \frac{\bar{\Theta}_1}{\zeta} \right|^2 \frac{1}{(l + 1/2)^2} \cos^2 \beta \sin \beta \tan \beta d\beta \quad (3.58)$$

given the fact we are working at high l we may simplify further and display the above expression as $l(l + 1)C_l/2\pi$ form:

$$\frac{l(l + 1)}{2\pi} C_l = \int_0^{\pi/2} d\beta \mathcal{P}_\zeta(k) \left| \frac{\bar{\Theta}_0}{\zeta} \right|^2 \cos \beta + 9 \int_0^{\pi/2} d\beta \mathcal{P}_\zeta(k) \left| \frac{\bar{\Theta}_1}{\zeta} \right|^2 \cos \beta \sin^2 \beta \quad (3.59)$$

The physical remaining of this equation is that $\pi/2 - \beta$ is the angle between the Fourier mode \mathbf{k} and the line of sight. The integration over $\cos \beta d\beta$ represents the averaging of such angles over the unit sphere, $\bar{\Theta}$ is the monopole, and the Doppler term has a $\sin \beta$ in amplitude($\sin^2 \beta$ in power) because only the line of sight component of the velocity is relevant.

Specific values. For $k \gg k_{\text{eq}}$, the photon perturbations at the time of recombination were:

$$\Theta_0(\eta_{\text{rec}}) = -\zeta \cos \frac{k\eta_{\text{rec}}}{\sqrt{3}}; \quad \Theta_1(\eta_{\text{rec}}) = \frac{\zeta}{\sqrt{3}} \sin \frac{k\eta_{\text{rec}}}{\sqrt{3}} \quad (3.60)$$

with the potential $\Phi \rightarrow 0$. This correctly predicts that the function $\bar{\Theta}_0/\zeta$ and $\bar{\Theta}_1/\zeta$ are oscillatory, and that this will give rise to oscillations in (3.59) since the integrands are dominated by $k \sim l/r_{\text{CMB}}$. Since the $\bar{\Theta}_0/\zeta$, $\bar{\Theta}_1/\zeta$ are squared, the period of oscillation is now:

$$\Delta k = \frac{\pi\sqrt{3}}{\eta_{\text{rec}}} \quad (3.61)$$

and this corresponds to oscillations in l of:

$$\Delta l = r_{\text{CMB}}\Delta k = \frac{\pi\sqrt{3}r_{\text{CMB}}}{\eta_{\text{rec}}} = \pi\sqrt{3}\frac{\eta_0}{\eta_{\text{rec}}} \approx 270 \quad (3.62)$$

for $\eta_0/\eta_{\text{rec}} = 50$. And this is indeed *what* we see. A second prediction from this approximation, which does not come out correctly, is the amplitude of fluctuations. At large l , where the amplitude over β smooths out the oscillations, we predict:

$$\frac{l(l+1)}{2\pi} C_l \rightarrow \mathcal{P}_\zeta(k) \quad (3.63)$$

which is wrong: it overpredicts the CMB fluctuations. There are two major reasons for this: first, the amplitude of $\bar{\Theta}_0$ as written above is only valid if k is much greater than k_{eq} , which is not true of modes relevant for CMB; and second photons can diffuse relative to the baryons since $\dot{\tau}$ is not infinite. Both of these facts bring down the fluctuation power. In fact, there is no range of k in which one can simultaneously neglect diffusion and take $k \gg k_{\text{eq}}$. The first effect can only be derived by numerical calculation, since there is no analytic solution to modes that are the order of the horizon scale, and are near matter-radiation equality. It brings a factor of ~ 4 suppression in C_l . The second effect can be treated analytically, which we do next.

3.4 The damping tail

At very small scales, we must consider the fact that photons have a finite mean free path. We will give two treatments of the effect: first an order-of-magnitude treatment, and then treatment base on the Boltzmann hierarchy.

Diffusion length. We will first try to estimate the comoving mean free path of photons is given by:

$$L_{\text{mfp}} = \frac{1}{n_e \sigma_T a} = \frac{a^2}{n_{H,0} \sigma_T x_e}, \quad (3.64)$$

where $n_{H,0} = 2 \cdot 10^{-7} \text{ cm}^{-3}$ is the comoving density of hydrogen atoms. Now the conformal time between scatterings is:

$$\Delta\eta = \frac{1}{L_{\text{mfp}}}. \quad (3.65)$$

The distance-squared traveled by a photon by diffusion adds incoherently after each scattering: (the number of scattering $\int d\eta/\eta$)

$$\Delta x^2 \sim \int L_{\text{mfp}}^2 \frac{d\eta}{\eta} = \int L_{\text{mfp}} d\eta = \frac{1}{n_{H,0} \sigma_T} \int d\eta \frac{a^2}{x_e}. \quad (3.66)$$

If recombination were instantaneous ($x_e = 1$ until η_{rec}), and we assume matter domination so $a \propto \eta^2$, this would imply:

$$\Delta x^2 \sim \frac{a^2(\eta_{\text{rec}})\eta_{\text{rec}}}{5n_{H,0}\sigma_T} \sim \frac{(10^{-3})^2(300\text{Mpc})}{5 \cdot 2 \cdot 10^{-7}\text{cm}^3 \cdot 7 \cdot 10^{-25}\text{cm}^2} \sim 140\text{Mpc}^2, \quad (3.67)$$

so a photon can actually travel about 12Mpc comoving prior to recombination. In reality, the distance is a little bit larger because x_e drops as hydrogen begins to recombine, and hence there's a rise in the integrand before the surface of last scattering at $x_e \sim 0.1$.

Boltzmann equation treatment. The formal way to treat the diffusion effects is by including the Θ_2 term in the Boltzmann equation. Leaving out the potential, and neglecting the Θ_3 term which is suppressed relative to Θ_2 by another factor of $\dot{\tau}$, we get:

$$\dot{\Theta}_0 = -k\Theta_1 \quad (3.68)$$

$$\dot{\Theta}_1 = \frac{1}{3}k(\Theta_0 - 2\Theta_2) + \dot{\tau} \left(\Theta_1 - \frac{1}{3}iv_b \right) \quad (3.69)$$

$$\dot{\Theta}_2 = \frac{2}{5}k\Theta_1 + \frac{9}{10}\dot{\tau}\Theta_2 \quad (3.70)$$

If we neglect baryon inertia ($R \ll 1$) so that the baryon come to the photon rest frame instantaneously then we can neglect the $\dot{\tau}$ term in $\dot{\Theta}_1$ because $v_b = -3i\Theta_1$. Then we find:

$$\frac{\partial}{\partial\eta} \begin{pmatrix} \Theta_0 \\ \Theta_1 \\ \Theta_2 \end{pmatrix} = \begin{pmatrix} 0 & -k & 0 \\ k/3 & 0 & -2k/3 \\ 0 & 2k/5 & 9\dot{\tau}/10 \end{pmatrix} \begin{pmatrix} \Theta_0 \\ \Theta_1 \\ \Theta_2 \end{pmatrix} \quad (3.71)$$

In practice $\dot{\tau}$ is varying, but on small scales, one may take a WKB approximation and treat it as approximately constant over a cycle. One may then determine the dispersion relation of the acoustic waves by looking at the eigenvalues of the 3x3 matrix. The determinant is:

$$\begin{vmatrix} -\omega & -k & 0 \\ k/3 & -\omega & -2k/3 \\ 0 & 2k/5 & 9\dot{\tau}/10 - \omega \end{vmatrix} = 0 \quad (3.72)$$

which gives:

$$-\frac{4}{5}k^2\omega + \left(\omega^2 + \frac{k^2}{3} \right) \left(\frac{9}{10}\dot{\tau} - \omega \right) = 0. \quad (3.73)$$

This is a cubic equation and has three roots. In the limit $|\dot{\tau}| \gg |\omega|$, the solutions are $\omega \pm ik/\sqrt{3}, 9\dot{\tau}/10$. We want to know the leading-order corrections to two oscillatory solutions(the exponentially decaying solution is not of interest). In this case, $|\omega| \gg |\dot{\tau}|$, so we approximate:

$$-\frac{4}{15}k^2\omega + \frac{9}{10}\dot{\tau} \left(\omega^2 + \frac{k^2}{3} \right) = 0 \quad (3.74)$$

We let $\omega \pm ik/\sqrt{3} + \varepsilon$:

$$-\frac{4}{5}k^2 \frac{\pm ik}{\sqrt{3}} + \frac{9}{10}\dot{\tau} \left(-\frac{1}{3}k^2 \pm \frac{2}{\sqrt{3}}ik\varepsilon + \frac{1}{3}k^2 \right) = 0 \quad (3.75)$$

The solution is:

$$\varepsilon = 4 \frac{k^2}{27\dot{\tau}}, \quad (3.76)$$

so

$$\omega = \pm \frac{ik}{\sqrt{3}} + 4 \frac{k^2}{27\dot{\tau}} \quad (3.77)$$

Since $\dot{\tau} < 0$ this means that the acoustic waves decay. The amplitude decays by a factor

$$\exp \left(- \int \frac{4k^2}{27|\dot{\tau}|} d\eta \right). \quad (3.78)$$

This is usually written as e^{-k^2/k_D^2} , where the damping scale is:

$$k_D^{-2} = \int \frac{4}{27|\dot{\tau}|} d\eta = \frac{4}{27} \int \frac{d\eta}{n_e \sigma_T a} \quad (3.79)$$

Thus wavenumbers smaller than the photon diffusion length are wiped out. In reality, there are finite baryon inertia corrections to this equation, and also the photons develop polarization which causes additional anisotropic scattering the factor of 4/27 should be 8/45.

3.5 Cosmology from the CMB power spectrum

We have seen that the CMB power spectrum is quite rich in features. It has the Sachs-Wolfe plateau at low l , then a series of acoustic peaks, and finally a damping tail. This spectrum allows us to obtain a number of cosmological observables.

- **Amplitude and slope.** The overall normalization and tilt of the CMB power spectrum allow one to estimate $\mathcal{P}(k)$ and the spectral index n_s .
- **Baryon density.** The baryon density $\Omega_b h^2$ has two major imprints on the CMB power spectrum: since baryons are pressureless, they decrease the sound speed and hence reduce the sound horizon. This stretches all the acoustic peaks to higher l . Baryons are attracted to dark matter potential wells(the $ik\Psi$ term in the baryon velocity equation), and thus the acoustic oscillation in $\Theta_0 - \Phi$ is offset: the positive extremes of $\Theta_0 - \Phi$ are larger than the negative extremes. Since the odd-numbered acoustic peaks are associated with $\Theta_0 - \Phi > 0$, they are enhanced relative to the even peaks. This effect increases if $\Omega_b h^2$ is increased.
- **Matter density.** If the matter density $\Omega_m h^2$ is increased, then the matter-radiation equality occurs earlier. This suppresses the high- l power spectrum (relative to the SW plateau) even more since the decaying potential during radiation era that drives the acoustic oscillations in our earlier calculation does not occur. Also, the ISW effect, which enhances the first peak because the universe is not completely matter-dominated at recombination, is suppressed.
- **Distance to the surface of the last scattering.** The peaks positions in the CMB power spectrum are determined by the comoving angular diameter distance to the surface of last scattering, r . If r is increased then the peaks move to the right. Historically

this was of importance in ruling out open Universe models. A key issue here is parameter degeneracy: the situation where multiple parameters affect a feature. The CMB power spectrum slope is affected by both matter density and the primordial slope n_s , but not in the same way(matter density suppresses only the peak region and produces a unique suppression of the first peak). Two other degeneracies that will encounter later are reionization and tensors, which also tilts the spectrum, but they produce unique features in the polarization that already have(reionization) or soon will(tensor) break the degeneracy.

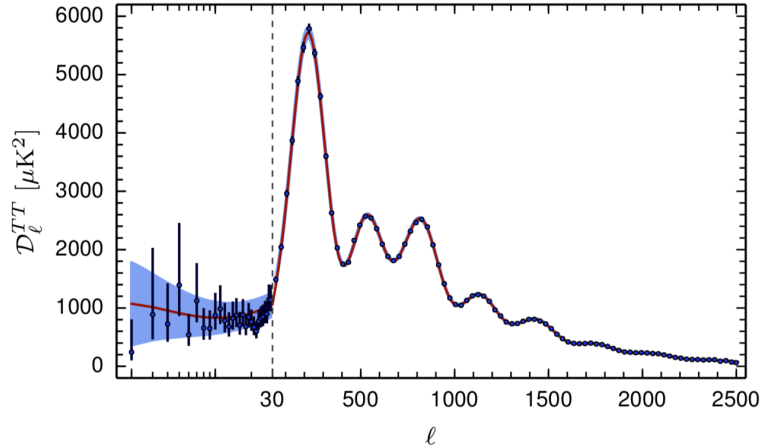


Figure 3.4: TT -angular power spectrum by Planck collaboration 2015. The dashed vertical line at $l = 30$ correspond to the change of map between commander($l = 2 - 29$) and SMICA($l = 30 - 2500$). Data shows an astonishing matching with the CMB model for higher l , however, al low l is cosmic variance(theoretical error) dominated. The unique easy solution to fix these statistical mismatch is to switch from this universe to another, take data and combine them. Credit: <https://www.cosmos.esa.int/web/planck/planck-collaboration>.

3.6 CMB Polarization

So far we have treated the CMB as unpolarized. This picture is incorrect since it affects the statistic properties generated via Thomson scattering process. This small polarized signal is about 10% of the total intensity coming from the CMB temperature alone, so indeed, it is not negligible. This statistical polarized signal has already provided various significative information about the primordial statistic and its consistency and has the potential to keep shedding some new light by opening a new window to the nature of inflation, recombination, and reionization.

3.6.1 Polarized Boltzmann equation

We have assumed that the photons have a scalar phase space density $f(\hat{x}^i, p, \hat{p}^i, \eta)$. In reality, there are two photon polarizations, vertical $\hat{\theta}$ and horizontal $\hat{\phi}$, and the phase space density may be different in each one. Moreover, the two polarizations may be correlated if the

photons are polarized in a diagonal direction or have circular polarization. Generally, we write the phase space density as 2x2 Hermitian density matrix:

$$f = \begin{pmatrix} f_{\hat{\theta}\hat{\theta}} & f_{\hat{\theta}\hat{\phi}} \\ f_{\hat{\theta}\hat{\phi}} & f_{\hat{\phi}\hat{\phi}} \end{pmatrix} = \begin{pmatrix} f_I + f_Q & f_U + if_V \\ f_U - if_V & f_I - f_Q \end{pmatrix} \quad (3.80)$$

The phase space density viewed through a linear polarizing filter at position angle ψ is:

$$f(x^i, p, \hat{p}^i, \eta, \psi) = f_I + f_Q \cos(2\psi) + f_U \sin(2\psi). \quad (3.81)$$

The temperature perturbation that we have been studying has an analogue for polarization. We define the temperature polarization Θ as:

$$f_I = 1 / (\exp(p/T_{\gamma 0}(1 + \Theta)) - 1) \quad (3.82)$$

with

$$\Theta(x^i, p, \hat{p}^i, \eta) = \frac{f_I - f^{(0)}}{-p \partial f^{(0)} / \partial p} \quad (3.83)$$

Whereas for Q ,

$$Q(x^i, p, \hat{p}^i, \eta) = \frac{f_Q}{-p \partial f^{(0)} / \partial p} \quad (3.84)$$

and similarly for U and V . Thus our goal now is to characterize Θ, Q, U, V , as usual, we will work in Fourier space and arrange the \hat{z} axis in the direction of \mathbf{k} . The polarization will be created by Thomson scattering. Since Thomson scattering does not create circular polarization, we will not consider V . It is then convenient to write the polarization as a traceless-symmetric tensor field,

$$P_{ab} = \begin{pmatrix} Q & U \\ U & -Q \end{pmatrix} \quad (3.85)$$

Now we could deal with the Boltzmann equation for polarized phase space density is just like that for intensity and we write:

$$C[f] = \frac{Df}{d\eta}, \quad (3.86)$$

where $C[f]$ is the collision term, and the derivative $D/d\eta$ transports the 2x2 matrix according to:

$$\frac{Df_{ab}}{d\eta} = \frac{\partial}{\partial \eta} f_{ab} + \dot{x}^i \frac{\partial}{\partial x^i} f_{ab} + \dot{p} \frac{\partial}{\partial p} f_{ab} + \dot{\hat{p}} \frac{\partial}{\partial \hat{p}} f_{ab} + h_a^\mu \frac{(u \cdot \nabla) h_\mu^c}{u^0} h_b^\nu \frac{(u \cdot \nabla) h_\nu^d}{u^0} f_{ab} \quad (3.87)$$

where $a, b \in \hat{\theta}, \hat{\phi}$ are indices of 2-dimensional plane perpendicular to direction of photon propagation. In the last term h_a^μ is a 4-vector corresponding to the unit vector in the direction of a on the unit 2-sphere. This term accounts for the fact that the basis $\hat{\theta}, \hat{\phi}$ is not parallel-transported along the photon's trajectory, so the polarization can appear to rotate due to the choice of the coordinate system. At first order in perturbation theory, this effect must vanish since the polarization is first-order and any coordinate rotation is also first-order. A similar argument kills the $\dot{\hat{p}}^i$ term. Also \dot{x}^i multiplies a first-order term(a spatial gradient) so it can be replaced with its zeroth-order value \hat{p}^i . If one is looking at the polarized components, f_{ab} is first-order so one may replace \dot{p} with $-aH\hat{p}$. Thus the photon Boltzmann equation reduces to:

$$C[f_Q] = \dot{f}_Q + \dot{\hat{p}}^i \frac{\partial}{\partial x^i} f_Q - aH\hat{p} \frac{\partial}{\partial p} f_Q \quad (3.88)$$

similarly for U . Writing this in terms of the dimensionless Q and U , we get:

$$C[f_Q] = -p \frac{\partial f^{(0)}}{\partial p} \dot{Q} - Q \frac{\partial}{\partial \eta} \left(p \frac{\partial f^{(0)}}{\partial p} \right) - p \frac{\partial f^{(0)}}{\partial p} \hat{p}^i \frac{\partial}{\partial x^i} + a H p \partial \left(p \frac{\partial f^{(0)}}{\partial p} Q \right) \quad (3.89)$$

Since $f^{(0)}$ depends only on the combination of ap , the $\partial/\partial\eta$ term cancels against the part of fourth term where the derivative acts on $p\partial f^{(0)}/\partial p$. Then, after dividing through by $-\partial f^{(0)}/\partial p$, we get:

$$\frac{C[f_Q]}{-p\partial f^{(0)}/\partial p} = \dot{Q} + \hat{p}^i \frac{\partial}{\partial x^i} Q + a H p \frac{\partial f^{(0)}}{\partial p} \frac{\partial Q}{\partial p} \quad (3.90)$$

This is a remarkably simple equation: note that there is no gravity inside of it. Polarization is created only by the collision operator, which includes Thomson scattering. Lie the case for Θ , it will turn out that Q and U are frequency independent. We will write the right-hand side as $C[Q]$ so:

$$\dot{Q} + i \mathbf{k} \cdot \hat{p} Q = C[Q] \quad (3.91)$$

Spherical harmonic decomposition.

The decomposition of Q and U in spherical harmonics is not as straightforward as Θ they generate a traceless and symmetric tensor, with determined transformation properties. In order to the spherical harmonic of Q and U satisfies the same rotational properties as Θ_{lm} , we need to construct a tensor covariantly derived from the basis functions Y_{lm} . An option is by taking derivatives of Y_{lm} and generate a new tensor that respects the properties of the polarization vector, such as:

$$Y_{lm,ab}^E(\theta, \phi) = -\frac{2}{\sqrt{(l-1)l(l+1)(l+2)}} \left(D_a D_b - \frac{1}{2} g_{ab} D^2 \right) Y_{lm}(\theta, \phi) \quad (3.92)$$

$$Y_{lm,ab}^B(\theta, \phi) = -\frac{2}{\sqrt{(l-1)l(l+1)(l+2)}} (\varepsilon_{bc} D_a D_c + \varepsilon_{ac} D_b D_c) Y_{lm}(\theta, \phi) \quad (3.93)$$

Where D_a and D^2 are the covariant derivative and the Laplacian, respectively, on unitary 2-sphere with a metric and antisymmetric symbol:

$$g_{ab} = \begin{pmatrix} 1 & 0 \\ 0 & \sin^2 \theta \end{pmatrix}, \quad \varepsilon_{ab} = \frac{1}{\sin \theta} \begin{pmatrix} 0 & 1 \\ 1 & 0 \end{pmatrix} \quad (3.94)$$

This set of functions form a complete basis for a traceless-symmetric tensor field on the unit sphere. This completeness can be demonstrated by applying second derivative operators to any polarization field P_{ab} to get a scalar, and then expand the scalar in spherical harmonics. the normalization coefficients have been chosen so that:

$$\int Y_{lm,ab}^{E*} Y_{lm}^{E,ab} d^2 \hat{n} = 2 \quad (3.95)$$

and similarly for B . The factor 2 is useful because $|f_{ab}|^2$ actually double-counts the square of each Stokes parameter, i.e. it is $2(f_I^2 + f_Q^2 + f_U^2 + f_V^2)$. It is worth noting there is no $l=0$ or $l=1$ tensor field, which is a consequence of $e^{\pm 2i\psi}$ dependence of the polarized intensity.

One can see this as well by noting that traceless-symmetric derivative operators applied to Y_{00} and Y_{1m} give zero. In addition to rotational properties, which are equivalent to those of Y_{lm} , the tensor spherical harmonics have parity properties:

$$Y_{lm}(\hat{n}) = (-1)^l Y_{lm}(-\hat{n}), \quad Y_{lm}^E(\hat{n}) = (-1)^l Y_{lm}^E(-\hat{n}), \quad Y_{lm}^B(\hat{n}) = (-1)^{l+1} Y_{lm}^B(-\hat{n}). \quad (3.96)$$

The B -type spherical harmonic has an extra minus sign because its definition includes the Levi-Civita tensor. It is customary to express the polarized phase space density in E and B spherical harmonics:

$$\begin{pmatrix} Q(\hat{n}) & U(\hat{n}) \\ U(\hat{n}) & -Q(\hat{n}) \end{pmatrix} = \sum_{lm} (-i) \sqrt{4\pi(2l+1)} [E_{lm} Y_{lm,ab}^E(\hat{n}) + B_{lm} Y_{lm,ab}^B(\hat{n})] \quad (3.97)$$

in analogy to the temperature anisotropies. This equation is the analogue of the spherical harmonic decomposition for polarization. The E_{lm} and B_{lm} transform under rotations in the same way as Θ_{lm} .

Free streaming term. If the equation (3.91) is projected in this basis and after some tedious but straightforward algebra we obtain the streaming equation for the E and B modes:

$$\begin{aligned} \dot{E}_{lm} &= \frac{\sqrt{(l-2)(l+2)(l-m)(l+m)}}{l(2l+1)} k E_{l-1,m} - \frac{\sqrt{(l-1)(l+3)(l+1-m)(l+1+m)}}{(l+1)(2l+1)} k E_{l+1,m} \\ &\quad - \frac{2im}{l(l+1)} k B_{lm} + C[E_{lm}]. \end{aligned} \quad (3.98)$$

$$\begin{aligned} \dot{B}_{lm} &= \frac{\sqrt{(l-2)(l+2)(l-m)(l+m)}}{l(2l+1)} k B_{l-1,m} - \frac{\sqrt{(l-1)(l+3)(l+1-m)(l+1+m)}}{(l+1)(2l+1)} k B_{l+1,m} \\ &\quad + \frac{2im}{l(l+1)} k E_{lm} + C[B_{lm}] \end{aligned} \quad (3.99)$$

Where the $C[\cdot]$ denotes the collision operator. Particularly the collision operator for polarization depend only on the local phase space density of photons, and only the photon density at that particular frequency. Symmetry under rotation and parity dictate the shape that the collision terms should have, thus $C[E_{lm}]$ can depend only on quantities with the same angular momentum and parity, i.e. Θ and E_{lm} , whereas B_{lm} can only depend on B_{lm} . The freedom under the coordinate choice also demands that the companion coefficients must depend only on l , so we get:

$$C[E_{lm}] = \dot{\tau} E_{lm} - \dot{\tau} (\alpha_l \Theta_l + \beta_l E_{lm}); \quad C[B_{lm}] = \dot{\tau} B_{lm} - \dot{\tau} \gamma_l B_{lm} \quad (3.100)$$

the second term represents the terms that have been remitted after scattering. The easiest way to determine each coefficient is just by studying the $m = 0$ case, in which the E type spherical harmonics Y_{lm}^E have only Q polarization and the B modes only U . Thus we may derive α, β, γ by taking $m = 0$ and keeping only the Q/U polarization. There is then a separate vertical 'north-south' temperature perturbation Θ_V and a horizontal 'east-west' polarization Θ_H , given by

$$\Theta_V = \Theta + Q, \quad \Theta_H = \Theta - Q. \quad (3.101)$$

One can estimate the post-scattering intensity and polarization by looking at the polarization-resolved differential scattering cross section from the incoming direction and polarization at the baryon rest frame \hat{p}' and ζ' to the outgoing \hat{p} and ζ . The component of the collision term due to re-scattered radiation is:

$$C[\Theta_V]_{r.s.} = |\dot{\tau}| \int d^2\hat{p}' \left[\frac{dP_{V \rightarrow V}}{d\Omega} \Theta_V(\hat{p}') + \frac{dP_{H \rightarrow V}}{d\Omega} \Theta_H(\hat{p}') \right] \quad (3.102)$$

and the polarization differential probability is

$$\frac{dP_{\zeta' \rightarrow \zeta}}{d\Omega} \Theta_V(\hat{p}' \rightarrow \hat{p}) = \frac{3}{8\pi} (\zeta \cdot \zeta')^2 \quad (3.103)$$

where ζ is given by:

$$\zeta_V = (\cos \theta \cos \phi, \cos \theta \sin \phi, -\sin \phi), \quad \zeta_H = (\sin \phi, \cos \phi, 0) \quad (3.104)$$

and the differential probability are:

$$\frac{dP_{H \rightarrow H}}{d\Omega} \Theta_V(\hat{p}' \rightarrow \hat{p}) = \frac{3}{8\pi} \cos^2 \Delta\phi \quad (3.105)$$

$$\frac{dP_{H \rightarrow V}}{d\Omega} \Theta_V(\hat{p}' \rightarrow \hat{p}) = \frac{3}{8\pi} \cos^2 \theta \sin^2 \Delta\phi \quad (3.106)$$

$$\frac{dP_{V \rightarrow H}}{d\Omega} \Theta_V(\hat{p}' \rightarrow \hat{p}) = \frac{3}{8\pi} \cos^2 \theta' \sin^2 \Delta\phi \quad (3.107)$$

$$\frac{dP_{V \rightarrow V}}{d\Omega} \Theta_V(\hat{p}' \rightarrow \hat{p}) = \frac{3}{8\pi} (\cos \theta \cos \theta' \cos \Delta\phi + \sin \theta \sin \theta')^2 \quad (3.108)$$

where $\Delta\phi = \phi - \phi'$. Since we are looking from $m = 0$ modes, we may angle average over $\Delta\phi$ and then get:

$$C[\Theta_V(\hat{p})]_{r.s.} = \frac{3|\dot{\tau}|}{4} \int \left[\left(\frac{1}{2} \cos^2 \theta \cos^2 \theta' + \sin^2 \theta \sin^2 \theta' \right) \Theta_V(\hat{p}') + \frac{1}{2} \cos^2 \theta \Theta_H(\hat{p}') \right] \sin \theta' d\theta' \quad (3.109)$$

$$C[\Theta_H(\hat{p})]_{r.s.} = \frac{3|\dot{\tau}|}{4} \left[\frac{1}{2} \cos^2 \theta' \Theta_V(\hat{p}') + \frac{1}{2} \Theta_H(\hat{p}') \right] \sin \theta' d\theta' \quad (3.110)$$

Using $Q = (\Theta_V - \Theta_H)/2$, thus:

$$C[Q(\hat{p})]_{r.s.} = \frac{3 \sin \theta |\dot{\tau}|}{8} \int d\theta' \sin \theta' \left[\left(\frac{1}{2} - \frac{3}{2} \cos^2 \theta' \right) \Theta(\hat{p}') + \frac{3}{2} \sin^2 \theta' Q(\hat{p}') \right] \quad (3.111)$$

this equation can be simplified if we recall the values of spherical harmonics,

$$Y_{20} = \sqrt{\frac{5}{16\pi}} (3 \cos^2 \theta - 1), \quad Y_{20,\hat{\theta}\hat{\theta}}^E = \sqrt{\frac{15}{32\pi}} \sin^2 \theta \quad (3.112)$$

and we note that only spherical harmonics with $l = 2$ are involved. Moreover, if we transform to harmonic space, $C[E_{lm}]$ vanishes unless $l = 2$. For this special case, we get:

$$C[E_{20}]_{r.s.} = \left(-\frac{\sqrt{6}}{10} \Theta_{20} + \frac{3}{5} E_{20} \right) |\dot{\tau}| \quad (3.113)$$

so we identify $\alpha_2 = -\sqrt{6}/10$ and $\beta_2 = 3/5$. A similar calculation can be done for B modes and shows that the re-scattering term to be zero $\gamma_l = 0$. Finally, the overall system of equations for polarization is:

$$\dot{E}_{lm} = \frac{\sqrt{(l-2)(l+2)(l-m)(l+m)}}{l(2l+1)} k E_{l-1,m} - \frac{\sqrt{(l-1)(l+3)(l+1-m)(l+1+m)}}{(l+1)(2l+1)} k E_{l+1,m} \\ - \frac{2im}{l(l+1)} k B_{lm} - |\dot{\tau}| \left(E_{lm} + \frac{\sqrt{6}\Theta_{2m} - 6E_{2m}}{10} \delta_{l2} \right) \quad (3.114)$$

$$- \frac{2im}{l(l+1)} k B_{lm} - |\dot{\tau}| \left(E_{lm} + \frac{\sqrt{6}\Theta_{2m} - 6E_{2m}}{10} \delta_{l2} \right) \quad (3.115)$$

$$\dot{B}_{lm} = \frac{\sqrt{(l-2)(l+2)(l-m)(l+m)}}{l(2l+1)} k B_{l-1,m} - \frac{\sqrt{(l-1)(l+3)(l+1-m)(l+1+m)}}{(l+1)(2l+1)} k B_{l+1,m} \\ + \frac{2im}{l(l+1)} k E_{lm} - |\dot{\tau}| B_{lm} \quad (3.116)$$

There are separate E type and B type power spectra,

$$\langle a_{lm}^{E*} a_{l'm'}^E \rangle = C_l^{EE} \delta_{ll'} \delta_{mm'} \quad \langle a_{lm}^{B*} a_{l'm'}^B \rangle = C_l^{BB} \delta_{ll'} \delta_{mm'} \quad (3.118)$$

Because E has the same parity as temperature, it is also possible to have a temperature-polarization spectrum:

$$\langle a_{lm}^{*} a_{l'm'}^E \rangle = C_l^{\Theta E} \delta_{ll'} \delta_{mm'} \quad (3.119)$$

The power spectra for the scalars can be determined using the same method as for temperature, i.e. integrating over wavenumbers and angles to get:

$$C_l^{EE} = 4\pi \int d \ln k \mathcal{P}_\zeta(k) \left| \frac{E_l}{\zeta} \right|^2 \quad (3.120)$$

$$C_l^{\Theta E} = 4\pi \int d \ln k \mathcal{P}_\zeta(k) \text{Re} \left[\frac{\Theta_l^*}{\zeta} \frac{E_l}{\zeta} \right] \quad (3.121)$$

although the real part in the integrand is unnecessary for scalars since Θ_l/ζ and E_l/ζ are real.

Recombination epoch

Polarization can be generated at recombination because of the finite thickness of the last scattering surface. The finite optical depth $|\dot{\tau}| < \infty$ allows a Θ_2 to be generated, and then converted into polarization. We can get an approximate sense for the magnitude of the polarization by using the tight-coupling limit:

$$\dot{\Theta}_2 = \frac{2}{5} k \Theta_1 + \frac{9}{10} \dot{\tau} \Theta_2, \quad (3.122)$$

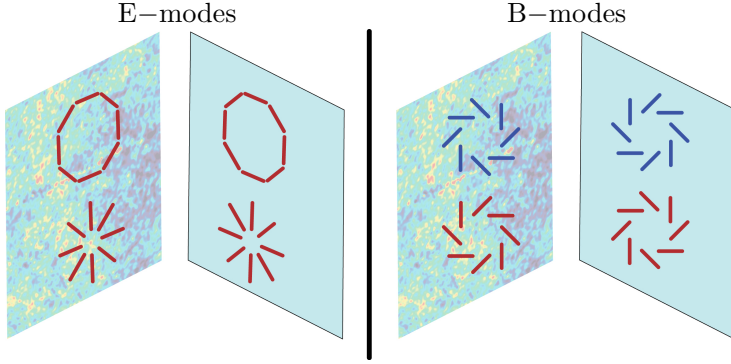


Figure 3.5: E-modes and B-modes patterns: The E-modes or curl free patterns are symmetric under reflection, whereas the B-modes or divergenless pattern are antisymmetric under reflection. Credit: <https://writescience.wordpress.com/2014/04/11/>

and supposing that the two terms on the right side approximately balance, which should be true if $\dot{\tau}$ is large. Then:

$$\Theta_2 \approx \frac{4k}{9|\dot{\tau}|} \Theta_1 \quad (3.123)$$

The polarization generated by the source term is:

$$\dot{E}_2 \approx -\frac{\sqrt{6}}{10} |\dot{\tau}| \Theta_2 \approx -\frac{2\sqrt{6}}{45} k \Theta_1. \quad (3.124)$$

Thus right after recombination, we should have a polarization field of

$$E_2(\eta_{\text{rec}}) \approx -\frac{2\sqrt{6}}{45} k \Delta \eta_{\text{lss}} \Theta_1, \quad (3.125)$$

where $\Delta \eta_{\text{lss}}$ is the width of the last scattering surface, i.e. the time during which the above equations are valid. But Θ_1 is an oscillating function; in the small-scale limit we have

$$\Theta_1 \approx -\frac{\zeta}{\sqrt{3}} \sin \frac{k \eta_{\text{rec}}}{\sqrt{3}} \exp(-k^2/k_D^2) \quad (3.126)$$

so

$$E_2(\eta_{\text{rec}}) \approx \frac{2\sqrt{2}}{45} k \Delta \eta_{\text{lss}} \sin \frac{k \eta_{\text{rec}}}{\sqrt{3}} \exp(-k^2/k_D^2) \quad (3.127)$$

This is an oscillating function, which rapidly goes to zero at large k , and also has an exponential cutoff. It is proportional to the width of the surface of the last scattering. It is smaller than Θ_1 by a factor of $k \eta_{\text{lss}}$. In order to determine what the polarization looks like today, we need to do a radiative transfer calculation. This is analogous to the spherical Bessel function calculation for temperature, except that the polarization equations are more complicated and the solution is a tensor spherical Bessel function. Qualitatively, however, the results are similar to those for temperature: the power spectrum C_l^{EE} today is an integral over $\mathcal{P}(k)$ weighted heavily at $k \sim l r_{\text{CMB}}$. because E_2 has a sine instead of a cosine dependence, the results are. First, The E -type polarization power spectrum C_l^{EE} shows acoustic oscillations, but 180° out of phase with $C_l^{\Theta\Theta}(\sin^2 \text{vs.} \cos^2)$. Second, The cross-correlation $C_l^{\Theta E}$ is 90° out of phase with both ($\sin \cos$).

Reionization epoch.

Theory predicts that the universe should have become neutral at $z \sim 1200$ and the existence of acoustic oscillations confirms that this picture is correct. However, we know that universe must have become reionized again from studies of hydrogen(Lyman- α) absorption lines in quasars. A neutral intergalactic medium would present an optical depth of $\sim 10^4$ and all flux blueward of Lyman- α in the quasar rest frame would be wiped out. Instead what is observed is a complex series of absorption features whose fractional transmission increases with redshift, being about 50% at $z \sim 3$ and becoming complete above $z \sim 6$. This implies that some mechanism reionized almost all the gas in the universe sometime before $z = 6$. The most likely candidate is UV radiation from an early generation of stars. Reionization causes an additional source of optical depth between us and recombination surface. If reionization were a step function at $z = z_{\text{ri}}$, with post-reionization electron abundance x_e , the this optical depth is

$$\tau_{\text{ri}} = \int n_e \sigma_T dt = \frac{\sigma_T n_{H0} x_e}{H_0} \int_0^{z_{\text{ri}}} (1+z)^3 \frac{dz}{(1+z) \sqrt{\Omega_\lambda + \Omega_m (1+z)^3}}. \quad (3.128)$$

If z_{ri} is large then the cosmological constant has only a minor influence; removing it reduces the integral to:

$$\tau_{\text{ri}} \approx \frac{2\sigma_T n_{H0} x_e}{3\Omega_m^{1/2} H_0} (1+z_{\text{ri}})^{3/2}. \quad (3.129)$$

The usual assumption is that at reionization, H became ionized to H^+ and He to He^+ , which gives $x_e = 1.08$ (1 electron from H and 0.08 from He). $He \rightarrow He^+$ is predicted by simulations to occur at the same time as $H \rightarrow H^+$ because of the spectrum of the starts. Under these conditions, we get:

$$\tau_{\text{ri}} \approx 0.0023 (1+z_{\text{ri}})^{3/2}. \quad (3.130)$$

The requirement of $z_{\text{ri}} > 6$ from the quasar absorption features implies $\tau_{\text{ri}} > 0.043$. In order to measure τ_{ri} we must understand its impact on the CMB. If one studies the Boltzmann equation, one can see that all of the high multipoles in the CMB have terms in the $\dot{\Theta}$ equation that contain $-|\dot{\tau}| \Theta_l$ for $l \geq 1$. These terms become inactive after recombination, but turn on again due to reionization. This implies that all of the modes that were inside the horizon at reionization (hence have temperature anisotropies dominates by large l) are suppressed by a factor of $\exp(-\tau_{\text{ri}})$. The condition for this to occur is roughly $k\eta_{\text{ri}} \gg 1$, or

$$l = k(\eta_0 - \eta_{\text{ri}}) \gg \frac{\eta_0 - \eta_{\text{ri}}}{-\eta_{\text{ri}}}. \quad (3.131)$$

Within this range the power spectrum, which depends on Θ_l^2 , is suppressed by a factor:

$$C_l \rightarrow C_l \exp(-2\tau_{\text{ri}}). \quad (3.132)$$

Therefore reionization causes a suppression of all the high multipoles. This makes sense: the additional scattering wipes out small-scale structure. The second effect of reionization is on the CMB polarization. For modes that were outside the horizon at recombination, we found in the temperature anisotropy section that

$$\Theta_l(\eta) = -\frac{1}{5} \zeta j_l(k\eta), \quad (3.133)$$

and in particular

$$\Theta_2(\eta_{\text{ri}}) = -\frac{1}{5}\zeta j_l(k\eta_{\text{ri}}), \quad (3.134)$$

If the scattering from reionization were instantaneous(it is not) then this immediately generates E -mode polarization:

$$E_2(\eta_{\text{ri}}) = \frac{\sqrt{6}}{50}\tau_{\text{ri}}\zeta j_2(k\eta_{\text{ri}}). \quad (3.135)$$

The free-streaming converts this into a polarization today at $l \sim k(\eta_0 - \eta_{\text{ri}})$. Since the spherical Bessel function is dominated by arguments near ~ 3 , we thus expect E -mode polarization to peak at

$$l \sim 3 \frac{\eta_0 - \eta_{\text{ri}}}{\eta_{\text{ri}}} \quad (3.136)$$

and have an amplitude proportional to τ_{ri} . In the power spectrum one expects:

$$C_l^{EE} \propto \tau_{\text{ri}}^2 \quad \text{and} \quad C_l^{\Theta E} \propto \tau_{\text{ri}}. \quad (3.137)$$

The expected polarization per $\ln l$, $\sqrt{l(l+1)C_l^{EE}/2\pi}$ is order $\tau_{\text{ri}}\sqrt{\mathcal{P}} \sim 10^{-6}$, i.e. at μK level; thet factor $\sqrt{6}/50$ makes this even lower. Nevertheless, this polarization feature at low l it was detected by Planck, which finds $\tau_{\text{ri}} = 0.087 \pm$ and $z_{\text{ri}} = 11.0 \pm 1.4$.

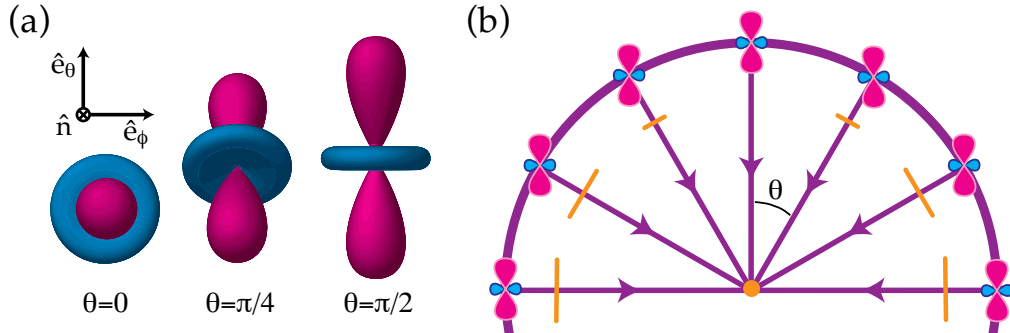


Figure 3.6: The transformation of quadrupole anisotropies into linear polarization. In different regions the plane wave modulation of the quadrupole can change its sign but not its polarization sense. (a) The orientation of the quadrupole moment with respect to the scattering direction \hat{n} determines the sense and magnitude of the polarization. It is aligned with the cold(red, long) lobe in the $e_\theta \otimes e_\phi$ tangent plane. (b) In spherical coordinates where $n \cdot k = \cos \theta$, the polarization points north-south Q with magnitude varying as $\sin 2\theta$ for scalar fluctuations. Credit: <http://background.uchicago.edu/~whu/polar/webversion/polar.html>

Gravitational waves

Primordial gravitational waves are expected to be very weak, and their imprint on the CMB temperature fluctuations would be very hard to disentangle from that of the density fluctuations. In polarization, however, they have a unique signature: the B -type polarization,

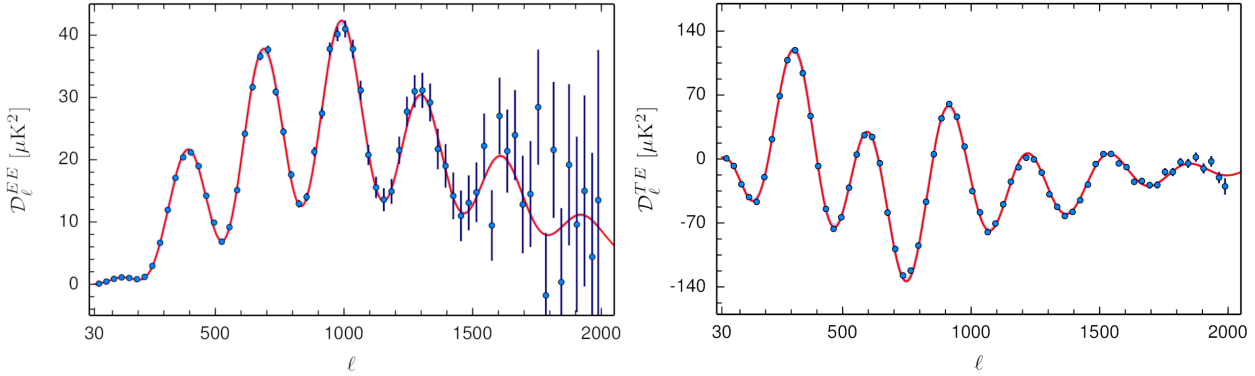


Figure 3.7: EE and TE angular power spectrum. Remarkably the red curves are not a fit, they are the model using the parameters inferred from the TT -angular power spectrum. Therefore these plot show the consistency of the theoretical framework [32].

which is not generated by density perturbations is given by

$$C_l^{BB} = 8\pi \int d \ln k \mathcal{P}_h(k) \left| \frac{B_l(k)}{h} \right|^2. \quad (3.138)$$

However, we may make an educated estimate as follows. The rate of generation of photon quadrupole at the recombination surface is:

$$\dot{\Theta}_2 \sim -\frac{\dot{E}}{5} \equiv \frac{2}{5\sqrt{3}}\dot{h}, \quad (3.139)$$

where we have written the gravitational wave amplitude in terms of $h = (h_+ \mp ih_x)/\sqrt{2}$ instead of E to avoid confusion with the polarization. This occurs throughout the time of the last scattering, so during this surface Θ_2 is of order

$$\Theta_2 \sim \frac{2}{5\sqrt{3}}\dot{h}\Delta\eta_{\text{lss}}. \quad (3.140)$$

Thomson scattering then generates E -type polarization:

$$\dot{E}_2 \sim -\frac{\sqrt{6}}{10}|\dot{\tau}|\Theta \sim -\frac{\sqrt{2}}{25}\dot{h}\Delta\eta_{\text{lss}}. \quad (3.141)$$

The dominant gravitational wave modes will be those that enter the horizon at recombination $k \sim 1/\eta_{\text{rec}}$: modes that enter earlier adiabatically decayed away, and those that enter later have $h \neq 0$ but $\dot{h} \approx 0$. For these waves, $\dot{h} \sim h/\eta_{\text{rec}}$, and the typical polarization is:

$$\frac{\sqrt{2}}{25} \frac{\Delta\eta_{\text{lss}}}{\eta_{\text{rec}}} h_{\text{rms}} \sim 10^{-7} r^{1/2}. \quad (3.142)$$

This is at scale of $l \sim k\eta_0 \sim \eta_0/\eta_{\text{rec}} \sim 50$, i.e. a few degrees. However for typical models with $r \sim 0.1$ the amplitude is down in the range of 100nK, and a more careful calculation gives a somewhat lower number. This makes gravitational waves one of the most difficult problems in observational cosmology. Nevertheless, there is an enormous prize: measuring

r and hence setting the energy scale of the inflationary epoch. Gravitational waves also generate polarization at reionization, however, this is on the largest scales (l of a few) where foregrounds are most severe.

Gravitational wave phenomenology

A few results follow easily from the above equations:

- Thomson scattering of the local quadrupole Θ_{2m} of the temperature field is the only source for polarization.
- Generation of polarization can only happen in regions where the optical depth is high enough to have Thomson scattering but not so high as to wash out the quadrupole. The two such possibilities are the recombination surface and reionization.
- Thomson scattering can only generate $l = 2$ E -type polarization; the free-streaming terms are needed to generate everything else.
- The mixing of E into B -type polarization occurs via a single term in the \dot{B}_{lm} equation that has a factor of m . Therefore for scalar perturbations ($m = 0$), there is no way to generate B -type polarization. On the other hand, tensors can generate it.

3.7 CMB systematics

No discussion of the CMB would be complete without a brief mention of the problems facing experimentalist who measure such tiny signals. Here we give an incomplete list:

- **The ground.** The CMB polarization fluctuations are a few μK , but the ground is at $\sim 300\text{K}$. Therefore if even a small amount of ground radiation diffracts into the telescope it is a serious problem. Ground-based experiments must take care to minimize diffraction, and also take advantage of the fact that the sky rotates relative to the ground so that the two effects can be separated. Going to space also helps but is expensive.
- **The atmosphere.** The Earth's atmosphere contains H₂O and O₂ molecules that radiate in the microwave bands. Humidity variations can masquerade as CMB anisotropies. These move relative to the sky and do not repeat from day to day, so once again there are ways to separate them, nevertheless, they are so large that they must be very carefully removed. Balloon or space experiments have an advantage as they rise above most of the water vapor.
- **Beams.** Precise measurement of the CMB fluctuations requires that one understand the beam (i.e. how the response to a source varies depending on how far it is off the boresight) very well. These are usually determined by diffraction: the resolution of an experiment is no better than $\theta = \lambda/D$. But to measure CMB power spectrum to 1%, we need to know the Fourier transform of the beam to 0.5%. Often one uses a bright microwave source such as a planet for this purpose.
- **Intensity → polarization leakage.** Since the CMB temperature fluctuations are much brighter than polarization one must make sure that the two polarizations measured by the instrument have the same relative calibration and that features such as

polarized diffraction spikes are well understood. The CMB temperature fluctuations are much fainter than the ground, so one might think they are less of a problem, but they are fixed to the sky which may make them more pernicious than the ground pick-up.

- **Response to magnetic flux.** The Earth's magnetic field can affect some types of microwave detectors, especially those using SQUIDs to measure current. These must be carefully shielded using superconducting cages.

There are also foregrounds: objects that emit microwaves that are not the CMB.

- **Active galactic nuclei.** These emit synchrotron radiation that is often time dependent. They have a different spectrum than the CMB, tilted to lower frequencies than a blackbody. The brighter ones can be recognized easily in CMB maps and are usually pointlike but the fainter ones may not. Some experiments, must do a statistical subtraction of AGN.
- **Star-forming galaxies.** These emit synchrotron, free-free radiation, and also thermal radiation from dust grains that have been heated by absorption of starlight. They are much fainter than AGN but with several emission, mechanisms may have complex spectra. To date, they have not been a problem but the next generation of higher-frequency CMB experiments ($\geq 150\text{GHz}$) could face significant difficulties, especially at small angular scales.
- **Galactic synchrotron.** Our own Milky Way emits synchrotron radiation, which fills the entire sky and at low frequencies (422 GHz) contributes tens of μK even at high Galactic latitude. The synchrotron is highly polarized which makes it a special problem for CMB experiments. It is steeply frequency-dependent, being much brighter at low frequency, so maps at e.g. 400 MHz are often used to assess contamination.
- **Galactic free-free radiation.** This is present but not the dominant foreground at any frequency. It has a well-understood spectral dependence, $I_\nu \propto \nu^{-0.15}$, so it is most important at low frequency. It is intrinsically unpolarized in the optically thin regime, and its source, warm ionized gas, is also traced at optical wavelengths by diffuse H α emission.
- **Galactic dust.** Interstellar dust absorbs starlight and can re-radiate it at infrared wavelengths; a small fraction of the energy emerges in the microwave via the Rayleigh-Jeans tail. The emission is weakly ($\sim 5\%$) polarized due to the alignment of the dust grains with the magnetic field. There is also evidence for an additional dust emission process, possibly electric dipole radiation from spinning dust grains, or thermal fluctuations of the magnetic moment of iron-bearing grains. Thermal dust emission dominates the Galactic foreground above $\sim 80\text{GHz}$.

The foregrounds are a serious problem, but by rejecting data from the Galactic plane (where they are worst), using their frequency dependence, and incorporating data from other wavelengths, they have so far been overcome. They will, however, represent a major challenge, especially for gravitational wave detection.

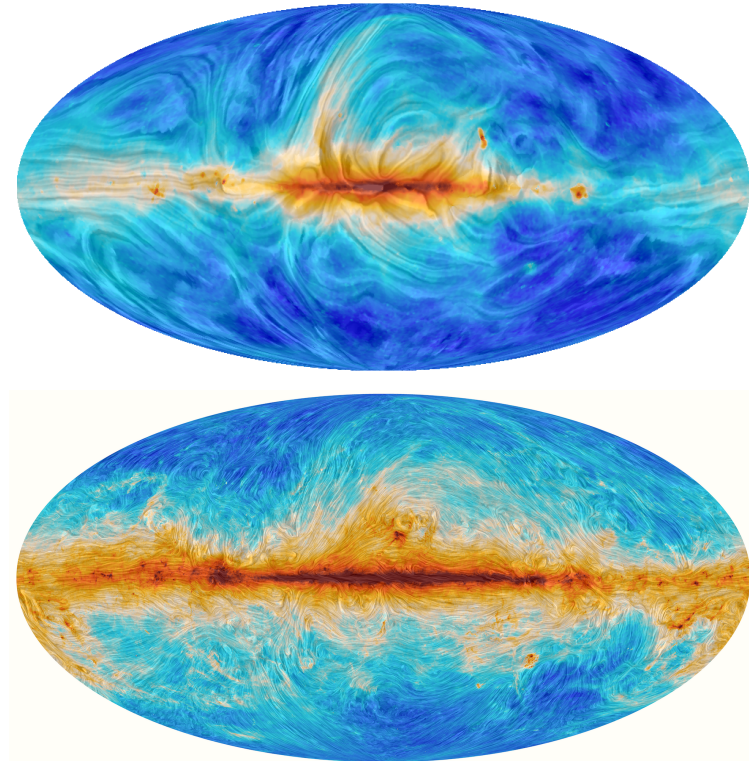


Figure 3.8: LFI at 30GHz Commander map: The top figure shows the magnetic fields and the intensity of polarized radiation synchrotron radiation measured from LFI at 30GHz. The bottom figure shows the magnetic fields and the intensity of polarized radiation synchrotron radiation measured from HFI at 353GHz. These two figures are important to understand the status of the current observation of B modes from CMB. They correspond to the main spurious sources on the galactic plane that must be characterized and eliminated. Credit: <https://www.cosmos.esa.int/web/planck/planck-collaboration>.

Chapter 4

Features

The simplest models of cosmic inflation [5], [27], [6], [28] predict both scalar and tensor primordial fluctuations, characterized by a set of nearly scale invariant power spectra. While cosmic microwave background (CMB) observations have enabled us to tightly constrain the power spectrum of scalar perturbations, a detection of primordial gravity waves (in the form of B-modes) remains a pending challenge. Current efforts to observe the CMB polarization will reach the limits of cosmic variance, allowing us to either measure or constrain the tensor-to-scalar ratio r down to $r \sim 0.01 - 0.002$ [18, 29, 30, 31]. The observation of B-modes in the CMB would give us access to the value of the Hubble expansion rate H during inflation, reinforcing the idea that the Hot Big Bang era was preceded by a stage of dramatic accelerated expansion.

Although current CMB observations are compatible with a nearly scale invariant power spectrum for curvature perturbations [32], there are some hints of scale dependent features present in the spectrum at certain multipoles [33, ?, 34, 35]. The shape and size of such features could in principle allow us to discriminate the type of physics that played a role during inflation, since their appearance in the primordial spectra would invalidate the simplest models of inflation, forcing us to consider models in which non-trivial degrees of freedom interacted with primordial curvature fluctuations around horizon crossing [32, 36, 37, 38, 39, 40, 41, 42, 43, 44, 45, 46, 47, 48, 49, 50, 51, 52] (see also [53, 54, 55] for early work on features of the tensor spectrum and [56] for an up-to-date review). The prospects of unveiling physics beyond the single-field slow-roll paradigm has also propelled new ideas to analyze the presence of such features in 21 cm and Large Scale Structure observations [57, 58, 59, 60].

The effective field theory (EFT) approach to inflation [61, 62] is particularly useful to understand the appearance of features in the primordial spectra. This formalism allows one to study models of inflation beyond the canonical single field paradigm by incorporating the sound speed at which curvature fluctuations propagate, as a parameter in the Lagrangian for perturbations. Within this framework, features are the consequence of time variations of background quantities appearing in the Lagrangian describing the dynamics of the lowest energy fluctuations. These time variations break – in a controlled way – the standard behavior required in single field slow-roll inflation, producing localized features in the spectra, though without invalidating inflation as a mechanism to explain the origin of primordial fluctuations

in a way compatible with observations. Given that the source of features may be traced back to background parameters that affect the evolution of all perturbations, features appearing in different n -point correlation functions would be necessarily correlated [63, 64, 65, 66, 67, 4, 68, 69, 70, 71, 72, 73]. In the case of scalar perturbations, a powerful way to study such time-dependent departures from slow-roll is the joint estimator analysis of two- and three-point correlation functions [71], since a detection of correlated signals in the power spectrum and bispectrum would increase the statistical significance of these features.

In this article we explore the possibility of establishing a novel class of cross correlation between spectra. Specifically, the questions we wish to address are the following: *If features in the primordial scalar power spectrum are confirmed, would they also show up in the tensor power spectrum? In addition, if the scale suppression of the angular power spectrum in the multipole range $4 \leq \ell \leq 50$ is found to be of primordial origin, what type of signal should we expect in the angular power spectrum of B-modes?* To that end, we study the effect of time dependent backgrounds on the dynamics of fluctuations in order to correlate features in the power spectra of scalar and tensor modes. Our main result is that features $\Delta\mathcal{P}_T/\mathcal{P}_T$, appearing in the tensor power spectrum \mathcal{P}_T , are correlated to features $\Delta\mathcal{P}_S/\mathcal{P}_S$, appearing in the scalar spectrum \mathcal{P}_S in Fourier space, in the following way

$$\frac{d^2}{d \ln k^2} \left(\frac{\Delta\mathcal{P}_T}{\mathcal{P}_T} \right) = 6\varepsilon_0 \frac{\Delta\mathcal{P}_S}{\mathcal{P}_S}, \quad (4.1)$$

where ε_0 is the (constant) average value of the slow-roll parameter $\varepsilon = -\dot{H}/H^2$. This expression tells us that any feature appearing in the tensor spectrum is in general suppressed with respect to those appearing in the scalar spectrum [74]. This suppression is two-fold: On the one hand, ε_0 must be small in order to keep inflation valid as a mechanism to produce fluctuations over a large range of scales. On the other hand, the $\ln k$ -derivatives must be large in order for features to be observable in the scalar power spectrum.* Note that this approach is model independent since it takes the scalar power spectrum data as an input without reference to the mechanism that produces the features.

Our results show that any strong departure of scale invariance in the scalar spectrum must come together with a consequential departure in the tensor spectrum, but at a level that is too small to be observed. As a corollary, any future observation of scale invariance departures in the tensor spectrum cannot be of primordial origin, unless some exotic mechanism underlies their origin. For example, models where the only background quantity experiencing rapid variations is the tensor sound speed will have features only in the tensor spectrum [75]. On the other hand, non Bunch-Davies initial conditions may lead to features in the two spectra with the same amplitude [76]. In this work, however, we are interested in predicting the scale dependence of the tensor spectrum from the scalar power spectrum, highlighting the perspective of a joint analysis of the two spectra. Having this in mind, in the particular case of the observed deficit of the angular power spectrum around $\ell \sim 20$, we conclude that coming CMB polarization experiments should not encounter any scale dependence of the spectrum around that region.

*As we shall see in the next section, observable features in the spectra must have an identifiable structure over a range of scales smaller than $\ln k$. This implies that $\ln k$ -derivatives acting on either $\Delta\mathcal{P}_T$ or $\Delta\mathcal{P}_S$ must be large.

The article is organized as follows: In Section 4.1 we present the method used and derive the correlation of the two power spectra for the cases where *i*) features appear due to sudden variations of the Hubble scale, and *ii*) variations in both the Hubble scale and the sound speed are responsible for features. In Section 4.2, we present results for the tensor power spectrum in the low ℓ region, modeling the features in the scalar signal with a Gaussian and a cosine function. Finally, we conclude in Section 4.3.

4.1 Correlation of power spectra

In this section we apply the methods elaborated in [65, 4] to correlate features appearing in the tensor and scalar power spectra. Our method is based on the *in-in* formalism to study the evolution of quantum fluctuations on a time dependent quasi-de Sitter background [23, 22]. Another widely used method to study features is the so called generalized slow-roll formalism [77, 78, 79, 80].

4.1.1 Preliminaries

Let us set the ground for the computation by first writing down the quadratic actions for the scalar and tensor perturbations in Fourier space. For the scalar part we will consider the primordial curvature perturbation \mathcal{R} in comoving gauge. On the other hand, for the tensor part we will work with the traceless and transverse perturbation γ_{ij} as:

$$\gamma_{ij}(\mathbf{k}, \tau) \equiv h_+(\mathbf{k}, \tau)e_{ij}^+(\mathbf{k}) + h_\times(\mathbf{k}, \tau)e_{ij}^\times(\mathbf{k}), \quad (4.2)$$

where \mathbf{k} is the wave vector (or momenta), and $e_{ij}^+(\mathbf{k})$ and $e_{ij}^\times(\mathbf{k})$ are the elements of a time independent basis for tensors satisfying $\delta^{ij}e_{ij} = 0$ and $k^i e_{ij} = 0$. We may further define canonically normalized fields u and $f_{+,\times}$ as

$$u = z\mathcal{R}, \quad f_{+,\times} = a(t)h_{+,\times}, \quad z \equiv \sqrt{2\varepsilon}\frac{a}{c_s}, \quad (4.3)$$

where $a(t)$ is the scale factor, c_s is the sound speed of the curvature perturbations and $\varepsilon = -\dot{H}/H^2$ the first Hubble slow-roll parameter. In these variables, the quadratic actions for scalar and tensor modes in conformal time τ are found to be

$$S_S^{(2)} = \frac{1}{2} \int d\tau d^3k \left[(u')^2 + c_s^2 k^2 u^2 + \frac{z''}{z} u^2 \right], \quad (4.4)$$

$$S_T^{(2)} = \frac{1}{2} \int d\tau d^3k \left[(f')^2 + k^2 f^2 + \frac{a''}{a} f^2 \right], \quad (4.5)$$

where we have chosen units such that $m_{\text{Pl}} = 1$, while keeping only one polarization mode for simplicity. Notice that primes ($'$) represent derivatives with respect to τ . The background quantities z''/z and a''/a may be written as

$$\frac{z''}{z} = (aH)^2 \left(2 - \varepsilon + \frac{1}{2}\eta - s \right) \left(1 + \frac{1}{2}\eta - s \right) + aH \left(\frac{\eta'}{2} - s' \right), \quad (4.6)$$

$$\frac{a''}{a} = (aH)^2 (2 - \varepsilon), \quad (4.7)$$

where $\eta = \varepsilon'/\varepsilon aH$ and $s = c'_s/c_s aH$.

4.1.2 Rapidly time varying backgrounds

To describe the origin of features, we may split each action into a zeroth order term, that describes the evolution of fluctuations in a quasi-de Sitter spacetime, and an interaction term, that contains the rapidly varying contributions of the background. To do so, we will assume that the background is such that ε remains small ($\varepsilon \ll 1$) throughout the whole relevant period where features are sourced. To model this behavior we will take ε to be of the form:

$$\varepsilon = \varepsilon_0 + \Delta\varepsilon, \quad |\Delta\varepsilon| \ll \varepsilon_0, \quad (4.8)$$

where ε_0 is (for any practical purpose) a constant, and $\Delta\varepsilon(\tau)$ contains information about the sudden variations of the background. One could consider that $\varepsilon_0 = -\dot{H}_0/H_0^2$, where H_0 is the slowly varying part of the Hubble expansion rate. In the same manner, η will have two contributions:

$$\eta = \eta_0 + \Delta\eta, \quad \Delta\eta = -\frac{1}{\varepsilon_0}\tau\Delta\varepsilon', \quad (4.9)$$

where $\eta_0 = -\dot{\varepsilon}_0/H_0\varepsilon_0$. Given that we are taking ε_0 as a slowly varying function, we may neglect η_0 against $\Delta\eta$ and simply take

$$\eta = -\frac{1}{\varepsilon_0}\tau\Delta\varepsilon'. \quad (4.10)$$

We will additionally assume that η remains small at all times:

$$|\eta| \ll 1. \quad (4.11)$$

However, given that we are interested into understanding the effects of rapidly varying backgrounds, further derivatives of η could be large, and the following hierarchy may be satisfied:

$$|\eta| \ll |\tau\eta'| \ll |\tau^2\eta''|. \quad (4.12)$$

On the other hand, we may also consider rapid variations of the sound speed c_s admitting departures from the slowly varying value $c_0 = 1$:

$$\theta \equiv 1 - c_s^2 \ll 1, \quad |\theta| \ll |\tau\theta'| \ll |\tau^2\theta''|. \quad (4.13)$$

The hierarchies (4.12) and (4.13), together with eqs. (4.8) and (4.11), reflect what we mean by having a rapid varying background near a quasi-de Sitter state.

The previous assumptions allow us to rewrite z''/z and a''/a in the following way

$$\frac{z''}{z} = \frac{2}{\tau^2} \left(1 + \frac{1}{2}\delta_S(\tau) \right), \quad \frac{a''}{a} = \frac{2}{\tau^2} \left(1 + \frac{1}{2}\delta_T(\tau) \right), \quad (4.14)$$

where we have used $\tau \simeq -(aH)^{-1}(1 + \varepsilon)$, and introduced the quantities $\delta_S(\tau)$ and $\delta_T(\tau)$ to parametrize the rapid variations of the background:

$$\delta_S(\tau) = 3\varepsilon + \frac{1}{2}\eta - \frac{\tau}{2}\eta' - 3s + \tau s', \quad \delta_T(\tau) = 3\varepsilon. \quad (4.15)$$

By plugging these expressions back into the actions of eqs. (4.4) and (4.5) and treating the rapidly varying parts as interaction terms, we may split the theory as:

$$S_S^0 = \frac{1}{2} \int d\tau d^3k \left[(u')^2 + k^2 u^2 + \frac{2}{\tau^2} u^2 \right], \quad S_S^{\text{int}} = \frac{1}{2} \int d\tau d^3k \left[\frac{\delta_S(\tau)}{\tau^2} u^2 \right], \quad (4.16)$$

$$S_T^0 = \frac{1}{2} \int d\tau d^3k \left[(f')^2 + k^2 f^2 + \frac{2}{\tau^2} f^2 \right], \quad S_T^{\text{int}} = \frac{1}{2} \int d\tau d^3k \left[\frac{\delta_T(\tau)}{\tau^2} f^2 \right]. \quad (4.17)$$

Notice that eq. (4.12) implies a further hierarchy of the form

$$|\delta| \ll |\tau \delta'| \ll |\tau^2 \delta''|, \quad (4.18)$$

where δ stands for both δ_S and δ_T . Given that a change in e -folds dN is related to a change in conformal time by $dN = -d\tau/\tau$, the previous hierarchies simply tell us that δ_S and δ_T vary rapidly over an e -fold:

$$|\delta| \ll \left| \frac{d\delta}{dN} \right| \ll \left| \frac{d^2\delta}{dN^2} \right|. \quad (4.19)$$

As we shall see, these are the rapidly varying functions that source the appearance of features in the spectra.

4.1.3 In-in formalism

We may now use the standard *in-in* formalism (see [81] for a review), which provides a way to compute the effects of the rapid time varying background on n -point correlation functions. To simplify the discussion, let us focus our attention on the scalar sector of the theory (*i.e.* the u fluctuations), and then come back to the case of tensor modes. Firstly, the complete solution $u(\mathbf{k}, \tau)$ can be written in terms of interaction picture fields $u_I(\mathbf{k}, \tau)$ as

$$u(\mathbf{k}, \tau) = U^\dagger(\tau) u_I(\mathbf{k}, \tau) U(\tau), \quad (4.20)$$

where $U(\tau)$ is the propagator, given by

$$U(\tau) = \mathcal{T} \exp \left[-i \int_{-\infty_+}^{\tau} d\tau' H_I(\tau') \right].$$

Here \mathcal{T} is the time ordering symbol, and $\infty_+ = (1 + i\varepsilon)\infty$ is the usual prescription to choose the right vacuum in the infinite past. In addition, $H_I(\tau)$ is the interaction Hamiltonian, given by

$$H_I = -\frac{\delta_S(\tau)}{\tau^2} \frac{1}{2} \int d^3k u_I^2. \quad (4.21)$$

The interaction picture fields $u_I(\mathbf{k}, \tau)$ are given by free field solutions of the zeroth order action (*i.e.* with $\delta_S = 0$), written in terms of creation and annihilation operators $a_{\mathbf{k}}^\dagger$ and $a_{\mathbf{k}}$ as:

$$u_I(\mathbf{k}, \tau) \equiv a_{\mathbf{k}} u_k(\tau) + a_{-\mathbf{k}}^\dagger u_k^*(\tau). \quad (4.22)$$

The creation and annihilation operators satisfy the standard commutation relation $[a_{\mathbf{k}}, a_{\mathbf{k}'}^\dagger] = (2\pi)^3 \delta^{(3)}(\mathbf{k} - \mathbf{k}')$, whereas the mode functions $u_k(\tau)$ are given by mode solutions respecting Bunch-Davies initial conditions:

$$u_k(\tau) = \frac{1}{\sqrt{2k}} \left(1 - \frac{i}{k\tau} \right) e^{-ik\tau}. \quad (4.23)$$

Furthermore, the vacuum state $|0\rangle$ is defined to satisfy $a_{\mathbf{k}}|0\rangle = 0$. By expanding the propagator $U(\tau)$, we may compute corrections to the two point function as The power spectrum $\mathcal{P}_{\mathcal{R}}(k, \tau)$ of the primordial curvature perturbation \mathcal{R} (evaluated at a given time τ) is related to the two point function $\langle u(\mathbf{k}, \tau)u(\mathbf{k}', \tau) \rangle$ as follows:

$$\frac{1}{z^2} \langle u(\mathbf{k}, \tau)u(\mathbf{k}', \tau) \rangle \equiv \frac{2\pi^2}{k^3} \delta^{(3)}(\mathbf{k} - \mathbf{k}') \mathcal{P}_{\mathcal{R}}(k, \tau). \quad (4.24)$$

We are interested in the power spectrum of super horizon modes at the end of inflation $\mathcal{P}_{\mathcal{R}}(k)$, which corresponds to the $\tau \rightarrow 0$ limit of $\mathcal{P}_{\mathcal{R}}(k, \tau)$. By taking into account the splitting of the theory into the zeroth order quasi-de Sitter part and the interaction part, we finally obtain

$$\mathcal{P}_{\mathcal{R}}(k) = \mathcal{P}_S^0 + \Delta \mathcal{P}_S(k), \quad \mathcal{P}_S^0(k) = \frac{H_0^2}{8\pi^2 \varepsilon_0}, \quad (4.25)$$

where \mathcal{P}_S^0 corresponds to the standard power spectrum for curvature perturbations in a quasi-de Sitter space-time, and $\Delta \mathcal{P}_S(k)$ contains the deviations from scale invariance induced by the rapidly varying background[†] [4]

$$\Delta_S(k) \equiv \frac{\Delta \mathcal{P}_S}{\mathcal{P}_S^0} = \frac{i}{4k^3} \int_{-\infty}^{\infty} d\tau \left[\frac{\theta''''}{8} + \frac{\delta_H''}{2\tau^2} - \frac{\delta_H}{\tau^4} \right] e^{2ik\tau}, \quad (4.26)$$

where θ is defined in (4.13) and δ_H is given by

$$\delta_H(\tau) = 3\varepsilon + \frac{1}{2}\eta - \frac{\tau}{2}\eta'. \quad (4.27)$$

Notice that the integration in eq. (4.26) is performed over the whole real line $(-\infty, +\infty)$, which from now on will be omitted. To derive eq. (4.26) we did the following trick [65]: We extended the τ -integration domain from $(-\infty, 0)$ to $(-\infty, +\infty)$ by imposing that both θ and δ_H are antisymmetric functions with respect to the interchange $\tau \rightarrow -\tau$.

We may now repeat all of the previous steps to compute the way that features appear in the tensor power spectrum. We find

$$\mathcal{P}_T(k) = \mathcal{P}_T^0 + \Delta \mathcal{P}_T(k), \quad \mathcal{P}_T^0(k) = \frac{H_0^2}{2\pi^2},$$

where $\Delta \mathcal{P}_T(k)$ is given by

$$\Delta_T(k) \equiv \frac{\Delta \mathcal{P}_T}{\mathcal{P}_T^0} = \frac{i}{4k^3} \int d\tau \left[\frac{\delta_T''}{2\tau^2} - \frac{\delta_T}{\tau^4} \right] e^{2ik\tau}. \quad (4.28)$$

[†]Notice that in eq. (4.26) time derivatives may be interchanged by factors of $-2ik$. Therefore, the appearance of four derivatives in θ might be deceiving, as the original expression [4] leading to eq. (4.26) had no time derivatives acting on θ . Having time derivatives acting on both θ and δ_H in eq. (4.26) allows one to have a single function of time being Fourier-transformed at the right hand side of the equation.

Equations (4.26) and (4.28) are the basic equations that we will exploit to obtain the desired correlation between the two sectors of the theory. Before deducing such a relation, let us notice that the hierarchy of eq. (4.18) necessarily implies a hierarchy in Fourier space affecting the spectra, that reads

$$|\Delta(k)| \ll \left| \frac{d\Delta(k)}{d \ln k} \right| \ll \left| \frac{d^2 \Delta(k)}{d \ln k^2} \right|, \quad (4.29)$$

where $\Delta(k)$ stands for both $\Delta_S(k)$ and $\Delta_T(k)$.

4.1.4 Features from varying Hubble parameters

In this subsection we consider the case where $c_s = 1$ for all times, so that $\delta_S = \delta_H$, and any observable feature is the outcome of sudden variations of $H(t)$. Firstly, because of the hierarchy (4.18) satisfied by δ_T , eq. (4.28) may be simplified as:

$$\Delta_T(k) = \frac{i}{8k^3} \int d\tau \frac{\delta''_T}{\tau^2} e^{2ik\tau}. \quad (4.30)$$

Furthermore, because of eq. (4.15), we see that eq. (4.30) may be rewritten in terms of η as:

$$\Delta_T(k) = -\frac{3i\varepsilon_0}{8k^3} \int d\tau \frac{\eta'}{\tau^3} e^{2ik\tau}. \quad (4.31)$$

This expression may now be Fourier inverted, leading to a formal expression for η' in terms of $\Delta_T(k)$ as

$$\eta' = \frac{1}{3\varepsilon_0} \int dk \left[\frac{d^3}{d \ln k^3} \Delta_T(k) \right] e^{-2ik\tau}. \quad (4.32)$$

Next, we may use the hierarchy of eq. (4.18) satisfied by δ_S to rewrite eq. (4.26) as

$$\Delta_S(k) = -\frac{i}{16k^3} \int d\tau \frac{1}{\tau} \eta''' e^{2ik\tau}, \quad (4.33)$$

where we used the fact that $\delta_H \simeq -\tau\eta'/2$. As a last step, we may insert the expression for η' in eq. (4.32) back into eq. (4.33), to obtain the main result of this work:

$$\frac{d^2}{d \ln k^2} \Delta_T = 6\varepsilon_0 \Delta_S. \quad (4.34)$$

This equation offers the desired link between features in the tensor and scalar spectra. Notice from eq. (4.31) that even though we have assumed that $\varepsilon \ll 1$, the piece $\Delta_T(k)$ could in principle be large. However, from eq. (4.34), we see that features in the tensor power spectrum are highly suppressed with respect to those in the scalar spectrum. This is not only due to the presence of ε_0 [74], but also due to the double $\ln k$ -derivative acting on $\Delta_T(k)$, on account of the hierarchy (4.29).

In the next subsection we extend this result to the more general case in which rapid variations of the sound speed are also allowed. As we shall see, in this case too, tensor features remain generically suppressed.

4.1.5 Including the effects of a varying sound speed

In the EFT of inflation [61, 62], the quadratic part of the action may exhibit a non-trivial sound speed for the perturbations, which could also lead to the presence of features in the scalar power spectrum [82, 83]. In general the evolution of $c_s(t)$ is independent of the evolution of H . That means that if features are generated by the simultaneous rapid variation of both c_s and H , then the scalar and tensor power spectra would exhibit uncorrelated oscillatory features. This is because \mathcal{P}_S would have features sourced by both c_s and H while \mathcal{P}_T would have features sourced by H alone. We would then have a relation of the form

$$\Delta_S = \frac{1}{6\varepsilon_0} \frac{d^2}{d \ln k^2} \Delta_T + \Delta_c, \quad (4.35)$$

where Δ_c represents the features sourced by variations of the sound speed c_s .

There are however intuitive reasons to expect that, at least in certain classes of models, variations of c_s and H happen in synchrony. An example of such a situation is the case where the inflationary valley admits turns, which is typical in multifield inflation [82]. In these scenarios, as the inflaton traverses a curve in the field space, there are instant deviations from slow-roll produced by “centrifugal” effects. Furthermore, the existence of such turns is responsible for a non-trivial sound speed [84]. The two quantities should thus be related since they stem from the same source. Another situation where c_s and H vary simultaneously is in $P(X, \varphi)$ models, where the kinetic term of the inflaton has a non-trivial structure. In these cases a reduction of the rapidity of the vacuum expectation value of the inflaton would inevitably induce a change in both c_s and H .

To capture the aforementioned situations, in [68], a one parameter relation between the Hubble slow-roll parameter η and the sound speed was proposed. This had the form

$$\eta = \eta_0 - \frac{\alpha}{2} \tau \theta', \quad (4.36)$$

with $\alpha \in \mathbb{R}$ and $\theta = 1 - c_s^2$. It was also shown to hold within several classes of models including $P(X, \varphi)$ and multifield models, with α admitting specific values for each case.

Using this fact, one may now relate θ to η in eq. (4.26) and follow the exact same steps to obtain a generic relation between the scalar and tensor power spectra in the case where both the sound speed and the Hubble radius experience sudden variations:

$$\frac{d^2}{d \ln k^2} \Delta_T = 6\varepsilon_0 \frac{\alpha}{1 + \alpha} \Delta_S, \quad \alpha \neq -1, \quad (4.37)$$

and for the special case of $\alpha \simeq -1$:

$$\frac{d}{d \ln k} \Delta_T = -\frac{6}{5} \varepsilon_0 \Delta_S. \quad (4.38)$$

We see that in these set-up’s too, deviations of the tensor power spectrum from scale invariance are suppressed by the slow-roll parameter ε as well as a double and a single momentum integral which smoothes out any acute variation of the scalar spectrum.

Before discussing quantitative features of these results, let us stress once more that the simple forms of eqs. (4.34), (4.37) and (4.38) are leading order expressions based on the assumption that any observable feature satisfy the following: *i*) it is sharp, in the sense that any departure from scale invariance should take place within few e-folds, and *ii*) it doesn't disrupt inflation, that is, ε remains small through out the whole dynamics.

4.2 A quantitative discussion

We now discuss the results of the previous section in two interesting situations. First, we consider the case in which resonant features are present throughout the whole spectra, and second, the case of the low ℓ power deficit observed in the scalar power spectrum. For this discussion, it will be useful to write concrete expressions relating features in the spectra and the rapidly varying contributions to the slow-roll parameters $\Delta\varepsilon$ and $\Delta\eta$. By Fourier inverting eq. (4.33) for the general case where the sound speed also contributes to features, these are found to be given by [4]

$$\Delta\eta(\tau) = \frac{i}{\pi} \frac{\alpha}{1+\alpha} \int dk \left[\frac{d}{dk} \frac{\Delta\mathcal{P}_S}{\mathcal{P}_S^0} \right] e^{2ik\tau}, \quad \Delta\varepsilon(\tau) = \frac{i\varepsilon_0}{\pi} \frac{\alpha}{1+\alpha} \int dk \left[\frac{1}{k} \frac{\Delta\mathcal{P}_S}{\mathcal{P}_S^0} \right] e^{2ik\tau}, \quad (4.39)$$

with $\Delta\varepsilon$ following from the relation $\Delta\eta = -\tau\Delta\varepsilon'/\varepsilon_0$. Note that the coefficient $\frac{\alpha}{1+\alpha}$ in eq. (4.39) is an $\mathcal{O}(1)$ number for any α so its specific value has no impact on the results. We thus set it to one in what follows and work with eq. (4.34). The only case where it plays a role is when $\alpha \simeq -1$, in which the next to leading time derivative dominates in the RHS of eq. (4.26) leading to the following expressions:

$$\Delta\eta(\tau) = -\frac{i}{5\pi} \int dk k \left[\frac{d^2}{dk^2} \frac{\Delta\mathcal{P}_S}{\mathcal{P}_S^0} \right] e^{2ik\tau}, \quad \Delta\varepsilon(\tau) = -\frac{i\varepsilon_0}{5\pi} \int dk \left[\frac{d}{dk} \frac{\Delta\mathcal{P}_S}{\mathcal{P}_S^0} \right] e^{2ik\tau}. \quad (4.40)$$

4.2.1 Resonant features

This type of scale dependence is relevant in models of inflation where the potential is periodic or semi-periodic, such as axion monodromy inflation [85], or models like Natural Inflation [86]. Inflationary scenarios involving axions usually require super-Planckian field range, and hence, they are good candidates for the production of primordial gravitational waves [87, 88].

To acquire an idea of the possible impact of resonant features on the tensor power spectrum, we model the resonant part of the scalar power spectrum as

$$\Delta_S(k) = A \cos(\Omega \log(k/k_*) + \phi), \quad (4.41)$$

where A parametrizes the amplitude of the feature, while Ω and ϕ denote the frequency and the phase of the oscillation, respectively. To be concrete, we will consider the following values $A = 0.028$, $\Omega = 30$ and $\phi/2\pi = 0.634$, which were found to constitute the best fit in the analysis of resonant features by Planck [7]. In addition, we set $k_* = 0.05$ [Mpc] $^{-1}$ as a reference scale.

Case for $\alpha \neq -1$

Using the parametrization (4.41) as a input, we numerically obtain the shape of the tensor spectrum feature via eq. (4.34), while the slow-roll parameters are reconstructed from eq. (4.39). The results are shown in the plots of figure 4.1. There we see that features in the tensor power spectrum are present, albeit with an amplitude of $\Delta_T \sim 10^{-6}$ making them observationally irrelevant. This is a complementary argument in support of the claim that tensor features stemming from axionic potentials should be suppressed due to the smallness of the decay constant of the axion [89].

Case for $\alpha \simeq -1$

Next, we consider the special case of $\alpha \simeq -1$ for the resonance features. We numerically solve eqs. (4.38) and (4.40) and plot the results in figure 4.2. As can be seen, even though there is an order of magnitude enhancement with respect to the general case, the amplitude of the deviation from a scale invariant spectrum still remains extremely small. Furthermore, in this case η can reach values up to $\eta \sim 0.8$. This does not invalidate the hierarchy (4.12), as to go from eq. (4.6) to eq. (4.14) one really requires $\eta/2$ to be much smaller than 1.

4.2.2 Predictions for the low ℓ tensor power spectrum

The low ℓ multipole region is the main observational window into CMB polarization since it is not contaminated by lensing effects. In addition, it is where the low ℓ deficit takes place in the scalar power spectrum [32, 36, 37, 38, 39, 40, 41, 42]. We focus in the $\ell < 50$ region, roughly corresponding to $0.0002 \lesssim k \lesssim 0.004$ [Mpc] $^{-1}$, which is the band that CMB polarization observatories focus on.

In order to get a quantitative look into the tensor power spectrum we model the $\ell \sim 20$ dip in the angular power spectrum as a sharp Gaussian:

$$\Delta_S(k) = -Ae^{-\lambda(\ln(k/k_*)^2)}, \quad (4.42)$$

where k_* determines the location of the feature. We set $A = 0.15$, $\lambda = 15$ and $k_* = 0.002$ [Mpc] $^{-1}$, which are chosen to have a rough fit with the observed power deficit. In addition, we choose $\varepsilon_0 = 0.0068$ [7].

Case with $\alpha \neq -1$

We solve eqs. (4.34) and (4.39) with the parametrization (4.42) as an input, with the results shown in the plots of figure 4.3. We see that for a realistic amplitude A the tensor power spectrum exhibits a feature of amplitude $\Delta_T \sim 10^{-9}$.

Case with $\alpha \simeq -1$

In the special case of $\alpha \simeq -1$, we see that the tensor spectrum and the slow-roll parameters, now given by eqs. (4.38) and (4.40) respectively, exhibit a feature which is enhanced by an order of magnitude compared to the previous case. However, as seen in figure 4.4, the amplitude still remains extremely small.

4.3 Conclusions

We have studied the possible appearance of scale dependent features in the power spectrum of primordial tensor perturbations due to non-trivial inflationary dynamics in a model independent way. Our main result is eq. (4.34) – or eqs. (4.37), (4.38) in the more general case of EFT’s with a sound speed – which consist of relations linking features in the tensor power spectrum to those appearing in the scalar power spectrum, allowing us to estimate the amplitude and shape of the former given the latter. In general, we find that the tensor spectrum is expected to be featureless: Indeed, eq. (4.34) shows that any feature appearing in the tensor spectrum is generically suppressed with respect to those appearing in the scalar one for two reasons: firstly due to slow-roll [74], and more importantly, due to the fact that features should in general be sharp enough in order to leave an imprint in the CMB.

One may wonder about other mechanisms producing features in the tensor sector of the theory. For instance, in principle, we could consider a Lagrangian describing the dynamics of tensor modes with a sound speed c_t experiencing rapid variations producing features in the tensor spectrum. However, in [90] it was shown that under a disformal transformation, models with a non-trivial tensor sound speed (and canonical scalar sector) map into models with a non-trivial scalar sound speed (and canonical tensor sector). Since the spectra are invariant under such a transformation, our formalism to relate features in the tensor spectrum to those appearing in the scalar spectrum would continue to be valid. Moreover, in the special case where only c_t varies, the disformal transformation would lead to an equivalent system where both c_s and H vary, but in such a way that the scalar spectrum remains featureless [75]. Given that we are interested in understanding the consequences of features in the scalar spectrum on the tensor one, this class of situations is out of our scope.

Current CMB observations show the existence of departures from scale invariance in the power spectrum of primordial curvature perturbations in the multipole range $\ell \sim 20$. If we interpret this behavior as the result of the dynamics of inflation, we are led to conclude that the tensor power spectrum will not show any consequential departure from scale invariance in this region. The importance of this conclusion may be appreciated more clearly by inverting the statement: If tensor modes are observed to have strong departures from scale invariance in the aforementioned multipole range, then we will have good reasons to suspect that the departures appearing in the scalar spectrum are not of primordial origin.

4.4 Figures

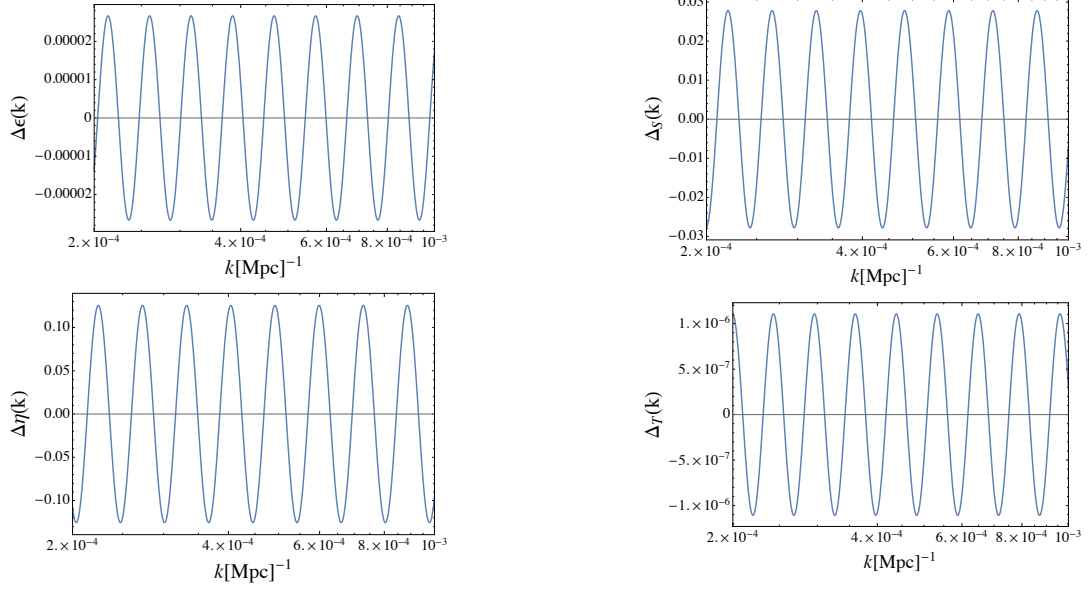


Figure 4.1: The first two slow-roll parameters $\Delta\eta$ and $\Delta\epsilon$ (left panels) using eq. (4.39) and $\frac{\Delta P_S}{P_S^0}(k)$, $\frac{\Delta P_T}{P_T^0}(k)$ (right panels) related by eq. (4.34), in the case of the resonant feature (4.41). We have used $A = 0.028$, $\Omega = 30$, $\phi/2\pi = 0.634$, $k_* = 0.05[\text{Mpc}]^{-1}$ and $\epsilon_0 = 0.0068$.

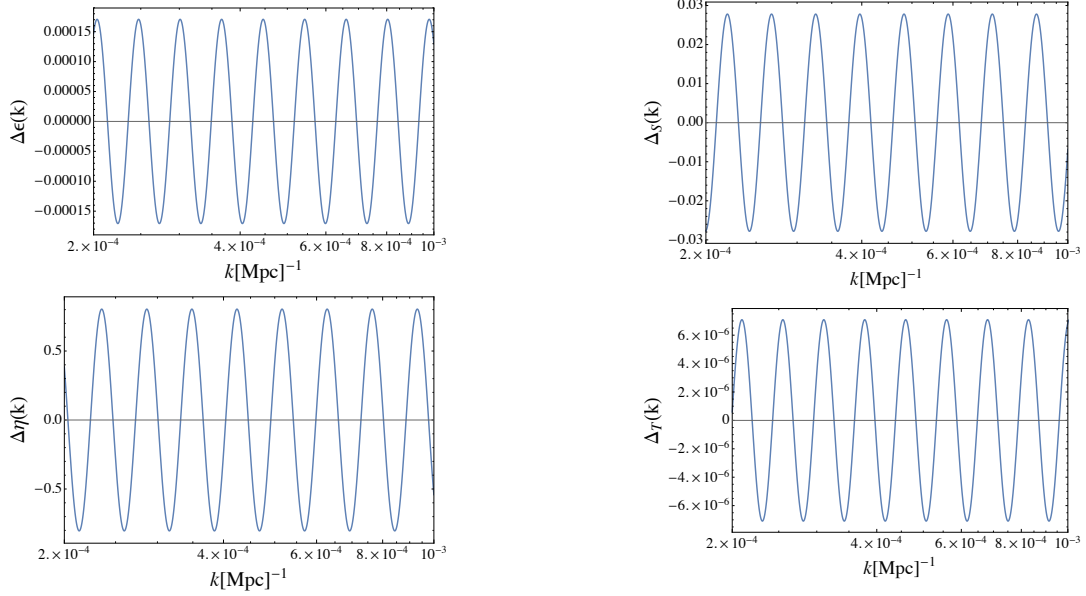


Figure 4.2: The first two slow-roll parameters $\Delta\eta$ and $\Delta\varepsilon$ (left panels) using eq. (4.40) and $\frac{\Delta P_S}{P_S^0}(k)$, $\frac{\Delta P_T}{P_T^0}(k)$ (right panels) related by eq. (4.38), in the case of the resonant feature (4.41). We have used $A = 0.028$, $\Omega = 30$, $\phi/2\pi = 0.634$, $k_* = 0.05[\text{Mpc}]^{-1}$ and $\varepsilon_0 = 0.0068$.

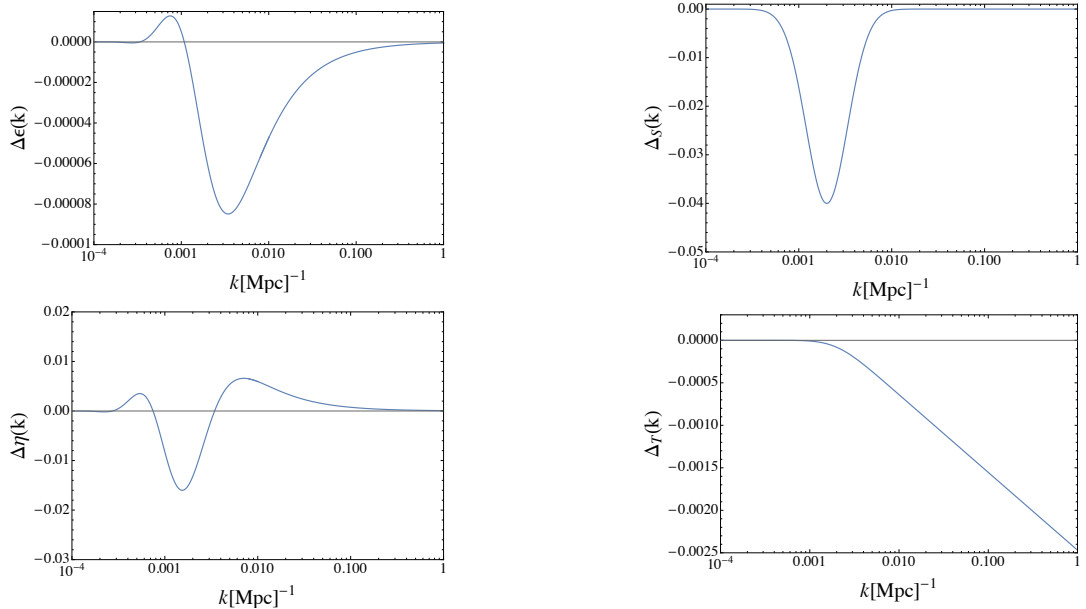


Figure 4.3: The first two slow-roll parameters $\Delta\eta$ and $\Delta\varepsilon$ (left panels) using eq. (4.39) and $\frac{\Delta P_S}{P_S^0}(k)$, $\frac{\Delta P_T}{P_T^0}(k)$ (right panels) related by eq. (4.34), in the case of the Gaussian feature (4.42). We have used $A = -0.15$, $\lambda = 15$, $k^* = 0.002[\text{Mpc}]^{-1}$ and $\varepsilon_0 = 0.0068$.

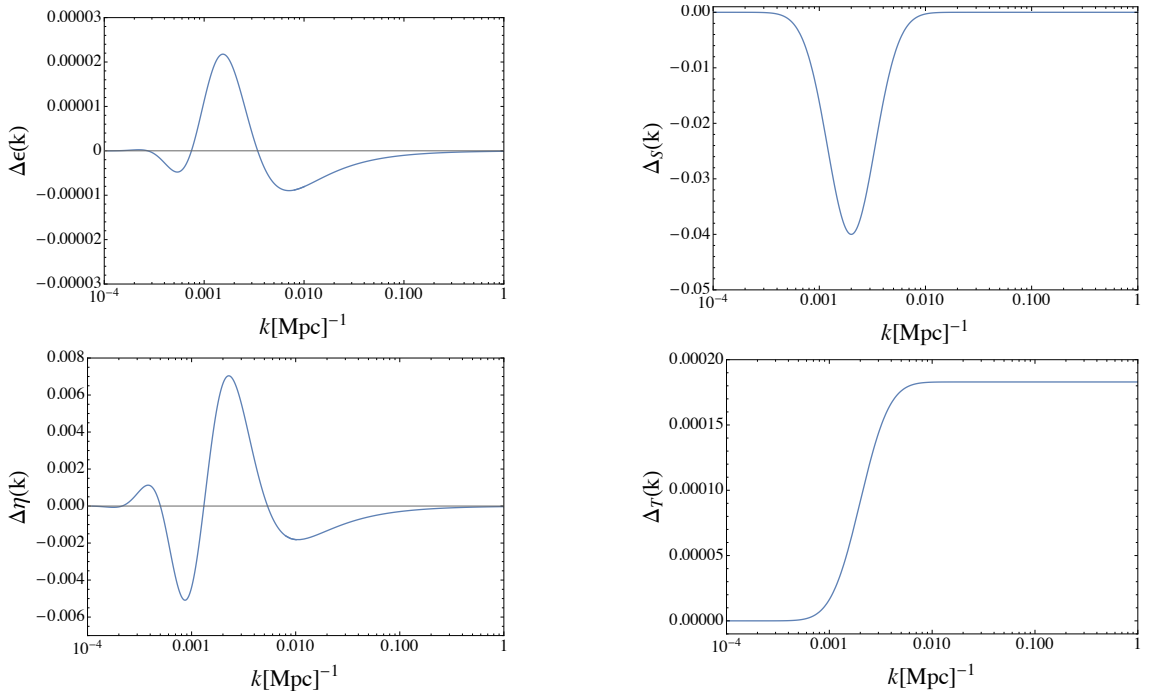


Figure 4.4: Plot of the first two slow-roll parameters $\Delta\eta$ and $\Delta\varepsilon$ (left panels) using eq. (4.40) and $\frac{\Delta P_S}{P_S^0}(k)$, $\frac{\Delta P_T}{P_T^0}(k)$ (right panels) related by eq. (4.38), in the case of the Gaussian feature (4.42). We have used $A = -0.15$, $\lambda = 15$, $k^* = 0.002[\text{Mpc}]^{-1}$ and $\varepsilon_0 = 0.0068$.

Chapter 5

Consistency relations

It is by now well understood that Maldacena's consistency relation $f_{\text{NL}} = 5(1 - n_s)/12$ [23], linking together the amount of local (squeezed) non-Gaussianity f_{NL} with the spectral index $n_s - 1$, and valid for attractor models of single field inflation [91, 92, 93, 94, 95, 96, 97, 98], cannot be directly observed. A correct account of the observable amount of primordial local non-Gaussianity yields [99, 3, 100, 1, 101]

$$f_{\text{NL}}^{\text{obs}} = 0 + \mathcal{O}(k_L^2/k_S^2), \quad (5.1)$$

where $\mathcal{O}(k_L^2/k_S^2)$ stands for non-Gaussianity produced by non-primordial phenomena such as gravitational lensing and redshift perturbations (the so called projection effects [102, 103]). This result may be understood as coming from a cancellation between the primordial value predicted in co-moving gauge $5(1 - n_s)/12$, and a correction $-5(1 - n_s)/12 + \mathcal{O}(k_L/k_S)$ that arises after considering a change of coordinates rendering gauge invariant observables. This coordinate change corresponds to a transformation from co-moving coordinates to the so called conformal Fermi coordinates [2, 3].

It appears to be entirely reasonable that the cancellation leading to (5.1) is only effective when the prediction of primordial non-Gaussianity corresponds to $f_{\text{NL}} = 5(1 - n_s)/12$. This is because Maldacena's consistency relation itself may be thought of as the consequence of a space-time reparametrization linking short- and long-wavelength curvature perturbations realized with the help of a symmetry of the system under a simultaneous spatial dilation and a field reparametrization [91]. Thus, any measurement of local non-Gaussianity would directly rule out single field models of slow-roll inflation [5, 27, 6, 28, 104] (attractor models of inflation), but it would not rule out other classes of inflation. In particular, one would be seriously motivated to consider more exotic models of inflation such as curvaton scenarios [105], multi-field models [106], or non-attractor models of inflation (that is, models for which the background depends on the initial conditions [107, 108, 109, 110, 111]). For instance, in the case of ultra slow-roll inflation [112, 107], one finds $f_{\text{NL}} = 5/2$, from where it seems unlikely that a cancellation could happen.

In this article, we show that there is a slightly more general class of non-Gaussian consistency relations, of which Maldacena's relation is an example. This generalization emerges

from a space-time reparametrization (linking short- and long-wavelength curvature perturbations) that is realized with the help of a more general symmetry. This time, the symmetry transformation involves both a time dilation and a spatial dilation. We will show that this symmetry is approximate in the case of $\varepsilon \ll 1$ (where ε is the standard first slow-roll parameter), but exact in the case of ultra slow-roll (independently of the value of ε). In a previous work [111] a few of us have already investigated the derivation of non-Gaussian consistency relations valid for non-attractor models using symmetry arguments. The difference between the present work and ref. [111] is that the symmetry used here involves a space-time reparametrization affecting the action of curvature perturbations, whereas the symmetry explored in [111] corresponds to a symmetry of the full action driving inflation.*

The existence of a more general consistency relation (coming from space-time reparametrizations) suggests that the vanishing of eq. (5.1) may be effective under more general conditions, valid beyond the attractor single field models of inflation. In particular, one could expect (5.1) to be valid in the extreme case of ultra slow-roll inflation. We will argue that this is indeed the case in a companion article [114], where the use of conformal Fermi coordinates is considered for the case of non-attractor models.

We have organized this article as follows: In Section 5.1 we offer a review of the derivation of the standard consistency relation for single field slow-roll inflation (attractor inflation). In Section 5.2 we derive the generalized version of the consistency relation. We do this first for the simple case $\varepsilon \rightarrow 0$, and then extend this result to the more subtle case $\varepsilon \neq 0$, where we pay some attention to the particular case of ultra slow-roll inflation. Then, in Section 5.3 we briefly discuss our results, and ask how they could be modified by deviations from the canonical models of inflation for which our results are strictly valid. Finally, in Section 5.4 we present our conclusions.

5.1 Review of the consistency relation derivation

Let us start by reviewing the derivation of the standard consistency relation for single field slow-roll attractor inflation, in which the curvature perturbation freezes on superhorizon scales. We will closely follow the discussion of ref. [94], (see also the derivations in refs. [91, 95]), but with a perspective that will show to be useful for generalizing the relation later on.

The metric line element describing a perturbed FRW spacetime, in co-moving gauge may be written as:

$$ds^2 = a^2(\tau) \left[-N^2 d\tau^2 + 2N_i d\tau dx^i + e^{2\zeta} dx^2 \right], \quad (5.1)$$

where a is the usual scale factor. We have adopted conformal time τ , which is related to cosmological time t via $d\tau = dt/a$. The lapse $\delta N = N - 1$ and shift N_i functions respect constraint equations that are found by varying the action of the perturbations. The linear

*While completing this work we have become aware that Finelli et al. [113] are finishing an article on the same subject, possibly arriving to similar conclusions.

solutions are given by:[†]

$$\delta N = \frac{1}{\mathcal{H}} \partial_0 \zeta, \quad N_i = -\partial_i \frac{\zeta}{\mathcal{H}} + \varepsilon \frac{\partial_i}{\partial^2} \partial_0 \zeta. \quad (5.2)$$

After replacing these solutions back into the action, one obtains a cubic action describing a single scalar degree of freedom ζ . Now, let us consider the following transformations of coordinates and fields:

$$x = e^g x', \quad (5.3)$$

$$\tau = \tau', \quad (5.4)$$

$$\zeta = \zeta' + \Delta\zeta, \quad (5.5)$$

where g and $\Delta\zeta$ are functions of τ' only. We would like to know how these relations affect the form of the ζ -action for a certain choice of g and $\Delta\zeta$. Given that g and $\Delta\zeta$ are taken as perturbations, this would require us to consider the full initial action, Einstein-Hilbert plus scalar field, including the background contributions (this is because (5.3) implies that some background terms will be promoted to perturbations). Instead of examining this change by inserting (5.3)-(5.5) in the full action explicitly, we may analyze the way in which the metric (5.1) is affected. This will allow us to infer how the action itself is affected by the transformation. To proceed, first notice that (5.3) and (5.4) imply

$$dx^i = e^g dx'^i + e^g \partial_0 g x'^i d\tau', \quad (5.6)$$

$$d\tau = d\tau'. \quad (5.7)$$

In second place, recall that N and N_i were already fixed in terms of ζ , and so they must change according to (5.5). This is because we are examining how the transformations alter the form of the ζ -action after N and N_i were solved. One finds:

$$\delta N = \delta N' + \frac{1}{\mathcal{H}} \partial_0 \Delta\zeta, \quad (5.8)$$

$$N_i = N'_i + \partial_i \Delta\psi, \quad (5.9)$$

where $\Delta\psi$ is such that

$$\partial^2 \Delta\psi = -\partial^2 \frac{\Delta\zeta}{\mathcal{H}} + \varepsilon \partial_0 \Delta\zeta. \quad (5.10)$$

Given that we are choosing $\Delta\zeta$ to be x' -independent, $\Delta\psi$ satisfies the simpler equation $\partial^2 \Delta\psi = \varepsilon \partial_0 \Delta\zeta$. This equation is solved by $\Delta\psi = \frac{1}{6} x^i x_i \varepsilon \partial_0 \Delta\zeta$, and so we may write:

$$\partial^i \Delta\psi = \frac{1}{3} x'^i \varepsilon \partial_0 \Delta\zeta. \quad (5.11)$$

Then, replacing all of these results back into the metric (5.1), we obtain:

$$\begin{aligned} ds^2 = & a^2(\tau') \left[-e^{2\delta N' + \frac{2}{\mathcal{H}} \partial_0 \Delta\zeta} d\tau'^2 \right. \\ & \left. + 2 \left(N'_i + \partial_0 g x'_i + \frac{1}{3} x'_i \varepsilon \partial_0 \Delta\zeta \right) d\tau' dx'^i + e^{2\zeta' + 2\Delta\zeta + 2g} dx'^2 \right]. \end{aligned} \quad (5.12)$$

[†]In this work we assume regular Bunch-Davies initial conditions. For a discussion on the effect of considering different initial states, see [115].

It is important to keep the perturbations appearing in the term proportional to dx'^2 up to third order at least. In this case, we have kept $\Delta\zeta$ and g exactly as they appear from the definition of the transformations (5.3)-(5.5). On the other hand, in those terms proportional to $d\tau'^2$ and $d\tau'dx'^i$ we must keep the perturbations up to first order at least. The reason for doing this is that we want to understand how (5.3)-(5.5) change the form of the ζ -action up to third order. Given that the cubic action depends on the linear contributions to δN and N_i , we do not need to worry about contributions coming from $\Delta\zeta$ and g beyond linear order in terms proportional to $d\tau'^2$ and $d\tau'dx'^i$.

Next, notice that if we choose both g and $\Delta\zeta$ constant, and demand them to satisfy $\Delta\zeta = -g$ we end up with

$$ds^2 = a^2(\tau') \left[-N'^2 d\tau'^2 + 2N'_i d\tau' dx'^i + e^{2\zeta'} dx'^2 \right]. \quad (5.13)$$

This metric has exactly the same form of (5.1), and therefore the action for ζ' , obtained by using this metric, has the same form as the one for ζ . This in turn, implies that both ζ and ζ' are solutions of the same system of equations of motion. Moreover, these solutions are connected through the relation:

$$\zeta(\tau, x) = \zeta'(\tau', x') - g. \quad (5.14)$$

Since $\tau = \tau'$ and $x = e^g x'$, we may write instead:

$$\zeta(\tau, x) = \zeta'(\tau, e^{-g} x) - g. \quad (5.15)$$

This relation may be used to derive the squeezed limit of the bispectrum in terms of the power spectrum of the perturbations. First, let us consider a splitting of ζ into short- and long-wavelength contributions of the form:

$$\zeta = \zeta_S + \zeta_L. \quad (5.16)$$

Here, ζ_L is such that it contains modes that have exited the horizon. For all purposes, ζ_L is x -independent. In addition, if we are interested in attractor models of single field inflation, ζ_L is also τ -independent. Then, if in eq. (5.15) we choose $g = -\zeta_L$ (or, equivalently $\Delta\zeta = \zeta_L$), we end up with

$$\zeta_S(\tau, x) = \zeta'(\tau, e^{\zeta_L} x). \quad (5.17)$$

In other words, the long wavelength mode of ζ has been absorbed via a coordinate transformation.[‡] Relation (5.17) tells us that $\zeta_S(\tau, x)$ may be expressed in terms of a fluctuation ζ' that is a solution of the same system of equations satisfied by ζ , but with $e^{\zeta_L} x$ instead of x in the spatial argument. In other words, we have non-linear information about how the long-wavelength mode ζ_L modulates the short wavelength mode ζ_S . Next, let us consider the 2-point correlation function $\langle \zeta_S(\tau, \mathbf{x}) \zeta_S(\tau, \mathbf{y}) \rangle \equiv \langle \zeta_S \zeta_S \rangle(\tau, |\mathbf{x} - \mathbf{y}|)$. Equation (5.17) tells us that

$$\langle \zeta_S \zeta_S \rangle(\tau, |\mathbf{x} - \mathbf{y}|) = \langle \zeta' \zeta' \rangle(\tau, e^{\zeta_L} |\mathbf{x} - \mathbf{y}|). \quad (5.18)$$

[‡]This reveals that ζ corresponds to an adiabatic mode [8, 116], and that the evolution of the short wavelength contribution $\zeta_S(\tau, x)$ may be thought of as that of a perturbation ζ' on a new redefined background (obtained by the absorption of ζ_L).

Notice that $\langle \zeta' \zeta' \rangle(\tau, |\mathbf{x} - \mathbf{y}|)$ is nothing but the usual 2-point correlation function of the curvature perturbation in co-moving gauge (because ζ' is a solution of the full system). Expanding the previous relation in powers of ζ_L , we obtain

$$\langle \zeta_S \zeta_S \rangle(\tau, |\mathbf{x} - \mathbf{y}|) = \langle \zeta' \zeta' \rangle(\tau, |\mathbf{x} - \mathbf{y}|) + \zeta_L \frac{d}{d \ln |\mathbf{x} - \mathbf{y}|} \langle \zeta' \zeta' \rangle(\tau, |\mathbf{x} - \mathbf{y}|) + \dots \quad (5.19)$$

Then, by writing the fields in Fourier space as

$$\zeta(\mathbf{x}) = \frac{1}{(2\pi)^3} \int d^3k \zeta(\mathbf{k}) e^{i\mathbf{k}\cdot\mathbf{x}}, \quad (5.20)$$

we end up with

$$\langle \zeta_S \zeta_S \rangle(\mathbf{k}_1, \mathbf{k}_2) = \langle \zeta' \zeta' \rangle(\mathbf{k}_1, \mathbf{k}_2) - \zeta_L(\mathbf{k}_L) [n_s(k_S, \tau) - 1] P_\zeta(\tau, k_S), \quad (5.21)$$

where we have defined $\mathbf{k}_L = \mathbf{k}_1 + \mathbf{k}_2$ and $\mathbf{k}_S = (\mathbf{k}_1 - \mathbf{k}_2)/2$. In the previous expressions, the power spectrum $P_\zeta(\tau, k)$ and its spectral index $n_s(k) - 1$ are defined as

$$P_\zeta(\tau, k) = \int d^3r e^{-i\mathbf{k}\cdot\mathbf{r}} \langle \zeta \zeta \rangle(\tau, r), \quad (5.22)$$

$$n_s(k, \tau) - 1 = \frac{\partial}{\partial \ln k} \ln(k^3 P_\zeta(\tau, k)), \quad (5.23)$$

with $\mathbf{r} \equiv |\mathbf{x} - \mathbf{y}|$.

The first term at the rhs of eq. (5.21) is independent of ζ_L , so by correlating eq. (5.21) with $\zeta_L(\mathbf{k}_3)$, we obtain

$$\langle \zeta_L(\mathbf{k}_3) \langle \zeta_S \zeta_S \rangle(\mathbf{k}_1, \mathbf{k}_2) \rangle = -\langle \zeta_L(\mathbf{k}_3) \zeta_L(\mathbf{k}_L) \rangle [n_s(k_S, \tau) - 1] P_\zeta(\tau, k_S). \quad (5.24)$$

The squeezed limit of the bispectrum appears as the formal limit:

$$\lim_{k_3 \rightarrow 0} (2\pi)^3 \delta(\mathbf{k}_1 + \mathbf{k}_2 + \mathbf{k}_3) B_\zeta(\mathbf{k}_1, \mathbf{k}_2, \mathbf{k}_3) = \langle \zeta_L(\mathbf{k}_3) \langle \zeta_S \zeta_S \rangle(\mathbf{k}_1, \mathbf{k}_2) \rangle. \quad (5.25)$$

Thus, putting together eqs. (5.24) and (5.25) we see that the squeezed limit acquires the form:

$$B_\zeta(\mathbf{k}_1, \mathbf{k}_2, \mathbf{k}_3) = -[n_s(k_S, \tau) - 1] P_\zeta(k_S) P_\zeta(k_L). \quad (5.26)$$

This corresponds to Maldacena's well known consistency relation. It was obtained with the help of transformation (5.17) linking short- and long-wavelength co-moving curvature perturbations ζ_S and ζ_L through a "complete" curvature perturbation ζ' (that is, a curvature perturbation for which there has been no separation of scales). In other words, (5.26) gives us information on how the long wavelength mode ζ_L modulates the short wavelength mode ζ_S .

5.2 A generalized consistency relation

We would like to count with a consistency relation valid for cases in which the long mode ζ_L is time dependent, that is, when the curvature perturbation evolves on super-horizon scales. For simplicity, let us first attempt this in the formal limit $\varepsilon \rightarrow 0$. We will consider the case $\varepsilon \neq 0$ in Section 5.2.3.

5.2.1 Case with $\varepsilon \rightarrow 0$

If $\varepsilon = 0$, the Hubble parameter $H = \dot{a}/a$ is a constant, and the scale factor a is given by

$$a(\tau) = -\frac{1}{H\tau}, \quad (5.1)$$

Then, let us consider the following transformations:

$$x = e^g x', \quad (5.2)$$

$$\tau = e^f \tau', \quad (5.3)$$

$$\zeta = \zeta' + \Delta\zeta. \quad (5.4)$$

Here the quantities g , f and $\Delta\zeta$ are all functions of τ' . For concreteness, let us assume that $\tau = \tau'$ at a given reference time τ_* . This implies that $f = 0$ at $\tau' = \tau_*$. To make this explicit, one could write f as $f(\tau') = \int_{\tau_*}^{\tau'} d\tau h$ (this will not be important though). This choice is completely arbitrary, and one could certainly fix initial conditions for f and g in other ways, without modifying the main conclusions of this section. The change of coordinates implies:

$$dx^i = e^g dx'^i + e^g \partial_0 g x'^i d\tau', \quad (5.5)$$

$$d\tau = e^f d\tau' (1 + \tau' \partial_0 f). \quad (5.6)$$

Note that now $\partial_0 \equiv \partial_{\tau'}$. Replacing these relations back into the metric (5.1), we find:

$$\begin{aligned} ds^2 &= a^2(\tau') \left[-e^{2\delta N' - 2\tau' \partial_0 \Delta\zeta + 2\tau' \partial_0 f} d\tau'^2 \right. \\ &\quad \left. + 2(N'_i + \partial_0 g x'_i) d\tau' dx'^i + e^{2\zeta' + 2\Delta\zeta + 2g - 2f} dx'^2 \right]. \end{aligned} \quad (5.7)$$

As before, let us recall that the perturbations appearing together with δN and N_i may be treated up to linear order. On the other hand, those appearing together with ζ' must be treated up to cubic order. In this case, we are treating them exactly. Now, notice that if we demand that g is constant, and that

$$\Delta\zeta + g - f = 0, \quad (5.8)$$

the metric reduces back to (5.13). Then, we conclude that the ζ -action is invariant under the transformations (5.2)-(5.4). Therefore, we have two solutions ζ and ζ' related through the following relation

$$\zeta(\tau, x) = \zeta'(e^{-f}\tau, e^{-g}x) - g + f. \quad (5.9)$$

In order to deduce the squeezed limit of the bispectrum in this class of models, let us now again consider the splitting

$$\zeta = \zeta_S + \zeta_L. \quad (5.10)$$

Recall that this time we are assuming that ζ_L depends on time. As we did with (5.15), let us choose f and g in such a way that $\Delta\zeta = \zeta_L$:

$$-g + f = \zeta_L(\tau). \quad (5.11)$$

Given that $f = 0$ for $\tau = \tau_*$, the previous relation sets the constant g as $g = -\zeta_L(\tau_*)$. Then we find that f is given by

$$f = \zeta_L(\tau) - \zeta_L(\tau_*). \quad (5.12)$$

This leads to a relation between ζ_S and ζ' given by:

$$\zeta_S(\tau, x) = \zeta'(e^{-[\zeta_L(\tau) - \zeta_L(\tau_*)]}\tau, e^{\zeta_L(\tau_*)}x). \quad (5.13)$$

If $\zeta_L(\tau)$ does not evolve, then $\zeta_L(\tau) = \zeta_L(\tau_*)$, and we recover eq. (5.17). We may now compute the power spectrum of ζ_S . Up to first order in ζ_L , it is direct to find in Fourier space

$$\begin{aligned} \langle \zeta_S \zeta_S \rangle(\mathbf{k}_1, \mathbf{k}_2) &= \langle \zeta' \zeta' \rangle(\mathbf{k}_1, \mathbf{k}_2) - [\zeta_L(\mathbf{k}_L) - \zeta_L^*(\mathbf{k}_L)] \frac{d}{d \ln \tau} P_\zeta(\tau, k_S) \\ &\quad - \zeta_L^*(\mathbf{k}_L) [n_s(k_S, \tau) - 1] P_\zeta(\tau, k_S). \end{aligned} \quad (5.14)$$

Correlating this expression with $\zeta_L(\mathbf{k}_3)$, we end up with

$$\begin{aligned} \langle \zeta_L(\mathbf{k}_3) \langle \zeta_S \zeta_S \rangle(\mathbf{k}_1, \mathbf{k}_2) \rangle &= -\langle \zeta_L(\mathbf{k}_3) [\zeta_L(\mathbf{k}_L) - \zeta_L^*(\mathbf{k}_L)] \rangle \frac{d}{d \ln \tau} P_\zeta(\tau, k_S) \\ &\quad - \langle \zeta_L(\mathbf{k}_3) \zeta_L^*(\mathbf{k}_L) \rangle [n_s(k_S, \tau) - 1] P_\zeta(\tau, k_S). \end{aligned} \quad (5.15)$$

This expression involves the correlation of $\zeta_L(\mathbf{k}_3)$ evaluated at a given time τ , with $\zeta_L^*(\mathbf{k}_3)$ which is evaluated at the reference time $\tau = \tau_*$. When superhorizon modes freeze, the first line cancels and there is no difference between $\zeta_L^*(\mathbf{k}_3)$ and $\zeta_L(\mathbf{k}_3)$, so we end up with Maldacena's standard attractor result. However, if ζ_L grows on superhorizon scales fast enough for ζ_L^* to become subdominant, and for the first line to dominate the second one, we end up with

$$B_\zeta(\mathbf{k}_1, \mathbf{k}_2, \mathbf{k}_3) = -P_\zeta(k_L) \frac{d}{d \ln \tau} P_\zeta(k_S). \quad (5.16)$$

This is one of our main results. Equation (5.16) tells us that under a substantial super-horizon growth, the squeezed limit is dominated by a time derivative of the power spectrum.

5.2.2 Non-Gaussianity in ultra slow-roll inflation

Before considering the more general case in which $\varepsilon \neq 0$, let us briefly analyze (5.16) in the context of ultra slow-roll inflation, where the inflaton field moves over a constant potential and, as a consequence, the curvature perturbation evolves exponentially after horizon crossing. The salient feature of this model is the rapid decay of ε , which is found to be given by

$$\varepsilon \propto \frac{1}{H^2 a^6}. \quad (5.17)$$

Although $\varepsilon \rightarrow 0$ very fast, the value of η is found to be large:

$$\eta = -6 \left(1 - \frac{\varepsilon}{3}\right). \quad (5.18)$$

The linear equation of motion respected by ζ on super-horizon scales is given by

$$\frac{d}{dt} \left(\varepsilon a^3 \dot{\zeta} \right) = 0. \quad (5.19)$$

Then, neglecting terms subleading in ε , one finds that $\zeta \propto \tau^{-3}$. In other words, the power spectrum on superhorizon scales behaves as:

$$P_\zeta(k) \propto \tau^{-6}. \quad (5.20)$$

Using this result back into (5.16), we find that the bispectrum in ultra slow-roll is given by

$$B_\zeta(\mathbf{k}_1, \mathbf{k}_2, \mathbf{k}_3) = 6P_\zeta(k_L)P_\zeta(k_S), \quad (5.21)$$

which coincides with the well known expression previously found in the literature [108, 111].

One should be careful with the result (5.21), even though it coincides with the known squeezed limit for ultra slow-roll inflation. Recall that we are judging the effect of the transformations (5.2)-(5.4) on the ζ -action from their effect on the metric. This implies that we are neglecting terms proportional to ε in the metric that could, according to eq. (5.18), have a sizable impact on the action due to time derivatives of ε . Strictly speaking, at this point in our derivation the result of eq. (5.16) is valid as long as $\varepsilon \ll 1$ together with $\eta \ll 1$. But under these conditions it is hard (or impossible) to have a sizable super-horizon growth of ζ that could lead to an interesting situation where eq. (5.16) could be used. To understand this issue more closely, let us analyze the case $\varepsilon \neq 0$ in what follows.

5.2.3 Case with $\varepsilon \neq 0$

Let us now analyze the more general case in which $\varepsilon \neq 0$. Here, we may consider the following transformation of coordinates and fields:

$$x = e^g x', \quad (5.22)$$

$$a(\tau) = e^{-f} a(\tau'), \quad (5.23)$$

$$\zeta = \zeta' + \Delta\zeta. \quad (5.24)$$

Notice that we are defining the time reparametrization in terms of the scale factor a in order to keep the transformation in the spatial part of the metric (which involves $a(\tau)$) valid to all orders in the perturbation f . The effect of this transformation on the rest of the metric may be computed up to linear order. With this in mind, it is possible to derive that the time reparametrization to linear order is given by $\tau = \tau' - \frac{1}{\mathcal{H}}f$, where $\mathcal{H} = a^{-1}\partial_0 a$. Then, the transformations lead to:

$$dx^i = e^g dx'^i + e^g \partial_0 g x'^i d\tau', \quad (5.25)$$

$$d\tau = d\tau' + \left((1 - \varepsilon)f - \frac{1}{\mathcal{H}}\partial_0 f \right) d\tau', \quad (5.26)$$

where we used $\partial_0 \mathcal{H} = (1 - \varepsilon)\mathcal{H}^2$. Plugging these transformations back into the action (5.1), one finds:

$$\begin{aligned} ds^2 = & a^2(\tau') \left[-e^{2\delta N' + 2\frac{1}{\mathcal{H}}\partial_0 \Delta\zeta - 2\varepsilon f - 2\frac{1}{\mathcal{H}}\partial_0 f} d\tau'^2 \right. \\ & \left. + 2(N'_i + \partial_0 g x'_i + \frac{1}{3}x'_i \varepsilon \partial_0 \Delta\zeta) d\tau' dx'^i + e^{2\zeta' + 2\Delta\zeta + 2g - 2f} dx'^2 \right]. \end{aligned} \quad (5.27)$$

Now, consider the following conditions on g and f :

$$\partial_0 \Delta\zeta - \varepsilon \mathcal{H}f - \partial_0 f = 0, \quad (5.28)$$

$$\Delta\zeta + g - f = 0. \quad (5.29)$$

It is direct to see that these two equations imply:

$$\partial_0 g = -\varepsilon \mathcal{H}f. \quad (5.30)$$

Then, the metric becomes

$$ds^2 = a^2(\tau') \left[-e^{2\delta N'} d\tau'^2 + 2(N'_i + \Delta N_i) d\tau' dx'^i + e^{2\zeta'} dx'^2 \right], \quad (5.31)$$

where we have defined ΔN_i as

$$\Delta N_i = -\varepsilon \mathcal{H}f x'_i + \frac{1}{3} x'_i \varepsilon (\varepsilon \mathcal{H}f + \partial_0 f), \quad (5.32)$$

and where f is such that it is a solution of eq. (5.28). Now, it is clear from this result that the ζ -action will not be invariant under the present transformation unless either $\Delta N_i = 0$, or ΔN_i leads to the appearance of a total derivative. This second option will not be true in general, and ΔN_i will imply terms in the action that are proportional to ε and η .

At this point, the metric of eq. (5.31) differs from the original metric of eq. (5.1) by the fact that ΔN_i does not vanish. The difference is of order ε , as expected from the analysis of Section 5.2.1. In what follows, let us explore what would be required to satisfy the condition $\Delta N_i = 0$, independently of the size of ε (that is, we will not assume that ε is small). First, it is direct to see that $\Delta N_i = 0$ is equivalent to

$$\partial_0(a^{-2}\mathcal{H}^{-1}f) = 0. \quad (5.33)$$

This implies that f must have the following dependence on time:

$$f = C a^2 \mathcal{H}, \quad (5.34)$$

where C is an integration constant that may be chosen conveniently. Note that here we cannot adopt the condition $f = 0$ at a given time $\tau = \tau_*$. This is because of the way in which f is introduced in eq. (5.23). Now, according to eq. (5.28), the solution for f given by eq. (5.34) must be compatible with $\Delta\zeta$. In other words, it must be possible to choose C in such a way that

$$\partial_0 \Delta\zeta = 3CH^2 a^4, \quad (5.35)$$

(where we have used $\mathcal{H} = Ha$). This corresponds to a strong restriction on $\Delta\zeta$, which has not been chosen yet. As in the previous subsections, we are interested in identifying $\Delta\zeta$ as:

$$\Delta\zeta = \zeta_L. \quad (5.36)$$

Inserting this back into (5.35), we see that $\Delta N_i = 0$ is only possible if (remember that in eq. (5.35) $\partial_0 \equiv \partial_\tau$)

$$\dot{\zeta}_L = 3CH^2 a^3. \quad (5.37)$$

Of course, this behavior is not guaranteed in general. However, in the particular case of ultra slow-roll inflation one has $\varepsilon \propto 1/H^2 a^6$, and so we may rewrite (5.37) as

$$\dot{\zeta}_L \propto \frac{1}{\varepsilon a^3}, \quad (5.38)$$

which is nothing but (5.19). As a consequence, we see that in ultra slow-roll inflation one has $\Delta N_i = 0$ independently of the value of ε . Therefore, we have shown that the transformations (5.22)-(5.24) with f , g and $\Delta\zeta$ chosen as in (5.34), (5.30), and (5.36) respectively, correspond to an exact symmetry of the action for curvature perturbations in ultra slow-roll inflation (independent of the size of ε). This should not come as a surprise. Similar to exponential inflation, ultra slow-roll inflation never ends, and so the size of ε (which dilutes as $\sim a^{-6}$) cannot be regarded as a fundamental quantity describing the state of inflation.

The final step is to deduce an expression for ζ_S . This is found to be

$$\zeta_S(\tau, x) = \zeta'(e^{-\zeta_L - g}\tau, e^{-g}x), \quad (5.39)$$

with g the solution of eq. (5.30). It is straightforward to see that g will contribute terms that are subleading in ε , and so we recover the expression (5.16) found in Section 5.2.1. This in turn, leads to the well known result (5.21).

5.3 Discussion

Now that we know that (5.16) is valid for ultra slow-roll inflation, but not for general situations with $\varepsilon \neq 0$, we would like to anticipate how this result could change once we consider models that depart from the exact ultra slow-roll behavior. First, if the action describing single field inflation is canonical, then all of the couplings appearing in the ζ -action will consist of time derivatives of H , such as ε and η . Given that the action remains invariant under the set of transformations (5.22)-(5.24) in the case of ultra slow-roll, then models with a background close to ultra slow-roll have departures at most proportional to

$$6 + \eta.$$

However, in order to have a small spectral index in models close to ultra slow-roll it is necessary to have $|6 + \eta| \ll 1$, and so it would not be possible to have large departures from (5.16) unless the spectral index becomes incompatible with observations. Another possibility is to consider non-canonical models of inflation. In this class of models one has an additional parameter, the sound speed c_s , which is not directly related to variations of H . This time, the action for ζ could have terms (parametrizing departures from the ultra slow-roll case) proportional to:

$$\left(1 - \frac{1}{c_s^2}\right)\eta.$$

This type of departure would not be suppressed for small values of c_s , and one could expect sizable modifications to the result shown in (5.21). In fact, a direct computation shows that the modification to (5.21) due to c_s is given by [110]

$$B_\zeta(\mathbf{k}_1, \mathbf{k}_2, \mathbf{k}_3) \simeq \frac{6}{c_s^2} P_\zeta(k_L) P_\zeta(k_S). \quad (5.1)$$

This result has also been obtained through symmetry arguments [111] pertaining the structure of the Lagrangian of $P(X)$ -theories of inflation [?], but not through symmetry arguments related to space-time parametrizations, as considered here. Given that c_s appears as a consequence of non-gravitational interactions, it seems reasonable to assume that a space-time reparametrization leading to (5.1) does not exist.

5.4 Conclusions

We have generalized the well known non-Gaussian consistency relation (5.24) to a broader class of relations that is able to cope with those classes of models where the curvature perturbation ζ evolves on super-horizon scales. This relation is given by eq. (5.15), and in the case where the super-horizon growth dominates, it leads to:

$$B_\zeta(\mathbf{k}_1, \mathbf{k}_2, \mathbf{k}_3) = -P_\zeta(k_L) \frac{d}{d \ln \tau} P_\zeta(k_S). \quad (5.1)$$

The standard non-Gaussian consistency relation (5.24) can be understood a symmetry involving a simultaneous spatial dilation and a reparametrization of the curvature perturbation. In the case of (5.1), the symmetry involves a time dilation together with a reparametrization of the curvature perturbation. In both cases, the reparametrization is induced by super-horizon evolution of the long-wavelength contributions of the curvature perturbation. While this symmetry is approximate in general when $\varepsilon \ll 1$, it becomes exact in the case of ultra slow-roll, independently of the value of ε . (It is also exact when $\varepsilon = 0$.)

Our result complements previous studies on consistency relations derived from symmetries of quasi-de Sitter spacetimes [116, 117, 118, 119, 120, 121, 122] applied to the context in which curvature perturbations freeze at horizon crossing. In addition, our result substantiates one more time the well known violation to the standard consistency relation found by the authors of ref. [108]. However, our result raises the question how the non-Gaussianity expressed in (5.1) would survive the transition from a non-attractor phase—in which ultra slow-roll is dominant—to an attractor phase where standard slow-roll inflation is dominant (before inflation ends).

Given that the expression leading to (5.1) involves a time derivative of the power spectrum, one may suspect that once the non-attractor phase concludes, and the modes stop evolving on super-horizon scales, this contribution would become suppressed. In this case, the transition to the new phase would imply a leading contribution to the bispectrum dictated by the scale dependence of the power spectrum (through $n_s - 1$). Strictly speaking, our expression cannot describe this transition. This is because during such a transition the system is no longer invariant under the set of transformations (5.22)-(5.24).

One could speculate that in such a transition (from non-attractor to attractor, see also [123]) the amount of non-Gaussianity in the form of (5.1) could be transferred to a form of non-Gaussianity that is described by (5.24). But this would necessarily imply an unacceptably large value of the spectral index $n_s - 1$. Another possibility is that, instead of (5.1), the

bispectrum produced during ultra slow-roll has to be read as

$$B_\zeta(\mathbf{k}_1, \mathbf{k}_2, \mathbf{k}_3) \simeq 6P_\zeta(k_L)P_\zeta(k_S), \quad (5.2)$$

without taking into consideration the time derivative appearing in the expression preceding it. In other words, the factor 6 implied by the τ -derivative becomes engraved on the distribution of superhorizon modes, and survives until the modes re-enter the horizon much after inflation. Given that ultra slow-roll inflation has gained some prominence as a transient period of inflation that could explain certain phenomena associated to primordial physics [124, 125], this seems to be a relevant issue to clarify. In [114] we will study this issue more closely, by introducing the use of conformal Fermi coordinates [3, 100, 1]. There, we will argue that the non-Gaussianity produced in non-attractor models such as ultra slow-roll is non-observable ($f_{\text{NL}}^{\text{obs}} = 0$).

Chapter 6

Conformal Fermi Coordinates and vanishing f_{NL}

The theory of cosmological perturbations assumes an external observer with unlimited access to all places and at all times with complete knowledge of the entire ensemble of modes of different fields and their properties; under this treatment, this type of observers are outside the experiment or "outside the box"(our universe). Nevertheless, that is not our case. Instead, we are observers confined in a 4-dimensional spacetime influenced and subordinated by its dynamics. Under this perspective, we are observers inside of the experiment, which at the same time is merely one realization of other similar alternatives, with limited access to the entire ensemble of fields modes.

Due to this fact, we can not have full access to the entire universe restricting our knowledge and information available to just a causally connected small region of space from which we extract local cosmological data. The way in which we formally deal with the influence of spacetime dynamics on us is by using the Conformal Fermi Coordinates(CFC). First introduced [2], in the context of an observer trajectory near strong gravitational fields(Fermi coordinates), but ultimately incorporated and revived in a cosmological context [3] [1] adapted to a conformal scenario to study the primordial curvature power spectrum and bispectrum of our universe.

This section is organized as follows, in the first part, we will introduce the theoretical framework that this chapter relies on defining some tools such as the notion of Fermi coordinates for a generic manifold, and the Fermi normal coordinates, geodesic congruence, and the flatness theorem. Then we jump in an intermediate step which are the Fermi coordinates applied to an FRW universe and finally, dive into the conformal Fermi coordinates and their predictions.

6.1 Fermi Normal Coordinates

In the mathematical theory of Riemannian geometry, the Fermi coordinates are local coordinates that are adapted to a geodesic. More formally, suppose \mathcal{M} is an 4-dimensional Riemannian manifold, γ a geodesic that lives in \mathcal{M} , and P any point along γ , then there exist local coordinates (t, x_1, x_2, x_3) around P such that:

- For small t , $(t, 0, 0, 0)$ represents a geodesics near P .
- On γ the 3-metric tensor is the Euclidean metric δ_{ij} .
- On γ all the Christoffel symbols vanish.

Such coordinates are called Fermi coordinates and are named after the Italian physicist Enrico Fermi. The above properties are only valid on the geodesic. For example, if all Christoffel symbols vanish near P , then the manifold is flat near P . It is said that we can introduce local inertial coordinates/Fermi normal coordinates for any timelike geodesic. Physically, Fermi normal coordinates represent the frame of reference of an inertial observer(as us in our universe) whose metric (along its worldline) looks like a diagonal matrix $\eta_{\mu\nu} = \text{diag}(-1, +1, +1, +1)$. This requires that three coordinates be spacelike and one timelike. Also, this coordinates can be extended for lightlike geodesics, but with other treatments.

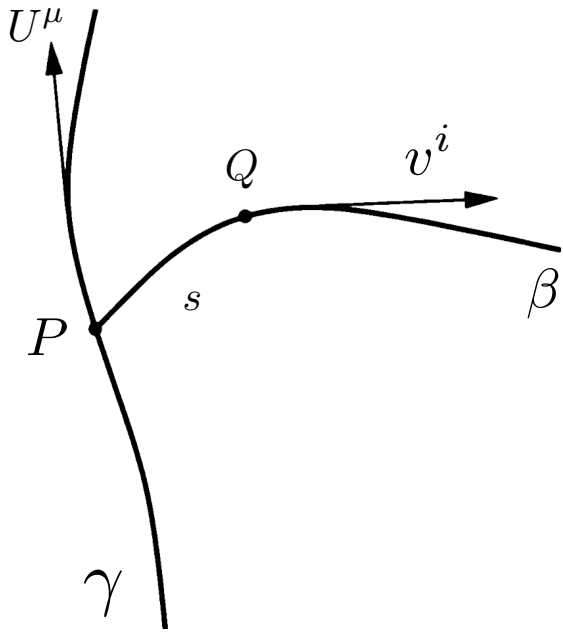


Figure 6.1: Geometrical construction of Fermi coordinates

For a given point in spacetime, it is always possible to find a coordinate system $x^{\alpha'}$ such that:

$$g_{\alpha'\beta'}(P) = \eta_{\alpha'\beta'}(P), \quad \Gamma_{\beta'\gamma'}^{\alpha'}(P) = 0 \quad (6.1)$$

where $\eta_{\mu\nu} = \text{diag}(-1, 1, 1, 1)$ is the Minkowski metric. Such a coordinate system will be called Lorentz inertial frame at P . We note that it is not possible to also set all the derivatives of the connection to zero when the spacetime is curved, the physical interpretation of the *local flatness theorem* is that a free-falling observer see no effect of gravity in their immediate vicinity, as required by the Einstein equivalence's principle. For concreteness we will take the geodesic to be timelike and we will adopt a geometric proof of the theorem. We will show that we can introduce coordinates $x^\mu = (t_P, x^i)$ such that near γ , the metric can be expressed as

$$g_{00}(x) = -1 - R_{0i0j}(t_P, \mathbf{x}_p(t_P))x^i x^j, \quad (6.2)$$

$$g_{0i}(x) = -\frac{2}{3}R_{0jik}(t_P, \mathbf{x}_p(t_P))x^j x^k, \quad (6.3)$$

$$g_{ij}(x) = \delta_{ij} - \frac{1}{3}R_{ikjl}(t_P, \mathbf{x}_p(t_P))x^k x^l. \quad (6.4)$$

These coordinates are known as Fermi Normal Coordinates, and t_P is the proper time along the geodesic γ , on which the spatial coordinate x^i are all zero. The components of Riemann tensor are evaluated on γ , and *they depend on t_P only*. It is obvious that (6.2) enforces $g_{\mu\nu} = \eta_{\mu\nu}$ and $\Gamma_{\alpha\beta}^\mu|_\gamma = 0$. Then the local-flatness theorem therefore holds everywhere on the geodesic.

6.1.1 Geometric construction

We will use $x^\alpha = (t, x^a)$ to denote the Fermi normal coordinates, and $x^{\alpha'}$ will refer to an arbitrary coordinate system. We imagine we are given a spacetime with a metric $g_{\alpha'\beta'}$ expressed in these coordinates. We will consider a geodesic γ in this spacetime. Its tangent vector $U^{\alpha'}$ and we let t be the proper time along γ . On this geodesic we select a point \mathcal{O} at which we set $t = 0$. At this point we construct an orthonormal system an orthonormal basis $(e_\mu)^{\alpha'}$ (the subscript μ serves to label the 4-basis vectors), and we identify $(e_t)^{\alpha'}$ with the tangent vector $U^{\alpha'}$ at \mathcal{O} . From this we construct a basis everywhere on γ by parallel transporting $(e_\mu)^{\alpha'}$ away from \mathcal{O} . Our basis therefore satisfies

$$(e_\mu)_{;\beta'}^{\alpha'} U^{\beta'} = 0 \quad (e_t)^{\alpha'} = U^{\alpha'}, \quad (6.5)$$

as well as

$$g_{\alpha'\beta'}(e_\mu)^{\alpha'}(e_\nu)^{\beta'} = \eta_{\mu\nu}, \quad (6.6)$$

everywhere on γ . Here, $\eta_{\mu\nu} = \text{diag}(-1, 1, 1, 1)$ is the Minkowski metric. Consider now a spatial-like geodesic β originating from a point P on γ , at which $t = t_P$. This geodesic has a tangent vector $v^{\alpha'}$, and we let s denote the proper distance along β ; we set $s = 0$ at P . We assume that $v^{\alpha'}$ is orthogonal to $u^{\alpha'}$ so that it admits a decomposition

$$v^{\alpha'}|_\gamma = \Omega^a(e_a)^{\alpha'} \quad (6.7)$$

To ensure that $v^{\alpha'}$ is properly normalized, the expansion coefficient must be properly normalized $\delta_{ab}\Omega^a\Omega^b = 1$. By choosing a different coefficient Ω^a we can construct a new geodesic β that are also orthogonal to γ at P . We shall denote this entire family of spatial-like geodesics as $\beta(t, \Omega^a)$. The Fermi normal coordinates of a point Q located away of the geodesic γ is

constructed as follows. First we find a unique geodesic that passes through Q and intersects γ orthogonally. We label the intersection as P and we name the geodesic $\beta(t_Q, \Omega_Q^a)$ with $t_Q = t_P$ and Ω_Q^a the expansion coefficients of $v^{\alpha'}$ at that point. We then assign to Q new coordinates:

$$x^0 = t_P, \quad x^a = \Omega_Q^a s_Q \quad (6.8)$$

where the s_Q is the proper distance from P to Q . These are the Fermi normal coordinates of the point Q , therefore, $x^\alpha = (t, \Omega^a s)$, and we must now figure out how these coordinates are related to $x^{\alpha'}$, the original system.

6.1.2 Coordinates transformation

We note first that we can describe a family of geodesics $\beta(t, \Omega^a)$ by the relations of the form $x^{\alpha'}(t, \Omega^a, s)$. In this parameter t and Ω^a serve to specify which geodesic, and s the proper distance to along the geodesic. If we substitute $s = 0$ in these relations, we recover the description of the timelike geodesic γ in terms of its proper time; the parameters Ω^a are the irrelevant. The tangent to the geodesics $\beta(t, \Omega^a)$ is

$$v^{\alpha'} = \left(\frac{\partial x^{\alpha'}}{\partial s} \right) \Big|_{t, \Omega^a}. \quad (6.9)$$

This vector is a solution to the geodesic equation subjected to the initial condition $v^{\alpha'}|_{s=0} = \Omega^a (e_a)^{\alpha'}$. But the geodesic is invariant under a rescaling of the affine parameter, $s \rightarrow s/c$, in which c is a constant. Under this rescaling $v^{\alpha'} \rightarrow cv^{\alpha'}$ and as a consequence we have that $\Omega^{\alpha'} \rightarrow c\Omega^{\alpha'}$. We have therefore established the identity $x^{\alpha'}(t, \Omega^a, s) = x^{\alpha'}(t, c\Omega^a, s/c)$, and a special case we find

$$x^{\alpha'}(t, \Omega^a, s) = x^{\alpha'}(t, s\Omega^a, 1) = x^{\alpha'}(x^\alpha) \quad (6.10)$$

by virtue of the equation (6.8), this relation is the desired transformation between $x^{\alpha'}$ and x^α (Fermi normal coordinates). Now as a consequence we have:

$$\Omega^a (e_a)^{\alpha'} = v^{\alpha'} \Big|_\gamma = \frac{\partial x^{\alpha'}}{\partial s} \Big|_{s=0} = \frac{\partial x^{\alpha'}}{\partial x^a} \Big|_{s=0} \Omega^a \quad (6.11)$$

which shows that

$$\frac{\partial x^{\alpha'}}{\partial x^a} = (e_a)^{\alpha'} \quad (6.12)$$

from previous equations observations we also have :

$$\frac{\partial x^{\alpha'}}{\partial t} \Big|_\gamma = U^{\alpha'} = (e_t)^{\alpha'} \quad (6.13)$$

finally Eqs. (6.12) (6.13) tell us that on γ , $\frac{\partial x^{\alpha'}}{\partial x^\mu} = (e_\mu)^{\alpha'}$.

Deviation vectors ξ^α

Suppose now that in the relations $x^{\alpha'}(t, \Omega^a, s)$, the parameters Ω^a are varied while keeping t and s fixed. This defines new curves that connects different geodesic β at the same proper distance s from their common intersection point P on γ . This is very similar to the construction described in section 6.1.1, and the vectors

$$\xi_a^\alpha = \frac{\partial x^\alpha}{\partial \Omega^a} \Big|_{t,s} \quad (6.14)$$

are deviation vectors relating geodesics $\beta(t, \Omega^a)$ with different coefficient Ω^a . Similarly,

$$\xi_t^{\alpha'} = \frac{\partial x^{\alpha'}}{\partial t} \Big|_{s, \Omega^a} \quad (6.15)$$

are deviation vectors relating different geodesics $\beta(t, \Omega^a)$ that start at different points on γ , but share the same coefficient Ω^a . The four vectors defined in equation (6.14) and (6.15) satisfies the geodesic equation (6.35); it must be kept in mind that in this equation, the tangent vector is $v^{\alpha'}$, not $U^{\alpha'}$, and the affine parameter is s not t .

Metric on γ

The components of the metric in the Fermi Normal coordinates are related to the old components by general relation

$$g_{\mu\nu}(x) = \frac{\partial x^{\mu'}}{\partial x^\mu} \frac{\partial x^{\nu'}}{\partial x^\nu} g_{\mu'\nu'}(x'(x)) \quad (6.16)$$

Evaluating this on γ yields $g_{\mu\nu}(x)|_\gamma = (e_\mu)^{\mu'}(e_\nu)^{\nu'} g_{\mu'\nu'}(x'(x))$, after using (6.13),(6.12). This states that in the Fermi normal coordinates, the metric is Minkowski everywhere on the geodesic γ .

First derivatives of the metric on γ

To evaluate the Christoffel symbols in the Fermi normal coordinates, we recall from the curves (6.10) that the curves $x^0 = t$, $x^a = \Omega^a s$ are geodesics so that these relations must be solutions to the geodesics equation,

$$\frac{d^2 x^\alpha}{ds^2} + \Gamma_{\beta\gamma}^\alpha \frac{dx^\beta}{ds} \frac{dx^\gamma}{ds} = 0 \quad (6.17)$$

This gives $\Gamma_{ab}^\alpha(t)\Omega^a\Omega^b = 0$. On γ the Christoffel symbols are functions of t only, and are therefore independent of Ω^a . Since these coefficients are arbitrary, we conclude that $\Gamma_{ab}^\alpha = 0$. To obtain the remaining components we recall that the basis vectors $(e_\mu)^\alpha$ are parallel transported along γ , so that

$$\frac{d(e_\mu)^\alpha}{dt} + \Gamma_{\beta\gamma}^\alpha (e_\mu)^\beta (e_t)^\gamma = 0 \quad (6.18)$$

since $(e_\mu)^\gamma = U^\alpha$. By virtue of (6.13), (6.12) we have $(e_\mu)^\alpha = \delta_\mu^\alpha$ in the Fermi coordinates, and the parallel-transport equation implies $\Gamma_{\beta t}^\gamma|_\gamma = 0$. The Christoffel symbols are therefore all zero on γ . We shall write this as

$$g_{\alpha\beta,\gamma}|_\gamma = 0 \quad (6.19)$$

This proves that the Fermi normal coordinates enforce the local- flatness theorem everywhere on the geodesic γ .

Second derivatives of the metric γ

We next turn to the second derivatives of the metric or the first derivatives of the connection. From the fact that $\Gamma_{\beta\gamma}^\alpha$ is everywhere on γ , we obtain immediately

$$\Gamma_{\beta\gamma,t}^\alpha|_\gamma = 0. \quad (6.20)$$

From the definition of the Riemann tensor, we also get

$$\Gamma_{\beta,t,\gamma}^\alpha|_\gamma = R_{\beta\gamma t}^\alpha|_\gamma = 0 \quad (6.21)$$

The other components are harder to come by. For these we must involve the deviation vectors ξ_a^α introduced in Section 6.1.2. These vectors satisfy the geodesic equation, (6.35), which we will fully write as

$$\frac{d^2\xi^\mu}{ds^2} + 2\Gamma_{\beta\gamma}^\alpha v^\beta \frac{d\xi^\gamma}{ds} + (R_{\beta\gamma\delta}^\alpha + \Gamma_{\beta\gamma,\delta}^\alpha - \Gamma_{\gamma\mu}^\alpha \Gamma_{\beta\delta}^\mu + \Gamma_{\delta\mu}^\alpha \Gamma_{\beta\gamma}^\mu) v^\beta \xi^\gamma v^\delta = 0 \quad (6.22)$$

According to (6.9), (6.10), (6.14) and (6.15), we have that $v^\alpha = \Omega^a \delta_a^\alpha$, $\xi_t^\alpha = \delta_t^\alpha$, and $\xi_a^\alpha = s \delta_a^\alpha$ in the Fermi coordinates. If we substitute $\xi^\alpha = \xi_t^\alpha$ in the geodesic deviation equation and evaluate it at $s = 0$, we find $\Gamma_{bt,c}^\alpha|_\gamma = R_{bct}^\alpha|_\gamma$, which is just a special case of (6.35): To learn something new, let us substitute $\xi^\alpha = \xi_a^\alpha$ instead. In this case we find

$$2\gamma_{ab}^\alpha \Omega^b + s (R_{bad}^\alpha + \Gamma_{ab,d}^\alpha - \Gamma_{a\mu}^\alpha \Gamma_{bd}^\mu + \Gamma_{du}^\alpha \Gamma_{ab}^\mu) \Omega^a \Omega^b = 0 \quad (6.23)$$

Before evaluating this on γ , we expand the first term in power of s :

$$\Gamma_{ab}^\alpha = \Gamma_{ab}^\alpha|_\gamma + s \Gamma_{ab,\mu}^\alpha|_\gamma v^\mu + \mathcal{O}(s^2) = s \Gamma_{ab,d}^\alpha|_\gamma \Omega^d + \mathcal{O}(s^2) \quad (6.24)$$

Dividing through by s and the evaluating on γ , we arrive at

$$R_{bad}^\alpha + 3\Gamma_{ab,d}^\alpha|_\gamma \Omega^b \Omega^d = 0 \quad (6.25)$$

Because the coefficient Ω^a are arbitrary, we conclude that quantity within the brackets, properly symmetrized in the indices b and d , must vanish a little algebra finally reveals that:

$$\Gamma_{ab,c}^\alpha|_\gamma = -\frac{1}{3} (R_{abc}^\alpha + R_{bac}^\alpha)|_\gamma \quad (6.26)$$

equations (6.20), (6.21), (6.26) give the complete set of derivatives of the Christoffel symbols on γ . It is now a simple matter to turn these equations into statements regarding the second derivatives of the metric at γ . Because the metric is Minkowski everywhere on the geodesics, only the spatial derivatives are non-zero. These are given by

$$g_{tt,ab} = -2R_{tatb}|_\gamma, g_{ta,bd} = -\frac{2}{3}(R_{tbac} + R_{tcab})|_\gamma, g_{ab,cd} = -\frac{1}{3}(R_{acbd} + R_{adbd})|_\gamma \quad (6.27)$$

From the local flatness theorem and (6.27) we recover (6.2), the expansion of the metric around γ , to the second in spatial displacement x^a .

6.2 Congruence of timelike geodesics

Let \mathcal{O} be an open region in spacetime. A congruence in \mathcal{O} is a family of curves such that though each point in \mathcal{O} there passes one and only one curve from this family. The tensor B can be expressed as:

$$B_{ij} = \frac{1}{3}\theta\delta_{ij} + \sigma_{ij} + \omega_{ij} \quad (6.28)$$

where $\theta = B_i^i$ is the expansion scalar as the trace part of B_{ij} , $\sigma_{ij} = B_{(ij)} - \frac{1}{3}\theta\delta_{ij}$ is the shear tensor as the symmetric-trace free part of B_{ij} , and $\omega_{ij} = B_{[i,j]}$ is the rotation tensor as the antisymmetric part of B_{ij} . And theta is the fractional change of volume per unit time. And the volume change is not affected by the shear and rotations tensors. (And the curves do not intersect; picture this as a tight bundle of copper wires.) In this section, we will be interested in congruences of timelike geodesics, which means that each curve in the family is a time-like geodesics. We wish to determine how such congruence evolves with time. More precisely stated, we want to determine the behavior of the deviations vector ξ^μ between two neighboring geodesics in the congruence, as a function of proper time τ along the reference geodesic (central geodesic). The geometric setup is the same as the previous section with the following relations

$$U^\mu U_\mu = -1, \quad U_{;\nu}^\mu U^\nu = 0, \quad U_{;\nu}^\mu \xi^\nu = \xi_{;\nu}^\mu U^\nu, \quad U^\mu \xi_\mu = 0 \quad (6.29)$$

where U^μ is tangent to geodesics. Notice in particular that ξ^μ is orthogonal to U^μ : The deviation vector points in the directions transverse to the flow of the congruence.

6.3 Transverse metric

Given the congruence and associated timelike vector field U^μ , the spacetime metric $g_{\mu\nu}$ can be decomposed into a longitudinal part $-U_\mu U_\nu$ and transverse part $h_{\mu\nu}$ given by

$$h_{\mu\nu} = g_{\mu\nu} + U_\mu U_\nu \quad (6.30)$$

The transverse metric is purely "spatial", in the sense that it is orthogonal to U^μ : $U^\mu h_{\mu\nu} = h_{\mu\nu} U^\mu$. It is effectively three dimensional: in a comoving Lorentz frame at some point P within the congruence, $U_\alpha = (-1, 0, 0, 0)$, $g_{\mu\nu} = \text{diag}(-1, 1, 1, 1)$, and $h_{\mu\nu} = \text{diag}(0, 1, 1, 1)$. We may also note relations $h_\mu^\mu = 3$ and $h_\rho^\mu h_\nu^\rho = h_\nu^\mu$.

6.3.1 Kinematics

We now introduce the tensor field $B_{\mu\nu}$ defined as:

$$B_{\mu\nu} = U_{\mu;\nu} \quad (6.31)$$

Like $h_{\mu\nu}$, this tensor is purely *transverse*, which implies that is constant along the geodesic ($U^\mu B_{\mu\nu} = U^\mu U_{\mu;\nu} = \frac{1}{2}(U_\mu U^\mu)_{;\nu} = 0$) and self transported ($B_{\mu\nu} U^\nu = U_{\mu;\nu} U^\nu = 0$). Moreover,

it determines the evolution of the deviation vector. From the Lie derivatives we know that $\xi_{;\nu}^{\mu} U^{\nu} = U_{;\nu}^{\mu} \xi^{\nu}$ we immediately obtain:

$$\frac{d}{dt} \xi^{\mu} = \xi_{;\nu}^{\mu} U^{\nu} = B_{\nu}^{\mu} \xi^{\nu} \quad (6.32)$$

and we see that B_{ν}^{μ} measures the failure of ξ^{μ} to be parallel transported along the congruence.

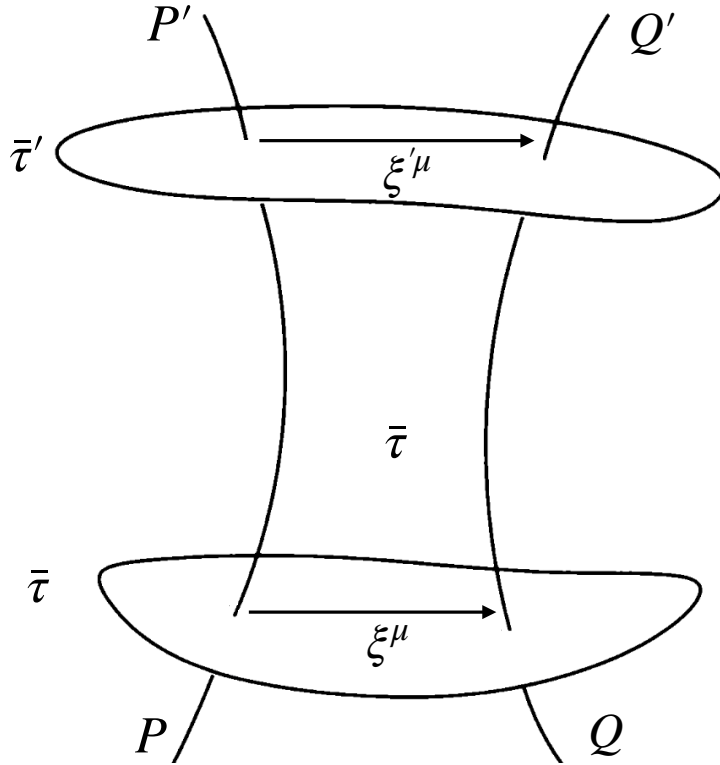


Figure 6.2: Geodesic congruence

6.4 Geodesic deviation

The geometrical meaning of the Riemann tensor is best illustrated by examining the behavior of neighboring geodesics. Consider two such geodesics, γ_0 and γ_1 , each described by relations $x^{\alpha}(t)$ in which t is the affine parameter; the geodesics can be either spacelike, timelike, or null. We want to develop the notion of a *deviation vector* between these two geodesics, and derive an evolution equation for this vector.

For this purpose we introduce, in the space between γ_0 and γ_1 , an entire family of interpolating geodesics fig. 6.2. To each geodesics we assign a label $s \in [0, 1]$, such that γ_0 comes with label $s = 0$ and γ_1 with $s = 1$. We collectively describe these geodesics with relations $x^{\alpha}(s, t)$, in which s serves to specify which geodesic at t is the affine parameter along the

specified geodesic. The vector field $U^\alpha = \partial x^\alpha / \partial t$ is tangent to the geodesics, and it satisfies the equation $U^{\alpha;\beta} U^\beta = 0$. If we keep t fixed in the relations $x^\alpha(s, t)$ and vary s instead, we obtain another family of curves, labelled by t and parameterized by s ; in general these curves will not be geodesics. The family has $\xi^\alpha = \partial x^\alpha / \partial s$ as its tangent vector field, and the restriction for this vector to γ_0 , $\xi^\alpha|_{s=0}$, gives a meaningful notion of a deviation vector between γ_0 and γ_1 . We wish to derive an expression for its acceleration,

$$\frac{D^2 \xi^\mu}{dt^2} = (\xi^\alpha_{;\beta} U^\beta)_{;\gamma} U^\gamma \quad (6.33)$$

in which it is understood that all quantities are evaluated on γ_0 . In flat spacetime the geodesic γ_0 and γ_1 are straight, and although their separation may change with t , this change is necessarily linear: $D^2 \xi^\alpha / dt^2 = 0$ in flat spacetime. A non-zero result for $D^2 \xi^\alpha / dt^2 = 0$ will, therefore, reveal the presence of curvature, and indeed, this vector will be found to be proportional to the Riemann tensor. It follows at once from the relations $U^\alpha = \partial x^\alpha / \partial t$ and $\xi^\alpha = \partial x^\alpha / \partial s$ that $\partial U^\alpha / \partial s = \partial \xi^\alpha / \partial t$, which can be written in covariant form as

$$\mathcal{L}_u \xi^\alpha = \mathcal{L}_\xi U^\alpha = 0 \rightarrow \xi^\alpha_{;\beta} U^\beta = U^\alpha_{;\beta} \xi^\beta. \quad (6.34)$$

We also have at our disposal the geodesic equation, $U^\alpha_{;\beta} U^\beta = 0$. These equations can be combined to prove that $\xi^\alpha U_\alpha$ is constant along γ_0 so we can set $\xi^\alpha U_\alpha = 0$. This means that the curves $t = \text{constant}$ cross γ_0 orthogonally, and adds weight to interpretation of ξ^α as a deviation vector. We may now calculate the acceleration that both geodesics γ_0 and γ_1 experience, starting from the equation 6.33, as a result :

$$\frac{D^2 \xi^\mu}{dt^2} = -R^\mu_{\nu\rho\lambda} U^\nu \xi^\rho U^\lambda \quad (6.35)$$

This is the *geodesics deviation equation*. It shows that curvature produces a relative acceleration between two neighboring geodesics; even if they start parallel, curvature prevents the geodesics from remaining parallel.

6.4.1 Raychaudhuri's equation

We now want to derive an evolution equation for θ , expansion scalar. We begin by developing an equation for $B_{\mu\nu}$ itself:

$$B_{\mu\nu;\rho} U^\rho = U_{\mu;\nu\rho} U^\rho = -B_{\mu\rho} B^\rho_\nu - R_{\mu\rho\nu\lambda} U^\rho U^\lambda \quad (6.36)$$

The equation for θ is obtained by taking the trace:

$$\frac{d\theta}{dt} = -B^{\mu\nu} B_{\nu\mu} - R_{\mu\nu} U^\mu U^\nu \quad (6.37)$$

it is easy to check that $B^{\mu\nu} B_{\nu\mu} = \frac{1}{3}\theta^2 + \sigma^{\mu\nu} \sigma_{\mu\nu} - \omega^{\mu\nu} \omega_{\mu\nu}$. Making the substitution, we arrive at

$$\frac{d\theta}{dt} = -\frac{1}{3}\theta^2 - \sigma^{\mu\nu} \sigma_{\mu\nu} + \omega^{\mu\nu} \omega_{\mu\nu} - R_{\mu\nu} U^\mu U^\nu \quad (6.38)$$

This is the *Raychaudhuri's equation* for the congruence of timelike geodesics. We note that since the shear and rotation tensor are purely spatial, $\sigma^{\mu\nu}\sigma_{\mu\nu} \geq 0$ and $\omega^{\mu\nu}\omega_{\mu\nu} \geq 0$, with the equality sign holding if and only if the tensor is identically zero. As an illustrative example let us consider the congruence of comoving world lines in an expanding universe with metric:

$$ds^2 = -dt^2 + a^2(t)d\mathbf{x}^2 \quad (6.39)$$

where $a(t)$ is the scale factor. The tangent vector field $-\partial_\alpha t$, and a quick calculation reveals that

$$B_{\mu\nu} = U_{\mu;\nu} = \frac{\dot{a}}{a}h_{\mu\nu} \quad (6.40)$$

where an overdot indicates a differentiation with respect to t . This shows that the shear and rotation tensor are both zero for this congruence. The expansion, on the other hand, is given by:

$$\theta = 3\frac{\dot{a}}{a} = \frac{1}{a^3}\frac{da^3}{dt} \quad (6.41)$$

This illustrates rather well the general statement that the expansion H is the fractional rate of change of the congruence's cross-sectional volume(which is here proportional to a^3). The interpretation of θ is the fractional rate of change of ΔV , the congruence's cross-sectional volume:

$$\theta = \frac{1}{\Delta V} \frac{d\Delta V}{dt} \quad (6.42)$$

cross-section and cross-sectional volume γ from the congruence, and on the geodesic pick up a point P at which $t = t_P$. Construct, in a small neighbourhood around P , a small set $\delta\Sigma(t_P)$ of points P' such that through each of these point pass another geodesic from this congruence, and (ii) at each point P' , t is equal to t_P . This set form a three dimensional region, a small segment of the hypersurface $t = t_P$. We assume that the parametrization has been adjusted so that γ intersects $\delta\Sigma(t_P)$ orthogonally (there is no requirement that other geodesics do, as the congruence may not be hypersurface orthogonal). We shall call $\delta\Sigma(t_P)$ the congruence's cross section around the geodesic γ , at proper time $t = t_P$. We want to calculate the change of this volume in this hypersurface and compare it with the volume $\delta\Sigma(t_Q)$, where Q is a neighbouring point on γ .

We introduce coordinate $\delta\Sigma(t_P)$ by assigning a label $y^i(i = 1, 2, 3)$ to each point P' in the set. Recalling that through each of these points there passes a geodesic from the congruence, we see that we may use y^i to label the geodesics themselves. By demanding that each geodesic keep its label as it moves away from $\delta\Sigma(t_P)$, we simultaneously obtain a coordinate system x^i in $\delta\Sigma(t_Q)$ or any other cross section. Therefore, this construction defines a coordinate system (t, x^i) in a neighbourhood of the geodesics γ , and there exists a transformation between this system and the originally in use: $x^\mu = x^\mu(t, y^i)$. Because x^i is constant along the geodesics, we have

$$U^\mu = \frac{\partial x^\mu}{\partial t} \Big|_{y^a} \quad (6.43)$$

On the other hand, the vectors:

$$(e_i)^\mu = \left(\frac{\partial x^\mu}{\partial x^i} \right)_t \quad (6.44)$$

are tangent to the cross sections. These relations implies that $\mathcal{L}_U(e_i)^\mu = 0$, and we also have $U_\mu(e_i)^\mu = 0$ holding on γ (and only on γ). We now introduce the three-tensor h_{ij} defined by

$$h_{ij} = g_{\mu\nu}(e_i)^\mu(e_j)^\nu \quad (6.45)$$

This act as a metric tensor on $\delta\Sigma(t)$: For displacement confined to the cross-section (so that $dt = 0$), $x^\mu = x^\mu(t, y^i)$ and

$$ds^2 = g_{\mu\nu} dx^\mu dx^\nu = g_{\mu\nu} \left(\frac{\partial x^\mu}{\partial y^i} dy^i \right) \left(\frac{\partial x^\nu}{\partial y^j} dy^j \right) = g_{\mu\nu} (e_i)^\mu (e_j)^\nu dy^i dy^j = h_{ij} dy^i dy^j \quad (6.46)$$

Thus, $h_{\mu\nu}$ is the three-dimensional metric on the congruence's cross section. Because γ is orthogonal to its cross-section ($U_\mu(e_i)^\mu = 0$), we have that $h_{ij} = h_{\mu\nu}(e_i)^\mu (e_j)^\nu$ on γ , where $h_{\mu\nu} = g_{\mu\nu} + U_\mu U_\nu$ is the transverse metric, if we define h^{ij} to be the inverse h_{ij} , then it is easy to check that

$$h^{\mu\nu} = h^{ij} (e_i)^\mu (e_j)^\nu \quad (6.47)$$

On γ the three dimensional volume element on the cross-section, or cross-sectional volume, is $\Delta V = \sqrt{h} d^3y$, where $h = \det[h_{ij}]$ because the coordinate y^i are comoving (since the geodesic moves with a constant value of its coordinates) and d^3y does not change as the cross section $\Delta\Sigma(t)$ evolves from $t = t_P$ to $t = t_Q$. A change in ΔV comes entirely from a change in \sqrt{h} :

$$\frac{1}{\Delta V} \frac{d\Delta V}{dt} = \frac{1}{\sqrt{h}} \frac{d\sqrt{h}}{dt} = \frac{1}{2} h^{ij} \frac{dh_{ij}}{dt} \quad (6.48)$$

The rate of change of a three-metric:

$$\frac{dh_{ij}}{dt} = (g_{\mu\nu}(e_i)^\mu (e_j)^\nu)_{;\rho} U^\rho \quad (6.49)$$

$$= g_{\mu\nu}(e_i)^\mu_{;\rho} (e_j)^\nu U^\rho + g_{\mu\nu}(e_i)^\mu (e_j)^\nu_{;\rho} U^\rho \quad (6.50)$$

$$= g_{\mu\nu}(U^\mu_{;\rho}(e_i)^\rho)(e_j)^\nu + g_{\mu\nu}(e_i)^\mu (U^\nu_{;\rho}(e_j)^\rho) \quad (6.51)$$

$$= U_{\nu;\mu}(e_i)^\mu (e_j)^\nu + U_{\mu;\nu}(e_i)^\mu (e_j)^\nu \quad (6.52)$$

$$= (B_{\mu\nu} + B_{\nu\mu})(e_i)^\mu (e_j)^\nu \quad (6.53)$$

Multiplying by h^{ij} and evaluating on γ , so that (6.47) may be used, we obtain

$$h^{ij} \frac{dh_{ij}}{dt} = (B_{\mu\nu} + B_{\nu\mu}) h^{ij} (e_i)^\mu (e_j)^\nu = 2B_{\mu\nu} h^{\mu\nu} = 2B_{\mu\nu} g^{\mu\nu} = 2\theta \quad (6.54)$$

this establishes that local expansion rate is:

$$\theta = \frac{1}{\sqrt{h}} \frac{d}{dt} \sqrt{h} \quad (6.55)$$

6.5 Fermi Normal Coordinates (FNC) in FRW

First, we want to summarize the main results of the works [1, 3, 100, 126] about the construction of the so called Fermi coordinates (See also appendix A of [127]).

Consider a free falling observer along a timelike geodesic $h(\gamma)$ (from now on, the central geodesic). Let be P an arbitrary point on the central geodesic such that $P = h(\gamma_0)$. At this point(as we have already seen) it is possible to construct an orthonormal tetrad or vierbein, $\{(e_\gamma)^\mu; \gamma = 0, i\}$ which satisfies the condition $\eta_{\alpha\beta} = (e_\alpha)^\mu (e_\beta)^\nu g_{\mu\nu}$ that is parallel transported along $h(\gamma)$. Here $(e_0)^\mu$ is a tangent timelike 4-vector to h at P , and $(e_j)^\mu$ will be orthogonal

to h at P and then be a spacelike vector. The goal is to describe the spacetime in a neighbourhood of P . For that, let fix a point Q outside the central geodesic, and more importantly connected to P through the spacelike geodesic $g(\lambda)$ as it is shown in Figure (6.3). The affine parameter λ of this spatial-like geodesic $g(\lambda)$ is chosen in such a way that $Q = g(\lambda = 1)$, whose, generator vector, namely, \mathbf{v} , is normal to h at P (6.9) therefore, it can be decomposed as a linear combination of the spatial component of the vierbein $(e_j)^\mu$, moreover, the time component, t_F , of the Fermi coordinates is chosen to be the proper time τ of P at h , that a free falling observer experience. Hereafter x^μ will be the global coordinates, while x_F^μ the Fermi normal coordinates(or the conformal Fermi coordinates) Now, we need to find a map between these two coordinates, this is achieved by solving the geodesic equation for g (6.17):

$$\frac{d^2x^\mu}{d\lambda^2} + \Gamma_{\alpha\beta}^\mu \frac{dx^\alpha}{d\lambda} \frac{dx^\beta}{d\lambda} = 0. \quad (6.56)$$

as a power series on λ :

$$x^\mu(\lambda) = \sum_{n=0}^{\infty} \alpha_n^\mu \lambda^n, \quad (6.57)$$

with its initial conditions:

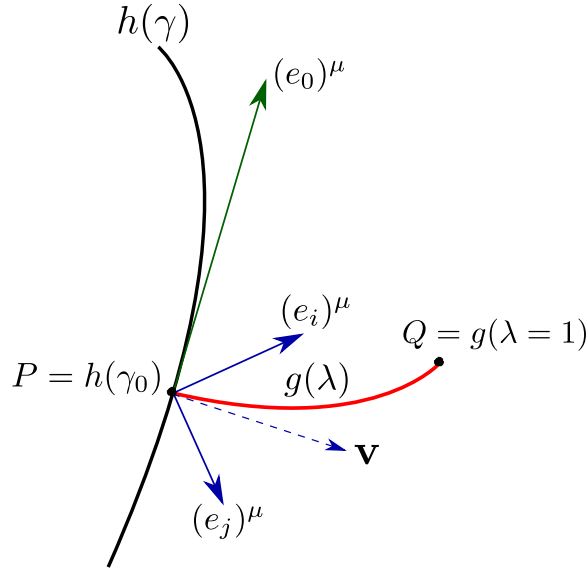


Figure 6.3: Geometrical construction of Fermi coordinates

$$\alpha_0^\mu = x^\mu(P) = (t_F, 0, 0, 0), \quad \alpha_1^\mu = \left. \frac{dx^\mu}{d\lambda} \right|_{\lambda=0} = x_F^i (e_i)^\mu. \quad (6.58)$$

The subsequent terms in this series expansion are found recursively by derivating (6.57) with respect to λ and using (6.56), with this, we find

$$\alpha_2^\mu = -\frac{1}{2} \left. \frac{d^2x^\mu}{d\lambda^2} \right|_{\lambda=0} = -\frac{1}{2} \Gamma_{\alpha\beta}^\mu \alpha_1^\alpha \alpha_1^\beta \quad (6.59)$$

$$\alpha_3^\mu = -\frac{1}{6} \left. \frac{d^3x^\mu}{d\lambda^3} \right|_{\lambda=0} = -\frac{1}{6} [\partial_\eta \Gamma_{\alpha\beta}^\mu (\alpha_1^\alpha \alpha_1^\beta \alpha_1^\eta) + 4 \Gamma_{\alpha\beta}^\mu \alpha_1^\alpha \alpha_2^\beta], \quad (6.60)$$

and so on. Now it is possible to write down the global coordinates as a function of Fermi normal coordinates:

$$x^\mu(x_F) = \alpha_0^\mu + (e_\sigma)^\mu x_F^\sigma - \frac{1}{2} \Gamma_{\alpha\beta}^\mu (e_\sigma)^\alpha (e_\rho)^\beta x_F^\sigma x_F^\rho + \mathcal{O}(x_F^3), \quad (6.61)$$

with corrections starting at $\mathcal{O}(x_F^3)$. If we denote $g_{\mu\nu}^F$ the metric in the FNC and $g_{\mu\nu}$ the metric in global coordinates, they are related by the usual transformation rule for any tensor.

$$g_{\mu\nu}^F(x_F) = \frac{\partial x^\alpha}{\partial x_F^\mu} \frac{\partial x^\beta}{\partial x_F^\nu} g_{\alpha\beta}(x(x_F)) \quad (6.62)$$

Where the Jacobian (6.62) has the form:

$$\begin{aligned} \frac{\partial x^\mu}{\partial x_F^\nu} &= (e_\nu)^\mu - \Gamma_{\alpha\beta}^\mu (e_\nu)^\alpha (e_j)^\beta x_F^j + \mathcal{O}(x_F^2) \\ &= (e_\nu)^\mu + A_{\nu j}^\mu x_F^j + \mathcal{O}(x_F^2) \end{aligned} \quad (6.63)$$

to be explicit the fact that we will only consider linear order terms along all the computations, we also expand the metric

$$\begin{aligned} g_{\alpha\beta}(x(x_F)) &= g_{\alpha\beta}|_P + \frac{\partial g_{\alpha\beta}}{\partial x^\mu}|_P x^\mu + \dots \\ &= g_{\alpha\beta}|_P + (e_j)^\mu (\partial_\mu g_{\alpha\beta})|_P x_F^j + \mathcal{O}(x_F^2). \end{aligned} \quad (6.64)$$

Now, expanding the metric al linear order (6.64), transforming the metric (6.62) using (6.63) and linearizing the metric:

$$g_{\mu\nu}^F(x_F) = \eta_{\mu\nu} + \nabla_\gamma g_{\alpha\beta}|_P (e_\mu)^\alpha (e_\nu)^\beta (e_j)^\gamma x_F^j + \mathcal{O}(x_F^2),$$

when the covariant derivative is compatible with the metric (absence of torsion), one has $\nabla_\gamma g_{\alpha\beta} = 0$. Then, the metric tensor in Fermi normal coordinates just correspond to a Minkowski metric

$$g_{\mu\nu}^F(x_F) = \eta_{\mu\nu} + \mathcal{O}(x_F^2). \quad (6.65)$$

6.5.1 Unperturbed FLRW Universe

As an example of application of the coordinates and to be explicit the fact that the first corrections to Minkowski begin in quadratic order in Fermi coordinates($|x_F|^2 H^2$), we will apply the recipe mentioned before and construct the line element for FLRW.

Consider the FLRW metric, written as

$$ds^2 = -dt^2 + a^2(t) \gamma_{ij} dx^i dx^j, \quad (6.66)$$

where a is the scale factor and t and x^i denotes the temporal and the spatial coordinate respectively. Furthermore, the above expression can be suitable written in conformal coordinates by using the conformal time $d\tau = \frac{dt}{a(t)}$, thus

$$ds^2 = a^2(\tau) (d\tau^2 + \gamma_{ij} dx^i dx^j), \quad (6.67)$$

where $\gamma_{ij} = \delta_{ij}(1 + \frac{K}{4}\delta_{ab}x^a x^b)^{-2}$. We will restrict to perform the computations considering the curvature constant $K = 0$. For computing the metric corrections for the FLRW universe, we need the Christoffel symbols for the metric (6.66), which are

$$\Gamma_{ij}^0 = a\dot{a}\delta_{ij}, \quad \Gamma_{i0}^k = \frac{\dot{a}}{a}\delta_i^k = H\delta_i^k. \quad (6.68)$$

To find the vierbein components, we impose the flatness condition (6.6)

$$\eta_{\alpha\beta} = (e_\alpha)^\mu (e_\beta)^\nu g_{\mu\nu}, \text{ then } (e_0)^\mu (e_0)^\nu g_{\mu\nu} = -1, \quad (e_i)^\mu (e_j)^\nu g_{\mu\nu} = \delta_{ij}. \quad (6.69)$$

Using the following ansatz

$$(e_0)^\mu = (\alpha, \mathbf{0}), \quad (e_i)^\mu = (0, \beta\delta_i^j) \quad (6.70)$$

is trivial to find that $\alpha = 1$ and $\beta = a(t)^{-1}$. Finally the vierbein becomes

$$(e_0)^\mu = (1, \mathbf{0}), \quad (e_i)^\mu = a(t)^{-1}(0, \delta_i^j). \quad (6.71)$$

Now we need to find the explicit form of (6.58), (6.59) and (6.60) once known the Christoffel symbols and the vierbein

$$\alpha_0^\mu = (t_F, \mathbf{0}), \quad \alpha_1^\mu = \frac{x_F^i}{a(t)}(0, \delta_i^j) \quad (6.72)$$

$$\alpha_2^0 = -\frac{1}{2}\Gamma_{ij}^0\alpha_1^i\alpha_1^j = -\frac{H}{2}x_F^i x_F^j \delta_{ij} = -\frac{H}{2}\vec{x}_F^2, \quad \alpha_2^k = -\frac{1}{2}\Gamma_{i0}^k\alpha_1^i \underbrace{\alpha_1^0}_{=0} = 0 \quad (6.73)$$

to compute (6.60) one have to consider

$$\partial_0\Gamma_{i0}^k = \dot{H}\delta_i^k, \quad \partial_0\Gamma_{ij}^0 = (\dot{a}^2 + a\ddot{a})\delta_{ij} = a^2(\dot{H} + 2H^2)\delta_{ij} \quad (6.74)$$

then

$$\alpha_3^0 = -\frac{1}{6} \left[\partial_0\Gamma_{ij}^0 \alpha_1^i \alpha_1^j \underbrace{\alpha_1^0}_{=0} + 4\Gamma_{ij}^0 \alpha_1^i \underbrace{\alpha_2^j}_{=0} \right] = 0 \quad (6.75)$$

$$\alpha_3^k = -\frac{1}{6} \left[\partial_0\Gamma_{i0}^k \alpha_1^i \underbrace{\alpha_1^0}_{=0} \alpha_1^j + 4\Gamma_{i0}^k \alpha_1^i \alpha_2^j \right] = \frac{H^2}{3a} x_F^k x_F^i x_F^j \delta_{ij} = \frac{H^2}{3a} x_F^k \vec{x}_F^2. \quad (6.76)$$

Replacing in (6.61) and separating by components, one finds that at quadratic order in x_F the coordinates sees as

$$x^0 = t = t_F - \frac{H}{2}\vec{x}_F^2 \quad (6.77)$$

$$x^i = \frac{x_F^i}{a} \left(1 + \frac{H^2}{3}\vec{x}_F^2 \right) \quad (6.78)$$

now, taking into account the transformation of the metric (6.62) one finds

$$g_{00}^F = \left(\frac{\partial t}{\partial t_F} \right)^2 g_{00} + \left(\frac{\partial x^i}{\partial t_F} \right) \left(\frac{\partial x^j}{\partial t_F} \right) g_{ij}, \quad (6.79)$$

$$g_{ij}^F = \left(\frac{\partial t}{\partial x_F^i} \right) \left(\frac{\partial t}{\partial x_F^j} \right) g_{00} + \left(\frac{\partial x^k}{\partial x_F^i} \right) \left(\frac{\partial x^l}{\partial x_F^j} \right) g_{kl}, \quad (6.80)$$

$$\frac{\partial t}{\partial t_F} = 1 - \frac{\dot{H}}{2} \bar{x}_F^2, \quad (6.81)$$

$$\frac{\partial x^i}{\partial t_F} = \frac{H}{2} \left[1 + \frac{(\dot{H} + 2H^2)}{3} \bar{x}_F^2 \right] x_F^i, \quad (6.82)$$

$$\frac{\partial x^k}{\partial x_F^i} = \frac{\delta_i^k}{a} \left(1 + \frac{H^2}{3} \bar{x}_F^2 \right) + \frac{2H^2}{3a} (x_F^l \delta_{li}) x_F^k. \quad (6.83)$$

Preserving only the zeroth and quadratic order terms, one obtains

$$g_{00}^F = -1 + (\dot{H} + H^2) \bar{x}_F^2, \quad g_{ij}^F = \delta_{ij} - \frac{H^2}{3} (\bar{x}_F^2 \delta_{ij} + x_{Fi} x_{Fj}) \quad (6.84)$$

it is possible performing a change of variable in the above equation to eliminate the term $x_{Fi} x_{Fj}$, since, this coordinate construction only fixes the gauge linearly at the central geodesic [102]. Finally one finds that the Fermi metric, including the second order corrections, is

$$ds^2 = - \left[1 - (\dot{H} + H^2) \bar{x}_F^2 \right] dt_F^2 + \left[1 - \frac{H^2}{2} \bar{x}_F^2 \right] d\bar{x}_F^2. \quad (6.85)$$

As an additional step, connecting with the results of [1], we may compute the geodesic expansion (this expression comes from solving the Raychaudhuri equation for a geodesic congruence), defined by

$$\theta = \frac{1}{3} \nabla_\mu U^\mu = \frac{1}{3} (\partial_\mu U^\mu + \Gamma_{\mu\lambda}^\mu U^\lambda) \quad (6.86)$$

Since $U^\mu = (e_0)^\mu$ and using the Christoffel symbols (6.68) and (??), one finds

$$\theta = H(t) \quad (6.87)$$

6.5.2 Perturbed FLRW Universe

In this section, we will follow the main results presented in the appendix C.2 of [102]. If we work with the perturbed metric defined by

$$g_{\mu\nu} = \eta_{\mu\nu} + h_{\mu\nu} = \begin{pmatrix} -1 + h_{00} & h_{0j} \\ h_{i0} & \delta_{ij} + h_{ij} \end{pmatrix}, \quad |h| \ll 1. \quad (6.88)$$

The construction of the Fermi coordinates now is respect to the metric (6.88). We will denote the Fermi coordinates respect to the perturbed metric like \bar{x}_F . To find the vierbein components, first, for $(e_0)^\mu$ we postulate the ansatz

$$(e_0)^\mu = (\alpha, v^i), \quad |v^i| \ll 1. \quad (6.89)$$

Here, v^i is the peculiar velocity of the observer. Using (6.69) with (6.89)

$$(\alpha \ v^i) \begin{pmatrix} -1 + h_{00} & h_{0j} \\ h_{i0} & \delta_{ij} + h_{ij} \end{pmatrix} \begin{pmatrix} \alpha \\ v^j \end{pmatrix} = -1 \quad (6.90)$$

$$\Rightarrow \alpha = \frac{1}{\sqrt{(1 - h_{00})}} \approx 1 + \frac{1}{2}h_{00}. \quad (6.91)$$

And for the spatial tetrad components, $(e_k)^\mu$, we use the ansatz $(e_k)^\mu = (\alpha_k, \beta_k^i)$ and use the flatness conditions to determine α_k and β_k^i , that reads

$$(e_k)^\mu (e_0)^\nu g_{\mu\nu} = 0 \quad \text{and} \quad (e_k)^\mu (e_l)^\nu g_{\mu\nu} = \delta_{kl} \quad (6.92)$$

following the same steps performed in (6.90)-(6.91), for (6.92) at linear order in $h_{\mu\nu}$ and v^i one finds that α and β are related by

$$\alpha_k = \beta_k^i (h_{i0} + v_i) \quad \text{and} \quad \beta_k^i \beta_l^j (\delta_{ij} + h_{ij}) = \delta_{kl}, \quad (6.93)$$

then one finds, at linear order in $h_{\mu\nu}$, α and β are

$$\beta_k^i = \delta_k^i - \frac{1}{2}h_j^i, \quad \text{and} \quad \alpha_k = (h_{k0} + v_k). \quad (6.94)$$

In consequence, the Vierbein associated with (6.88) is given by

$$(e_0)^\mu = \left(1 + \frac{1}{2}h_{00}, v^i \right), \quad (e_j)^\mu = \left(v_j + h_{0j}, \delta_j^i - \frac{1}{2}h_j^i \right). \quad (6.95)$$

Since $h_{\mu\nu}$ is a small perturbation, we have only considered linear terms of h along the computation. Particularly, the coordinate expansion (6.61) reduces to

$$x^\mu(\bar{x}_F) = P^\mu + (e_i)^\mu \bar{x}_F^i - \frac{1}{2}\Gamma_{ij}^\mu \bar{x}_F^i \bar{x}_F^j. \quad (6.96)$$

Where $P^\mu = x^\mu(P)$ are the global coordinates of the central geodesic, so that $v^i = \partial P^i / \partial x^0$. As stated before, the Fermi time component is defined by the proper time of an observer on the central geodesic, namely the proper time of P

$$\bar{x}_F^0 = \tau_P = \int \sqrt{g_{\mu\nu}|_P dx^\mu dx^\nu} \quad (6.97)$$

keeping only the linear contributions, then the conformal proper time is related to the global time by

$$x^0(P) = \bar{x}_F^0 + \frac{1}{2} \int_0^{\bar{x}_F^0} h_{00}(\mathbf{0}, \tau) d\tau. \quad (6.98)$$

On the other hand, the Christoffel symbols for (6.88) are given by

$$\Gamma_{ij}^\mu = \frac{1}{2} (h^\mu_{i,j} + h^\mu_{j,i} + h_{ij}^{,\mu}). \quad (6.99)$$

Finally, the coordinate expansion of the global coordinates in terms of Fermi normal coordinates is

$$x^0(\bar{x}_F) = \bar{x}_F^0 + \frac{1}{2} \int_0^{\bar{x}_F^0} h_{00}(\mathbf{0}, \tau) d\tau + (v_j + h_{0j}) \bar{x}_F^j + \frac{1}{4} (h_{0j,i} + h_{0i,j} + h'_{ij}) \bar{x}_F^i \bar{x}_F^j \quad (6.100)$$

$$x^k(\bar{x}_F) = P^k + \bar{x}_F^k - \frac{1}{2}h_i^k \bar{x}_F^i - \frac{1}{4} (h_{i,j}^k + h_{j,i}^k - h_{ij}^{,k}) \bar{x}_F^i \bar{x}_F^j. \quad (6.101)$$

6.6 Conformal Fermi Coordinates (CFC)

In this section, we will generalize the construction of Fermi Normal Coordinates(FNC) to local conformal coordinates that a free falling observer experiences. This set of coordinates are suitable constructed for an homogeneously and isotropically expanding space-time such a FLRW universe, moreover, they are required to make predictions for any cosmological purpose, since, these set of coordinates account the fact that any local observer is unable to capture any gravitation effect(curvature) much wider than the sound horizon in a description of metric perturbations. So, such ignorance is parametrized by hiding them into a new local effective metric, the Conformal Fermi Metric(CFC). Finally, is worth mentioning that this section has been influenced for [1], [100],[3], [126] as a result, we generalize and complement part of these work already started, incorporating a non-attractor scenario for the evolution of metric perturbations and deducing more relations. This section is organized as follows: in subsection 1) 2) 3).

As we know from the beginning of this chapter an inertial observer does not experience any gravitational effects on him/her as a consequence of the Einstein equivalence principle. Therefore, his/her local spacetime description is equivalent to a flat spacetime, which naturally induces a diffeomorphism between the global coordinates and this inertial frame:

$$g_{\mu\nu}^F(\bar{x}) = \frac{\partial x^\alpha}{\partial \bar{x}^\mu} \frac{\partial x^\beta}{\partial \bar{x}^\nu} g_{\alpha\beta}(x(\bar{x})) \quad (6.102)$$

where the bar denotes the *Conformal Fermi Coordinates*(CFC). These coordinates are the physical set of coordinates used for measurements. Due to the perturbative description of the metric fluctuations, these two set of coordinates slightly differs, thus a generic coordinate transformation has the form:

$$\tau(\bar{\tau}, \bar{x}) = \bar{\tau} + \xi^0(\bar{\tau}, \bar{x}), \quad \mathbf{x}^i(\bar{\tau}, \bar{x}) = \bar{x}^i + \xi^i(\bar{\tau}, \bar{x}), \quad (6.103)$$

where ξ^μ is a shift 4-vector, that is expansible perturbatively order by order such that:

$$\xi^\mu(\bar{\tau}, \bar{x}) = \xi^{\mu(0)}(\bar{\tau}, \bar{x}) + \xi^{\mu(1)}(\bar{\tau}, \bar{x}) + \xi^{\mu(2)}(\bar{\tau}, \bar{x}) + \dots, \quad (6.104)$$

and the induced FLRW metric now has the form of:

$$g_{\mu\nu}^F(\bar{x}) = a_F^2(\bar{\tau}) \bar{g}_{\mu\nu} = a_F^2(\bar{\tau}) [\eta_{\mu\nu} + h_{\mu\nu}^F(\bar{x})] = a_F^2(\bar{\tau}) \bar{g}_{\mu\nu}^F(\bar{x}), \quad h_{\mu\nu}^F(\bar{x}) = \mathcal{O}(\bar{x}^2) \quad (6.105)$$

where the super/subscripts denotes 'CFC' objects such as the spacetime scale factor $a_F(x)$ and the metric tensor $g_{\mu\nu}^F$, additionally, the conformal proper time is defined as

$$d\bar{\tau} = a_F^{-1}(P(\bar{t})) d\bar{t}, \quad (6.106)$$

where $\bar{\tau}$ is the conformal time coordinate for the conformal geodesic or simple the proper time, this allows us to construct surfaces of constant $\bar{\tau}$, spanned by space-like conformal geodesics with respect to the conformal metric $\bar{g}_{\mu\nu}^F = a_F^{-2}(x) g_{\mu\nu}^F$. We must emphasize that this set of coordinates physically fixes the gauge up to first order in gradients only, because the flatness requirement: $\bar{g}_{\mu\nu}^F|_P = \eta_{\mu\nu}$ and $\partial_\rho \bar{g}_{\mu\nu}^F|_P = 0$, just imposes restriction on the metric

and their first derivatives along the central geodesics. Additionally, the metric perturbations can be expressed in terms of the Riemann tensor (6.2):

$$h_{00}^F(\bar{x}) = -\bar{R}_{0k0l}^F|_P \bar{x}^k \bar{x}^l, \quad h_{0i}^F(\bar{x}) = -\frac{2}{3} \bar{R}_{0kil}^F|_P \bar{x}^k \bar{x}^l, \quad h_{ij}^F(\bar{x}) = -\frac{1}{3} \bar{R}_{ikjl}^F|_P \bar{x}^k \bar{x}^l \quad (6.107)$$

where $\bar{R}_{\mu\rho\nu\sigma}^F$ is the Riemann tensor of the conformal metric in CFC coordinates, and indices have been lowered with the conformal metric. In terms of global coordinates, $\bar{R}_{\mu\rho\nu\sigma}^F|_P$ is,

$$\bar{R}_{\mu\rho\nu\sigma}^F|_P = \bar{R}_{\alpha\beta\gamma\delta}|_P (\bar{e}_\mu)^\alpha_P (\bar{e}_\rho)^\beta_P (\bar{e}_\nu)^\gamma_P (\bar{e}_\delta)^\mu_P, \quad (6.108)$$

where the basis vectors at the central geodesic are given by $(\bar{e}_\nu)^\beta_P = a_F(P)(e_\nu)_P^\mu$. Furthermore, we need to determine the local induced scale factor $a_F(\bar{x})$ that contributes with its gradients to the Riemann tensor of the conformal Fermi Metric $\bar{g}_{\mu\nu}^F$, this function can be determined through a local expansion rate by taking the divergence of the time-like vector $\nabla_\mu U^\mu \propto H_F(\bar{\tau}, \bar{x}_c)$,

$$\frac{d}{d\bar{\tau}} \log a_F(P) = \frac{1}{a_F(\bar{\tau})} \frac{d}{d\bar{\tau}} \log a_F(P) = \frac{\nabla_\mu U^\mu}{3} \Big|_P \quad (6.109)$$

6.6.1 Construction of the CFC

The CFC coordinates $(\bar{\tau}, \bar{\mathbf{x}})$ for an inertial observer with timelike vector U^μ resembles a Minkowski space, whose first correction scales as $\bar{x}^i \bar{x}^j \partial_i \partial_j \zeta_L$ instead of $|\mathbf{x}|^2 H^2$, as in the case of Fermi normal coordinates. Particularly, its construction goes as follows:

- *Tetrad construction:* along the central geodesic at each point $P(\bar{\tau})$ is constructed an orthonormal system $\{(e_\nu)^\mu : \nu = 0, 1, 2, 3\}$ with respect to the timelike vector $U^\mu \equiv (e_0)^\mu$. These vectors are parallel transported along the central geodesic.
- *Conformal Fermi time:* given a Fermi scale factor a_F , we define the conformal Fermi time, $\bar{\tau}$, as the time coordinate, in (6.106) this allows us to define surfaces of constant $\bar{\tau}$, spanned by space-like conformal geodesics.
- *Spatial coordinates:* It is possible to construct a map from the global conformal coordinates to the CFC (6.17). The coordinates of a point Q inside the geodesic congruence are defined as the director vector that generates the spatial-like conformal geodesic that joins P with Q , this geodesic satisfies fig. ?? :

$$\frac{d^2 x^\mu}{d\lambda^2} + \bar{\Gamma}_{\alpha\beta}^\mu \frac{dx^\alpha}{d\lambda} \frac{dx^\beta}{d\lambda} = 0, \quad \text{with } \bar{\Gamma}_{\alpha\beta}^\mu = \Gamma_{\alpha\beta}^\mu - C_{\alpha\beta}^\mu \quad (6.110)$$

where $\bar{\Gamma}_{\alpha\beta}^\mu$ are the Christoffel symbols for the conformal metric $\bar{g}_{\mu\nu}^F$ and $C_{\alpha\beta}^\mu$ is defined by:

$$C_{\alpha\beta}^\mu = \delta_\alpha^\mu \nabla_\beta \ln a_F + \delta_\beta^\mu \nabla_\alpha \ln a_F - g_{\alpha\beta} g^{\mu\lambda} \nabla_\lambda \ln a_F. \quad (6.111)$$

Moreover, the first derivatives of a_F are constrained by the CFC metric and the gradient of a_F along the central geodesic must be along the time direction

$$\nabla_\mu \ln a_F|_{\bar{x}^i=0} = (\ln a_F)' a_F(e_0)_\mu \quad (6.112)$$

where the prime denotes derivatives with respect to $\bar{\tau}$, additionally the second derivative are constrained to the construction (6.105) $\nabla_\mu \nabla_\nu \ln a_F|_{\bar{x}^i=0}$. In particular, they exactly match the expression for an unperturbed FLRW. With this construction, we can now derive the explicit transformation law from the global coordinate system to CFC. In particular, one can solve (6.110) as a power expansion with affine parameter λ :

$$x^\mu(\lambda) = \sum_{n=0}^{\infty} \alpha_n^\mu \lambda^n. \quad (6.113)$$

This set of curves connect points that are in the same spatial hypersurfaces, particularly, we are interested in connecting any point P (with CFC coordinate $x^\mu(P) = (\bar{\tau}, 0)$) along the central geodesic with any point Q which in CFC has the coordinates $x^\mu(Q) = (\bar{\tau}, \bar{\mathbf{x}})$ in the same hypersurface. Since P is chosen as the spatial origin, we immediately have $\alpha_0^\mu = x^\mu(P)$. Additionally, rescaling λ such that $\lambda = 0$ corresponds to P and $\lambda = 1$ at Q . These spatial-like geodesics are generated by the perpendicular vector at $\lambda = 0$, $(\bar{e}_i)_P^\mu$, more explicitly:

$$\alpha_1^\mu = \frac{dx^\mu}{d\lambda} \Big|_{\lambda=0} = (\bar{e}_i)_P^\mu \bar{x}^i = a_F(P)(e_i)_P^\mu \bar{x}^i, \quad (6.114)$$

furthermore, higher order contributions can be computed recursively by taking successive derivatives to (6.110) :

$$x^\mu(\bar{\tau}, \bar{x}) = x^\mu(P) + a_F(P)(e_i)_P^\mu \bar{x}^i - \frac{a_F^2(P)}{2} \bar{\Gamma}_{\alpha\beta}^\mu|_P (e_i)_P^\alpha (e_j)_P^\beta \bar{x}^i \bar{x}^j \quad (6.115)$$

$$- \frac{a_F^3(P)}{6} (\partial_\gamma \bar{\Gamma}_{\alpha\beta}^\mu - 2 \bar{\Gamma}_{\sigma\alpha}^\mu \bar{\Gamma}_{\beta\gamma}^\sigma)|_P (e_i)_P^\alpha (e_j)_P^\beta (e_k)_P^\gamma \bar{x}^i \bar{x}^j \bar{x}^k + \dots \quad (6.116)$$

where all quantities are evaluated at the central geodesics. As a remark, we emphasize that just for brevity, \bar{x}^i was used instead of the distance to the central geodesic $\Delta \bar{x}^i = \bar{x}^i - \bar{x}_c^i$, and the basis vectors are given by:

$$(e_0)^\mu = a^{-1}(\tau) \left(1 + \frac{1}{2} h_{00}, V^i \right), \quad (e_j)^\mu = a^{-1}(\tau) \left(V_j + h_{0j}, \delta_j^i - \frac{1}{2} h_j^i \right), \quad (6.117)$$

or equivalently in the comoving gauge, using the ADM decomposition.

$$(e_0)^\mu = a^{-1}(\tau) (1 - N_1, V^i), \quad (e_j)^\mu = a^{-1}(\tau) (V_j + N_j, [1 - \zeta] \delta_j^i). \quad (6.118)$$

6.6.2 Mapping to CFC

In this section, we are going to find the explicit map between the global conformal coordinates, x^μ , and the CFC, \bar{x}^μ , to do that we are going to solve perturbatively, recursively and independently of the underlying inflationary background some of the expressions stated in the previous section. Let us start with the definition of the CFC basis vector:

$$\frac{\partial x^\mu(\bar{\tau}, \bar{\mathbf{x}}_c)}{\partial \bar{\tau}} = a_F(P)(e_0)_P^\mu, \quad (6.119)$$

considering the spatial coordinates $\mu = i$:

$$(\bar{e}_0)_P^i = a_F(\bar{\tau})(e_0)_P^i = \frac{a_F(\bar{\tau})}{a(\tau(\bar{\tau}, \bar{\mathbf{x}}_c))} V^i(x(\bar{\tau}, \bar{\mathbf{x}}_c)) \quad (6.120)$$

but, we know that $(e_0)_P^i$ is a first order in perturbation, so the zeroth order $\frac{a_F(P)}{a(P)}$ suffices, which is just 1. Therefore, from (6.119) we deduce:

$$x^i(\bar{\tau}, \bar{\mathbf{x}}_c) = \bar{x}_c^i + \int_{\bar{\tau}_*}^{\bar{\tau}} d\bar{s} V^i(\tau(\bar{\tau}, \bar{\mathbf{x}}_c), \bar{\mathbf{x}}_c) \quad (6.121)$$

where we have used $\mathbf{x} = \bar{\mathbf{x}}_c$. In the same manner from (6.119) if $\mu = 0$, the time shift is:

$$\tau(\bar{\tau}, \bar{\mathbf{x}}) = \bar{\tau} + \Delta\tau(\bar{\tau}, \bar{\mathbf{x}}_c) = \bar{\tau} + C_{\Delta\tau}(\bar{\mathbf{x}}_c) + \int_{\bar{\tau}_*}^{\bar{\tau}} d\bar{s} (\Delta a(\bar{s}, \bar{\mathbf{x}}_c) - N_1(\bar{s}, \bar{\mathbf{x}}_c)). \quad (6.122)$$

Now we already have the first terms of (6.113) associated to the spatial component (6.121) and the temporal component (6.122), we are able to extend the map recursively to neighboring points around the central geodesics. It is worth noting that due to the constraint (6.105) the conformal Christoffel symbols $\tilde{\Gamma}$ must be first order in perturbation and must contain gradients of ζ_L , thus we can neglect second order contributions coming from $a_F(P)/a(P)$, so the equation (6.115) simplifies to:

$$x^\mu(\bar{\tau}, \bar{x}) = x^\mu(P) + a_F(P)(e_i)_P^\mu \bar{x}^i - \frac{1}{2} \bar{\Gamma}_{\alpha\beta}^\mu |_P (e_i)_P^\alpha (e_j)_P^\beta \bar{x}^i \bar{x}^j \quad (6.123)$$

where the conformal Christoffel symbols are determined by:

$$\bar{\Gamma}_{\mu\nu}^\rho = \Gamma_{\mu\nu}^\rho - \delta_\mu^\rho \nabla_\nu \ln a_F - \delta_\nu^\rho \nabla_\mu \ln a_F + g_{\mu\nu} g^{\rho\sigma} \nabla_\sigma \ln a_F \quad (6.124)$$

and the scale factor gradient along the central geodesic:

$$\nabla_\mu \ln a_F|_P = -\frac{\mathcal{H}(P)}{a_F(P)} (e_0)_{\mu,P}, \quad (e_0)_{\mu,P} = g_{\mu\nu} (e_0)_P^\nu \quad (6.125)$$

with the local comoving Hubble expansion rate \mathcal{H}_F ,

$$\frac{\mathcal{H}(P)}{a_F(P)} = \frac{1}{a(\tau)} \left(\mathcal{H}(\tau) - \mathcal{H}(\tau) N_1(\tau, \mathbf{x}_c(\tau)) + \partial_0 \zeta(\tau, \mathbf{x}_c(\tau)) + \frac{1}{3} \partial_i V^i(\tau, \mathbf{x}_c(\tau)) \right). \quad (6.126)$$

Then, replacing (6.121), (6.122) into (6.123) we find a coordinate transformation, up to third order in gradient expansion, that looks like:

$$\tau(\bar{\tau}, \bar{\mathbf{x}}) = \bar{\tau} + \Delta\tau(\bar{\tau}, \bar{\mathbf{x}}_c) + F_i(\bar{\tau}, \bar{\mathbf{x}}_c) \bar{x}^i - \frac{1}{2} \bar{\Gamma}_{ij}^0(\bar{\tau}, \bar{\mathbf{x}}_c) \bar{x}^i \bar{x}^j + \dots \quad (6.127)$$

$$x^l(\bar{\tau}, \bar{\mathbf{x}}) = \bar{x}^l + \int_{\bar{\tau}_*}^{\bar{\tau}} d\bar{s} V^l(\bar{s}, \bar{\mathbf{x}}_c) + [\Delta a(\bar{\tau}, \bar{\mathbf{x}}_c) - \zeta_L(\bar{\tau}, \bar{\mathbf{x}}_c)] \bar{x}^l - \frac{1}{2} \bar{\Gamma}_{ij}^l(\bar{\tau}, \bar{\mathbf{x}}_c) \bar{x}^i \bar{x}^j + \dots \quad (6.128)$$

where we omitted the $\bar{\mathbf{x}}_c$ and it has been defined $F_i = N_i + V_i$. Finally, the above expression suggest the following parametrization for (6.103):

$$x^\mu(\bar{\tau}, \bar{\mathbf{x}}) = \bar{x}^\mu + \xi^{\mu(0)}(\bar{\tau}, \bar{\mathbf{x}}_c) + \xi^{\mu(1)}(\bar{\tau}, \bar{\mathbf{x}}) + \xi^{\mu(2)}(\bar{\tau}, \bar{\mathbf{x}}) + \dots \quad (6.129)$$

$$= \bar{x}^\mu + \xi^\mu(\bar{\tau}, \bar{\mathbf{x}}_c) + A_i^\mu(\bar{\tau}, \bar{\mathbf{x}}_c) \bar{x}^i + B_{ij}^\mu(\bar{\tau}, \bar{\mathbf{x}}_c) \bar{x}^i \bar{x}^j + \dots \quad (6.130)$$

Notice that all coefficients for this expansion have been evaluated at the central geodesic.

Peculiar velocity potential

Despite having the full construction of the map so far, we have not yet provided an analytical expression for the peculiar velocity potential, \mathcal{F} , and how this is related to the perturbations itself. In an unperturbed universe, we know that it must be zero because one can always set a reference system in which is exactly zero. However, in a perturbed universe, we know that it must depend on spatial gradients of curvature modes. In principle, V^i is unconstrained, but if we impose that the vierbein is parallel transported, particularly, by using U^μ is parallel transported by itself, one is able to derive a close relation to determine it:

$$U^\lambda \partial_\lambda U^\mu + \Gamma_{\alpha\beta}^\mu U^\alpha U^\beta = 0, \quad (6.131)$$

we find a relation between V^j , and the Lagrangian constraints N^j , N_1 , the time shift and the time lapse, respectively. Thus,

$$\partial_0 V^i + \mathcal{H} V^i = -\partial^i N_1 - \partial_0 N^i - \mathcal{H} N^i \quad (6.132)$$

If we define the velocity potential \mathcal{F} , such as, $F^i = V^i + N^i = \partial^i \mathcal{F}$, and substituting in the above equation, this reduces to:

$$\partial_0 F^i + \mathcal{H} F^i + \partial^i N_1 = 0 \rightarrow \partial_0 \mathcal{F} + \mathcal{H} \mathcal{F} + N_1 = C(\tau), \quad (6.133)$$

whose general solution is:

$$\mathcal{F}(\tau, \mathbf{x}) = e^{-\int_{\tau_*}^\tau ds \mathcal{H}(s)} \left[\tau_* C_{\mathcal{F}}(\tau_*, \mathbf{x}) - \int_{\tau_*}^\tau ds e^{\int_{\tau_*}^s d\omega \mathcal{H}(\omega)} N_1(s, \mathbf{x}) \right], \quad (6.134)$$

where the $C(\tau)$ was set to zero because only their spatial gradients matter contributes. In particular, it is possible reduce (6.134) for a quasi-de sitter limit by using the conformal Hubble parameter definition:

$$\mathcal{H}(\tau) = aH = \dot{a} = \frac{a'}{a} = \frac{d \ln a(\tau)}{d\tau} = \partial_\tau N \quad (6.135)$$

that is to say, the conformal Hubble parameter is just the conformal time derivatives of the number of e-folds, $N(\tau)$, so the integral in the exponential reduces to:

$$\exp \left(- \int_{\tau_*}^\tau ds \mathcal{H}(s) \right) = \exp(-N(\tau) + N(\tau_*)) = a(\tau_*)/a(\tau), \quad (6.136)$$

where we are using that the scale factor can be parametrized as $a(\tau) = a(\tau_*)e^{N(\tau)}$. Moreover, if we choose $\tau_* = -\infty$ as $N = 0$, the last expression simplifies to:

$$\exp \left(- \int_{\tau_*}^\tau ds \mathcal{H}(s) \right) = e^{-N(\tau)}. \quad (6.137)$$

Now for the remaining term in (6.134), we know from the ADM formalism that $N_1(\tau) = \partial_0 \zeta / \mathcal{H}$, so:

$$\int_{\tau_*}^\tau ds e^{\int_{\tau_*}^s d\omega \mathcal{H}(\omega)} N_1(s, \mathbf{x}) = \int_{\tau_*}^\tau ds e^{N(s)} \frac{\partial_0 \zeta}{\partial_\tau N}. \quad (6.138)$$

Additionally, if we take $\tau = -1/\mathcal{H} = -1/\partial_\tau N$ at first order. Using that N is a monotonic function of τ , we have $\tau = -\frac{d\tau}{dN}$, and by direct integration gives $N(\tau) = -\ln(\tau/\tau_*)$, so $\tau = \tau_* e^{-N}$. Replacing in (6.138) we find:

$$\begin{aligned} \int_{\tau_*}^{\tau} ds e^{\int_{\tau_*}^s d\omega \mathcal{H}(\omega)} N_1(s, \mathbf{x}) &= \int_{N_*}^N dN \frac{ds}{dN} e^{N(s)} \frac{\partial \zeta}{\partial N} = \int_{N_*}^N dN (-\tau_* e^{-N}) e^{N(s)} \frac{\partial \zeta}{\partial N} \\ &= -\tau_* \int_{N(\tau_*)}^{N(\tau)} dN \frac{\partial \zeta}{\partial N} = -\tau_*(\zeta(\tau, \mathbf{x}) - \zeta(\tau_*, \mathbf{x})). \end{aligned} \quad (6.139)$$

Thus, the peculiar velocity potential (6.134) reduces remarkably to:

$$\mathcal{F}(\tau, \mathbf{x}) = \tau(C_{\mathcal{F}}(\mathbf{x}) + \zeta(\tau, \mathbf{x}) - \zeta(\tau_*, \mathbf{x})). \quad (6.140)$$

Depending on the background behavior, the curvatures modes will evolve differently after horizon crossing; for attractor models if the modes are adiabatic they will freeze and therefore conserved [8]. This fact allow us to make robust prediction connecting inflationary models and observations. Thus for this scenario we know $\partial_0 \zeta_L(\tau, \mathbf{x}) \approx 0$, then $\zeta_L(\tau, \mathbf{x}) \approx \zeta_L(\tau_*, \mathbf{x})$ so the peculiar velocity potential becomes,

$$\mathcal{F}(\tau, \mathbf{x}) = \tau C_{\mathcal{F}}(\mathbf{x}) \quad (6.141)$$

and therefore the peculiar velocity,

$$V^i(\tau, \mathbf{x}) = \tau \partial^i (C_{\mathcal{F}}(\mathbf{x}) - \zeta_L(\tau, \mathbf{x})) \quad (6.142)$$

where we have ignored $\mathcal{O}(\varepsilon)$ terms. Since by construction we know that $C_{\mathcal{F}}$ is composed only by long modes, we at least know that it will be suppressed k_L , in particular its divergence(that influences \mathcal{H}_F):

$$\partial_i V^i(\tau, \mathbf{x}) = -\tau \partial^2 \zeta_L(\tau, \mathbf{x}) \propto k_L^2 \zeta_L(\tau, \mathbf{x}) \quad (6.143)$$

is k_L^2 suppressed, then terms that involve the divergence of the peculiar velocity can be safely ignored for attractor inflation.

On the other hand, for non-attractor inflation the peculiar velocity V^i becomes:

$$\begin{aligned} V^i(\tau, \mathbf{x}) &= \partial^i \mathcal{F} - N^i \\ &= \tau \partial^i (-\zeta(\tau_*, \mathbf{x}) + C_{\mathcal{F}}(\mathbf{x})) - \partial^i (\varepsilon \partial^{-2} \partial_0 \zeta(\tau, \mathbf{x})) \end{aligned} \quad (6.144)$$

whose divergence is:

$$\partial_i V^i(\tau, \mathbf{x}) = \tau \partial^2 (-\zeta(\tau_*, \mathbf{x}) + C_{\mathcal{F}}(\mathbf{x})) - \varepsilon \partial_0 \zeta(\tau, \mathbf{x}). \quad (6.145)$$

thus, the first term is k_L^2 suppressed, whereas the second $\varepsilon \propto a^{-6}$ and $\partial_0 \zeta \propto a^2$. So the divergence of the peculiar velocity potential is suppressed for this scenario too.

Conformal Scale Factor

In this section, we will derive a first order expression for the ratio between the local scale factor, a_F/a , and the global scale factor along the geodesic, this expression can be easily

be extended to points outside the central geodesic inside the local patch. We can find the local expansion rate as the fractional volume change that an inertial observer experiences along its world-line in a perturbed expanding spacetime. Physically, they cannot distinguish between long modes, ζ_L , of a wavelength longer than the sound horizon and the background, therefore, these observer infers a different and effective Hubble ratio given by (6.28):

$$H_F(\bar{\tau}) = \frac{1}{3} \nabla_\mu U^\mu. \quad (6.146)$$

Expanding the divergence of the 4-velocity:

$$\nabla_\mu U^\mu = \frac{1}{3} (\partial_\mu U^\mu + \Gamma_{\mu\lambda}^\mu U^\lambda) = \frac{3}{a} \mathcal{H} + \frac{3}{2} \frac{\mathcal{H}}{a} h_{00} + \frac{h'}{2a} + \frac{1}{a} \partial_j V^j, \quad (6.147)$$

using $h = \delta^{ij} h_{ij} = 2\zeta(\tau, x) \delta^{ij} \delta_{ij} = 6\zeta(\tau, x)$ and $h_{00} = -2\partial_0 \zeta / \mathcal{H}$, the above expression reduces to:

$$\nabla_\mu U^\mu = \frac{1}{a} (3\mathcal{H} + \partial_j V^j). \quad (6.148)$$

As we have seen in the previous subsection the peculiar velocity contribution is strongly suppressed, this physically can be viewed as long wavelength modes(which are almost constant) can not induce substantial deviation on an inertial observer, because their spatial gradients are very small, so safely we can ignore them. Nevertheless, in [122], the authors considered the local influence of long modes on short ones as an effective curved universe with $k \neq 0$, to derive the correction to Maldacena's consistency relation at 'order q^2 '. It is interesting to keep tracking those terms since they potentially could induce a complete f_{NL} vanishing, beyond the linear order. We left the impact of these terms for future work.

Backing to work, we need an expression for the modified scale factor. Let us consider the time derivative of the ratio $a_F(\bar{\tau})/a(\tau)$:

$$\frac{d}{d\tau} \left(\frac{a_F(\bar{\tau})}{a(\tau)} \right) = \frac{1}{a(\tau)} \frac{da_F(\bar{\tau})}{d\tau} + a_F(\bar{\tau}) \frac{da^{-1}(\tau)}{d\tau} = \frac{1}{a(\tau)} \frac{da_F(\bar{\tau})}{d\bar{\tau}} \frac{d\bar{\tau}}{d\tau} - \frac{a_F(\bar{\tau})}{a^2(\tau)} \frac{da(\tau)}{d\tau},$$

thus this slightly deviation becomes,

$$\frac{d \ln a_F(\bar{\tau})/a(\tau)}{d\tau} = \left(-\mathcal{H}(\tau) + \mathcal{H}_F(\bar{\tau}) \frac{d\bar{\tau}}{d\tau} \right). \quad (6.149)$$

It is easy to see that in the unperturbed universe limit, one recovers zero as expected. Finally, we must find $\frac{d\bar{\tau}}{d\tau}$, this can be achieved from the invariance of the line element between global and CFC coordinates along the central geodesic:

$$ds^2 = a^2(\tau) (\eta_{\mu\nu} + h_{\mu\nu}) dx^\mu dx^\nu = a_F^2(\bar{\tau}) \eta_{\mu\nu} d\bar{x}^\mu d\bar{x}^\nu. \quad (6.150)$$

By construction, an observer inertial only experience a temporal displacement in the CFC frame, thus $U^\mu d\bar{\tau} = (d\bar{\tau}, 0, 0, 0)$. Therefore the line element:

$$a^2(\tau) (\eta_{00} + h_{00}) d\tau^2 = a_F^2(\bar{\tau}) \eta_{00} d\bar{\tau}^2, \quad (6.151)$$

where h_{00} receives a contribution from long modes only, and extra contribution on l.h.s. have been neglected because they are second-order contributions. This implies

$$\frac{d\bar{\tau}}{d\tau} = \frac{a(\tau)}{a_F(\bar{\tau})} \left(1 - \frac{1}{2} h_{00}(\tau, \mathbf{x}_c) \right), \quad (6.152)$$

replacing in (6.149)

$$\frac{d \ln a_F(\bar{\tau})/a(\tau)}{d\tau} = \left[-\mathcal{H}(\tau) + \mathcal{H}_F(\bar{\tau}) \frac{a(\tau)}{a_F(\bar{\tau})} \left(1 - \frac{1}{2} h_{00}(\tau, \mathbf{x}_c) \right) \right] \quad (6.153)$$

using (6.147) in the above expression we find:

$$\frac{d \ln a_F(\bar{\tau})/a(\tau)}{d\tau} = \left(-\mathcal{H} \frac{h_{00}(\tau, \mathbf{x}_c)}{2} + \frac{1}{3} \partial_j V^j(\tau, \mathbf{x}_c) \right). \quad (6.154)$$

Which is a reduced expression for eq. (2.15) of [1]. Integrating the above equation:

$$\frac{a_F(\bar{\tau})}{a(\tau)} = \exp \left(C_{\Delta a}(\mathbf{x}_c) + \int_{\tau_*}^{\tau} ds \left(-\frac{1}{2} \mathcal{H}(\tau) h_{00}(\tau, \mathbf{x}_c) + \frac{1}{3} \partial_j V^j(\tau, \mathbf{x}_c) \right) \right), \quad (6.155)$$

where $C_{\Delta a}(\mathbf{x}_c)$ is a time independent field. To reduce the above expression, in the comoving gauge we have $h_{00} = -2\partial_0 \zeta/\mathcal{H}$ while the second term is k_L^2 suppressed, so the above expression becomes:

$$a_F(\bar{\tau}) = a(\tau) \exp \left(C_{\Delta a}(\mathbf{x}_c) + \int_{\tau_*}^{\tau} ds \partial_0 \zeta(s, \mathbf{x}_c) \right) \quad (6.156)$$

$$= a(\tau) (1 + \zeta(\tau, \mathbf{x}_c) - \zeta(\tau_*, \mathbf{x}_c) + C_{\Delta a}(\mathbf{x}_c) + \dots). \quad (6.157)$$

We realize that the scale factor shift is:

$$\Delta \left(\frac{a_F(\bar{\tau})}{a(\tau)} \right) = \frac{a_F(\bar{\tau})}{a(\tau)} - 1 = (\zeta(\tau, \mathbf{x}_c) - \zeta(\tau_*, \mathbf{x}_c) + C_{\Delta a}(\mathbf{x}_c)). \quad (6.158)$$

As we will see, the inflationary background behaviour determines the value of $C_{\Delta a}(\mathbf{x}_c)$.

Time shift ξ^0

Finally one needs an equation to determine the time shift ξ^0 induced by the map from the comoving global coordinates to the observer coordinates. This time shift not only affects the proper time that the inertial observer describes its neighborhood, but also the scale factor in a determined way. To compute this quantity one start with the global time dependence in terms of the Fermi conformal time, from (6.122) we know that the time shift is defined as:

$$\Delta\tau(\bar{\tau}, \bar{\mathbf{x}}_c) = C_{\Delta\tau}(\bar{\mathbf{x}}_c) + \int_{\bar{\tau}_*}^{\bar{\tau}} d\bar{s} \left[\frac{a_F}{a}(\bar{s}, \bar{\mathbf{x}}_c) - 1 - N_1(\bar{s}, \bar{\mathbf{x}}_c) \right].$$

Integrating this expression:

$$\begin{aligned} \Delta\tau(\bar{\tau}, \bar{\mathbf{x}}_c) &= C_{\Delta\tau}(\bar{\mathbf{x}}_c) + \int_{\bar{\tau}_*}^{\bar{\tau}} d\bar{s} \left(\zeta_L(\bar{s}, \bar{\mathbf{x}}_c) - \zeta_L(\bar{\tau}_*, \bar{\mathbf{x}}_c) + C_{\Delta a}(\bar{\mathbf{x}}_c) - \frac{\partial_0 \zeta_L(\bar{s}, \bar{\mathbf{x}}_c)}{\mathcal{H}} \right) \\ &= C_{\Delta\tau}(\bar{\mathbf{x}}_c) + \bar{\tau} C_{\Delta a}(\bar{\mathbf{x}}_c) \Big|_{\bar{\tau}_*}^{\bar{\tau}} + \bar{\tau} \zeta(\bar{\tau}, \bar{\mathbf{x}}_c) \Big|_{\bar{\tau}_*}^{\bar{\tau}} - \bar{\tau} \zeta(\bar{\tau}_*, \bar{\mathbf{x}}_c) \Big|_{\bar{\tau}_*}^{\bar{\tau}} \end{aligned} \quad (6.159)$$

Finally at the central geodesic $\bar{\mathbf{x}}_c$ we find

$$\Delta\tau(\bar{\tau}, \bar{\mathbf{x}}_c) = \bar{\tau}(\zeta(\bar{\tau}, \bar{\mathbf{x}}_c) - \zeta(\bar{\tau}_*, \bar{\mathbf{x}}_c)) + C_{\Delta\tau}(\bar{\mathbf{x}}_c) + C_{\Delta a}(\bar{\mathbf{x}}_c)(\bar{\tau} - \bar{\tau}_*). \quad (6.160)$$

This time shift is completely generic under the inflationary assumptions (whether SR or USR), but just valid along the central geodesic points $\bar{\mathbf{x}}_c$, however, it can easily be extended to its local neighbourhood around it by incorporating the next order time shift contributions, $\xi_L^{0(1)}(\bar{\tau}, \bar{\mathbf{x}})$, as gradients long wavelength modes, by doing so, we are able to recover the full-time shift map up to k_L^2 corrections. Adding its leading order corrections,

$$\begin{aligned}\Delta\tau(\bar{\tau}, \bar{\mathbf{x}}) &= \xi_L^0(\bar{\tau}, \bar{\mathbf{x}}) = \xi_L^{0(0)}(\bar{\tau}, \bar{\mathbf{x}}) + \xi_L^{0(1)}(\bar{\tau}, \bar{\mathbf{x}}) \\ &= \Delta\tau(\bar{\tau}, \bar{\mathbf{x}}_c) + \bar{\mathbf{x}}^i \partial_i \mathcal{F}(\bar{\tau}, \bar{\mathbf{x}}_c)\end{aligned}\quad (6.161)$$

From (6.140) we know $\partial_i \mathcal{F} = \bar{\tau} [\partial_i \zeta_L(\bar{\tau}, \bar{\mathbf{x}}_c) - \partial_i \zeta_L(\bar{\tau}_*, \bar{\mathbf{x}}_c) + \partial_i C_{\mathcal{F}}(\bar{\mathbf{x}}_c)]$, then the time shift becomes

$$\begin{aligned}\Delta\tau(\bar{\tau}, \bar{\mathbf{x}}) &= C_{\Delta\tau}(\bar{\mathbf{x}}_c) + C_{\Delta a}(\bar{\mathbf{x}}_c)(\bar{\tau} - \bar{\tau}_*) + \bar{\tau} (\zeta(\bar{\tau}, \bar{\mathbf{x}}_c) - \zeta(\bar{\tau}_*, \bar{\mathbf{x}}_c)) + \\ &\quad \bar{\mathbf{x}}^i \bar{\tau} [\partial_i \zeta_L(\bar{\tau}, \bar{\mathbf{x}}_c) - \partial_i \zeta_L(\bar{\tau}_*, \bar{\mathbf{x}}_c) + \partial_i C_{\mathcal{F}}(\bar{\mathbf{x}}_c)].\end{aligned}\quad (6.162)$$

Given this structure, one notices that the gradients can be resummed into the curvature perturbation:

$$\Delta\tau(\bar{\tau}, \bar{\mathbf{x}}) = \bar{\tau} (\zeta_L(\bar{\tau}, \bar{\mathbf{x}}) - \zeta_L(\bar{\tau}_*, \bar{\mathbf{x}})) + C_{\Delta\tau}(\bar{\mathbf{x}}_c) + C_{\Delta a}(\bar{\mathbf{x}}_c)(\bar{\tau} - \bar{\tau}_*) + \bar{\tau} \bar{\mathbf{x}}^i \partial_i C_{\mathcal{F}}(\bar{\mathbf{x}}_c) \quad (6.163)$$

notice that at this point we have not assumed anything about the 3 remnant fields that aroused from the integrations of equations (6.140), (6.156), (6.163), their fixing depends on the inflationary conditions whether is SR, USR or a combination of both as a phase transition between them and the physical flatness requirement that an inertial observer experience along the central geodesic.

Curvature Modes Transformation

Until now we have kept the discussion quite general: just a small diffeomorphism from the comoving coordinates to the observer coordinates, nevertheless, we have not concerned yet in quantities that are projected in observations, such a curvature perturbation. We start from the transformation of curvature perturbation ζ . We consider a coordinate transformation from $\mathbf{x} \rightarrow \bar{\mathbf{x}}$ (that in the case of attractor inflation does not change the hypersurfaces of constant τ). However, when the time coordinate is involved it is better to start from the definition of ζ in slices of spacetime on the surfaces Σ_τ [128], that by definition are related to the local number of e-folds $\delta N(x)$.

$$\zeta = \frac{\log \det(g_{ij}/a^2)}{6} \quad (6.164)$$

where g_{ij} is the induced metric on Σ_τ . We can use this formal definition to see how ζ transform under a small coordinate change, $x^\mu \rightarrow \bar{x}^\mu = x^\mu - \xi^\mu$. Denoting with a bar the transformed metric at leading order in ξ we have:

$$g_{\mu\nu} \rightarrow \bar{g}_{\mu\nu} = g_{\mu\nu} + 2\nabla_{(\mu} \xi_{\nu)} = g_{\mu\nu} + g_{\nu\rho} \nabla_\mu \xi^\rho + g_{\mu\rho} \nabla_\nu \xi^\rho, \quad (6.165)$$

so that:

$$\bar{g}_{ij}/a^2 = \delta_{ij} + \underbrace{(e^{2\xi} - 1)}_{=\Delta g} \delta_{ij} + 2\nabla_{(i} \xi_{j)}/a^2. \quad (6.166)$$

Using the relation $\log \det = \text{Tr} \log$, and working at quadratic order in perturbations,

$$\log(\bar{g}_{ij}/a^2) = 2\zeta\delta_{ij} + 2\nabla_{(i}\xi_{j)}/a^2 - 2\zeta(\partial_i\xi_j + \partial_j\xi_i + 2\mathcal{H}\xi^0\delta_{ij}). \quad (6.167)$$

We need now is an expression for $\nabla_{(i}\xi_{j)}/a^2$. First of all we know that:

$$\nabla_i\xi_j/a^2 = \partial_i\xi_j + 2\zeta\partial_i\xi_j + N_j\partial_i\xi^0 + g_{j\rho}\Gamma_{i\rho}^\rho\xi^\sigma/a^2, \quad (6.168)$$

with the following relevant contractions:

$$g_{jk}\Gamma_{il}^k\xi^l/a^2 = \delta_{jk}\Gamma_{il}^k\xi^l = -\mathcal{H}N_j\xi_i + \delta_{ij}\xi^l\partial_l\zeta - 2\xi_{[i}\partial_{j]}\zeta, \quad (6.169)$$

$$g_{jk}\Gamma_{i0}^k\xi^0/a^2 = e^{2\zeta}\delta_{jk}\Gamma_{i0}^k\xi^0 = \mathcal{H}\delta_{ij}\xi^0 + 2\mathcal{H}\zeta\xi^0\delta_{ij} + \xi^0\partial_0\zeta\delta_{ij} - \partial_{[i}N_{j]}\xi^0, \quad (6.170)$$

$$g_{j0}\Gamma_{i0}^k\xi^\sigma/a^2 = N_j\Gamma_{i0}^k\xi^\sigma = N_j\Gamma_{ik}^0\xi^k = N_j\mathcal{H}\delta_{ik}\xi^k = \mathcal{H}\xi_iN_j \quad (6.171)$$

Replacing in (6.167)

$$\log(\bar{g}_{ij}/a^2) = 2\zeta\delta_{ij} + 2\partial_{(i}\xi_{j)} + 2\mathcal{H}\xi^0\delta_{ij} + 2N_{(i}\partial_{j)}\xi^0 + 2\xi^\mu\partial_\mu\zeta\delta_{ij} + ..., \quad (6.172)$$

finally taking the trace, we obtain:

$$\bar{\zeta} = \frac{\text{Tr} \log(\bar{g}_{ij}/a^2)}{6} = \zeta + \frac{\partial_i\xi^i}{3} + \mathcal{H}\xi^0 + \frac{N^i\partial_i\xi^0}{3} + \xi^\mu\partial_\mu\zeta. \quad (6.173)$$

Splitting both ζ and $\bar{\zeta}$ into its long and short contribution, and assigning the long wavelength prescription $\xi^\mu = \xi_L^\mu$, we obtain the effective transformation for each modes,

$$\bar{\zeta}_L = \zeta_L + \frac{\partial_i\xi_L^i}{3} + \mathcal{H}\xi_L^0, \quad \bar{\zeta}_s = \zeta_s + \frac{N_s^i\partial_i\xi_L^0}{3} + \xi_L^\mu\partial_\mu\zeta_s, \quad (6.174)$$

where $N_i = N_i(\zeta)$ is the linear shift constraint. The above expression illustrates that the short modes transform effectively like a scalar field, plus small correction that vanishes for attractor inflation. As we will see in the forthcoming sections, this is due to the long modes gradients, they go to zero on super-Hubble scales, additionally, this term does not play any role in both the power spectrum(it cancels by symmetry) and the bispectrum(low order corrections).

Short Modes Transformation

As we have seen in the previous subsection, the short modes of curvature in CFC are represented by (6.174):

$$\bar{\zeta}_s(\bar{x}) = \zeta_s(\bar{x}) + \xi_L^\mu(\bar{x})\partial_\mu\zeta_s(\bar{x}) + \frac{1}{3}N_s^i(\bar{x})\partial_i\xi_L^0(\bar{x}) \quad (6.175)$$

$$= \zeta_s(x(\bar{x})) + \frac{1}{3}N_s^i(\bar{x})\partial_i\xi_L^0(\bar{x}). \quad (6.176)$$

So they transform effectively as a scalar field, plus a small correction generated by the time coordinate shift ξ^0 that couples to the time shift function N^i associated to the short modes. Notice that this small correction is k_L suppressed and as we will see do not contribute to the two-point correlation function. Explicitly the second term reads,

$$\partial_k\xi_L^0(\bar{\tau}, \bar{\mathbf{x}}) = \partial_k(\Delta\tau(\bar{\tau}, \bar{\mathbf{x}}_c) + \partial_i\mathcal{F}(\bar{\tau}, \bar{\mathbf{x}}_c)\bar{x}^i) = \partial_i\mathcal{F}(\bar{\tau}, \bar{\mathbf{x}}_c). \quad (6.177)$$

Which at first order, it is just the peculiar velocity gradient at $\bar{\mathbf{x}}_c$.

Long Modes Transformation

We start transforming the long wavelength curvature modes according to (6.174):

$$\bar{\zeta}_L(\bar{x}) = \zeta_L(\bar{x}) + \frac{1}{3} \partial_i \xi_L^i(\bar{x}) + \mathcal{H} \xi_L^0(\bar{x}). \quad (6.178)$$

From (6.127) we are able to identify the small temporal and spatial coordinate shift induced by the long wavelength modes as

$$\xi_L^0(\bar{\mathbf{x}}) = \Delta\tau(\bar{\tau}, \bar{\mathbf{x}}_c) + \partial_i \mathcal{F}(\bar{\tau}, \bar{\mathbf{x}}_c) \bar{x}^i, \quad (6.179)$$

$$\xi_L^i(\bar{\mathbf{x}}) = \int_{\bar{\tau}_*}^{\bar{\tau}} ds V^i(s, \bar{\mathbf{x}}_c) + \left[\frac{a_F}{a}(\bar{\tau}, \bar{\mathbf{x}}_c) - 1 - \zeta_L(\bar{\tau}, \bar{\mathbf{x}}_c) \right] \bar{x}^i - \frac{1}{2} \bar{\Gamma}_{jk}^i(\bar{\tau}, \bar{\mathbf{x}}_c) \bar{x}^j \bar{x}^k, \quad (6.180)$$

taking the spatial divergence and ignoring the peculiar velocity contribution, V^i , because is k_L^2 suppressed. The divergence of the spatial shift becomes,

$$\partial_i \xi_L^i(\bar{\mathbf{x}}) = 3 \left[\frac{a_F}{a}(\bar{\tau}, \bar{\mathbf{x}}_c) - 1 - \zeta_L(\bar{\tau}, \bar{\mathbf{x}}_c) \right] - 3(\bar{x}^k \partial_k \zeta_L(\bar{\mathbf{x}}) + \mathcal{H} \partial_k \mathcal{F}(\bar{\tau}, \bar{\mathbf{x}}_c) \bar{x}^k), \quad (6.181)$$

expanding long modes around the central geodesic $\zeta_L(\bar{\tau}, \bar{\mathbf{x}}) = \zeta_L(\bar{\tau}, \bar{\mathbf{x}}_c) + \bar{x}^i \partial_i \zeta_L(\bar{\tau}, \bar{\mathbf{x}}_c)$, and replacing it into (6.178),

$$\begin{aligned} \bar{\zeta}_L(\bar{x}) &= \zeta_L(\bar{\tau}, \bar{\mathbf{x}}_c) - \zeta_L(\bar{\tau}_*, \bar{\mathbf{x}}_c) + C_{\Delta a}(\bar{\mathbf{x}}_c) + \mathcal{H}(C_{\Delta\tau}(\bar{\mathbf{x}}_c) + C_{\Delta a}(\bar{\mathbf{x}}_c)(\bar{\tau} - \bar{\tau}_*) + \\ &\quad \bar{\tau}(\zeta(\bar{\tau}, \bar{\mathbf{x}}_c) - \zeta(\bar{\tau}_*, \bar{\mathbf{x}}_c))) + \mathcal{O}(\partial_i \partial_j \zeta_L(\bar{x})) \\ \bar{\zeta}_L(\bar{x}) &= \mathcal{H}(C_{\Delta\tau}(\bar{\mathbf{x}}_c) - \bar{\tau}_* C_{\Delta a}(\bar{\mathbf{x}}_c)) + \mathcal{O}(\partial_i \partial_j \zeta_L(\bar{x})). \end{aligned} \quad (6.182)$$

The above expression corresponds to the curvature of long modes in the CFC around the central geodesic. It is worth noting the consistency of this result since the physical ζ_L has been entirely removed up to second order in ζ via coordinate transformation modulo fields that depend on USR or SR condition. Remarkably this result generalizes the expression (6) in the early work [3], though a full and explicit demonstration, in which not only a spatial diffeomorphism is considered, but also generic one that is extended to the time coordinate.

Despite having analytical expressions for both short and long modes, we have not imposed any condition on the residual fields $C_{\Delta\tau}(\bar{\mathbf{x}}_c), C_{\Delta a}(\bar{\mathbf{x}}_c)$, which are just a combination of time-independent fields that came from integrating the equations for the scale factor a_F and the time shift ξ^0 , these quantities are determined by the condition that an inertial observer can not notice the gravitational background from long wavelengths ζ_L , that is to say, in the CFC frame the metric must be Minkowski, with their conformal Christoffel symbols (and their gradients) equals to zero, which is the mathematically equivalent to the statement that metric corrections start at quadratic order in the conformal Riemann tensor. Given this condition the long modes vanish along the central geodesic $\bar{\zeta}_L(\bar{\tau}, \bar{\mathbf{x}}) = 0$, this implies that in order to remove them completely up to second order inside the patch we require:

$$C_{\Delta\tau}(\bar{\mathbf{x}}_c) - \bar{\tau}_* C_{\Delta a}(\bar{\mathbf{x}}_c) = 0, \quad (6.183)$$

thus,

$$\bar{\zeta}_L(\bar{\mathbf{x}}) = \mathcal{O}(\bar{\mathbf{x}}^i \bar{\mathbf{x}}^j \partial_i \partial_j \zeta_L(\bar{\mathbf{x}}_c)) = \text{'curvature and tidal effects'}. \quad (6.184)$$

In effect, the long wavelength modes are subtracted completely up to second order in derivatives, inside the patch, which is one of the results of [3]. Additionally, the above physical requirement imposes constraints on the time shift and the local scale factor (6.187) that acquire the simple form:

$$\Delta\tau(\bar{\tau}, \bar{\mathbf{x}}) = \bar{\tau}(\zeta_L(\bar{\tau}, \bar{\mathbf{x}}) - \zeta_L(\bar{\tau}_*, \bar{\mathbf{x}})) + \bar{\tau}(C_{\Delta a}(\bar{\mathbf{x}}_c) + \bar{\mathbf{x}}^i \partial_i C_{\mathcal{F}}(\bar{\mathbf{x}}_c)) \quad (6.185)$$

$$a_F(\bar{\tau}) = a(\bar{\tau})(1 + \zeta_L(\bar{\tau}, \bar{\mathbf{x}}_c) - \zeta_L(\bar{\tau}_*, \bar{\mathbf{x}}_c) + C_{\Delta a}(\bar{\mathbf{x}}_c)) \quad (6.186)$$

where we used that the argument function change, $\mathbf{x} \rightarrow \bar{\mathbf{x}}$, induces an irrelevant higher order correction. The above expression is a reduction of (6.163) and (6.156) after the induced flatness condition for the CFC frame and the remaining residual field $C_{\Delta a}(\bar{\mathbf{x}})$ inside in both of them, depends on the single field background, specifically on the property whether its is attractor or not. For attractor inflation it is known that the superhorizon modes 'freezes' or they do not experience a considerable growth, then $\zeta_L(\bar{\tau}, \bar{\mathbf{x}}) \approx \zeta_L(\bar{\tau}_*, \bar{\mathbf{x}})$, therefore for fixing the CFC completely only $C_{\Delta a}(\bar{\mathbf{x}}_c)$ needs to be set. We observe that the remaining term for attractor inflation just correspond to a constant shift in the magnitud of the scale factor, therefore, it does not play any role, so it can be chosen such that, $C_{\Delta a}(\bar{\mathbf{x}}) = C_{\mathcal{F}}(\bar{\mathbf{x}}) = 0$, in consequence:

$$a_F(\bar{\tau}) = a(\tau), \quad \Delta\tau(\bar{\tau}, \bar{\mathbf{x}}) = \bar{\tau}\mathcal{O}(\partial_i \partial_j \zeta_L(\bar{\mathbf{x}}_c)), \quad (6.187)$$

for single field inflationary attractor models. This result have been obtained in [1] [3] [114]. On the other hand, for a non-attractor inflation one can set $C_{\Delta a}(\bar{\mathbf{x}}) = \zeta_L(\bar{\tau}_*, \bar{\mathbf{x}})$ in order to eliminate the gauge mode $\zeta_L(\bar{\tau}_*, \bar{\mathbf{x}})$ (or any arbitrariness in the choice of τ_*), then

$$a_F(\bar{\tau}) = a(\bar{\tau})(1 + \zeta_L(\bar{\tau}, \bar{\mathbf{x}})), \quad \Delta\tau(\bar{\tau}, \bar{\mathbf{x}}) = \bar{\tau}\zeta_L(\bar{\tau}, \bar{\mathbf{x}}) + \bar{\tau}\mathcal{O}(\partial_i \partial_j \zeta_L(\bar{\mathbf{x}}_c)), \quad (6.188)$$

as a consequence, it is obtained $C_{\Delta a}(\bar{\mathbf{x}}) = C_{\mathcal{F}}(\bar{\mathbf{x}}) = C_{\Delta\tau}(\bar{\mathbf{x}})/\bar{\tau}_* = \zeta_L(\bar{\tau}_*, \bar{\mathbf{x}})$, for attractor and non-attractor inflation due to ζ_L removal constraint. This was the last choice for residual field setting associated to the time integration of the three differential equations along this computations. This result resembles the equation (17) in [3] as a suggestion for "non-trivial backgrounds".

Second order map reconstruction

Until now we have computed the CFC expansion map recursively up to first order; nevertheless, it is also worth compute this expansion up to second order to incorporate higher order corrections in correlations function, but also the potential underlying non-linear symmetries behind this coordinate transformation. These corrective terms are reached by solving recursively the spatial-like geodesic equations which are contained in the geodesic congruence at a fixed global time in a locality around the central geodesic. Let start with the infinitesimal coordinate transformation (6.129):

$$\tau = \bar{\tau} + \xi_L^0(\bar{\tau}, \bar{\mathbf{x}}), \quad x^i = \bar{x}^i + \xi_L^i(\bar{\tau}, \bar{\mathbf{x}}) \quad (6.189)$$

the time and spatial shift can be expanded according to their spatial coordinate order around $\bar{\mathbf{x}}_c = 0$

$$\xi_L^\mu(\bar{\tau}, \bar{\mathbf{x}}) = \xi_L^{\mu(0)}(\bar{\tau}, \bar{\mathbf{x}}_c) + \xi_L^{\mu(1)}(\bar{\tau}, \bar{\mathbf{x}}) + \xi_L^{\mu(2)}(\bar{\tau}, \bar{\mathbf{x}}) + \dots \quad (6.190)$$

$\Gamma(\eta_{\mu\nu} + h_{\mu\nu})$	$C(a_F^{-1}) + C(a)$
$\bar{\Gamma}_{ij}^k$	$-\partial^k \zeta_L \delta_{ij} + \partial_i \zeta_L \delta_j^k + \partial_j \zeta_L \delta_i^k$
$\bar{\Gamma}_{ij}^0$	$\mathcal{H}(-F^k \delta_{ij} + F_i \delta_j^k + F_j \delta_i^k)$
	$-(\partial_0 \zeta_L + \partial_m V^m / 3) \delta_{ij}$

Table 6.1: In this table we collect the relevant CFC conformal metric Christoffel coefficients from [1]. We separate them into contributions from $\eta_{\mu\nu} + h_{\mu\nu}$ and those from the scale factor a^2/a_F^2 . The terms of the left(right) are useful for (non-)attractor models.

For attractor inflation both scale factor are the same (6.187), therefore, the conformal ratio in (6.158) is 1, as a consequence, the peculiar velocity potential $\partial^k \mathcal{F} = 0$, thus in this scenario the terms in the second column of table (6.1) do not contribute, so their contracted Christoffel symbols $\bar{\Gamma}_{ij}^k(\bar{\tau}, \bar{\mathbf{x}}_c), \bar{\Gamma}_{ij}^0(\bar{\tau}, \bar{\mathbf{x}}_c)$ are:

$$\bar{\Gamma}_{ij}^k(\bar{\tau}, \bar{\mathbf{x}}_c) \bar{x}^i \bar{x}^j = -\partial^k \zeta_L(\bar{\tau}, \bar{\mathbf{x}}_c) \bar{x}^2 + 2\bar{x}^i \partial_i \zeta_L(\bar{\tau}, \bar{\mathbf{x}}_c) \bar{x}^k \quad (6.191)$$

$$\bar{\Gamma}_{ij}^0(\bar{\tau}, \bar{\mathbf{x}}_c) \bar{x}^i \bar{x}^j = -\bar{\tau} \partial_i \partial_j \zeta_L(\bar{\tau}, \bar{\mathbf{x}}_c) \bar{x}^i \bar{x}^j. \quad (6.192)$$

Replacing in (6.129):

$$x^k(\bar{x}) = (1 - \zeta_L(\bar{\tau}, \bar{\mathbf{x}}_c) - \bar{x}^i \partial_i \zeta_L(\bar{\tau}, \bar{\mathbf{x}}_c)) \bar{x}^k + \frac{1}{2} \partial^k \zeta_L(\bar{\tau}, \bar{\mathbf{x}}_c) \bar{x}^2 \quad (6.193)$$

$$x^k(\bar{x}) = (1 - \zeta_L(\bar{\tau}, \bar{\mathbf{x}}_c)) \bar{x}^k + \frac{1}{2} \partial^k \zeta_L(\bar{\tau}, \bar{\mathbf{x}}_c) \bar{x}^2 \quad (6.194)$$

where in the second line the long mode gradient was re-summed. Notice that the above expression displays evidently the local absorption of long wavelength modes in the spatial CFC coordinate. Moreover, and remarkably the shape of the second order expansion of (6.193) (6.195) terms are compatible with dilation and SCT symmetries [116], [117], [120] in the comoving gauge by taking the dilation parameter $\lambda = \zeta_L(\bar{\tau}, \bar{\mathbf{x}}_c)$ and the symmetry generator vector $b^i = \partial^i \zeta_L(\bar{\tau}, \bar{\mathbf{x}}_c)$, when the modes behaves classically and they do not evolve. Finally, resumming the time shift terms, we get,

$$\tau(\bar{x}) = \bar{\tau} \left(1 + \frac{1}{2} \partial_i \partial_j \zeta_L(\bar{\tau}, \bar{\mathbf{x}}_c) \bar{x}^i \bar{x}^j \right). \quad (6.195)$$

In this case, the inertial observer's clock is synchronized only at the central geodesics and increases quadratically as the Hessian of ζ_L for nearby points, which can be completely be ignored(k_L^2 suppressed).

In contrast, for a non-attractor single field scenario the ratio between the two Fermi scale factor differs, and its ratio, a_F/a , is different from the unity, therefore $\partial^k \mathcal{F}$ has to be considered. Using the second column of table (6.1), one sees that the Christoffel symbols related to the spatial coordinate vanishes whereas time do not:

$$\begin{aligned} \bar{\Gamma}_{ij}^k(\bar{\tau}, \bar{\mathbf{x}}_c) \bar{x}^i \bar{x}^j &= (-\partial^k \zeta_L(\bar{\tau}, \bar{\mathbf{x}}_c) \bar{x}^2 + 2\bar{x}^i \partial_i \zeta_L(\bar{\tau}, \bar{\mathbf{x}}_c) \bar{x}^k) \\ &\quad - (-\partial^k \zeta_L(\bar{\tau}, \bar{\mathbf{x}}_c) \bar{x}^2 + 2\bar{x}^i \partial_i \zeta_L(\bar{\tau}, \bar{\mathbf{x}}_c) \bar{x}^k) = 0 \end{aligned} \quad (6.196)$$

$$\bar{\Gamma}_{ij}^0(\bar{\tau}, \bar{\mathbf{x}}_c) \bar{x}^i \bar{x}^j = -\bar{\tau} \partial_i \partial_j \zeta_L(\bar{\tau}, \bar{\mathbf{x}}_c) \bar{x}^i \bar{x}^j, \quad (6.197)$$

gathering the time shift terms altogether, one notice that a resummation is possible again:

$$\tau(\bar{x}) = \bar{\tau} (1 + \zeta_L(\bar{\tau}, \bar{\mathbf{x}}_c) + \bar{x}^i \partial_i \zeta_L(\bar{\tau}, \bar{\mathbf{x}}_c) + \frac{1}{2} \partial_i \partial_j \zeta_L(\bar{\tau}, \bar{\mathbf{x}}_c) \bar{x}^i \bar{x}^j) \quad (6.198)$$

therefore the global coordinates projected onto CFC reads,

$$\tau(\bar{x}) = \bar{\tau}(1 + \zeta_L(\bar{\tau}, \bar{\mathbf{x}})), \quad x^i(\bar{x}) = \bar{x}^i. \quad (6.199)$$

This is analog to the expressions (6.193) (6.195), but the long modes have been absorbed in the time coordinate instead. In consequence, one can obtain the new scale factor for this inflationary scenario as a first order mode expansion induced by the new time foliation,

$$a(\tau) = a(\tau(\bar{x})) = a(\bar{\tau} + \bar{\tau}\zeta_L(\bar{\tau}, \bar{\mathbf{x}})) = a(\bar{\tau})(1 + \mathcal{H}\bar{\tau}\zeta_L(\bar{\tau}, \bar{\mathbf{x}})) = a(\bar{\tau})(1 - \zeta_L(\bar{\tau}, \bar{\mathbf{x}})) \quad (6.200)$$

comparing with (6.188) we recognize:

$$a_F(\bar{\tau}) = a(\bar{\tau}) = a(\tau)(1 + \zeta_L(x)). \quad (6.201)$$

This corresponds to the same scale factor as a function but composed with an advanced or delayed time dictated by the induced time shift. Finally is worth mentioning that due to the smallness coordinate shift, the maps (6.193) (6.195) (6.199) they are easily invertible by just changing the function argument $\bar{x} \rightarrow x$ and most importantly, these type diffeomorphisms are useful to deduce correlation functions through shift symmetries [129] [113]. In previous sections, we showed the explicit mapping for both attractor and non-attractor

	Attractor	Non-attractor
$\xi_L^{0(0)}(\bar{\tau}, \bar{\mathbf{x}})$	0	$\bar{\tau}\zeta_L(\bar{\tau}, \bar{\mathbf{x}}_c)$
$\xi_L^{0(1)}(\bar{\tau}, \bar{\mathbf{x}})$	0	$\bar{\tau}\partial_i\zeta_L(\bar{\tau}, \bar{\mathbf{x}}_c)\bar{x}^i$
$\xi_L^{0(2)}(\bar{\tau}, \bar{\mathbf{x}})$	$\bar{\tau}\frac{1}{2}(\partial_i\partial_j\zeta_L(\bar{\tau}, \bar{\mathbf{x}}_c))\bar{x}^i\bar{x}^j$	$\bar{\tau}\frac{1}{2}(\partial_i\partial_j\zeta_L(\bar{\tau}, \bar{\mathbf{x}}_c))\bar{x}^i\bar{x}^j$
$\xi_L^{i(0)}(\bar{\tau}, \bar{\mathbf{x}})$	0	0
$\xi_L^{i(1)}(\bar{\tau}, \bar{\mathbf{x}})$	$-\zeta_L(\bar{\tau}, \bar{\mathbf{x}}_c)\bar{x}^i$	0
$\xi_L^{i(2)}(\bar{\tau}, \bar{\mathbf{x}})$	$-\partial_j\zeta_L(\bar{\tau}, \bar{\mathbf{x}}_c)\bar{x}^i\bar{x}^j + \frac{1}{2}\partial^i\zeta_L(\bar{\tau}, \bar{\mathbf{x}}_c)\bar{x}^2$	0
$a_F(\bar{\tau})$	$a(\tau)$	$a(\bar{\tau})$
$(\tilde{e}_0)^\mu$	$(1 - \partial_0\zeta_L/\mathcal{H}, V^i)$	$(1 + \zeta_L - \partial_0\zeta_L/\mathcal{H}, V^i)$
$(\tilde{e}_j)^\mu$	$(-\partial_j\zeta_L/\mathcal{H}, (1 - \zeta_L)\delta_j^i)$	$(-\partial_j\zeta_L/\mathcal{H}, \delta_j^i)$

Table 6.2: Results: this is a summary of the derived perturbative quantities for the CFC construction evaluated at the central geodesic. All the geometrical objects of interest are displayed here; in particular, notice the tetrad vectors for both types of scenarios in which the unobservable long modes have been absorbed either in the spatial components or the temporal components. In the last two lines the coordinates $(\bar{\tau}, \bar{\mathbf{x}}_c)$ was omitted for brevity.

scenarios. The physical interpretation of the induced CFC is different for each type of inflationary model. For non-attractor inflation, it is better redefine the comoving time slice for one that a inertial observed experiences, since the long modes keep evolving in time, so they effectively can be absorbed in another time varying function such as the scale factor as a suitable option leaving the spatial map intact. Schematically, if we start with a perturbed universe: $ds^2 = a^2(\tau) [-(d\tau)^2 + (1 + 2\zeta_L(x))(dx)^2]$. This can be arranged to $ds^2 = a^2(\tau)(1 + 2\zeta_L(x)) [-(1 - 2\zeta_L(x))(d\tau)^2 + (dx)^2]$ as the same manner for attractor case, moreover, one can locally absorb the long wavelength mode around \mathbf{x}_c by defining a new

time foliation, $d\bar{\tau} = (1 - \zeta_L(x))d\tau$, consequently, the scale factor transform under this time shift as $a(\tau + \Delta\tau) = a(\tau)(1 + \mathcal{H}\Delta\tau)$ this implies that $a(\tau(x)) = a(\bar{\tau})(1 - \zeta_L(\bar{x}))$. Therefore, if we ignore $\mathcal{O}(\zeta_L^2)$ corrections the line element in this new set of coordinates becomes $ds^2 = a^2(\bar{\tau})[-(d\bar{\tau})^2 + (d\bar{\mathbf{x}})^2]$ (conformally flat).

On the other hand, when inflation has reached an attractor phase(or simply attractor scenario) the modes superhorizon modes change their time behaviour and finally freeze thus conserved. Hence, the suitable alternative is a spatial diffeomorphism keeping the time component intact, $d\tau = d\bar{\tau}$. Qualitatively, if we start with a perturbed metric: $ds^2 = a^2(\tau)[- (d\tau)^2 + (1 + 2\zeta_L(x))(d\mathbf{x})^2]$ then the long wavelength perturbations can be absorbed by defining a new spatial coordinate, such as $d\bar{\mathbf{x}} = (1 + \zeta_L(x))d\mathbf{x}$. In consequence, the metric becomes conformally flat, $ds^2 = a^2(\bar{\tau})[-(d\bar{\tau})^2 + (d\bar{\mathbf{x}})^2]$.

6.7 Power Spectrum Of Short Modes in CFC

Given the last expression for the coordinate time shift, now we know an analytic expression for the short modes in CFC, using this, we proceed to compute the correlation function of the short modes.

$$\begin{aligned} \langle \bar{\zeta}_s(\bar{x}_2)\bar{\zeta}_s(\bar{x}_1) \rangle &= \left\langle \left[\zeta_s(\bar{x}_1) + \frac{1}{3}N_s^i(x(\bar{x}_1))\partial_i\xi_l^0(\bar{x}_1) \right] \left[\zeta_s(\bar{x}_2) + \frac{1}{3}N_s^i(x(\bar{x}_2))\partial_i\xi_l^0(\bar{x}_2) \right] \right\rangle \\ &= \langle \zeta_s(x_2)\zeta_s(x_1) \rangle + \frac{1}{3}\langle \zeta_s(x_1)N_s^i(x(\bar{x}_2)) \rangle \partial_i\xi_l^0(\bar{x}_2) + \frac{1}{3}\langle \zeta_s(x_2)N_s^i(x(\bar{x}_1)) \rangle \partial_i\xi_l^0(\bar{x}_1) + \dots \\ &= \langle \zeta_s(x_2)\zeta_s(x_1) \rangle + \frac{1}{3}\langle \zeta_s(x_1)N_s^i(x(\bar{x}_2)) \rangle F_i(\bar{\tau}, \bar{x}_c) + \frac{1}{3}\langle \zeta_s(x_2)N_s^i(x(\bar{x}_1)) \rangle F_i(\bar{\tau}, \bar{x}_c) + \dots \\ &= \langle \zeta_s\zeta_s \rangle(\tau, \mathbf{r}) + \frac{1}{3}F_i(\bar{\tau}, \bar{\mathbf{x}}_c)\langle \zeta_s N_s^i \rangle(\tau, -\mathbf{r}) + \frac{1}{3}F_i(\bar{\tau}, \bar{\mathbf{x}}_c)\langle \zeta_s N_s^i \rangle(\tau, \mathbf{r}) + \dots \end{aligned} \quad (6.202)$$

The time shift in the comoving gauge has the form: $N^i = \partial^i\psi = \partial^i(-\frac{\zeta}{\mathcal{H}} + \varepsilon\partial^{-2}\partial_0\zeta)$, then, its correlator with the short modes is,

$$\begin{aligned} \langle \zeta_s(\mathbf{x}_1)N_s^i(\mathbf{x}_2) \rangle &= \frac{1}{(2\pi)^3} \int d^3k e^{i\mathbf{k}(\mathbf{x}_1-\mathbf{x}_2)} ik^i \zeta(\mathbf{k})\psi(\mathbf{k}) \\ &= -\frac{1}{(2\pi)^3} \int d^3k e^{i\mathbf{k}(\mathbf{x}_2-\mathbf{x}_1)} ik^i \zeta(\mathbf{k})\psi(\mathbf{k}) \\ &= -\langle \zeta_s(\mathbf{x}_2)N_s^i(\mathbf{x}_1) \rangle. \end{aligned} \quad (6.203)$$

which implies the parity property $\langle \zeta_s N_s^i \rangle(-\mathbf{r}) = -\langle \zeta_s N_s^i \rangle(\mathbf{r})$. Therefore, the two last term of (6.202) cancel each other exactly, as a consequence, the correlation function for short modes transform effectively as a scalar field for both SR and USR inflationary models under a small induced diffeomorphism:

$$\langle \bar{\zeta}_s(\bar{x}_2)\bar{\zeta}_s(\bar{x}_1) \rangle = \langle \zeta_s(x_2)\zeta_s(x_1) \rangle = \langle \zeta_s\zeta_s \rangle(\tau, \mathbf{r}), \quad (6.204)$$

more explicitly, by expanding the r.h.s. of (6.204):

$$\langle \zeta_s\zeta_s \rangle(\tau, \mathbf{r}) = \langle \zeta_s\zeta_s \rangle(\bar{\tau}, \bar{\mathbf{r}}) + \xi^\mu(\bar{\tau}, \bar{\mathbf{r}})\partial_\mu \langle \zeta_s\zeta_s \rangle(\bar{\tau}, \bar{\mathbf{r}}) \quad (6.205)$$

where the global coordinates were expanded in terms of CFC $r^i = \bar{r}^i + \xi^i(\bar{\tau}, \bar{\mathbf{r}})$, $\tau = \bar{\tau} + \xi^0(\bar{\tau}, \bar{\mathbf{r}})$. Moreover, it is useful expand the coordinate shifts order by order, this separation allows us visualize each contribution of CFC coordinate expansion in a clear manner,

$$\begin{aligned}\langle \bar{\zeta}_s \bar{\zeta}_s \rangle(\bar{\mathbf{r}}) &= \langle \zeta_s \zeta_s \rangle(\bar{\mathbf{r}}) + \xi_L^0(\bar{\tau}, \bar{\mathbf{r}}) \partial_0 \langle \zeta_s \zeta_s \rangle(\bar{\mathbf{r}}) + \xi_L^i(\bar{\tau}, \bar{\mathbf{r}}) \partial_i \langle \zeta_s \zeta_s \rangle(\bar{\mathbf{r}}) \\ &= \langle \zeta_s \zeta_s \rangle(\bar{\mathbf{x}}) + (\xi_L^{0(0)}(\bar{\tau}, \bar{\mathbf{r}}) + \xi_L^{0(1)}(\bar{\tau}, \bar{\mathbf{r}})) \partial_0 \langle \zeta_s \zeta_s \rangle(\bar{\mathbf{r}}) \\ &\quad + (\xi_L^{i(0)}(\bar{\tau}, \bar{\mathbf{r}}) + \xi_L^{i(1)}(\bar{\tau}, \bar{\mathbf{r}})) \partial_i \langle \zeta_s \zeta_s \rangle(\bar{\mathbf{r}}).\end{aligned}$$

With this expression on hand, let's look at attractor inflation, as we have seen $\xi^0 = 0$, and keeping the first order terms, the 2-pt correlation function reads,

$$\langle \bar{\zeta}_s \bar{\zeta}_s \rangle(\bar{\mathbf{r}}) = \langle \zeta_s \zeta_s \rangle(\bar{\mathbf{r}}) + \zeta_L(\bar{\tau}, \bar{\mathbf{x}}_c) \bar{x}^i \partial_i \langle \zeta_s \zeta_s \rangle(\bar{\mathbf{r}}), \quad (6.206)$$

Fourier transforming this expression, we get

$$\bar{P}(\bar{\tau}, \bar{k}_s) = \left(1 + \zeta_L(\bar{\tau}, \bar{\mathbf{x}}_c) \frac{\partial \ln(k_s^3 P(\bar{\tau}, \bar{k}_s))}{\partial \ln k_s}\right) P(\bar{\tau}, \bar{k}_s). \quad (6.207)$$

On the other hand, for non-attractor inflation, it has been found that the spatial shift is $\xi^i = 0$, thus for (6.204) the time shift accounts. Replacing the first order contribution from (6.198) into (6.204)

$$\langle \bar{\zeta}_s \bar{\zeta}_s \rangle(\bar{\mathbf{r}}) = \langle \zeta_s \zeta_s \rangle(\bar{\mathbf{r}}) + \bar{\tau} \zeta_L(\bar{\tau}, \bar{\mathbf{x}}_c) \partial_0 \langle \zeta_s \zeta_s \rangle(\bar{\mathbf{r}}), \quad (6.208)$$

finally, Fourier transforming the short modes:

$$\bar{P}(\bar{\tau}, \bar{k}_s) = \left(1 + \zeta_L(\bar{\tau}, \bar{\mathbf{x}}_c) \frac{\partial \ln P(\bar{\tau}, \bar{k}_s)}{\partial \ln \bar{\tau}}\right) P(\bar{\tau}, \bar{k}_s). \quad (6.209)$$

6.8 Bispectrum Squeezed Limit

6.8.1 Observed f_{NL} in single field Attractor models

It is known that the squeezed limit of the three-point function is understood as the correlation between a long mode that modulates 2 point correlation function in Fourier space, the so called background wave argument. In the absence of modulation, the 2-point function does not experience any contribution from longer modes and thus remains the same. It is worth mentioning that in this limit for single field inflation only gravitational interactions matters, therefore, this limit is model independent; moreover, their quadratic corrections start at the second order as k_L^2/k_s^2 and they are a model dependent. [91] [93]. Thus in the limit $k_3 \rightarrow 0$, we know:

$$\lim_{k_3 \rightarrow 0} (2\pi)^3 \delta^3(\mathbf{k}_1 + \mathbf{k}_2 + \mathbf{k}_3) B(k_1, k_2, k_3) = \langle \zeta(\mathbf{k}_3) \langle \zeta(\mathbf{k}_1) \zeta(\mathbf{k}_2) \rangle \rangle \quad (6.210)$$

and this result is valid at any time during inflation. Particularly, for single field slow roll inflation from [23] They satisfy the well known Maldacena's consistency relation :

$$\lim_{k_3 \rightarrow 0} B_{\zeta \zeta \zeta}(k_1, k_2, k_3) = -(n_s - 1) P(k_3) P(k_1) \quad (6.211)$$

where the $P(k_i)$ correspond to the power spectrum of a determined model, that could depend for example, the speed of sound, and n_s correspond to the spectral index of the scalar power spectrum.

From CFC construction we know that the power spectrum receives a long mode contribution, which first order correction correspond to a dilatation by a factor ζ_L :

$$\bar{P}(\bar{\tau}, \bar{k}_s) = P(\bar{k}_s) + \zeta_L(\bar{\tau}, \bar{\mathbf{x}}_c) \frac{\partial \ln(k_s^3 P(\bar{k}_s))}{\partial \ln \bar{k}_s} P(\bar{k}_s) \quad (6.212)$$

by using (6.207), the squeezed limit of the bispectrum in the CFC:

$$\lim_{k_L \rightarrow 0} B_{\bar{\zeta}\bar{\zeta}\bar{\zeta}}(\bar{k}_L, \bar{k}_1, \bar{k}_2) = \lim_{k_L \rightarrow 0} B_{\zeta\zeta\zeta}(\bar{k}_L, \bar{k}_1, \bar{k}_2) + \frac{\partial \ln(\bar{k}_s^3 P(\bar{k}_s))}{\partial \ln k_s} P(\bar{k}_L) P(\bar{k}_s) \quad (6.213)$$

$$\lim_{k_L \rightarrow 0} B_{\bar{\zeta}\bar{\zeta}\bar{\zeta}}(\bar{k}_L, \bar{k}_1, \bar{k}_2) = -(n_s - 1) P(\bar{k}_L) P(\bar{k}_s) + (n_s - 1) P(\bar{k}_L) P(\bar{k}_s) \quad (6.214)$$

thus,

$$\lim_{k_L \rightarrow 0} B_{\bar{\zeta}\bar{\zeta}\bar{\zeta}}(\bar{k}_L, \bar{k}_1, \bar{k}_2) = 0 \quad (6.215)$$

as a consequence in the CFC frame the superhorizon long modes do not couple with short modes, or in simple words they do not interact gravitationally, as a consequence, a free-falling observer, measure a vanishing f_{NL} .

6.8.2 Observed f_{NL} in single field Non-attractor models

For the Non-attractor models, the situation is quite similar to a longer mode modulates the short scale physics changing the effective background. In this scenario, the squeezed limit of the three-point function is different, moreover, it violates the Maldacena's consistency relation for canonical single field inflation, producing a local non-gaussianity of $f_{NL} = 5/2$ [110, 111, 129, 113]. Which are model dependent and other non-gravitational contributions affect them for this limit. However, recent work has shown a suppression of the latest for a smooth transition by a factor $e^{-\Delta N}$, where ΔN means the duration of the transition between the non-attractor to the attractor phase in terms of the e-folding [130]. Our interest is the Non-attractor phase so we consider the former. For this scenario the squeezed limit for canonical single field reads:

$$\lim_{k_L \rightarrow 0} B_{\bar{\zeta}\bar{\zeta}\bar{\zeta}}(\bar{k}_L, \bar{k}_1, \bar{k}_2) = 6P(\bar{k}_L)P(\bar{k}_s) \quad (6.216)$$

Now considering (6.209), and the fact that ζ , the squeezed limit of the bispectrum in the CFC frame:

$$\lim_{k_L \rightarrow 0} B_{\bar{\zeta}\bar{\zeta}\bar{\zeta}}(\bar{k}_L, \bar{k}_1, \bar{k}_2) = B_{\zeta\zeta\zeta}(\bar{k}_L, \bar{k}_1, \bar{k}_2) + \frac{\partial \ln P(\bar{\tau}, \bar{k}_s)}{\partial \ln \bar{\tau}} P(\bar{k}_L) P(\bar{k}_s) \quad (6.217)$$

$$\lim_{k_L \rightarrow 0} B_{\bar{\zeta}\bar{\zeta}\bar{\zeta}}(\bar{k}_L, \bar{k}_1, \bar{k}_2) = 6P(\bar{k}_L)P(\bar{k}_s) - 6P(\bar{k}_L)P(\bar{k}_s) \quad (6.218)$$

thus,

$$\lim_{k_L \rightarrow 0} B_{\bar{\zeta}\bar{\zeta}\bar{\zeta}}(\bar{k}_L, \bar{k}_1, \bar{k}_2) = 0 \quad (6.219)$$

Thus for both scenarios, the result is the same: superhorizon physics do not affect shorter scales for an inertial observer, independently of the underlying background behavior. The interpretation of this result is elucidated by remembering the meaning of Conformal Fermi Coordinates, that is to say, that the equivalence principle guarantee that always exists sufficient small vicinity in which an inertial observer describe the spacetime as it were flat, that is to say, Minkowski, erasing in this way any small global curvature, in this footing these results are protected by the **Local Flatness Theorem**. In particular, for our interest superhorizon modes do not contribute to short scales (but big enough to be observable).

6.9 Discussion and conclusions

We have studied the computation of local non-Gaussianity accessible to inertial observers in canonical models of single field inflation. It was already known [99, 3, 101, 1] that observable local non-Gaussianity vanishes in the case of single field attractor models ($f_{NL}^{\text{obs}} = 0$) modulo projection effects. In this work, we have extended this result to the case of non-attractor models (ultra slow-roll) in which the standard derivation gives a sizable value $f_{NL} = 5/2$. This result (the standard result) was thought to represent a gross violation of Maldacena's consistency relation. We have instead shown that for both classes of models, the consistency relation is simply:

$$f_{NL}^{\text{obs}} = 0. \quad (6.220)$$

This result is noteworthy: In ultra slow-roll, comoving curvature perturbations experience an exponential superhorizon growth, and this growth was taken to be the natural explanation underlying large local non-Gaussianity. However, this is indeed not the case.

Our results shed new light on our understanding of the role of the bispectrum squeezed limit in inflation to test primordial cosmology. We now know that non-Gaussianity cannot discriminate between two drastically different regimes of inflation. Instead, we are forced to think of new ways of testing the evolution of curvature perturbations in non-attractor backgrounds. This is particularly important once we face the possibility that ultra slow-roll could be representative of a passing phase within a conventional slow-roll regime [124, 125].

To derive (6.220), we have re-examined the use of conformal Fermi coordinates introduced in ref. [3] and perfected in refs. [100, 1]. Our results complement these works. For instance, the vanishing of f_{NL}^{obs} in the case of non-attractor models required us to consider in detail the contribution of time-displacement of the CFC map that is irrelevant in the case of attractor models.

The previous remark offers a way to understand the vanishing of local f_{NL}^{obs} for the case of non-attractor models. To appreciate this, let us first focus on the case of attractor models. Notice that in the case of attractor models the freezing of the curvature perturbation can

be absorbed at superhorizon scales through a re-scaling of the coordinates, which, to linear order in the perturbations, looks like $\mathbf{x} \rightarrow \mathbf{x}' = \mathbf{x} + \zeta(\mathbf{x}_c)\mathbf{x}$, where ζ is the value of the mode at horizon crossing. It is precisely this scaling that gives rise to the modulation of small scale perturbations by long scale perturbations in comoving gauge. The map coefficients of eq. (6.193) show that in attractor inflation the local transformation corresponds to $\mathbf{x} \rightarrow \mathbf{x} = \bar{\mathbf{x}} - \zeta(\bar{\mathbf{x}}_c)\bar{\mathbf{x}}$. This transformation is opposite to the previous re-scaling, and therefore it cancels the effect of the modulation in comoving coordinates.

Now, something similar happens in the case of non-attractor models. Here, the curvature perturbation does not freeze on superhorizon scales. Instead, on superhorizon scales the mode acquires a time dependence that may be absorbed by a re-scaling of time $\tau \rightarrow \tau' = \tau - \zeta(\tau)\tau$ in the argument of the scale factor (in comoving coordinates). Similar to the case of attractor models, the map coefficients of eq. (6.199) show that in the non-attractor regime the local CFC transformation corresponds to $\tau(\bar{\tau}) = \bar{\tau} + \zeta(\bar{\tau})\bar{\tau}$, which is opposite to the previous re-scaling, and so it cancels the whole modulation effect.

More generally, and independently of whether we are looking into the attractor regime or the non-attractor regime, the cancellation may be understood as follows: The squeezed limit of the 3-point correlation function of canonical models of inflation is the consequence of a symmetry of the action for ζ under the special class of space-time reparametrization shown in Eqs. (5.2)-(5.3). This symmetry is exact in the two regimes that we have studied, but approximate in intermediate regimes. In addition, this symmetry dictates the way in which long-wavelength ζ -modes modulate their short wavelength counterparts. The CFC transformation is exactly the inverse of the symmetry transformation, and so the modulation deduced with the help of the symmetry is canceled by moving into the CFC frame.

At this point, it is important to emphasize that our computation was performed during inflation. That is, we have performed the CFC transformation while inflation takes place, and the result $B + \Delta B = 0$ found in Section 6.8 is strictly valid during inflation. The claim that the primordial contribution to $f_{\text{NL}}^{\text{obs}}$ vanishes for a late time observer must be a consequence of the CFC transformation, taking into account the entire cosmic history. This would require studying the transition from the non-attractor phase to the next phase, which presumably could be of the attractor class, a study began in [123, 130]. Given that both B and ΔB found in Section 6.8 are exactly the same (but of opposite signs) and determined by τ -derivatives and k -derivatives of the power spectrum, we expect that the transition will affect equally B and ΔB , in such a way that the net result would continue to be $B + \Delta B = 0$. Verifying this claim, which seems reasonable, is out of the scope of the present article.*

The vanishing of local non-Gaussianity in both attractor and non-attractor models of single field inflation might not necessarily be surprising after all. In both cases, after the inflaton scalar degree of freedom is swallowed by the gravitational field, the only dynamical scalar degree of freedom corresponds to the curvature perturbation. As a consequence, the interaction coupling together long and short wavelength modes is purely gravitational, and therefore

*In a recent article [130] (written simultaneously to this work), Cai *et al.* studied the effects on the bispectrum B of a transition from a non-attractor phase to an attractor phase. They discovered that the transition can drastically change the value of f_{NL} , suppressing its value if the transition is smooth. Then, the question would be: What happens with ΔB during such transitions?

the equivalence principle dictates that long wavelength physics cannot dictate the evolution of short wavelength dynamics, implying that any observable effect must be suppressed by a ratio of scales $\mathcal{O}(k_L/k_S)^2$. All of this calls for a better examination of the relation between the local ansatz and the squeezed limit of the bispectrum [131].

Our work leaves several open challenges ahead. First, we have focussed our interest in canonical models of inflation, namely, those in which the inflaton field is parametrized by a Lagrangian containing a canonical kinetic term. In this category, the ultra slow-roll regime is not fully realistic, and at best should be considered as a toy model allowing the study of perturbations under the extreme conditions of a non-attractor background. However, it has been shown that attractor regimes may appear more realistically within non-canonical models of inflation such as $P(X)$ models. In these models, one has non-gravitational interactions inducing a sound speed $c_s \neq 1$, and so we suspect that our result (6.220) will not hold in those cases. Nevertheless, this work (together with ref. [129]) calls for a better understanding of the non-Gaussianity predicted by non-attractor models in general.

Second, given that observable local non-Gaussianity vanishes in ultra slow-roll, in which curvature perturbations grow exponentially on superhorizon scales, one should revisit the status of other classes of inflation, such as multi-field inflation, where local non-Gaussianity may be significant (the first look into this issue has already been undertaken in ref.[114]). It is entirely feasible that in some models of multi-field inflation the amount of local non-Gaussianity may be understood as the consequence of a space-time symmetry dictating the way in which long-wavelength modes module short modes.

Third, a deeper understanding of our present result is in order. In the case of attractor models, Maldacena's consistency relation (and its vanishing) may be understood as a consequence of soft limit identities linking the non-linear interaction of long wavelength perturbations with shorter ones [116, 117, 118, 119, 120, 121, 122]. However, there were good reasons to suspect that these relations would not hold anymore in the case of non-attractor models [3]. Our results suggest that, regardless of the background, these identities continue to be valid, and in an inertial frame the gravitational interaction cannot be responsible for making long wavelength modes affect the local behavior of short wavelength modes.

Chapter 7

Window Functions and Deconvolution Method for The Cosmology Large Angular Scale Surveyor(CLASS)

7.1 Beams and window functions

Knowledge of the beam profiles is of critical importance for interpreting data from CMB experiments. In algorithms for recovering the CMB angular power spectrum from a map, the output angular power spectrum is divided by the window function to reveal the intrinsic angular power spectrum of the sky. Thus, the main beam and its transform (response function) directly affect cosmological analyses. Typically, the beam must be mapped to less than 30 dB of the peak to achieve 1% accuracy on the angular power spectrum. The CLASS 40GHz calibration is done entirely with the Moon profile, which fills the main lobes and side-lobes. For most other CMB experiments, insufficient knowledge of the beams affects both the calibration and window function.

Although it is traditional, and often acceptable, to parameterize beams with a single one or two-dimensional Gaussian form, such an approximation is not useful for CLASS. This is because at the level to which the beams must be characterized, they are intrinsically non-Gaussian. Moreover, the CLASS beams can be treated as azimuthally symmetric because each pixel is observed with multiple orientations. The symmetric beam approximation allows us avoid many of complications associated with asymmetric beams.

Figure 7.1 shows the beams in profile after symmetrization. In the Moon map analysis, the symmetrization procedure consists of smoothly interpolating the beam to 20×20 degrees with a two-dimensional spline and then azimuthally averaging in rings of width ~ 0.017 (degrees). Due to noise, the maximum value in a map is often not on the best symmetry axis, though it is generally within 1 pixel of it. The symmetrized beam has the same solid angle as the raw beam to $< 0.3\%$. The normalized symmetrized beam is called $b(\theta)$. Generally, the Hermite beams are used for space quantities, such as the window function, and the Moon maps are

used for real space calculations. In the following we discuss how the beams are parameterized, how the window functions are computed, and how the uncertainties in the window functions are propagated through to the CMB angular power spectrum. The notation is summarized in Table (7.1).

Table 7.1: Notation

Symbol	Description
Ω_B	Beam solid angle
σ_B	Width of a gaussian beam
FWHM	Full width at Half Maximum
$B(\theta)$	Beam profile normalized with $\int B(\theta)d\Omega = 1$
$b(\theta)$	Beam normalized to unity at $\theta = 0$
B_l	Beam response function of $B(\theta)$
b_l	Beam response function normalized to unity at $l = 0$
w_l^{TT}	Temperature Window function normalized to unity at $l = 0$
$\Sigma_{B,ll'}$	Beam covariance matrix for B_l
$\Sigma_{b,ll'}$	Beam covariance matrix for b_l
$\Sigma_{w,ll'}$	Temperature Window function covariance matrix

Mathematically the beam is a kernel used to convolved the sky, in other words the measured temperature anisotropies is different of the true sky qualitatively the beam function acts as a low pass filter for the angular multipoles, usually the multipoles $l = 0$ or $l = 1$ receives the true value because larger scales are unaffected. Particularly if an infinite resolution experiment were constructed the beam would be nothing but the delta function defined on the 2-sphere and the respective window function would be the unity. For intermediate resolution it is known that the wider the beam narrow the window function. This behavior can be captured by the simplest model: an azimuthally symmetric gaussian beam

$$B(\theta) = \exp\left(-\frac{1}{2}\frac{\theta^2}{\sigma^2}\right). \quad (7.1)$$

With θ the polar angle defined from the line of sight and σ the gaussian width. It is often in the literature define an equivalent quantity for the beam width called the full width at half maximum(FWHM), which is the angular separation in which Eq. 7.1 reaches 0.5 value.

$$\theta_{\text{FWHM}} = \sqrt{8 \ln 2} \sigma. \quad (7.2)$$

Moreover, it can be defined the gaussian beam normalized whose its solid angle, $\Omega_B = \int d\Omega B(\theta)$:

$$b(\theta) = \frac{1}{\Omega_B} \exp\left(-\frac{1}{2}\frac{\theta^2}{\sigma^2}\right). \quad (7.3)$$

This beam can be expanded in terms of spherical harmonics,

$$b(\theta) = \sum_{l=0}^{l_{\max}} \sum_m \sqrt{\frac{(2l+1)}{4\pi}} b_{lm} Y_{lm}(\theta, \phi), \quad (7.4)$$

with the expansion coefficient given by the projection:

$$b_{lm} = \sqrt{\frac{4\pi}{(2l+1)}} \int d\Omega b(\theta, \phi) Y_{lm}^*(\theta, \phi) \quad (7.5)$$

~~due to~~ $b(\theta)$ does not depend on ϕ coordinate, the unique modes with non vanishing contribution are the modes $m = 0$, ~~then the coefficients~~ $b_{lm} = b_l \delta_{0m}$:

$$b(\theta) = \sum_{l=0} b_l Y_{l0}(\theta, \phi), \text{ with } b_l = \int d\Omega b(\theta) P_l(\cos \theta) \quad (7.6)$$

the b_l 's approximately are,

$$b_l = \exp\left(-\frac{l(l+1)}{2} \sigma_b^2\right) \quad (7.7)$$

~~the~~ above expression defines the beam response function. Additionally, we can define similar quantities for polarization. For perfectly co-polar beam ~~the~~ and assuming fully polarized detectors, with no sensitivity to circular polarization ~~the~~ the beam Q and U Stokes parameter can be obtained from the azimuthally symmetric beam as

$$Q_b \pm iU_b = -b(\theta) e^{\pm 2i\phi} \quad (7.8)$$

~~this~~ can be expanded:

$$Q_b \pm iU_b = - \sum_{lm} \sqrt{\frac{2l+1}{4\pi}} (b_{lm}^E \mp i b_{lm}^B) {}_{\mp 2} Y_{lm}(\theta, \phi) \quad (7.9)$$

as a spin-2 field can be represented in spherical harmonic of spin-2, ${}_{\pm 2} Y_{lm}$. In the case of fully azimuthally symmetric beam [132], its harmonic spin-2 representation reduces to

$$b_l^P = -(8\pi) \frac{(l-2)!}{(l+2)!} \int d\theta \sin \theta b(\theta) {}_{-2} P_l^2(\cos \theta) \quad (7.10)$$

where the superscripts label $P = E, B$ and ${}_{-2} P_l^2$ is a Legendre polynomial of spin-2. As a main feature, its harmonic representation starts from $l = 2$, since the $l = 0, 1$ are erased when the rising and lowering operators of spin ± 2 acts over Y_l^m [132]. For an azimuthally symmetric beam:

$$b_l^P = \exp\left(-\frac{(l(l+1)-4)}{2} \sigma_b^2\right) \quad (7.11)$$

Beams in CMB analysis mathematically correspond to a kernel defined on the 2-sphere, acting on the true sky as

$$\tilde{T}(\hat{n}_2) = \int d\Omega_1 b(\hat{n}_2, \hat{n}_1) T(\hat{n}_1) \quad (7.12)$$

where \tilde{T} is the measured temperature in the direction \hat{n}_2 receiving temperature weighted contributions from \hat{n}_1 and noise has not been included. The importance of the beam in the analysis is that it weights the true power spectrum on the sky. Let's suppose we have generic scalar field defined on the 2-sphere as the CMB temperature fluctuations, this field can be decomposed into the spherical harmonic basis:

$$T(\hat{n}_1) = \sum_{lm} T_{lm} Y_{lm}(\hat{n}_1), \quad (7.13)$$

or compactly, in a coordinate free way:

$$|T\rangle = \sum_{lm} T_{lm} |lm\rangle \quad (7.14)$$

In the same manner the beam as a kernel in Eq.(7.12) is decomposed as

$$b(\hat{n}_2, \hat{n}_1) = \sum_{l_1 l_2} \sum_{m_1 m_2} b_{l_2 m_2 l_1 m_1} Y_{l_2 m_2}^*(\hat{n}_2) Y_{l_1 m_1}(\hat{n}_1) \quad (7.15)$$

where \hat{n}_1, \hat{n}_2 are two sky direction and $b_{l_2 m_2 l_1 m_1}$ are the components of the beam matrix that reduces to $b_{l_1} \delta_{l_1 l_2} \delta_{m_1 m_2}$ for symmetric beams. It is useful to define the beam operator as:

$$\hat{b} = \sum_{l_1 l_2} \sum_{m_1 m_2} b_{l_2 m_2 l_1 m_1} |l_2 m_2\rangle \langle l_1 m_1| \quad (7.16)$$

since reduce an analytic expression to an algebraic one. The convolution Eq.(7.12) is clearer

$$|\tilde{T}\rangle = \hat{b}|T\rangle = \sum_{l_1 l_2} \sum_{m_1 m_2} b_{l_2 m_2 l_1 m_1} T_{l_1 m_1} |l_2 m_2\rangle$$

where \tilde{T} is convolved temperature vector. The coordinate free representation is simpler to manipulate than real space convolution (7.12), but the real space convolution is more intuitive, for example a convolution is. Projecting in the real basis the Eq.(7.17) becomes

$$\tilde{T}(\hat{n}_2) = \sum_{l_1 l_2} \sum_{m_1 m_2} b_{l_2 m_2 l_1 m_1} T_{l_1 m_1} Y_{l_2 m_2}(\hat{n}_2) \quad (7.17)$$

in effect, we can identify easily the measured map coefficient $\tilde{T}_{l_2 m_2}$ as:

$$\tilde{T}_{l_2 m_2} = \sum_{l_1 m_1} b_{l_2 m_2 l_1 m_1} T_{l_1 m_1} \quad (7.18)$$

with this definition it easy to compute the power spectrum for temperature $\langle \tilde{T} | \tilde{T} \rangle$:

$$\langle \tilde{T} | \tilde{T} \rangle = \sum_{l'_1 l_2} \sum_{m'_2 m_1} \tilde{T}_{l'_2 m'_2} \tilde{T}_{l_2 m_2} \langle l'_2 m'_2 | l_2 m_2 \rangle = \sum_{l'_2 m'_2} \left(\tilde{T}_{l'_2 m'_2} \tilde{T}_{l_2 m_2} \right) \quad (7.19)$$

$$= \sum_{l'_2 m'_2} \left(\sum_{l'_1 l_1} \sum_{m'_1 m_1} b_{l'_2 m'_2 l'_1 m'_1}^* b_{l'_2 m'_2 l_1 m_1} T_{l'_1 m'_1} T_{l_1 m_1} \right) \quad (7.20)$$

Identifying the coefficients as:

$$|\tilde{T}_{l'_2 m'_2}|^2 = \sum_{l'_1 l_1} \sum_{m'_1 m_1} b_{l'_2 m'_2 l'_1 m'_1}^* b_{l'_2 m'_2 l_1 m_1} T_{l'_1 m'_1} T_{l_1 m_1} \quad (7.21)$$

Defining the ensemble average $\tilde{C}_{l'_2 m'_2} = \langle |\tilde{T}_{l'_2 m'_2}|^2 \rangle$:

$$\tilde{C}_{l'_2 m'_2} = \sum_{l'_1 l_1} \sum_{m'_1 m_1} b_{l'_2 m'_2 l'_1 m'_1}^* b_{l'_2 m'_2 l_1 m_1} C_{l'_1} \delta_{l'_1 l_1} \delta_{m'_1 m_1} = \sum_{l'_1} \sum_{m'_1} |b_{l'_2 m'_2 l'_1 m'_1}|^2 C_{l'_1} \quad (7.22)$$

Notice that despite the fact that T_{lm} 's do not have any correlation in m and l the measured \tilde{T}_{lm} 's are not absent of correlation. In general, beam asymmetries induce m -dependence for the measured angular power spectrum $\tilde{C}_{l'm'}$. Additionally, for estimating the primordial power spectrum we can take average over m and relabel l and m , therefore

$$\langle \tilde{C}_{l'} \rangle = \sum_l \frac{1}{(2l+1)} \sum_{mm'} |b_{l'm'lm}|^2 \langle C_l \rangle, \quad (7.23)$$

or compactly as

$$\langle \tilde{C}_{l'} \rangle = \sum_l M_{l'l} \langle C_l \rangle. \quad (7.24)$$

For a particular case in which matrix $M_{l'l}$ is nothing but the window function for a symmetric beam, $w_l \delta_{l'l}$, ones gets:

$$\langle \tilde{C}_{l'} \rangle = w_l \langle C_l \rangle \quad (7.25)$$

The above expression constitutes the direct relationship for the measured power spectra \tilde{C}_l and the true value C_l . The window function w_l in this case for temperature correspond to the weights for different multipoles, therefore its understanding its critical for any CMB analysis.

7.2 Moon temperature model

A measured moon map, \tilde{T} , can be modeled as the convolution between the moon as uniform disc T of an angular radius a , and a symmetric beam, B :

$$\tilde{T} = T * B + N, \quad (7.26)$$

where a small noise component N was added. This convolution can be represented in k-domain by applying the Fourier projector $\mathcal{F}^{-1}(\mathcal{F}(\cdot))$ and using the Fourier representation of the uniform disc, $2\pi a^2 J_1(ka)/ka$ with $J_1(x)$ the Bessel function of the first kind; thus,

$$\tilde{T}(\theta, \phi) = \frac{a}{(2\pi)} \int_{\mathbb{R}^2} d\mathbf{k} e^{i\mathbf{k}\cdot\mathbf{x}} \frac{J_1(ka)}{k} B(k) + N(\theta, \phi). \quad (7.27)$$

It is suitable use the rotational symmetry of the convolved signal by doing the following substitution: $x = \theta \cos \phi$, $y = \theta \sin \phi$; the identity $\cos \xi \cos \phi + \sin \xi \sin \phi = \cos(\xi - \phi)$; and making a change of variables $\xi - \phi = \psi$. So,

$$\tilde{T}(\theta) = \frac{a}{(2\pi)} \int_0^\infty \int_0^{2\pi} dk d\psi e^{ik\theta \cos \psi} J_1(ka) B(k) + N(\theta, \phi) \quad (7.28)$$

Additionally, by using the integral representation of the zeroth order Bessel function of the first kind, $2\pi J_0(z) = \int_0^{2\pi} d\psi e^{\pm iz \cos \psi}$ and taking the angular average of the noise $\langle N(\mathbf{x}) \rangle_\phi = N(\theta)$, then the observed temperature map is only a function of θ :

$$\tilde{T}(\theta) = 2\pi a \int_0^\infty dk J_0(k\theta) J_1(ka) B_0(k) + N(\theta), \quad (7.29)$$

where $B_0(k)$ is the 0-th Hankel transform of the beam defined by $B_0(k) = \int_0^\infty d\theta \theta B(\theta) J_0(k\theta)$. The above analytical expression is the model of the moon-beam convolution. Notice that it has been reduced from 2-dimensional convolution(two integrals) to a single 1-dimensional integral expression by using the rotational symmetry of both functions. This reduces the fitting computation process.

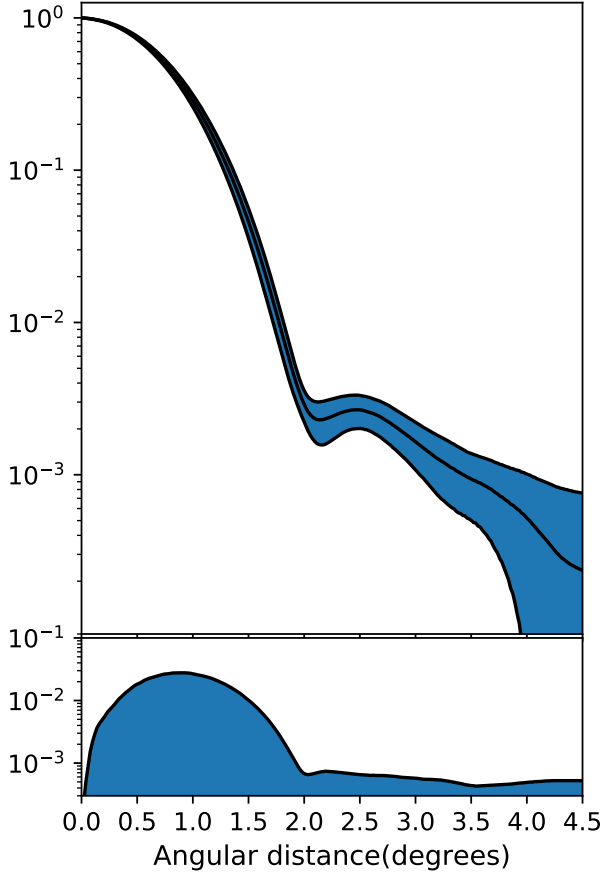


Figure 7.1: Average beam profile. The shaded region denotes a $1-\sigma$ of uncertainty envelope around the beam average along the season.

7.2.1 Beam fitting and deconvolution

Since the contribution from non-Gaussian components of the symmetrized beam modify significantly the CMB analysis, it is necessary quantify and parametrize these deviations with some complete basis. The natural way to capture these effect is by projecting the symmetrized beam into Hermite basis(as the quantum harmonic oscillator) since they parametrize these deviations from gaussianity. Thus the Hermite expansion is given by

$$B(\theta) = \sum_{j=0}^{N_{max}} a_{2j} B_{2j} \left(\frac{\theta}{\sigma_b} \right), \quad (7.30)$$

where θ is the angular distance from the beam center, σ_b correspond to the standard deviation of the gaussian component and B_j to their corrections. Explicitly the above expression is

$$B(\theta) = \sum_{j=0}^{N_{max}} a_{2j} H_{2j} \left(\frac{\theta}{\sigma_b} \right) \exp \left(-\frac{1}{2} \frac{\theta^2}{\sigma_b^2} \right), \quad (7.31)$$

where $2j$ is an even number. This expansion allows to capture and parametrize the small features that deviates from the gaussianity. This basis has already been implemented in [?]. Thus in order to obtain the beam shape from moon scans data, we need to fit a certain number of Hermite functions to the beam, this number can be estimated if we note that the $2n$ -Hermite polynomials have a maximum at $\theta_m = \pm \sigma_b \sqrt{2n}$, and then they decays Gaussianly, since our effective beam has its last relevant feature at ~ 4.0 deg. Fig.(7.1) which implies $\lfloor 2N_{max} \rfloor = 34$ this impose an upper limit, $N_{max} \leq 17$, for the beam expansion.

Replacing Eq.(7.31) into Eq.(7.29) each of these modes contributes as:

$$\tilde{T}_{2j}(\theta) = 2\pi a \int_0^\infty dk J_0(k\theta) J_1(ka) B_{0,2j}(k) \quad (7.32)$$

to the moon temperature field. The $\tilde{T}_{2j}(\theta)$ correspond to the temperature contribution of $B_{0,2j}(k)$, which is the 2D-Hankel transformation of $B_{2j}(\theta)$. Then the temperature map Eq.(7.29) can be expanded linearly as,

$$\tilde{T}(\theta) = \sum_j a_{2j} \tilde{T}_{2j}(\theta) + N(\theta). \quad (7.33)$$

Therefore, if the coefficients set a_{2j} are found, the beam shape Eq.(7.31) is determined. Due to we are interested only in the beam shape it is suitable to normalize the composed map at $\theta = 0$ to the unity. If $N(0) \ll \tilde{T}(0)$, then:

$$\hat{t}(\theta) = \frac{\int_0^\infty dk J_0(k\theta) J_1(ak) B_0(k)}{\int_0^\infty dk J_1(ak) B_0(k)} + n(\theta). \quad (7.34)$$

with $n(\theta) = N(\theta)/\tilde{T}(0)$. To Hankel transform the B_{2j} functions and convolve analytically the basis Eq.(7.32) to get Eq.(7.33),(7.34), we can use the fact that the even Hermite polynomials are composed by even monomials as:

$$\left(\frac{\theta}{\sigma_b} \right)^{2n} \exp \left(-\frac{\theta^2}{2\sigma_b^2} \right) \subseteq B_{2n}(\theta) = H_{2n} \left(\frac{\theta}{\sigma_b} \right) \exp \left(-\frac{1}{2} \frac{\theta^2}{\sigma_b^2} \right) \quad (7.35)$$

, whose Hankel transform are:

$$\mathcal{H}_0 \left[\left(\frac{\theta}{\sigma_b} \right)^{2n} \exp \left(-\frac{\theta^2}{2\sigma_b^2} \right) \right] (k) = 2^n \sigma_b^2 \Gamma(n+1) \cdot {}_1 F_1 \left(n+1; 1; \frac{-\sigma_b^2 k^2}{2} \right). \quad (7.36)$$

Where ${}_1 F_1(a, b, z)$ are the confluent hypergeometric functions of the first kind. This allows to obtain an analytical expression in Fourier representation for different Hermite modes, as a consequence, each component of the convolved basis, $\tilde{T}_{2j}(\theta)$, is determined exactly as an integral representation of known functions.

Returning to Eq.(7.34) and using the convolved Hermite basis Eq.(7.36), the normalized moon-beam model Eq.(7.32) can be expanded in terms of the components of this basis.

$$\hat{t}(\theta) = \frac{\sum_{j=0}^{N_{max}} a_{2j} \tilde{T}_{2j}(\theta)}{\sum_{j=0}^{N_{max}} a_{2j} \tilde{T}_{2j}(0)} + n(\theta) \quad (7.37)$$

The above expression is symmetric under a rescaling transformation $\tilde{T} \rightarrow a\tilde{T}$, therefore to avoid a scale degeneracy in the set coefficient $\{a_{2n}\}$, it is suitable choose one of them to unity, for instance a_0 , and proceed with the fitting procedure, thus

$$\hat{t}(\theta) = \frac{\tilde{T}_0(\theta) + \sum_{j=1}^{N_{max}} a_{2j} \tilde{T}_{2j}(\theta)}{\tilde{T}_0(0) + \sum_{j=1}^{N_{max}} a_{2j} \tilde{T}_{2j}(0)} + n(\theta) \quad (7.38)$$

The above expression gives the fitting coefficients for the set a_{2j} and its respective covariance matrix $\Sigma_{a,jj'}$. The figure 7.2 displays the symmetrized convolved moon signal, the fit to this signal and the deconvolved beam. After deconvolving the beam from the moon contributions,

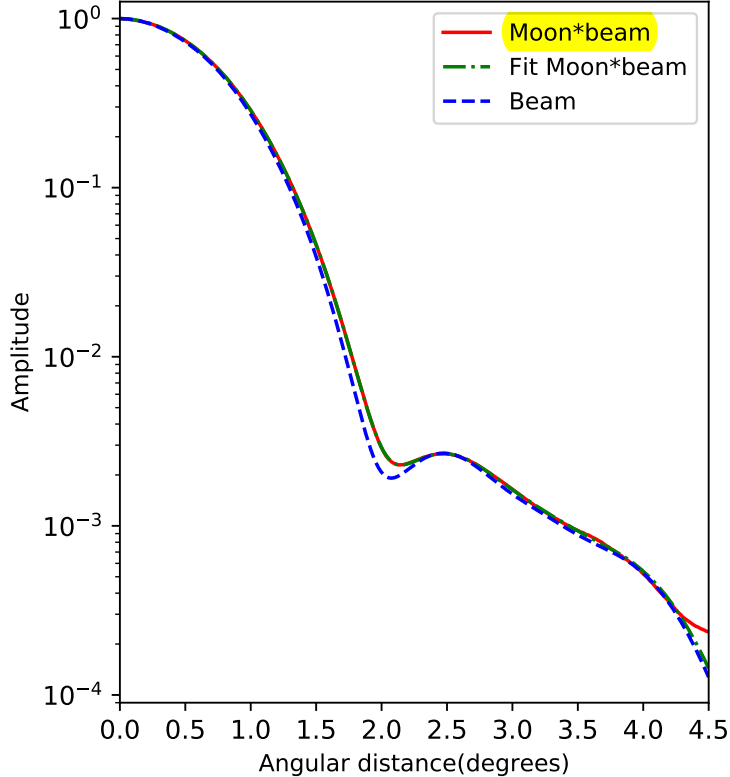


Figure 7.2: Beam profile: the red line represents the symmetrized convolved signal between the moon and the beam($T * B$) with its respective fit using Eq.(7.38)(green line), whereas the blue dashed line represent the deconvolved beam.

we can construct its window function using Eq.(3.8). The figure (7.6) shows the temperature window function with its fractional uncertainty included fig.(7.4) shows the uncertainties of the convolved beam compared with the beam. The red line represent their fractional deviation from the true value, showing that a deconvolution procedure is important for higher l .

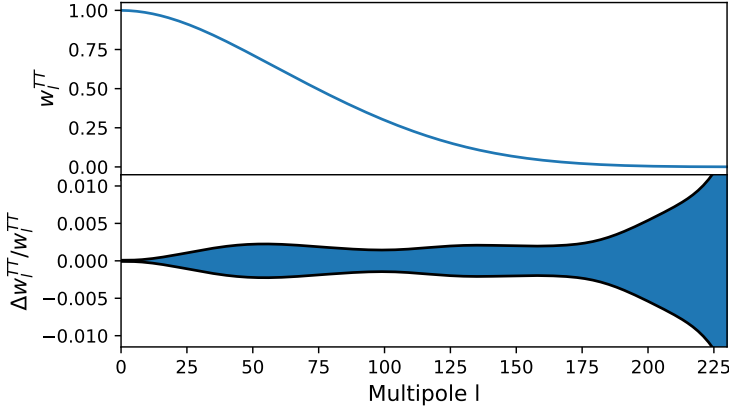


Figure 7.3: Temperature-temperature window function: The upper panel show the l dependence of the window function acting as low pass filter. The bottom panel shows its fractional uncertainty.

Table 7.2: Window function parameters

Parameter	Value
$\sigma_b(\text{deg})$	$0.67 \pm 1.04 \cdot 10^{-3}$
FWHM(deg)	$1.57 \pm 2.46 \cdot 10^{-3}$
$\Omega_b \cdot 10^{-4}(\text{sr})$	8.08 ± 0.02
$l^{w=0.5}$	~ 110
$l^{w=0.2}$	~ 165
N_{\max}	12
$l_{\max}[\frac{\Delta b_l}{b_l} \% < 0.01]$	~ 225

7.2.2 Uncertainty propagation

The procedure of combining power spectra requires the full covariance matrix of the individual cross-power spectra. The full covariance matrix for CMB analysis receives contribution from well known canonical principal sources: cosmic variance, instrument noise, mode coupling due to foreground mask, point source subtraction errors, uncertainty in the window function and the overall calibration uncertainty. This covariance matrix can be expanded as

$$\Sigma_{\text{full}} = \Sigma_{\text{c. variance}} + \Sigma_{\text{masking}} + \Sigma_{\text{point sources}} + \Sigma_{\text{beams}} \quad (7.39)$$

In this subsection we are concerned in the last term. These errors correspond to the uncertainty in the beam window function, w_l . These errors arise from fluctuations in the window function which causes the measured power spectrum \tilde{C}_l differ from our convolved spectrum $w_l C_l$, where w_l is the estimated window function. Cross window functions are computed as the product of beam response functions:

$$w_l^{ij} = b_l^i b_l^j \quad (7.40)$$

with $i, j = T, E, B$. When at least one component correspond to E or B the window function starts at $l = 2$, since the $l = 0, 1$ are erased when the rising and lowering operators of spin

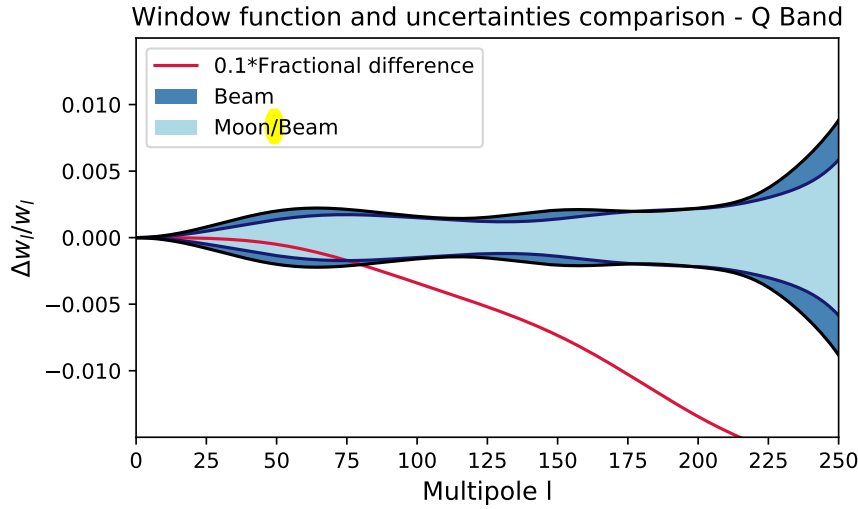


Figure 7.4: Fractional uncertainty comparison: The blue and the light blue contours represent the fractional uncertainty of beam and the convolved beam, respectively. The red line correspond to the fractional deviation between the convolved beam and the deconvolved beam, this effect is significant for higher l . The negative tendency can be interpreted as a lack of power for higher l since the convolution softens the small beam features that adds extra amplitude.

± 2 acts over Y_l^m [132] for uncertainty propagation.

The expansion Eq.(7.31) ~~systematically~~ provides a ~~easy~~ way to derive the covariance matrix associated; from this expansion the ~~deviation from the average comes~~ from the basis components

$$\Delta b_l^i = b_l^i(\vec{a}) - \langle b_l^i \rangle = \sum_{n=0}^N \frac{\partial b_l^i}{\partial a_n} (a_n - \langle a_n \rangle) = \sum_{n=0}^N \frac{\partial b_l^i}{\partial a_n} \Delta a_n \quad (7.41)$$

therefore the beam covariance matrix between b_l^i and $b_{l'}^j$ is defined as:

$$\Sigma_{b,ll'}^{ij} = \langle \Delta b_l^i \Delta b_{l'}^j \rangle = \sum_{n,n'} \frac{\partial b_l^i}{\partial a_n} \frac{\partial b_{l'}^j}{\partial a_{n'}} \langle \Delta a_n \Delta a_{n'} \rangle = \sum_{n,n'} \frac{\partial b_l^i}{\partial a_n} \frac{\partial b_{l'}^j}{\partial a_{n'}} \Sigma_{a,nn'}. \quad (7.42)$$

This matrix has units of sr^2 , and is independent of the Moon's temperature, and as expected its magnitude is ~~large at low l and at high l for calibration and sensitivity loss, respectively~~. Moreover, if we note that the beam is normalized by its solid angle, $b_l^i = B_l^i / B_{l=0}^T$ at $l = 0$, then the uncertainty at $l = 0$ is fixed to 0, but it increases at high l .

$$\Sigma_{b,ll'}^{ij} = \frac{1}{(B_{l=0}^T)^2} \left[\Sigma_{B,ll'}^{ij} + b_l^i b_{l'}^j \Sigma_{B,00}^{TT} - b_l^i \Sigma_{B,0l'}^{Tj} - b_{l'}^j \Sigma_{B,l0}^{iT} \right] \quad (7.43)$$

the diagonal above expression Eq.(7.43) gives us the standard deviation of the beam response function Fig.7.2 and its off-diagonal element have the information of modes coupling. In the same manner for the window function, w^I .

$$\Sigma_{w,ll'}^{IJ} = \langle \Delta w_l^I \Delta w_{l'}^J \rangle = w_l^I w_{l'}^J \left(\frac{\Sigma_{b,ll'}^{ij}}{b_l^i b_{l'}^j} + \frac{\Sigma_{b,ll'}^{i'j'}}{b_l^{i'} b_{l'}^{j'}} + \frac{\Sigma_{b,ll'}^{i'j}}{b_l^{i'} b_l^j} + \frac{\Sigma_{b,ll'}^{ij'}}{b_l^i b_{l'}^{j'}} \right) \quad (7.44)$$

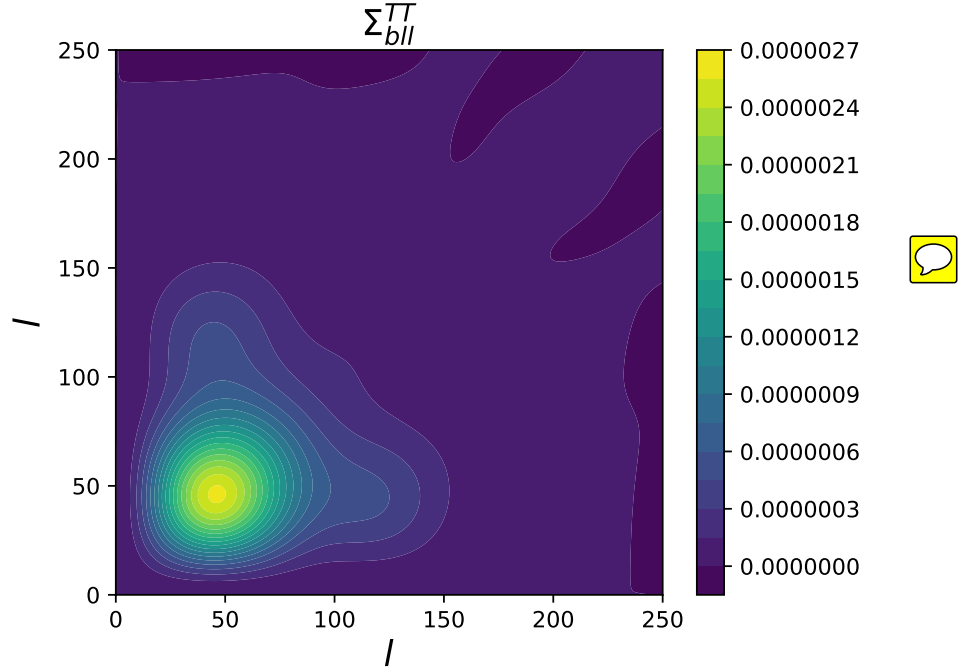


Figure 7.5: Temperature-temperature beam covariance matrix in harmonic representation.

where $I = ii'$, $J = jj'$ corresponding to T, E, B . This covariance matrix that enters directly to the likelihood function to constraint cosmological parameters and therefore is used for any CMB analysis. Moreover, to characterize it completely it is sufficient have knowledge about the beam covariance.

7.3 Conclusions

The main features of the beams in 40 GHz band(Q-band) for CLASS experiment have been presented in real and harmonic representation. The beam solid angle which are necessary for instrument calibration are given with 1% of precision. The uncertainties in the window function are typically $< 1.0\%$ at the range 0-200, multipoles of CLASS experiment is interested to constraint the reionization depth and a potential large angular scale B-mode signal. These values does not include all systematic effects.

We have also showed how the moon deconvolution formalism improved the window function analysis this construction is generic, systematic, and easy to implement, moreover, this semi-analytic method is computationally low cost, therefore it should be used as potential tool for beams characterization hereafter, especially for "in flight" calibration. In addition to this, we have not incorporated second order effects corresponding to the yearly variation of the moon angular diameter due to its proximity changes. We suspect that this constitutes a negligible effect compared to its average angular diameter seen from CLASS site location, even this annual variation can be absorbed as a noise.

In addition to this, we have provided a ~~systematic~~ formalism to propagate the beams errors into the ~~survey~~, likelihood, encapsulated in the beam covariance matrix. The components of covariance matrix are small, this can be attributed to the ~~instrument sensitivity and low noise~~, as a consequence, the small uncertainties implies that the solid angle is determined with high accuracy, ~~therefore keeping the detector calibration precise with high accuracy~~. Moreover, the low- l off-diagonal components shows a small and basis-dependent correlation that is worth mentioning, since it can induce small mode couplings, furthermore, the magnitude of its components are strictly smaller than its diagonal components, therefore, approximated matrix inversion procedures suitable fit for this covariance matrix, reducing the computational cost of its inversion. For all these reasons, the Hermite functions ~~used as a basis~~, keep being the appropriate basis to capture the beam deviation from gaussianity.

7.4 Chapter Appendix

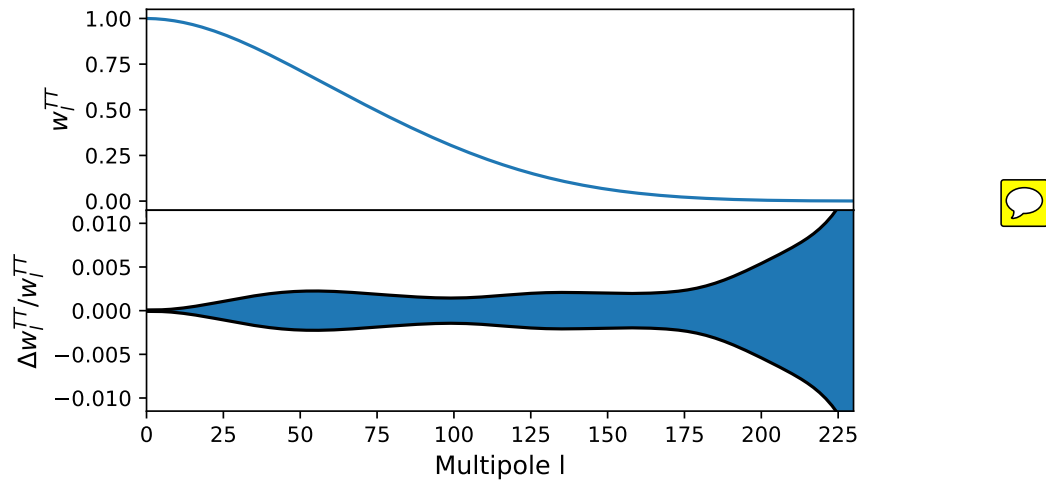


Figure 7.6: Temperature-Temperature window function: The upper panel show the l dependence of the window function acting as low pass filter. The bottom panel shows its fractional uncertainty.

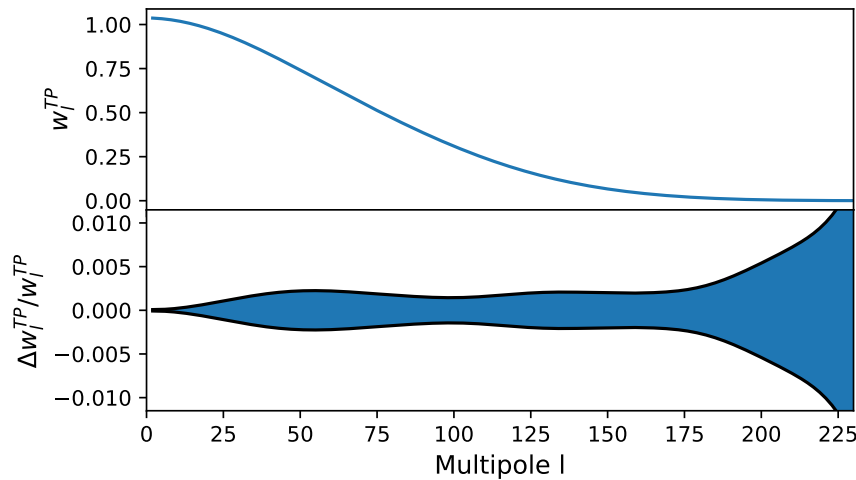


Figure 7.7: Temperature-Polarization window function. $P = E, B$. The upper panel show the l dependence of the window function acting as low pass filter. The bottom panel shows its fractional uncertainty.

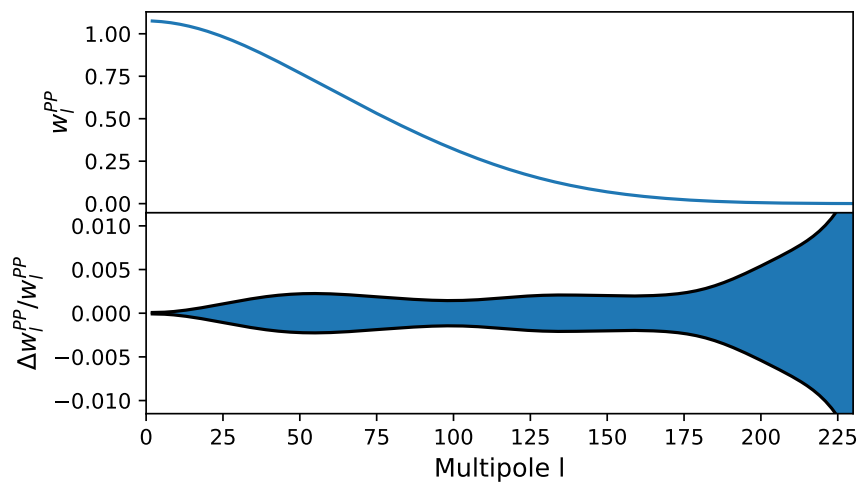


Figure 7.8: Polarization-Polarization window function. $P = E, B$. The upper panel show the l dependence of the window function acting as low pass filter. The bottom panel shows its fractional uncertainty.

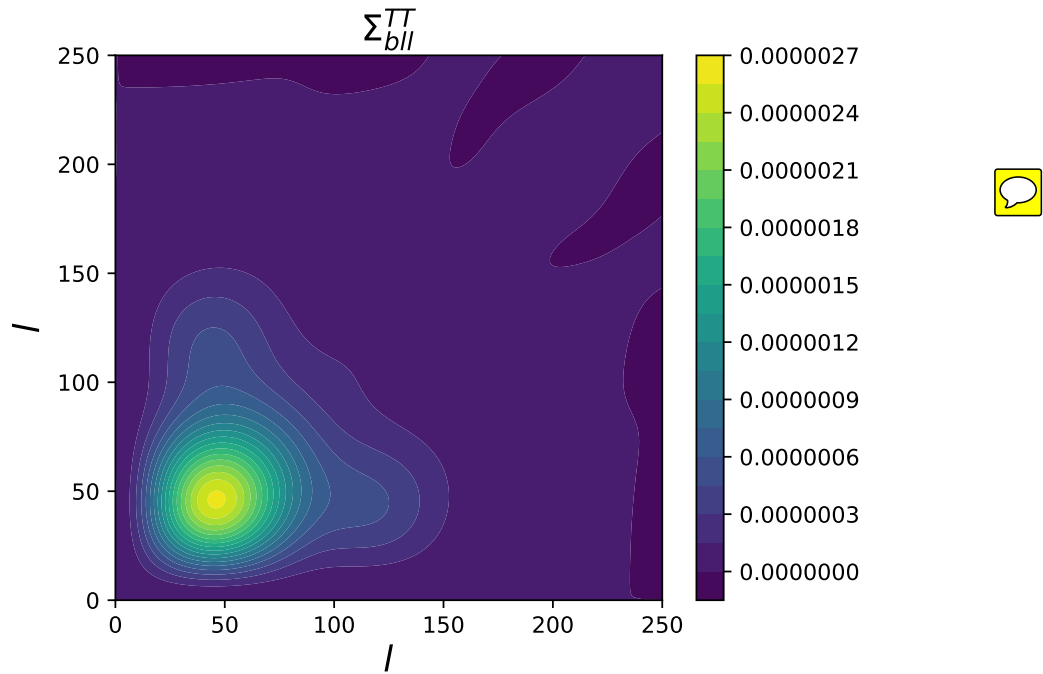


Figure 7.9: Temperature-Temperature beam covariance matrix in harmonic representation.

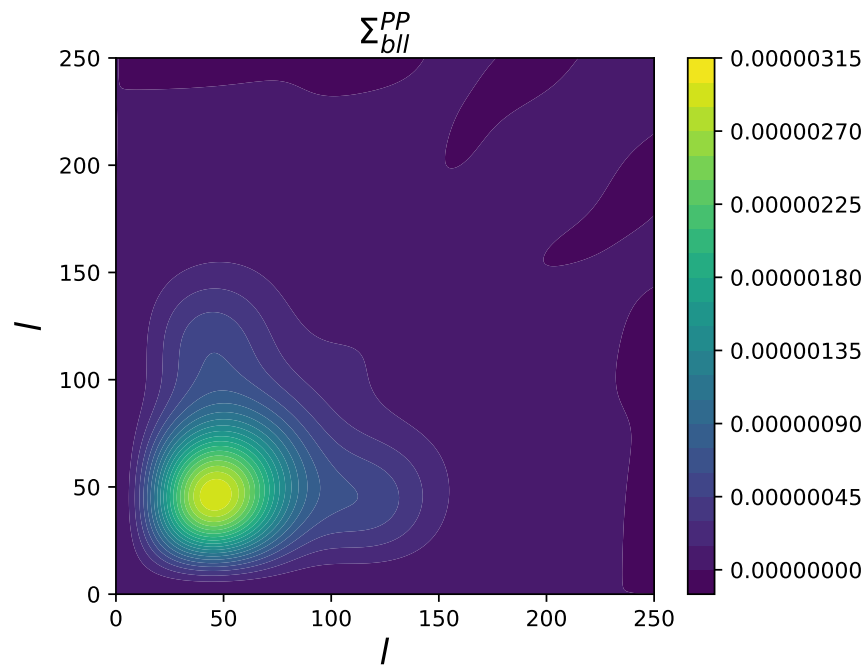


Figure 7.10: Polarization-Polarization beam covariance matrix in harmonic representation.

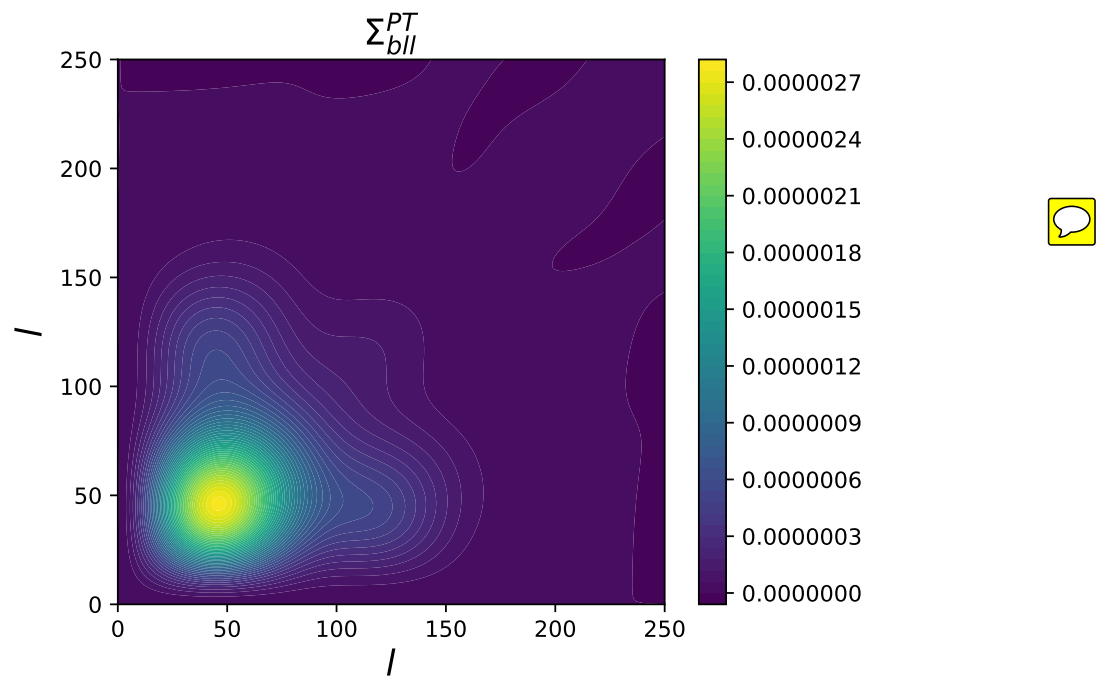


Figure 7.11: Polarization-Temperature beam covariance matrix in harmonic representation.

Bibliography

- [1] Giovanni Cabass, Enrico Pajer, and Fabian Schmidt. How Gaussian can our Universe be? *JCAP*, 1701(01):003, 2017.
- [2] F. K. Manasse and C. W. Misner. Fermi Normal Coordinates and Some Basic Concepts in Differential Geometry. *J. Math. Phys.*, 4:735–745, 1963.
- [3] Enrico Pajer, Fabian Schmidt, and Matias Zaldarriaga. The Observed Squeezed Limit of Cosmological Three-Point Functions. *Phys. Rev.*, D88(8):083502, 2013.
- [4] Gonzalo A. Palma. Untangling features in the primordial spectra. *JCAP*, 1504(04):035, 2015.
- [5] Alan H. Guth. The Inflationary Universe: A Possible Solution to the Horizon and Flatness Problems. *Phys. Rev.*, D23:347–356, 1981.
- [6] Alexei A. Starobinsky. A New Type of Isotropic Cosmological Models Without Singularity. *Phys. Lett.*, B91:99–102, 1980. [,771(1980)].
- [7] P. A. R. Ade et al. Planck 2015 results. XX. Constraints on inflation. *Astron. Astrophys.*, 594:A20, 2016.
- [8] Steven Weinberg. Adiabatic modes in cosmology. *Phys. Rev.*, D67:123504, 2003.
- [9] Scott Dodelson. Coherent phase argument for inflation. *AIP Conf. Proc.*, 689:184–196, 2003. [,184(2003)].
- [10] Daniel Baumann. Tasi lectures on inflation. *arXiv preprint arXiv:0907.5424*, 2009.
- [11] Csaba Csaki, Nemanja Kaloper, Javi Serra, and John Terning. Inflation from Broken Scale Invariance. *Phys. Rev. Lett.*, 113:161302, 2014.
- [12] D. S. Salopek and J. R. Bond. Nonlinear evolution of long wavelength metric fluctuations in inflationary models. *Phys. Rev.*, D42:3936–3962, 1990.
- [13] James M. Bardeen, Paul J. Steinhardt, and Michael S. Turner. Spontaneous Creation of Almost Scale - Free Density Perturbations in an Inflationary Universe. *Phys. Rev.*, D28:679, 1983.

- [14] Yi Wang. Inflation, Cosmic Perturbations and Non-Gaussianities. *Commun. Theor. Phys.*, 62:109–166, 2014.
- [15] P. A. R. Ade et al. Improved Constraints on Cosmology and Foregrounds from BICEP2 and Keck Array Cosmic Microwave Background Data with Inclusion of 95 GHz Band. *Phys. Rev. Lett.*, 116:031302, 2016.
- [16] R. J. Thornton et al. The Atacama Cosmology Telescope: The polarization-sensitive ACTPol instrument. *Astrophys. J. Suppl.*, 227(2):21, 2016.
- [17] P. A. R. Ade et al. A Measurement of the Cosmic Microwave Background B-Mode Polarization Power Spectrum at Sub-Degree Scales with POLARBEAR. *Astrophys. J.*, 794(2):171, 2014.
- [18] Kathleen Harrington et al. The Cosmology Large Angular Scale Surveyor. *Proc. SPIE Int. Soc. Opt. Eng.*, 9914:99141K, 2016.
- [19] Natalie N. Gandilo et al. The Primordial Inflation Polarization Explorer (PIPER). *Proc. SPIE Int. Soc. Opt. Eng.*, 9914:99141J, 2016.
- [20] B. P. Crill et al. SPIDER: A Balloon-borne Large-scale CMB Polarimeter. *Proc. SPIE Int. Soc. Opt. Eng.*, 7010:2P, 2008.
- [21] James N Fry and Enrique Gaztanaga. Biasing and hierarchical statistics in large-scale structure. *The Astrophysical Journal*, 413:447–452, 1993.
- [22] Steven Weinberg. Quantum contributions to cosmological correlations. *Phys. Rev.*, D72:043514, 2005.
- [23] Juan Martin Maldacena. Non-Gaussian features of primordial fluctuations in single field inflationary models. *JHEP*, 05:013, 2003.
- [24] Scott Dodelson. *Modern cosmology*. Elsevier, 2003.
- [25] David H Lyth and Andrew R Liddle. *The primordial density perturbation: Cosmology, inflation and the origin of structure*. Cambridge University Press, 2009.
- [26] Wayne Hu and Martin White. Acoustic signatures in the cosmic microwave background. *The Astrophysical Journal*, 471(1):30, 1996.
- [27] Andrei D. Linde. A New Inflationary Universe Scenario: A Possible Solution of the Horizon, Flatness, Homogeneity, Isotropy and Primordial Monopole Problems. *Phys. Lett.*, 108B:389–393, 1982.
- [28] Andreas Albrecht and Paul J. Steinhardt. Cosmology for Grand Unified Theories with Radiatively Induced Symmetry Breaking. *Phys. Rev. Lett.*, 48:1220–1223, 1982.
- [29] Kevork N. Abazajian et al. CMB-S4 Science Book, First Edition. 2016.
- [30] A. Suzuki et al. The POLARBEAR-2 and the Simons Array Experiment. *J. Low.*

Temp. Phys., 184(3-4):805–810, 2016.

- [31] Z. Ahmed et al. BICEP3: a 95GHz refracting telescope for degree-scale CMB polarization. *Proc. SPIE Int. Soc. Opt. Eng.*, 9153:91531N, 2014.
- [32] N. Aghanim et al. Planck 2015 results. XI. CMB power spectra, likelihoods, and robustness of parameters. *Astron. Astrophys.*, 594:A11, 2016.
- [33] Dhiraj Kumar Hazra, Arman Shafieloo, and George F. Smoot. Reconstruction of broad features in the primordial spectrum and inflaton potential from Planck. *JCAP*, 1312:035, 2013.
- [34] Dhiraj Kumar Hazra, Arman Shafieloo, and Tarun Souradeep. Primordial power spectrum from Planck. *JCAP*, 1411(11):011, 2014.
- [35] Paul Hunt and Subir Sarkar. Search for features in the spectrum of primordial perturbations using Planck and other datasets. *JCAP*, 1512(12):052, 2015.
- [36] C. L. Bennett, A. Banday, K. M. Gorski, G. Hinshaw, P. Jackson, P. Keegstra, A. Kogut, George F. Smoot, D. T. Wilkinson, and E. L. Wright. Four year COBE DMR cosmic microwave background observations: Maps and basic results. *Astrophys. J.*, 464:L1–L4, 1996.
- [37] G. Hinshaw et al. First year Wilkinson Microwave Anisotropy Probe (WMAP) observations: The Angular power spectrum. *Astrophys. J. Suppl.*, 148:135, 2003.
- [38] D. N. Spergel et al. First year Wilkinson Microwave Anisotropy Probe (WMAP) observations: Determination of cosmological parameters. *Astrophys. J. Suppl.*, 148:175–194, 2003.
- [39] H. V. Peiris et al. First year Wilkinson Microwave Anisotropy Probe (WMAP) observations: Implications for inflation. *Astrophys. J. Suppl.*, 148:213–231, 2003.
- [40] P. A. R. Ade et al. Planck 2013 results. XVI. Cosmological parameters. *Astron. Astrophys.*, 571:A16, 2014.
- [41] P. A. R. Ade et al. Planck 2015 results. XIII. Cosmological parameters. *Astron. Astrophys.*, 594:A13, 2016.
- [42] P. A. R. Ade et al. Planck 2013 results. XV. CMB power spectra and likelihood. *Astron. Astrophys.*, 571:A15, 2014.
- [43] Micol Benetti and Jailson S. Alcaniz. Bayesian analysis of inflationary features in Planck and SDSS data. *Phys. Rev.*, D94(2):023526, 2016.
- [44] Camila P. Novaes, Micol Benetti, and Armando Bernui. Primordial Non-Gaussianities of inflationary step-like models. 2015.
- [45] Micol Benetti. Updating constraints on inflationary features in the primordial power

- spectrum with the Planck data. *Phys. Rev.*, D88:087302, 2013.
- [46] Stefano Gariazzo, Olga Mena, Hector Ramirez, and Lotfi Boubekeur. Primordial power spectrum features in phenomenological descriptions of inflation. *Phys. Dark Univ.*, 17:38–45, 2017.
- [47] Amjad Ashoorioon, Axel Krause, and Krzysztof Turzynski. Energy Transfer in Multi Field Inflation and Cosmological Perturbations. *JCAP*, 0902:014, 2009.
- [48] Stefano Gariazzo, Laura Lopez-Honorez, and Olga Mena. Primordial Power Spectrum features and f_{NL} constraints. *Phys. Rev.*, D92(6):063510, 2015.
- [49] Xian Gao and Jinn-Ouk Gong. Towards general patterns of features in multi-field inflation. *JHEP*, 08:115, 2015.
- [50] Yi-Fu Cai, Elisa G. M. Ferreira, Bin Hu, and Jerome Quintin. Searching for features of a string-inspired inflationary model with cosmological observations. *Phys. Rev.*, D92(12):121303, 2015.
- [51] Alexander Gallego Cadavid, Antonio Enea Romano, and Stefano Gariazzo. CMB anomalies and the effects of local features of the inflaton potential. *Eur. Phys. J.*, C77(4):242, 2017.
- [52] Dhiraj Kumar Hazra, Arman Shafieloo, George F. Smoot, and Alexei A. Starobinsky. Primordial features and Planck polarization. *JCAP*, 1609(09):009, 2016.
- [53] David Polarski and Alexei A. Starobinsky. Structure of primordial gravitational waves spectrum in a double inflationary model. *Phys. Lett.*, B356:196–204, 1995.
- [54] J. Lesgourgues, D. Polarski, and Alexei A. Starobinsky. How large can be the primordial gravitational wave background in inflationary models? *Mon. Not. Roy. Astron. Soc.*, 308:281–288, 1999.
- [55] David Polarski. Direct detection of primordial gravitational waves in a BSI inflationary model. *Phys. Lett.*, B458:13–18, 1999.
- [56] Jens Chluba, Jan Hamann, and Subodh P. Patil. Features and New Physical Scales in Primordial Observables: Theory and Observation. *Int. J. Mod. Phys.*, D24(10):1530023, 2015.
- [57] Xingang Chen, P. Daniel Meerburg, and Moritz Munchmeyer. The Future of Primordial Features with 21 cm Tomography. *JCAP*, 1609(09):023, 2016.
- [58] Yidong Xu, Jan Hamann, and Xuelei Chen. Precise measurements of inflationary features with 21 cm observations. *Phys. Rev.*, D94(12):123518, 2016.
- [59] Xingang Chen, Cora Dvorkin, Zhiqi Huang, Mohammad Hossein Namjoo, and Licia Verde. The Future of Primordial Features with Large-Scale Structure Surveys. *JCAP*, 1611(11):014, 2016.

- [60] Mario Ballardini, Fabio Finelli, Cosimo Fedeli, and Lauro Moscardini. Probing primordial features with future galaxy surveys. *JCAP*, 1610:041, 2016. [Erratum: *JCAP*1804,no.04,E01(2018)].
- [61] Clifford Cheung, Paolo Creminelli, A. Liam Fitzpatrick, Jared Kaplan, and Leonardo Senatore. The Effective Field Theory of Inflation. *JHEP*, 03:014, 2008.
- [62] Steven Weinberg. Effective Field Theory for Inflation. *Phys. Rev.*, D77:123541, 2008.
- [63] Ana Achucarro, Vicente Atal, Bin Hu, Pablo Ortiz, and Jesus Torrado. Inflation with moderately sharp features in the speed of sound: Generalized slow roll and in-in formalism for power spectrum and bispectrum. *Phys. Rev.*, D90(2):023511, 2014.
- [64] Ana Achucarro, Vicente Atal, Pablo Ortiz, and Jesus Torrado. Localized correlated features in the CMB power spectrum and primordial bispectrum from a transient reduction in the speed of sound. *Phys. Rev.*, D89(10):103006, 2014.
- [65] Ana Achucarro, Jinn-Ouk Gong, Gonzalo A. Palma, and Subodh P. Patil. Correlating features in the primordial spectra. *Phys. Rev.*, D87(12):121301, 2013.
- [66] Jinn-Ouk Gong, Koenraad Schalm, and Gary Shiu. Correlating correlation functions of primordial perturbations. *Phys. Rev.*, D89(6):063540, 2014.
- [67] J. R. Fergusson, H. F. Gruetjen, E. P. S. Shellard, and B. Wallisch. Polyspectra searches for sharp oscillatory features in cosmic microwave sky data. *Phys. Rev.*, D91(12):123506, 2015.
- [68] Sander Mooij, Gonzalo A. Palma, Grigoris Panotopoulos, and Alex Soto. Consistency relations for sharp features in the primordial spectra. *JCAP*, 1510(10):062, 2015. [Erratum: *JCAP*1602,no.02,E01(2016)].
- [69] Alexander Gallego Cadavid, Antonio Enea Romano, and Stefano Gariazzo. Effects of local features of the inflaton potential on the spectrum and bispectrum of primordial perturbations. *Eur. Phys. J.*, C76(7):385, 2016.
- [70] Jesus Torrado, Bin Hu, and Ana Achucarro. Robust predictions for an oscillatory bispectrum in Planck 2015 data from transient reductions in the speed of sound of the inflaton. *Phys. Rev.*, D96(8):083515, 2017.
- [71] P. Daniel Meerburg, Moritz Munchmeyer, and Benjamin Wandelt. Joint resonant CMB power spectrum and bispectrum estimation. *Phys. Rev.*, D93(4):043536, 2016.
- [72] Stephen Appleby, Jinn-Ouk Gong, Dhiraj Kumar Hazra, Arman Shafieloo, and Spyros Sypsas. Direct search for features in the primordial bispectrum. *Phys. Lett.*, B760:297–301, 2016.
- [73] Sander Mooij, Gonzalo A. Palma, Grigoris Panotopoulos, and Alex Soto. Consistency relations for sharp inflationary non-Gaussian features. *JCAP*, 1609(09):004, 2016.

- [74] Wayne Hu. Generalized slow roll for tensor fluctuations. *Phys. Rev.*, D89(12):123503, 2014.
- [75] Yong Cai, Yu-Tong Wang, and Yun-Song Piao. Is there an effect of a nontrivial c_T during inflation? *Phys. Rev.*, D93(6):063005, 2016.
- [76] Benedict J. Broy. Corrections to n_s and n_t from high scale physics. *Phys. Rev.*, D94(10):103508, 2016. [Addendum: Phys. Rev.D94,no.10,109901(2016)].
- [77] Ewan D. Stewart. The Spectrum of density perturbations produced during inflation to leading order in a general slow roll approximation. *Phys. Rev.*, D65:103508, 2002.
- [78] Jeongyeol Choe, Jinn-Ouk Gong, and Ewan D. Stewart. Second order general slow-roll power spectrum. *JCAP*, 0407:012, 2004.
- [79] Peter Adshead, Wayne Hu, Cora Dvorkin, and Hiranya V. Peiris. Fast Computation of Bispectrum Features with Generalized Slow Roll. *Phys. Rev.*, D84:043519, 2011.
- [80] Cora Dvorkin and Wayne Hu. Generalized Slow Roll for Large Power Spectrum Features. *Phys. Rev.*, D81:023518, 2010.
- [81] Daniel Baumann. Inflation. In *Physics of the large and the small, TASI 09, proceedings of the Theoretical Advanced Study Institute in Elementary Particle Physics, Boulder, Colorado, USA, 1-26 June 2009*, pages 523–686, 2011.
- [82] Ana Achucarro, Jinn-Ouk Gong, Sjoerd Hardeman, Gonzalo A. Palma, and Subodh P. Patil. Mass hierarchies and non-decoupling in multi-scalar field dynamics. *Phys. Rev.*, D84:043502, 2011.
- [83] Ana Achucarro, Jinn-Ouk Gong, Sjoerd Hardeman, Gonzalo A. Palma, and Subodh P. Patil. Features of heavy physics in the CMB power spectrum. *JCAP*, 1101:030, 2011.
- [84] Andrew J. Tolley and Mark Wyman. The Gelaton Scenario: Equilateral non-Gaussianity from multi-field dynamics. *Phys. Rev.*, D81:043502, 2010.
- [85] Raphael Flauger, Liam McAllister, Enrico Pajer, Alexander Westphal, and Gang Xu. Oscillations in the CMB from Axion Monodromy Inflation. *JCAP*, 1006:009, 2010.
- [86] Katherine Freese, Joshua A. Frieman, and Angela V. Olinto. Natural inflation with pseudo - Nambu-Goldstone bosons. *Phys. Rev. Lett.*, 65:3233–3236, 1990.
- [87] David H. Lyth. What would we learn by detecting a gravitational wave signal in the cosmic microwave background anisotropy? *Phys. Rev. Lett.*, 78:1861–1863, 1997.
- [88] Richard Easther, William H. Kinney, and Brian A. Powell. The Lyth bound and the end of inflation. *JCAP*, 0608:004, 2006.
- [89] Ippei Obata and Jiro Soda. Oscillating Chiral Tensor Spectrum from Axionic Inflation. *Phys. Rev.*, D94(4):044062, 2016.

- [90] Paolo Creminelli, Jerome Gleyzes, Jorge Norena, and Filippo Vernizzi. Resilience of the standard predictions for primordial tensor modes. *Phys. Rev. Lett.*, 113(23):231301, 2014.
- [91] Paolo Creminelli and Matias Zaldarriaga. Single field consistency relation for the 3-point function. *JCAP*, 0410:006, 2004.
- [92] David Seery and James E. Lidsey. Primordial non-Gaussianities in single field inflation. *JCAP*, 0506:003, 2005.
- [93] Xingang Chen, Min-xin Huang, Shamit Kachru, and Gary Shiu. Observational signatures and non-Gaussianities of general single field inflation. *JCAP*, 0701:002, 2007.
- [94] Clifford Cheung, A. Liam Fitzpatrick, Jared Kaplan, and Leonardo Senatore. On the consistency relation of the 3-point function in single field inflation. *JCAP*, 0802:021, 2008.
- [95] Jonathan Ganc and Eiichiro Komatsu. A new method for calculating the primordial bispectrum in the squeezed limit. *JCAP*, 1012:009, 2010.
- [96] Sebastien Renaux-Petel. On the squeezed limit of the bispectrum in general single field inflation. *JCAP*, 1010:020, 2010.
- [97] Nilay Kundu, Ashish Shukla, and Sandip P. Trivedi. Constraints from Conformal Symmetry on the Three Point Scalar Correlator in Inflation. *JHEP*, 04:061, 2015.
- [98] Nilay Kundu, Ashish Shukla, and Sandip P. Trivedi. Ward Identities for Scale and Special Conformal Transformations in Inflation. *JHEP*, 01:046, 2016.
- [99] Takahiro Tanaka and Yuko Urakawa. Dominance of gauge artifact in the consistency relation for the primordial bispectrum. *JCAP*, 1105:014, 2011.
- [100] Liang Dai, Enrico Pajer, and Fabian Schmidt. Conformal Fermi Coordinates. *JCAP*, 1511(11):043, 2015.
- [101] Yuichiro Tada and Vincent Vennin. Squeezed bispectrum in the δN formalism: local observer effect in field space. *JCAP*, 1702(02):021, 2017.
- [102] Tobias Baldauf, Uros Seljak, Leonardo Senatore, and Matias Zaldarriaga. Galaxy Bias and non-Linear Structure Formation in General Relativity. *JCAP*, 1110:031, 2011.
- [103] Jaiyul Yoo, A. Liam Fitzpatrick, and Matias Zaldarriaga. A New Perspective on Galaxy Clustering as a Cosmological Probe: General Relativistic Effects. *Phys. Rev.*, D80:083514, 2009.
- [104] Viatcheslav F. Mukhanov and G. V. Chibisov. Quantum Fluctuations and a Nonsingular Universe. *JETP Lett.*, 33:532–535, 1981. [Pisma Zh. Eksp. Teor. Fiz. 33, 549 (1981)].
- [105] Misao Sasaki, Jussi Valiviita, and David Wands. Non-Gaussianity of the primordial

- perturbation in the curvaton model. *Phys. Rev.*, D74:103003, 2006.
- [106] Christian T. Byrnes, Ki-Young Choi, and Lisa M. H. Hall. Conditions for large non-Gaussianity in two-field slow-roll inflation. *JCAP*, 0810:008, 2008.
- [107] William H. Kinney. Horizon crossing and inflation with large eta. *Phys. Rev.*, D72:023515, 2005.
- [108] Mohammad Hossein Namjoo, Hassan Firouzjahi, and Misao Sasaki. Violation of non-Gaussianity consistency relation in a single field inflationary model. *Europhys. Lett.*, 101:39001, 2013.
- [109] Jerome Martin, Hayato Motohashi, and Teruaki Suyama. Ultra Slow-Roll Inflation and the non-Gaussianity Consistency Relation. *Phys. Rev.*, D87(2):023514, 2013.
- [110] Xingang Chen, Hassan Firouzjahi, Mohammad Hossein Namjoo, and Misao Sasaki. A Single Field Inflation Model with Large Local Non-Gaussianity. *EPL*, 102(5):59001, 2013.
- [111] Sander Mooij and Gonzalo A. Palma. Consistently violating the non-Gaussian consistency relation. *JCAP*, 1511(11):025, 2015.
- [112] N. C. Tsamis and Richard P. Woodard. Improved estimates of cosmological perturbations. *Phys. Rev.*, D69:084005, 2004.
- [113] Bernardo Finelli, Garrett Goon, Enrico Pajer, and Luca Santoni. Soft Theorems For Shift-Symmetric Cosmologies. *Phys. Rev.*, D97(6):063531, 2018.
- [114] Rafael Bravo, Sander Mooij, Gonzalo A. Palma, and Bastian Pradenas. Vanishing of local non-Gaussianity in canonical single field inflation. 2017.
- [115] Sandipan Kundu. Non-Gaussianity Consistency Relations, Initial States and Back-reaction. *JCAP*, 1404:016, 2014.
- [116] Paolo Creminelli, Jorge Norena, and Marko Simonovic. Conformal consistency relations for single-field inflation. *JCAP*, 1207:052, 2012.
- [117] Kurt Hinterbichler, Lam Hui, and Justin Khoury. Conformal Symmetries of Adiabatic Modes in Cosmology. *JCAP*, 1208:017, 2012.
- [118] Leonardo Senatore and Matias Zaldarriaga. A Note on the Consistency Condition of Primordial Fluctuations. *JCAP*, 1208:001, 2012.
- [119] Valentin Assassi, Daniel Baumann, and Daniel Green. On Soft Limits of Inflationary Correlation Functions. *JCAP*, 1211:047, 2012.
- [120] Kurt Hinterbichler, Lam Hui, and Justin Khoury. An Infinite Set of Ward Identities for Adiabatic Modes in Cosmology. *JCAP*, 1401:039, 2014.
- [121] Walter D. Goldberger, Lam Hui, and Alberto Nicolis. One-particle-irreducible consis-

- tency relations for cosmological perturbations. *Phys. Rev.*, D87(10):103520, 2013.
- [122] Paolo Creminelli, Ashley Perko, Leonardo Senatore, Marko Simonovi?, and Gabriele Trevisan. The Physical Squeezed Limit: Consistency Relations at Order q^2 . *JCAP*, 1311:015, 2013.
- [123] Yi-Fu Cai, Jinn-Ouk Gong, Dong-Gang Wang, and Ziwei Wang. Features from the non-attractor beginning of inflation. *JCAP*, 1610(10):017, 2016.
- [124] Cristiano Germani and Tomislav Prokopec. On primordial black holes from an inflection point. *Phys. Dark Univ.*, 18:6–10, 2017.
- [125] Konstantinos Dimopoulos. Ultra slow-roll inflation demystified. *Phys. Lett.*, B775:262–265, 2017.
- [126] Liang Dai, Enrico Pajer, and Fabian Schmidt. On Separate Universes. *JCAP*, 1510(10):059, 2015.
- [127] Fabian Schmidt and Donghui Jeong. Large-Scale Structure with Gravitational Waves II: Shear. *Phys. Rev.*, D86:083513, 2012.
- [128] Mafalda Dias, Joseph Elliston, Jonathan Frazer, David Mulryne, and David Seery. The curvature perturbation at second order. *JCAP*, 1502(02):040, 2015.
- [129] Rafael Bravo, Sander Mooij, Gonzalo A. Palma, and Bastian Pradenas. A generalized non-Gaussian consistency relation for single field inflation. 2017.
- [130] Yi-Fu Cai, Xingang Chen, Mohammad Hossein Namjoo, Misao Sasaki, Dong-Gang Wang, and Ziwei Wang. Revisiting non-Gaussianity from non-attractor inflation models. 2018.
- [131] Roland de Putter, Olivier Dore, Daniel Green, and Joel Meyers. Single-Field Inflation and the Local Ansatz: Distinguishability and Consistency. *Phys. Rev.*, D95(6):063501, 2017.
- [132] P Fosalba, O Doré, and FR Bouchet. Elliptical beams in cmb temperature and polarization anisotropy experiments: An analytic approach. *Physical Review D*, 65(6):063003, 2002.